wasser infrastruktur ressourcen

Organic Micropollutants, Metals and Total Suspended Solids in Urban Stormwater Runoff from an Industrial Area: Evaluation of Occurrence, Behaviour and Removal Efficiency

Philipp Baum

Organic Micropollutants, Metals and Total Suspended Solids in Urban Stormwater Runoff from an Industrial Area: Evaluation of Occurrence, Behaviour and Removal Efficiency

Dipl.-Ing. Philipp Baum

Kaiserslautern

2023

Organic Micropollutants, Metals and Total Suspended Solids in Urban Stormwater Runoff from an Industrial Area: Evaluation of Occurrence, Behaviour and Removal Efficiency

vom Fachbereich Bauingenieurwesen der Rheinland-Pfälzischen Technischen Universität Kaiserslautern-Landau zur Erlangung des akademischen Grades Doktor-Ingenieur (Dr.-Ing.) genehmigte Dissertation

Vorgelegt von

Dipl.-Ing. Philipp Baum

Dekan Prof. Dr.-Ing. Hamid Sadegh-Azar

Prüfungskommission

Vorsitzende Prof. Dr.-Ing. Heidrun Steinmetz

1. Berichterstatter Prof. Dr.-Ing. Ulrich Dittmer

2. Berichterstatterin Prof. Dr. rer. nat. habil. Brigitte Helmreich

Datum der Prüfung 14.12.2022

Kaiserslautern 2023

(D 386)

Acknowledgements

Kurzfassung

Feststoffe gelten schon seit längerer Zeit als Indikator für die Verschmutzung von urbanem Regenwasserabfluss. Es gibt nur jedoch wenige Studien, die die Ver-schmutzung mit organischen Mikroverunreinigungen und Metallen sowohl in der gelösten als auch in der partikulären Phase sowie über verschiedene Partikelgrö-ßenklassen hinweg untersucht haben. Gerade diese Verteilung spielt jedoch eine wichtige Rolle für ein besseres Verständnis und die Optimierung von Maßnahmen zur Behandlung von urbanem Regenwasser. Ziel dieser Arbeit war es daher, die Zusammensetzung von Partikeln im städtischen Regenwasser im Hinblick auf ihre physikalisch-chemischen Eigenschaften (Partikelgrößenverteilung und organischer Gehalt) sowie das Aufkommen von organischen Mikroverunreinigungen und Metal-len, ihre Bindung an die Partikel und ihre Entfernung aus dem urbanen Abfluss zu untersuchen.

Es wurde eine kontinuierliche langzeit Messkampagne an einer zentralen Regen-wasserbehandlungsanlage in einem Gewerbegebiet durchgeführt. Die Regenwas-serabflüsse wurden mit großvolumigen Probenahmebehältern beprobt welche vo-lumenproportional zum Abfluss an den beiden Auslässen der Anlage gefüllt wur-den. Dies ermöglichte die Bestimmung der mittleren Ereigniskonzentrationen sowie der fracht-bezogenen Wirkungsgrade der Behandlungsanlage für verschiedene Pa-rameter. In jeder Probe wurden die Konzentrationen der abfiltrierbaren Stoffe (AFS) über verschiedene Partikelgrößenfraktionen (< 63 µm, 63 – 125 µm, 125 – 250 µm, 250 – 2000 µm) sowie deren organischer Anteil gemessen. Darüber hinaus wurden die Konzentrationen und die Phasenverteilung von 5 Metallen (Chrom, Kupfer, Zink, Cadmium, Blei) und 29 organischen Spurenstoffen, darunter polyzyklische aromatische Kohlenwasserstoffe, Industriechemikalien (z. B. Organophosphate, Alkyphenole) und Biozide, in verschiedenen Partikelgrößenfraktionen analysiert.

In dieser Studie wurden über einen Zeitraum von fast 2,5 Jahren insgesamt 36 Probenahmeereignisse in zwei Probenahmezeiträumen (2015 – 2016 und 2017 – 2019) an der Regenwasserbehandlungsanlage in Freiburg Haid erfasst und unter-sucht. Bei 22 dieser Ereignisse wurde das Vorkommen von organischen Mikrover-unreinigungen und bei 17 Ereignissen das Vorkommen von Metallen bestimmt. Die Auswertung der mittleren AFS-Ereigniskonzentration zeigte, dass der Feinfraktion der Feststoffe eine besondere Bedeutung zukommt, da sie eine mehr als doppelt so hohe mittlere Ereigniskonzentration (34 mg L^{-1}) aufweist wie die gröbere Partikel-fraktion (14,9 mg L^{-1}).

Hinsichtlich der transportierten Feststofffracht hatten die Feststoffe < 63 µm einen mittleren Anteil von 61 %, die Fraktion 63 – 125 µm einen Anteil von 13 %, die Fraktion 125 – 250 µm einen Anteil von 6 % und die Fraktion 250 – 2000 µm einen An-teil von 9 % an der gesamten Feststoffmasse. Was den organischen Anteil der Fest-stoffe

betrifft, so zeigten die Ergebnisse eine deutliche Zunahme des organischen Anteils mit zunehmender Partikelgröße (gemessen als Glühverlust).

Wie auch bei den Feststoffen wurden die höchsten Konzentrationen der untersuch-ten organischen Spurenstoffe und Metalle in der Partikelgrößenfraktion < 63 µm gefunden. Die Feinfraktion der Partikel transportierte auch die größte Fracht an or-ganischen Spurenstoffen und Metallen. Daher wurde in dieser Studie die Beladung der Festoffe mit organischen Spurenstoffen oder Metallen bzw. die partikelgebun-dene Spurenstoff-/Metallkonzentration berechnet. Für die meisten Substanzen wurde eine ziemlich gleichmäßige Verteilung über die kleinsten drei Partikelgrö-ßenfraktionen festgestellt. Es konnte eine gewisse Korrelation des organischen An-teils mit dem Aufkommen an organischen Spurenstoffen und Metallen gezeigt wer-den, so dass davon ausgegangen werden kann, dass die partikelgebundene Kon-zentration durch den organischen Anteil der Partikel beeinflusst wird. Da jedoch u.a. die größten partikelgebundenen Schadstofffrachten mit Partikeln < 63 µm transportiert werden, stellt die Feinfraktion die relevante Partikelgröße im urbanen Regenwasserabfluss dar.

Bezogen auf den Gesamtwirkungsgrad (Sedimentationswirkungsgrad und Spei-cher-wirkungsgrad) konnte die untersuchte Anlage in dieser Studie die Belastung durch Feinpartikel nur um ca. ein Viertel reduzieren. Die größeren Partikelgrößen-klassen wurden in den meisten Fällen um weit mehr als die Hälfte reduziert. Würde man das gesamte Größenspektrum von AFS als Proxy zur Abschätzung der Reini-gungsleistung von Metallen und organischen Spurenstoffen heranziehen, würde diese zu hoch ange-setzt und damit die tatsächliche Schadstofffracht, die in die Umwelt gelangt, unter-schätzt werden. Die Untersuchung, ob die Partikelgrößenfrak-tion < 63 µm besser ge-eignet wäre, zeigte jedoch, dass selbst für Stoffe mit einer hohen Neigung zur Adsorp-tion an Partikel (z. B. Cr, Cu, IND, GHI) der Gesamtwir-kungsgrad der Behandlung durch die Feinfraktion überschätzt wurde.

Schlagworte: Abfiltrierbare Stoffe, Metalle, organische Spurenstoffe, Partikelgrö-ßen-verteilung, urbane Regenwasser Qualität.

Abstract

Particulate matter has been considered an indicator for the pollution of urban storm-water runoff for quite some time. There are only few studies that have investi-gated the contamination with organic micropollutants and metals both in the dis-solved and particulate phase as well as across different particle size classes.Yet, this distribution plays an important role in better understanding and optimising ur-ban stormwater treatment measures.Therefore, this work aimed at assessing the composition of par-ticulate matter in urban stormwater in terms of the physico-chemical properties (par-ticle size distribution and organic content), as well as the occurrence of organic mi-cropollutants and metals, their association to particulate matter and their removal from urban runoff.

An intensive long term monitoring campaign at a centralised stormwater treatment facility of an industrial area was conducted. The stormwater runoff was sampled with large volume sampling tanks filled volume-proportional to the runoff at the two outlets of the facility. This allowed the determination of the event mean concentra-tions as well as the load-related removal efficiencies of the treatment facility for dif-ferent parameters. Within each sample the concentrations of total suspended solids across dif-ferent particle size fractions (< 63 µm, 63 – 125 µm, 125 – 250 µm, 250 – 2000 µm) were measured as well as their organic content. Furthermore, the concen-trations and the phase distibution of 5 metals (Chromium, Copper, Zinc, Cadmium, Lead) and 29 organic micropollutants including polycyclic aromatic hydrocarbons, industrial chemi-cals (e.g. organophosphates, alkyphenols) and biocides were ana-lysed across different particle size fractions.

In this study, over a period of almost 2.5 years, a total of 36 sampling events were recorded and investigated within two sampling periods (2015 – 2016 and 2017 – 2019) at the rainwater treatment facility in Freiburg Haid. The occurrence of organic mi-cropollutants was determined in 22 of these events and the occurrence of metals in 17. The evaluation of the event mean concentration of total suspended solids showed that the fine fraction of the solids is of particular importance, as it showed an event mean concentration more than twice as high (34 mg L^{-1}) as the coarser par-ticle fraction (14.9 mg L^{-1}).

Regarding the occurrence of total suspened solids in terms of the transported solid load, the solids < 63 µm accounted for a mean proportion of 61 %, the fraction 63 – 125 µm for 13 %, the fraction 125 – 250 µm for 6 % and the fraction 250 – 2000 µm for 9 % of the total solid mass. In terms of the organic content of the solids, the re-sults showed a clear increase of the organic content with increasing particle size (measured as loss on ignition).

As in the case of solids, the highest concentrations of the organic micropollutants and metals investigated were found in the particle size fraction < 63 μm. This fine fraction of the particles also accounted for the largest load of organic micropollutants and metals. Therefore, the particle loading with organic micropollutants or metals respectively the particle-bound micropollutant/metal concentration was calculated in this study. For most substances, a rather equal distribution over the smallest three particle size fractions was found. A certain correlation of the organic content with the occurrence of organic micropollutants and metals could be shown, therfore it can be assumed that the particle-bound concentration is certainly influenced by the organic content of the particulate matter. However, due to the fact that, among other things, the largest particle-bound pollutant loads are transported with particles < 63 μm, the fine fraction represents the relevant particle size in urban stormwater runoff.

Regarding the total treatment efficiency (including sedimentation efficiency and volume retention), the investigated facility in this study was able to reduce the load of fine particles by only a quarter. The larger particle size classes were reduced by far more than half in most cases. If total suspended solids in its entire particle size range were used as a proxy to estimate the removal efficiency of metals and organic micropollutants, the efficiency would be overestimatd and the actual pollutant load released into the environment would thus be underestimated. However, the investigation, weather the particle size fraction < 63 μm would be more suitable, showed that even for substances with a high tendency to adsorb onto particles (e.g. Cr, Cu, IND, GHI), the total treatment efficiency was still overestimated by the fine fraction.

Table of Contents

List of Figures

List of Tables

List of Abbrevations

4NP	4-nonylphenol
4tOP	4-tert-ocylphenol
AADT[°]	Annual average daily traffic
AA-EQS	Average annual EQS
ACY	Acenaphthylene
ADWP	Antecedent dry weather period
AFS63	Abfiltrierbare Stoffe < 63 µm (AFS german equivalent forTSS)
Al	Aluminum
ANT	Anthracene
BaA	Benzo[a]anthracene
BaP	Benzo[a]pyrene
BbF	Benzo[b]fluoranthene
BkF	Benzo[k]fluoranthene
BT	Benzothiazole
CAF	Caffein
CAN	Acenaphthene
CBZ	Carbamazepine
Cd	Cadmium
CHR	Chrysene
Co	Cobalt
COD	Chemical oxygen demand
Cr	Chromium
Cu	Copper
CWD	Clear water discharge
DBA	Dibenzo[ah]anthracene
DEET	N,N-diethyl-m-toluamide
DOC	Dissolved organic carbon
DOM	Dissolved organic matter
EC	Electrical conductivity
EMC	Event mean concentration
EPA	Environmental Protection Agency
EQS	Environmental quality standard
EU	European Union
fd	Partitioning index – dissolved fraction
Fe	Iron

FLE	Fluorene
FLU	Fluoranthene
fOC	Mass fraction of organic carbon
fp	Partitioning index – particular fraction
GC	Gas chromatography
GHI	Benzo[ghi]perylene
GSM	Global System for Mobile Communications
HMW	Heavy molecular weight
HPLC	High performance liquid chromatography
ICP	Inductivly coupled plasma
IND	Indeno[1,2,3-cd]pyrene
IQA	Interquartile range
ISWA	Institut for Sanitary Engineering, Water Quality, and Waste Management
KD	Equilibrium phase distribution coefficient
KOC	Adsorption coefficient normalised to organic carbon content
KOW	Octanol-water partition coefficient
LID	Lidocain
LMW	Light molecular weight
LOI	Loss on ignition
LOQ	Limit of quantification
LVST	Large volume sampling tank
MAC-EQS	Maximum allowable concentration EQS
MCP	Mecoprop
Mn	Manganese
MS	Mass spectrometry
MTBT	2-methylthiobenzothiazole
NAP	Naphthalene
Ni	Nickel
OM	Organic matter
PAH	Polycyclic aromatic hydrocarbon
Pb	Lead
PHE	Phenantrene
PM	Particular matter
POC	Particulate organic carbon
POM	Particular organic matter
PSD	Particle size distribution
PYR	Pyrene
r	Pearson correlation coefficient
RDS	Road deposited solids
RFM	Regenwasserbehandlungsanlge Freiburger Modell (stormwater treat-ment facility Freiburg model)

rs	Spearman correlation coefficient
SD	Standard diviation
SE	Sampling event
SSA	Specific surface area
SSC	Small sampling container
TBY	Terbutryn
TCEP	Tris(2-chlorethyl)phosphate
TCPP	Tris(1-chloro-2-propyl)phosphate
TOC	Total organic carbon
TPP	Triphenylphosphate
TSS	Total suspended solids
TSS63	Total suspended solids < 63 µm
W	Tungsten (or Wolfram)
WFD	Water Framework Directive
Zn	Zinc

1   Introduction

In 2010 the United Nations General Assembly recognized the human right to water and sanitation. Thereby, they acknowledged that clean drinking water is essential to the realization of all human rights (United Nations General Assembly 2010). Moreover, the world's water resources are indispensable for all life on earth and therefore most valuable. However, industrialization, population growth and the increasing urbanization in the last decades have negative impacts on the water resources. Particularly urban surface waters are directly affected by anthropogenic activities that can influence the hydromorphology as well as the water quality (Larsen et al. 2016).

In our modern society, chemical substances became part of the daily life. Therefore, it is hardly surprising that with the improved analytical methods, substances such as pharmaceuticals, industrial chemicals, personal care products as well as pesticides are detected in the range of nanograms to micrograms per litre in the aquatic environment. In the last years, occurrence, fate and the effects of organic micropollutants on the aquatic environment and on the human health became a new challenge for the scientific world. Various research groups all over the world carried out monitoring campaigns to better understand their impact in the urban water cycle (Luo et al. 2014).

At the European level, the issue of emerging chemical substances and their threat to the aquatic environment, is addressed by the European Water Framework Directive (WFD). Herein, a list of substances or groups of substances of priority concern in surface waters with regards to their wide-ranging use and their high concentrations in rivers, lakes and coastal waters, is identified. This list will be consistently reviewed and updated if appropriate. In the current form, it comprises 45 priority substances (PS) mainly organic compounds including multiple pesticides, several polycyclic aromatic hydrocarbons (PAHs) other industrial chemicals, such as flame retardants, plasticisers as well as pharmaceuticals and some heavy metals. To achieve and maintain a good ecological as well as chemical status of the surface waters, the cause of pollution should be identified and emissions should be dealt with at source, in "the most economically and environmentally effective manner" (Directive 2013/39/EU).

Besides discharges of wastewater treatment plants (WWTPs) and combined sewer overflow (CSO) being sources for organic micropollutants, urban stormwater runoff has been recognized as a major pathway of a vast number of pollutants (Makepeace et al. 1995; Holten Lützhøft et al. 2009). The pollution of urban runoff varies depending of the catchment area and the anthropogenic activities within that catchment. Pollutants usually monitored in urban stormwater runoff include organic matter, metals, nutrients, organic micropollutants, pathogenic microorganisms, and solids (particulate matter) (Hvitved-Jacobsen et al. 2010). The pollution of urban stormwater runoff has different points of origin. It is traffic related (e.g., tyre wear particles, break wear, and

fluid leakage), it contains materials from dry and wet atmospheric deposition or substances which can be released from roofs or buildings that are all washed off during a rain-event (Davis et al. 2001; McKenzie et al. 2009; Becouze-Lareure et al. 2015; Markiewicz et al. 2017)

Particulate matter (PM) being referred to as a pollutant in urban stormwater, relates to the fact, that PM can directly influence the aquatic ecosystem of the receiving waters. For example, high amounts of PM are affecting the penetration of light into the water column and thereby influencing the energy assimilation of macrophytes and algae which will also impacts primary consumers. The deposition and settling of PM into the river beds can also affect the development and the survival of salmonid eggs and larvae (Bilotta und Brazier 2008). Furthermore, different studies showed that organic micropollutants and metals are associated with particles in urban stormwater runoff (Gromaire et al. 1999; Grant S.B. et al. 2003; Huber et al. 2016). PM transports these substances including hazardous and toxic substances into the surface waters and thereby not only influences physicochemical variables of the receiving water but also poses a threat to the organisms living in the water and in the bottom sediments (Gosset et al. 2017).

Particles found in stormwater runoff are of different origin. In addition to traffic related activities (Drapper et al. 2000; McKenzie et al. 2009; Gunawardana et al. 2014), surrounding soil (Qian et al. 2011; Zhang et al. 2015) as well as wet and dry atmospheric deposition (Sabin et al. 2006; Wang et al. 2016) are the main sources. There have been multiple investigations regarding the concentration of total suspended solids (TSS) in stormwater runoff from different surfaces. There are variations of several orders of magnitude between different catchments. The highest concentrations can be found in street and highway run-off (Lygren et al. 1984; Bannerman et al. 1993). In addition to the mere occurrence of solids, their particle size distribution (PSD) plays a very important role in urban stormwater runoff and needs to be considered as a crucial factor due to the fact that it has a significant influence on the adsorption of pollutants (Badin et al. 2008; Li et al. 2015). Several studies investigated the particle size distribution (PSD) of urban stormwater runoff and they have shown that it contains particles in a wide spectrum of size, ranging from submicron colloids (< 1 µm) to gravel sized particles (Sartor und Boyd 1972; Ball und Abustan 1995; Sansalone und Buchberger 1997a; Grout et al. 1999). Regarding the contamination, different pollutants are associated with particles of different size. There have been numerous investigations about heavy metals and PAHs associated with particles in different size fractions, indicating that the fine particle fraction is contaminated the most (Sartor et al. 1974; Wilber und Hunter 1979; Evans et al. 1990; Revitt et al. 1990; Xanthopoulos und Hahn 1990; Marsalek und Marsalek 1997; Herngren et al. 2010). However, regarding the contamination of stormwater particles with other organic micropollutants than PAHs, only few studies were conducted so far. Mostly just the partitioning between dissolved and particulate phase was investigated an very rarely the partitioning within different size fractions (Zgheib et al. 2011; Björklund et al. 2009; Kalmykova et al. 2013).

The majority of technical solutions for the treatment of urban stormwater runoff are based on the physical principles of sedimentation or filtration, for example settling tanks, detention ponds or retention soil filters (RSF). With regards to the dominating role of solids in urban runoff this seems appropriate. However, the performance of these treatment systems is sensitive to the PSD (for RSF, this applies only to a lesser extent, as adsorption processes also play a role in the treatment of urban runoff). In terms of separating the fine and heavily contaminated size fraction sedimentation becomes less efficient (Charters et al. 2015). Concerning the classical end-of-pipe emission reduction of priority substances in urban stormwater runoff, a good knowledge about the partitioning of these substances within different particle size fractions is of particular importance (Hilliges et al. 2013; Maniquiz-Redillas und Kim 2014).

This work aimed at assessing the composition of particulate matter in urban stormwater in terms of the physico-chemical properties (particle size distribution, organic content), as well as the occurrence of organic micropollutants and metals. There are new regulations on stormwater management in Germany in which the requirement of stormwater treatment is based on TSS < 63 µm (DWA 2020). For this reason, this study investigated whether the particle fraction <63 µm is more contaminated with organic micropollutants and metals than the coarse fraction. The association of PM and pollutants with regard to their physico-chemical properties was one of the main focus areas of this work. Furthermore, another objective of this work was to investigate whether TSS or a specific size class is a suitable proxy to adequately represent the contamination with organic micropollutants and metals.

The thesis is structured as follows. In Chapter 2, the relevant theoretical foundations for the topic of this thesis are presented and an overview of the current state of knowledge is given. Chapter 3 presents the distinct objectives of this work in detail. The following Chapter 4 presents the material and methods used for the research project carried out, Chapter 5 presents the results and their discussion and finally Chapter 6 contains the conclusion of the thesis and suggestions for future research approaches.

The basics outlined in Chapter 2 are divided into several sub-chapters. First, some important terms used in the thesis are defined to create a common understanding (2.1). Next, the topic of urban stormwater quality is highlighted (2.2). Here, among other things, measurement methods of physico-chemical characteristics of PM relevant to this work are presented. Also, measurement programmes and results of other research groups are shown and discussed thus giving an overview about the state of knowledge. Along with the scientific principles of adsorption described herein, Chapter 2 enables the understanding and interpretation of the results of the conducted monitoring campaign. In order to investigate the objectives of the work described in Chapter 3, an intensive long-term monitoring campaign was carried out. In Chapter 4, the investigated catchment area and the sampled stormwater treatment facility are presented and the methodological approach as well as the performed laboratory analyses are explained. This chapter also includes the statistical methods used for the evaluation of

the measurement results as well as further calculation approaches that were applied in the evaluation of the results. Chapter 5 presents and discusses the results of the monitoring campaign. For a better understanding of the samples and the evaluated results, the rainfall and runoff events are characterised first (5.1). Next, the results of the PM analysis (5.2), more precisely their PSD (< 63 μm, 63 – 125 μm, 125 – 250 μm, 250 – 2000 μm), as well as their respective organic content and the occurrence of TSS (concentrations and loads) within the four different particle size fractions are presented. Based on this, the efficiency of the treatment facility is evaluated and correlations between the investigated parameters and the rainfall and runoff characteristics are examined. Subsequently, the results of the organic micropollutant and metal analysis are evaluated and discussed (5.3 and 5.4). The focus lies on the occurrence (concentrations and loads) in the dissolved and particulate phase as well as the particulate bound pollutant concentrations of the individual particle size fractions. The phase distribution and the association with organic matter (OM) are also evaluated. The treatment efficiency of the investigated facility with respect to the retention of organic micropollutants and metals is shown. Finally, the suitability of TSS as a proxy with regard to the contamination with the examined substances as well as to their retention by the treatment facility is investigated and discussed. At the end of the thesis, Chapter 6 draws a conclusion based on the results presented and gives recommendations for future research programmes.

2 Fundamentals and State of Knowledge

This chapter is intended to provide a basis for a better understanding of the key issues relevant to the objectives of this thesis. It includes scientific fundamentals on important processes (e.g. adsorption) and on the physico-chemical properties of solids in urban stormwater runoff. In addition, relevant literature data are compiled, which serve for the later classification and interpretation of the own measurement results.

2.1 Definition of Terms

Solids, particles, and sediments are terms used in this thesis to describe the same. Namely, particulate matter (PM) present in urban runoff as a result of atmospheric desposition, inputs from soil or originating from anthropogenic activities (e.g. tyre wear) etc.

In the context of this work, organic micropollutants are defined as persistent synthetic or natural chemical substances occurring in the aquatic environment in low concentrations (in the range of ng L^{-1} to µg L^{-1}). These compounds contain carbon atoms that are covalently bound to other atoms. Due to their persistent nature, organic micropollutants may have detrimental effects on the environment and humans in these low concentrations.

Traditionally, metals are often divided into heavy metals and light metals according to their density. Heavy metals have densities of five grams per cubic centimetre and more (Holleman et al. 2007). In this study they are referred to as metals. Metals are widespread in nature (soil and water), some of them (e.g. Copper and Zinc) are vital trace elements. However, metal ions can have toxic effects on organisms even in low concentrations.

2.2 Urban Stormwater Quality

Urban stormwater runoff is recognised as a major nonpoint source of contaminants having negative effects on the water quality of surface waters (Burton und Pitt 2001). Makepeace et al. (1995) published an extensive literature review of stormwater pollution research and distinguished hazardous effects of pollutants with regard to humans and aquatic life. Their work highlights especially solids, metals, hydrocarbons and nutrients as the most critical contaminants.

However it is important to note, that measurement results are influenced by the way samples are taken, prepared and analysed. Thus, different measurement programmes are not necessarily comparable and do not contribute to a generally valid gain of knowledge (Welker und Dittmer 2005).

2.2.1 Particulate Matter in Urban Stormwater

Particulate matter (PM) is commonly referred to as sediments or solids. Samples of urban stormwater often are classified into two fractions, the "particulate" and the "dissolved" fraction. The particulate fraction usually consists of particles > 0.45 μm and is also called total suspended solids (TSS). The dissolved fraction contains everything that passes through a membrane or a filter with a pore size of 0.45 μm. However, 0.45 μm is a conventional limit because it is known that the dissolved fraction is not truly dissolved but contains colloidal matter (Brown und Peake 2003; Lead J. R. et al. 1997). These colloids are ranging in sizes from 1 nm to 1 μm (Everett 1988).

PM is recognized as a major pollutant in stormwater not only due to their direct impacts on salmonid fish, phytoplankton and macrophytes (Bash und Bernman 2001; Bilotta und Brazier 2008) but also due to their capability of adsorbing toxic pollutants such as metals and organic micropollutants (Morrison et al. 1988; Herngren et al. 2005; Lau und Stenstrom 2005; Gasperi et al. 2009) and thereby having a significant effect on the receiving water quality. The organic content of PM plays a major role in the adsorption of pollutants (cf. 2.3.2)

2.2.1.1 Sources and Occurrence

PM found in urban stormwater runoff is of different origin. Besides traffic related activities (Gunawardana et al. 2014; Drapper et al. 2000; McKenzie et al. 2009), surrounding soil (Zhang et al. 2015; Qian et al. 2011) as well as wet and dry atmospheric deposition (Sabin et al. 2005; Wang et al. 2016) are the main sources.

There have been multiple investigations regarding the concentration of TSS in stormwater runoff from different surfaces. Dierschke (2014) gives an overview about the various studies from different countries. There are variations of several orders of magnitude between different catchments. The highest concentrations can be found in street and highway runoff. Bannerman et al. (1993) investigated the runoff from different streets (feeder, collector and arterial streets) in residential, commercial and industrial areas. The TSS concentrations range from 173 – 763 mg L^{-1}. Lygren et al. (1984) studied highway runoffs in Norway and found TSS runoff concentrations ranging from 162 – 2420 mg L^{-1}. In the literature review of Makepeace et al. (1995) the total range of TSS in stormwater is given as 1.0 – 36,200 mg L^{-1}.

Summary: PM in runoff has multiple sources. Traffic activities, soil, as well as wet and dry deposition are the main sources. In terms of occurrence, a very wide range of TSS concentrations (up to several grams per liter) is apparent. The occurrence is strongly

dependent on the investigated catchment area. Heavily trafficked roads show the highest load of solids.

2.2.1.2 Particle Composition and Flocculation

PM in urban stomwater runoff has different origins and it consists of different materials and elements (Fedotov et al. 2014). In addition to various mineral components, anthropogenic as well as natural organic components can be found (Gunawardana et al. 2012). Particles in the urban environment can be seen as a heterogeneous mixture originating from different sources and their characterisation can be complex since various physical, chemical, and biological factors affect their structure (Adachi und Tainosho 2004). As Beckwith et al. (1986) noted, particles are subject to a complex mixing processes that occur both during transport and on surfaces, for example, on roads. This can lead to changes in the chemical composition of the particles. Such compositional changes are also common in inputs of natural soil particles found on road surfaces. In addition, due to frequent traffic activities, traffic-related particles can combine with mineral soil constituents to form unique mixtures (Kreider et al. 2010).

Flocculation is caused by collisions and subsequent adherence of primary and/or secondary particles to each other. The physico-chemical forces acting on the particles can be attractive or repulsive. If the resulting net force is attractive under appropriate conditions, the particles are bound together. Repulsive forces for example are caused by negative surface charge of particles. The Van der Waals forces represent an important attractive force which decreases rapidly with increasing distance from the particle surface. Parameters such as pH, solids concentration, organic content and temperature have influences on the particle behavior. High pH values tend to contribute to particle dispersion whereas low pH values increase flocculation. Since pH values in urban surface runoff are usually in a range not far from neutral, the influence of pH fluctuations cannot be considered significant in the field. A higher particle concentration increases the frequency of inter-particle collisions and thus tends to increase the formation of flocs. Increased temperature increases Brownian motion, which theoretically also leads to more frequent particle collisions, yet investigations of van Leussen (1994) suggest that Brownian molecular motion is usually negligible as a cause of particle collision. As also shown by studies on particles from stormwater infiltration basins, OM plays a major role in the formation of particle agglomerates (Badin et al. 2009; El-Mufleh et al. 2013). Organic polymers that can be formed by decomposition of plant residues, for example, easily adhere to clay particles, since they do not carry a surface charge and thus no repulsive forces occur. Thus, long polymer chains can adhere to several particles at the same time and form flocs with a high binding strength (Hillebrand 2008).

In addition to effects on the settling behavior of particles - the settling velocity of a particle aggregate, for instance, can differ significantly from the settling velocity of the primary particle - flocculation also influences the laboratory analysis of the particulate fine fraction, for example (Baum et al. 2018; Welker et al. 2019).

Summary: Particulate matter in urban stormwater runoff is composed of a variety of materials and elements. It can be considered as a heterogeneous mixture originating from different sources. The particle structure is influenced by various physical, chemical and biological factors. Electric charges on the outer particle surface are mainly responsible for the cohesion of particles. Flocculation is caused by collisions and subsequent adhesion of primary and/or secondary particles to each other and influences the settling properties of particles as well as the laboratory analysis of the particulate fine fraction (cf. 4.3.1). Organic matter has a very strong influence on flocculation.

2.2.1.3 Particle Size Distribution

In sedimentology and soil science, particle size distributions (PSD) are used for classification and nomenclature of soils, sediments and sedimentary rocks and allow conclusions on the formation and on certain properties of these natural materials. Tab. 2.1 shows such a classification according to ISO 14688-1:2017 (2017). Since particles in the real environment are usually not perfect spheres, geometric dimensions and equivalent diameters of measurable characteristics are used in relation to the sphere.

Tab. 2.1:   Particle size scale according to ISO 14688-1:2017 (2017)

Descriptive terminology		Particle size (mm)
boulder	large boulder	> 630
	boulder	> 200 and ≤ 630
	cobble	> 63 and ≤ 200
gravel	coarse gravel	> 20 and ≤ 63
	medium gravel	> 6.3 and ≤ 20
	fine gravel	> 2.0 and ≤ 6.3
sand	coarse sand	> 0.63 and ≤ 2.0
	medium sand	> 0.2 and ≤ 0.63
	fine sand	> 0.063 and ≤ 0.20
silt	coarse silt	> 0.02 and ≤ 0.063
	medium silt	> 0.0063 and ≤ 0.02
	fine silt	> 0.002 and ≤ 0.0063
clay		≤ 0.002

The particle size is closely related to the cohesion and thus to the flocculation tendency. While particles >63 µm can be considered non-cohesive, particles <63 µm are cohesive above a certain clay content because the concentration of clay minerals is responsible for cohesion (Raudkivi 1982). For example, coarse silt exhibits little to no cohesive behaviour (Wu et al. 2018), and although the finest rock flour particles can

have the size of clay, they are not clay minerals and therefore show no cohesive behaviour (Craig 2004).

Due to the above mentioned issue, as well as the fact that the particle size has a significant influence on the adsorption of pollutants (Bian und Zhu 2009; Li et al. 2015), it must be considered as a crucial parameter. The role of particle size in the adsorption process will be further highlighted in Chapter 2.3.1. Furthermore, in addition to the density, the size of the particles also has an influence on the settling velocity and is thus also significant for the treatment of urban stormwater runoff (cf. 2.2.1.6, formula 2.1)

Typical measurement methods used to determine particle size distribution in urban stormwater runoff are: Sieving, laser diffraction, digital image analysis, and counting methods such as the Coulter Counter. The classical sieving method has a measurement range between 20 μm and several centimeters. Sieves with different mesh sizes are stacked from fine to coarse and the sample is passed through the individual sieves from above by means of vibration. With a high fine particulate content (< 63 μm), wet sieving should be used (Gelhardt et al. 2017). The representation of the PSD in sieve analysis is limited by the number of sieves used, since each sieve corresponds to one data point. Information on the distribution within the sieve fractions is missing. Laser diffraction has a measurement range between 10 nm and 1 to 2 mm and shows a very high resolution, especially in the nanometer range. Laser diffraction measures particle size distributions by measuring the angular variation in intensity of light scattered as a laser beam passes through a dispersed particulate sample. Large particles scatter light at small angles relative to the laser beam and small particles scatter light at large angles. The angular scattering intensity data is then analyzed to calculate the size of the particles responsible for creating the scattering pattern. The particle size is reported as a volume equivalent sphere diameter. In digital image analysis, which has become more important in recent years, the particles are recorded two-dimensionally by cameras, pixelated and finally the area pixels and the circumference are analyzed and counted by the use of software. With this method, particle size distributions as well as shape distributions can be measured. The typical measurement range is between 1 μm and 3 mm. Counting methods such as the Coulter Counter are rarely used. It is based on the electric field interference method. Particles are passed through two electrodes and their volume is determined by the change in mean electrical conductivity.

When comparing PSDs from different measurement methods and programs, it is important to ensure that the sample population has not been reduced in size. Whereas the sample can still be classified in the centimeter range in sieve analysis, particle analyses with laser diffraction or digital image analysis are usually limited to just a few millimeters at the top. Therefore, for these measurements, the total sample may have to be reduced to the measuring range of the instruments by pre-sieving. The separated coarse fraction should be taken into account for the determination of the PSD, otherwise the grading curve will shift and suggest a finer composition. Furthermore, when

using an automatic sieve shaker with a 63 µm sieve, for example, particles with a length of up to 89 µm can pass through the mesh of the sieve on the diagonal. This means that the PSD tends to be finer than, for instance, when using laser diffraction methods, which determine the particle size on the basis of the scattered light equivalent diameter.

Urban stormwater runoff transports a wide range of particles of different sizes. It ranges from colloids with sizes < 1 µm (Kalmykova et al. 2013) to gravel with sizes above 10,000 µm (Sansalone et al. 1998). PSD from urban runoff needs to be distinguished from road deposited solids (RDS) as they differ considerably. Fig. 2.1 compares the PSD of urban stormwater runoff from international studies found in literature. Whereas Fig. 2.2 shows the PSD found in RDS. In comparison, it can be seen that urban runoff shows a finer PSD than RDS. RDS are mostly collected as dry samples by street sweeping or vacuuming whereas runoff samples are obviously collected wet. Besides different rain characteristics and surface properties (e.g. roughness or slope) the wash-off effect results in a finer PSD (Vaze und Chiew 2002; Zhao und Li 2013; Hong et al. 2016; Gelhardt et al. 2017).

Summary: Particle size plays a significant role in the context of stormwater management due to its influence on the settling velocity, flocculation, and adsorption of pollutants. Urban stormwater runoff contains a wide range of particles with different sizes. When comparing the PSD of different measurement programs, attention must be paid to the selected measurement method and to the fact that the entire population of particles is included in the evaluation even if sample pre-treatment was required. PSD from stormwater runoff samples tends to have a finer composition than PSD from RDS due to wash-off effects.
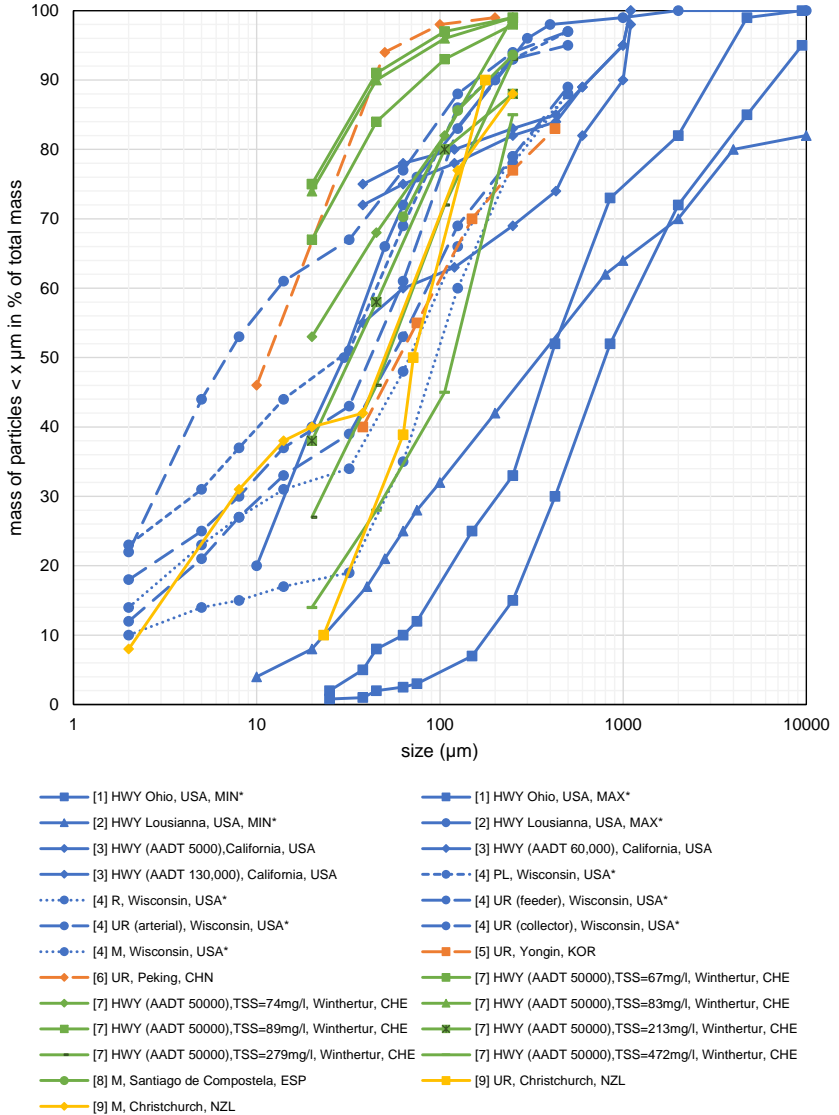
Fig. 2.1:   Comparison of particle size distribution in urban stormwater runoff (HWY = high-way, solid line, UR = urban road, long dashed line, PL = parking lot, angular dashed line, R = residential, dotted line, M = mixed catchment, dotted line, *mean values/composite sample, details Tab. A.1)
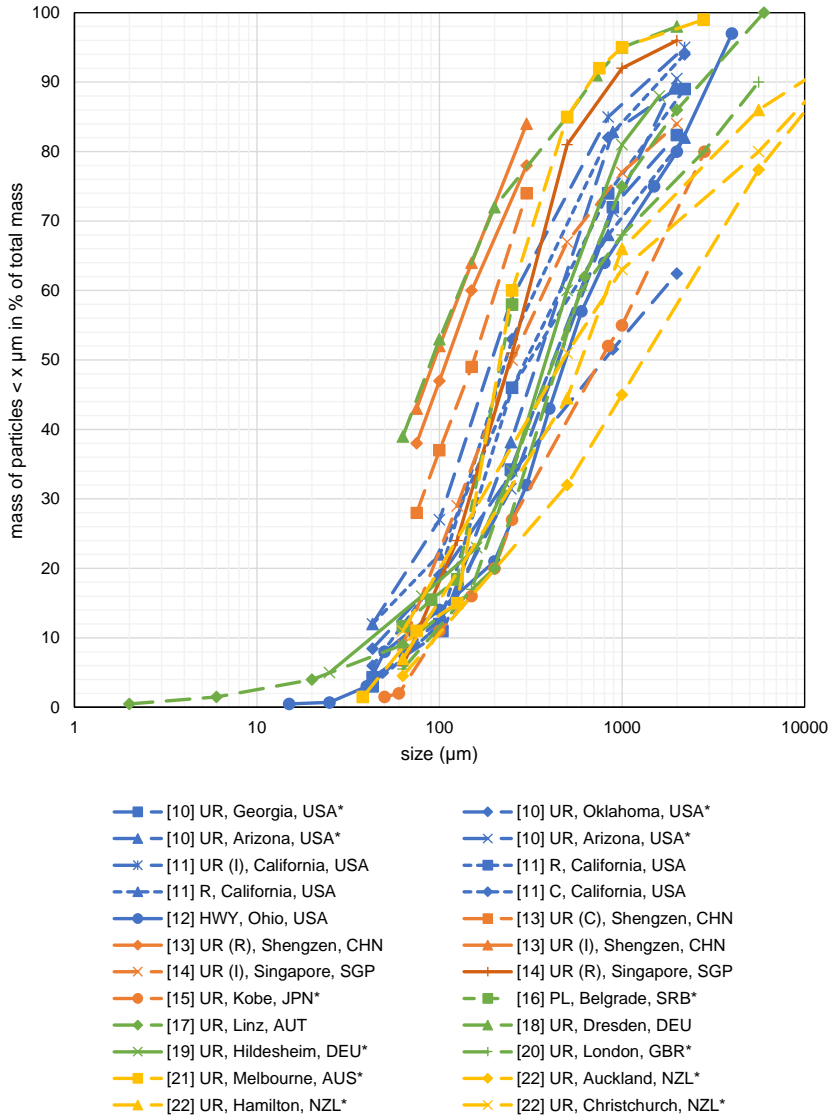
Fig. 2.2: Comparison of particle size distribution in road deposited solids (HWY = highway, solid line, UR = urban road, long dashed line, PL = parking lot, angular dashed line, R = residential area, dotted line, C = commercial area, dashed line, M = mixed catchment, dotted line, *mean values/composite sample, details Tab. A.1)

2.2.1.4   Particle Density

The density ρ of a body is defined as its mass per volume. It is often expressed in grams per cubic centimeter or in kilograms per cubic meter. The density is an important parameter with regard to the settling behavior, since it directly influences the weigth of the particles as well as their settling velocity. Frequently, the density of particles is considered to be equivalent to the density of sand (quartz), which is 2.65 g cm^{-3}, and the actual particle density is seldom determined (Cristina et al. 2002). The determination of density, essentially is a volume determination of a sample with known mass and it is based on volume displacement. Common measurement methods for particles and soil samples use different kind of pycnometers (Sartorius AG 1999).

There only have been a few studies that investigated the density of stormwater particles so far. An overview about the studies and their results is given Tab. 2.2. Cristina et al. (2002) and Sansalone und Tribouillard (1999) investigated particles from highways in Cincinnati, Ohio. However, Cristina et al. (2002) focused on PSD and density of PM that was carried by snow and snowmelt runoff, whereas Sansalone und Tribouillard (1999) focused on RDS collected by wet and dry vacuuming. Butler et al. (1992) also investigated RDS collected by manual brushing and vacuuming in London, U.K. Bäckström M. (2002) studied the density of sediments that where collected by a sweeping machine at a road area in the central part of Luleå, Sweden. Jacopin et al. (1999) investigated stormwater solids that were manually collected from traps installed on the bottom of a detention basin in Bordeaux, France. Andral et al. (1999) studied particles from stormwater runoff of a highway located in the Hérault department in France. The samples were collected manually from the influent of a collection channel. Lin (2003) carried out research on samples of stormwater runoff from an elevated section of an interstate highway in Baton Rouge, Louisiana. Zanders (2005) examined RDS gathered by vacuuming a 30 cm wide road-side gutter in Hamilton, New Zealand

For the interpretation of the results, it is important to note that particles in urban areas, especially those generated by traffic activity, such as tire and road wear, are mixtures of materials of different densities. They consist of metallic, mineral and organic components, including vegetation or abrasion. In general, OM has a density well below 2 g cm^{-3}. For instance, tire wear has a density of about 1.15 g cm^{-3} in its raw form (Banerjee et al. 2016) and due to frictional processes is usually found as a joint product with mineral and bituminous road wear. Metallic abrasion or constituents are assumed to be present only in the case of iron with a significant share in the composition. Iron is predominantly present in its oxidized form, so the approximate density of the constituent is assumed to be 5.25 g cm^{-3} (Čabanová et al. 2019). Minerals have a density between 2.5 g cm^{-3} (chlorite) and 2.82 g cm^{-3} (muscovite) (Gunawardana et al. 2012). Thus, it can be assumed that measured values above this range contain metallic components and values below this range contain more organic matter.

Summary: There are only few monitoring programs in the context of stormwater runoff which also measure the density of solids. The particles often consist of a mixture of

materials with different densities. The density is an important parameter with regard to the settling behavior because it directly influences the settling velocity.

Tab. 2.2:   Summary of reported density values

Size range (µm)	Density (g cm^{-3})	Matrix	Location	References
< 63 63 – 150 150 – 300 300 – 600 600 – 1000 > 1000	2.19 – 2.56 2.13 – 2.51 2.26 – 2.83 2.02 – 2.41 1.99 – 2,59 1.89 – 2.53	RDS	London, U.K.	Butler et al. 1992
< 50 50 – 100 100 – 500 500 – 1000	2.38 – 2.65 2.53 – 2.86 2.50 – 2.82 2.20 – 2.27	Road Runoff	Hérault depart-ment, France	Andral et al. 1999
< 32 32 – 63 63 – 125 125 – 250 250 – 500 500 – 1000 1000 – 2000	2.14 2.15 2.19 2.33 2.53 2.54 2.39	RDS	Hamilton, New Zealand	Zanders 2005
15 – 75 75 – 4750	2.75 2.86	RDS (snowmelt)	Cincinnati, Ohio	Cristina et al. 2002
< 75 75 – 152	2.61 2.58	RDS	Luleå, Sweden	Bäckström M. 2002
All sizes	2.70 – 3.011	RDS	Cincinnati, Ohio	Sansalone und Tribouillard 1999
All sizes	2.20 – 2.27	Stormwater de-tention basin	Bordeaux, France	Jacopin et al. 1999
All sizes	2.24	Combined sewer detention basin	Bordeaux, France	Jacopin et al. 1999

2.2.1.5   Organic Content

Organic material, or organic matter (OM) refers to carbon-based compounds found in the natural, terrestrial and aquatic environment. In the aquatic environment OM can be further distinguished into particulate organic matter (POM) or dissolved organic matter (DOM). For the description of OM, mostly only the carbon-containing compounds are considered and these are indicated as sum parameter total or dissolved

organic carbon (TOC or DOC). There are two main methods for determining the organic content: firstly, the determination of TOC or DOC and secondly, loss on ignition (LOI). TOC or DOC are determined by oxidizing the sample and measuring the CO_2 released in the process. LOI also represents the amount of carbon-containing compounds. The measurement is based on a thermogravimetric principle whereby a sample of known dry mass is incinerated at a defined temperature (often 550 °C) under the influence of oxygen. By subtracting the mineral residue from the dry mass, the LOI is determined as the organic content in percentage of the total sample.

OM in urban stormwater runoff is mainly vegetation-related (plant debris, pollen, etc.) and traffic-related (abrasion from tires and bituminous roadways). In addition, there are other possible natural (e.g. animal excrements, soil particles) and anthropogenic (e.g. waste) sources (Rogge et al. 1993; Xie et al. 1999; Goonetilleke et al. 2005). In the investigations of Rogge et al. (1993), organic particles from anthropogenic sources were found increasingly in the fine particle fraction and organics from natural sources were dominant in the coarse particle fraction.

Badin et al. (2009) studied the aggregation of stormwater sediments from a detention basin. Their results indicate that OM strongly affects the aggregation of particles (cf. 2.2.1.2). El-Mufleh et al. (2014b) report similar findings. Furthermore the binding of organic pollutants is, among other physico-chemical properties, strongly controlled by the content of organic carbon (Shea 1988; Kalmykova et al. 2013). The overall results of El-Mufleh et al. (2014a) confirms that PAHs are bound to OM, as described in other literature (Karickhoff et al. 1979; Chiou et al. 1998; Weber 2001). Bedsides organic pollutants, different studies show that metals also associated to organic carbon fractions (Lair et al. 2007; El-Mufleh et al. 2014b). The investigations of Charlesworth und Lees (1999), Hamilton et al. (1984) and Robertson et al. (2003) indicate that copper displays a higher affinity to OM. Saulais et al. (2011) carried out research on stormwater sediments of an infiltration basin and their results show that zinc, cadmium and cupper are mainly associated with carbonate and organic matter fractions. The role of organic content in the adsorption process will further be addressed in 2.3.2.

Summary: OM in urban stormwater runoff comes primarily from vegetation and traffic-related sources. For laboratory determination the sum parameters TOC and DOC as well as LOI are used, which cover the carbon containing compounds of the samples. OM plays a very important role in the flocculation of particles as well as in the adsorption of pollutants to particles.

2.2.1.6 Particle Settling Velocities

The settling behavior of particles is of great importance for urban stormwater treatment (Sample et al. 2012; Dierkes et al. 2015). The settling velocity of a particle in a viscous fluid depends on several factors: size, density and shape of the particle, the flow regime, the particle concentration and of course the fluid viscosity (Burton und Pitt 2001).

According to Stokes' formula, the settling velocity v_s (m s^{-1}) of a sphere of known density moving in a fluid is calculated as follows:

$$v_s = \frac{g\, d_s^2}{18\, \eta}\, (\rho_s - \rho_f) \qquad\qquad (2.1)$$

Where g is the gravitational acceleration (m s^{-1}), d_s the diameter of the sphere, ρ_s the density of the sphere (kg m^{-3}), ρ_f the density of the fluid (kg m^{-3}) and η the dynamic viscosity (kg (m s)$^{-1}$). It must be noted, however, that this formula is only valid for low Reynolds numbers (approx. < 0.25). The Reynolds number is a dimensionless parameter used in fluid mechanics and can be understood as the ratio of inertial to viscous forces. The Reynolds number (Re) is calculated as follows

$$Re = \frac{v_s\, d_s}{\nu} \qquad\qquad (2.2)$$

Where ν is the kinematic viscosity (m² s^{-1}).

In the real environment, however, the particles found in urban stormwater runoff do not have a spherical shape as assumed in Stokes' formula. For these amorphous structures with the same density and volume, the sinking behavior changes in comparison to a sphere. These "real" particles settle comparatively slower. For natural particles such as sand, which deviate from the spherical shape, the settling velocity of particles with a diameter d_n can be approximated by semiempirical formulas (Hallermeier 1981; Dietrich 1982). But this will not be discussed in further detail here.

However, for a general understanding of the subject matter discussed in this work, it should be mentioned that the settling behavior of solids as they are present in ubran stormwater runoff is more complex and subject to certain interactions. Because the solids in ubran stormwater runoff are mixtures of many different materials, shapes, densities, particle sizes, and particle concentrations. For example, the presence of many particles will alter the velocity field (Kaskas 1970). High concentrations of solids can have both accelerating and decelerating effects on the settling velocity. As the particle sizes in the solids mixture vary, they settle differently with increasing deviation between the smallest and largest fractions. Fine fractions, for example, can be slowed down by the counterflow generated by the large particles (Koglin 1971; Brauer und Thiele 1973). For increasing concentrations of solids, increasing settling velocities can be expected. An increase in the settling velocity of real effluents of higher concentration was also observed by Aiguier et al. (1996).

Several researchers have developed experimental methods for measuring the particle settling velocities of stormwater samples (Aiguier et al. 1996; Lucas-Aiguier et al. 1998). Those methods were developed in the United States (Pisano 1996), in Germany (Michelbach und Wöhrle 1993; Pisano und Brombach 1996), in the U.K. (Walling und Woodward 1993; Tyack et al. 1996) and in France (Chebbo 1992). However the devices, the required sample pretreatment and the operating procedures vary quite substantially, as do the published results (Aiguier et al. 1996; Gelhardt 2020). Recently, Chebbo und Gromaire (2009) developed a new method, called VICAS (a French acronym for

"effluent settling velocity" – "Vitesse de chute en assainissement"). This method is based on the homogeneous suspension principle. Gelhardt et al. (2017) present a novel approach based on the device from Michelbach und Wöhrle (1993) with some adjustments.

Tab. 2.3 gives an overview about the mentioned methods and their specifications. In her work, Gelhardt (2020) compares the most commonly used measurement methods for determining settling velocities based on a literature review of a total of 26 studies. The evaluation of the measurement methods and their frequencies of use shows that although there is a solid basis of studies in which settling velocities have been measured, the use of different, specially developed devices, makes it difficult to compare the results. Furthermore, she points out uncertainties in the reproduction of measurement results in the investigation of runoff samples. These are uncertainties in sampling and sample splitting as well as changes in particle characteristics due to "uncontrolled" sample aging. All these issues are closely related to the tendency of the samples to flocculate and are among the same issues that affect the determination of TSS < 63 μm.

Summary: Knowledge of particle settling velocities in urban stormwater runoff is important to evaluate the retention of solids and associated pollutants by treatment systems using the principle of sedimentation. Particle size and shape as well as particle composition (density and organic content) and particle concentration have a significant influence on the settling velocity of the particles. For the empirical determination of the settling velocities of particles from urban runoff samples, research groups have used specially developed devices. However, the lack of comparability of the results from different methods is a major limitation.

Tab. 2.3: Overview about methods for the determination of settling velocities in stormwater runoff

References	Principle	Sedimentation height [mm]	Sample preparation	Sample volume [L]	Liquid in device	Range of settling velocities
Walling und Woodward 1993	Elutriation	N/D	None required	10 – 50	Stormwater	According to flow and diameter of columns
Tyack et al. 1996	Floating layer	1750	3 hrs. of settlement in the column	5	Stormwater	0.018 – 2.7
Michelbach und Wöhrle 1993	Floating layer	700	2 hrs. of settlement in an Imhoff cone	1	Water	0.01 – 17.5
Chebbo 1992	Floating layer	1815	Wet sieving of particles < & > 50 µm	20	Water	0.0197 – 8
Chebbo 1992	Homogeneous suspension	200		20	Water	0.0014 – 0.41
Pisano 1996	Homogeneous suspension	2250	Sieving over 2 mm	40 – 50	Stormwater	N/D
Chebbo und Gromaire 2009	Homogeneous suspension	600	Sieving over 2 mm	4.5	Stormwater	N/D

2.2.2 Organic Micropollutants in Urban Stormwater

2.2.2.1 Sources and Occurrence

Among the first organic micropollutants to be investigated in stormwater runoff were PAHs. In the 1970s, urban stormwater runoff was already recognized as a source of anthropogenic PAHs (Wakeham 1977; MacKenzie und Hunter 1979). With the introduction of the Water Framework Directive (Directive 2000/60/EC) and the priority pollutants listed in the amending directive (Directive 2013/39/EU), the investigations were expanded to include further substances. Müller et al. (2020) show the most important sources identified for these substances in their literature review. Besides wet and dry atmospheric deposition (Petrucci et al. 2014; Gromaire et al. 2015), mainly serving as a transportation vector (Marsalek et al. 2008), the identified sources are drainage surfaces including building surface materials like facades (Burkhardt et al. 2011) and roofs (Gromaire et al. 2015) or paved surfaces and roads. These drainage surfaces are directly affected by the source of anthropogenic activities. In which vehicular transportation contributes to the emission of organic micropollutants through exhaust emission (Markiewicz et al. 2017), road abrasion (Hvitved-Jacobsen et al. 2010) and car washing (Björklund 2010) for example. Road maintenance (Meland et al. 2010), industrial activities (Becouze-Lareure et al. 2019), construction activities and littering were also identified as possible pollutant sources.

There have been numerous investigations concerning micropollutants in urban runoff with different objectives and especially different substances. Some of the research teams focus on specific groups of chemicals. Björklund (2011) for example focused on plasticisers (phthalates), Regnery und Püttmann (2009) investigated Organophosphates (OPs) which can be used as flame retardants or plasticisers. Less frequently, the investigations cover a broader spectrum of different substances. Wicke et al. (2015) sampled about 90 storm events and analysed them for more than 100 substances. Launay (2017) gives a partial overview about studies conducted in urban runoff. The highlighted investigations cover substances of the following groups: Biocides, industrial chemicals, flame retardants, plasticiser and PAHs. The amended overview can be seen in Tab. 2.5. Additional information about the analysed fractions of the studies can be found in Tab. 2.4.

Summary: A wide substance spectrum of various organic micropollutants is found in urban stormwater runoff (e.g., biocides, household and industrial chemicals, flame retardants, plasticizers, PAHs). The substances either reach the surfaces directly, or are transported there, e.g. by dry and wet deposition (or are a direct component of surfaces/materials). Subsequently, they are washed off by stormwater runoff.

Tab. 2.4: Analysed fraction of studies shown in Tab. 2.5

study	homogenised	dissolved	particulate
Wicke et al. (2015)	x		
Gasperi et al. (2014)		x	x
Birch et al. (2011)	x		
Bollmann et al. (2014)	x		
Kalmykova et al. (2013)	x	x	
Björklund et al. (2009)	x		
Reddy und Quinn (1997)	x	x	
Zeng et al. (2004; Kloepfer et al.)	x	x	
Regnery und Püttmann (2009)	x		

Tab. 2.5: Range of concentrations of organic micropollutants found in stormwater runoff in urban catchments in ng L^{-1} (Launay 2017)

	Reference	Wicke et al., 2015	Gasperi et al., 2014	Birch et al., 2011	Bollmann et al., 2014	Kalmykova et al., 2013	Björklund et al., 2009	Reddy and Quinn, 1997	Zeng et al., 2004	Kloepfer et al., 2005	Regnery and Püttmann, 2010
	Country	Germany	France	Denmark	Denmark	Sweden	Sweden	USA	USA	Germany	Germany
Biocides	MCPA			<10-18							
	Mecoprop	<LOD-6,900	1-2								
	Carbendazim	<LOD-1,500	7-195		10-306						
	Isoproturon	<LOD-120	16-469	<10-44	<LOD-150						
	Diuron	<LOD-600	25-795	<10-55	1-100						
	Terbutryn	<LOD-360			10-1,840						
Household/ industrial chemicals	4-tert-octylphenol	<LOD-1,000	35-72			110-820					
	4-nonylphenol	<LOD-5,800	187-509	<100-430		270-1,100	100-1,200				
	Bisphenol A	<LOD-500	207-817			484-827					
	DEHP	<LOD-14,000		<500-8,500		2,300-3,000	<1,000-5,000				
	1H-benzotriazole	10-3,600									
	Benzothiazole	160-3,200						100-500	230-555	1,000-4,000	
	MTBT	50-540						40-200	36-160		
Flame retar- dants/ plasti- cisers	TIBP	<LOD-660									2-1,478
	TBP	<LOD-340									4-417
	TCEP	<LOD-2,700									23-275
	TCPP	<LOD-260									16-5,791
	TDCPP	<LOD-5,600									<LOD-73
	TBEP										<LOD-1,616
PAHs	Fluoranthene	10-3,200	97-217*	<10-550		30-120					
	Pyrene	10-2,900	88-176*	<10-560		50-190					
	Σ16 EPA PAHs	30-11,000	892-1,362*	30-4,383		<300-550					

*: Range of average values

2.2.2.2 Association with Particulate Matter

As mentioned in chapter 2.2.1 among others PM is recognized as a significant pollutant due to the fact that it serves as carrier for other constituents.

In-depth knowledge about the association of micropollutants with different particle size fractions is of great importance as the majority of technical solutions for the treatment of urban stormwater runoff are based on the physical principles of sedimentation or filtration. The performance of these treatment systems however is very sensitive to the PSD.

Herngren et al. (2010) reviewed the results of various different studies for PAHs and concluded that the literature reports contradictory findings. For example, Choi und Chen (1976), Zuofeng (1987) and Evans et al. (1990) found out, that PAHs show a tendency to be associated with the silt and clay fraction (< 50 µm). However, the results of Readman et al. (1984) show a decrease in PAH with decreasing particle size from sand to clay (100 to 10 µm). Hoffman et al. (1984) noted that in stormwater PAHs show a maxima within the 125 – 150 µm range as well as below 45 µm. On the other hand, Simpson et al. (1998) found high PAH concentrations in the coarse particle fraction (300 – 1180 µm and > 1180 µm) that also contained a high content of organic carbon. The association with the fine particle fraction was attributed to its relatively large specific surface area as well as its electrostatic surface charge. Correlations with the organic content were also shown. These relationships are discussed in more detail in the chapter on the adsorption process (cf. 2.3)

Regarding other micropollutants only studies were found that investigated the partitioning between dissolved and particulate phase (Reddy und Quinn 1997; Zgheib et al. 2011; Kalmykova et al. 2013; Cladière et al. 2013; Gasperi et al. 2014) or studied the micropollutant load directly on sediments (Gasperi et al. 2009; Carpenter et al. 2016; Jiang et al. 2016). However without partitioning in different size fractions.

Summary: Depending on their physical chemical properties, many substances tend to adsorb to particles in urban surface runoff. Especially with regard to the treatment of stormwater, a profound knowledge of this issue is of major importance. Many studies indicate that particle size is a crucial criterion in this respect. Previous studies mainly focused on PAHs. With regard to other substances and their relationship to different particle size classes, only few studies have been conducted so far.

2.2.3 Metals in Urban Stormwater

2.2.3.1 Sources and Occurrence

The identification of metal sources can sometimes be complicated due their geogenic as well as anthropogenic origin (Loganathan et al. 2013). Furthermore the fact that most elements have more than one origin, makes it difficult to determine the dominant source. Moreover, there is a high degree of heterogeneity in the water quality data of

stormwater runoff from different sites. This can be attributed to differing background levels, types of uses and method-specific factors (Göbel et al. 2007; Huber et al. 2016).

However, metals were among the first pollutants to be analysed early on in studies of stormwater runoff (Bradford 1977). In the meantime, there have been many studies worldwide that have looked at metals in runoff and were able to identify their sources of origin. The sources listed in chapter 2.2.1.1 can mainly also be applied to metals. One of the major sources of metals identified is vehicular traffic. Tab. 2.6 shows some specific metal sources of vehicular traffic.

In road runoff, heavy metals can be present in both dissolved and particulate form (Huber et al. 2016; Gnecco et al. 2019). Especially for Pb and Cu, but also for Zn, the particulate fraction is often higher than the dissolved fraction (Huber et al. 2016). The distinction between dissolved and particulate fraction is important for the treatment of stormwater runoff, as dissolved and particulate pollutants need to be treated with different treatment principles.

Tab. 2.6: Specific sources of metals released by vehicular traffic in urban areas (adapted by Müller et al. (2020))

Specific source	metals	References
Exhaust	Mn, Ni	Preciado und Li (2006); Duong und Lee (2011)
Tire wear	Cd, Cu, Zn	Muschack (1990); Councell et al. (2004); Legret und Pagotto (1999); McKenzie et al. (2009)
Tire studs wear	W	Huber et al. (2016)
Engine and vehicle body wear	Cr, Ni	Gupta et al. (1981); Ward (1990)
Body paint wear	Pb	Kayhanian (2012)
Wheel balance weights wear	Pb, Fe, Zn	Root (2000); Donald I. Bleiwas (2006)
Commercial car washing facilities	Pb, Cd, Cr, Zn	Sörme et al. (2001)

Summary: Metals are found in both dissolved and particulate forms in urban stormwater runoff. Many studies have addressed their occurrence. Traffic-related activities have been found to be the most important anthropogenic source.

2.2.3.2   Association with Particulate Matter

In regards to the association of metals with different particle size, the results of the published research show a higher consistency as the research on organic micropollutants (see chapter 2.2.2.2.) Li et al. (2006) shows an overview about the findings of several monitoring campaigns (Sansalone und Buchberger 1997a; Roger et al. 1998; German und Svensson 2002; Morquecho und Pitt 2003; Lau und Stenstrom 2005).

Overall, the metal concentrations are increasing with decreasing particle size. Further research that has not been listed by Li et al. (2006) confirms that tendency (Biggins und Harrison 1980; Bryan Ellis und Revitt 1982; Stone und Marsalek 1996; Birch und Scollen 2003; Sutherland 2003; Herngren et al. 2006). For example, Herngren et al. (2006) studied concentrations of eight metals (Zn, Fe, Pb, Cd, Cu, Al, Mn) in five different particle size fractions in urban stormwater runoff and found that most of the metals were adsorbed to particles < 150 μm. For all elements the highest concentrations were consistently found in the fraction 0,45 – 75 μm. Similar behaviour was shown by Birch und Scollen (2003). They analysed road dust for Co, Cr, Cu, Fe, Mn, Ni, Pb, Zn and found the highest concentrations in the fraction < 62 μm.

Summary: Many studies have investigated the association of metals with different particle size fractions. There is a clear trend that the highest particulate metal concentrations are found in the fine particle size fractions.

2.3   Adsorption Process

Generally speaking, adsorption is the accumulation of a substance (sorptive/adsorptive) on the surface of a solid (sorbent/adsorbent), more precisely at the interface between the two phases (Sparks 2003). A distinction is made between two types of adsorption. Physical adsorption, also called physisorption, in which the adsorbed substance (sorbate/adsorbate) does not form any chemical bonds with the adsorbent. The adsorbate usually adheres through electrostatic interactions. The chemical bonds within adsorbed molecules remain intact, but might become polarised (aligned according to the electrical charges). The adsorption energy in physisorption is between 4 and 40 kJ mol^{-1}. The other type is chemisorption, in which chemical bonds are formed (hydrogen and covalent bonds) between the sorptive and the sorbent. Here, the adsorption energy is in the range of 40 – 420 kJ mol^{-1}. Chemisorption results from the interaction between functional groups on the surface of a solid and the ions in the surrounding solution (Bradl 2004).

The adsorption process of pollutants onto stormwater sediments is complex and influenced by the physico chemical properties of the substance, of the particulate matter as well as of the stormwater itself (Fig. 2.3). Usually adsorption is a reversible process of two simultaneous occurring reactions: adsorption and desorption. If both reactions have an equal rate, the adsorption equilibrium is reached (Margot 2015).
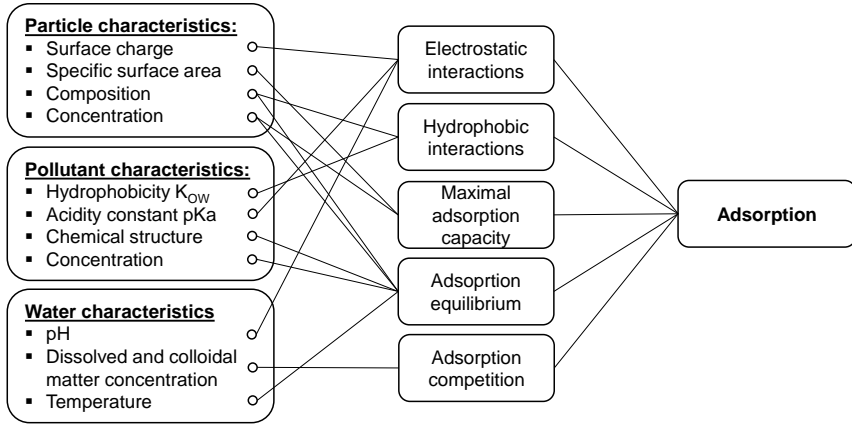
Fig. 2.3: Main factors influencing the adsorption of micropollutants onto particulate matter (adapted from Margot 2015).

The adsorption equilibrium on particulate matter can be described by empirical adsorption isotherms. These compare the concentration of the sorbate (C_s) with the concentration of the sorptive (C_{eq}) under equilibrium conditions at constant temperature. The simplest case describes a linear relationship between C_s and C_{eq}:

$$C_s = K_d\, C_{eq} \qquad\qquad (2.3)$$

K_d (L kg^{-1}), the adsorption coefficient (or solid-water partitioning coefficient), indicates the concentration ratio. For the linear adsorption isotherm, K_d corresponds to the slope of the adsorption isotherm. At low pollutant concentrations (e.g. < 1µg L^{-1}) and relatively high concentrations of particulate matter (> 100 mg L^{-1}), the linear model is often considered (saturation of the particulate matter neglected). In cases with higher pollutant concentrations, the Freundlich and the Langmuir model show a better accuracy due to the fact that it considers the saturation of adsorption sites (Wium-Andersen et al. 2012).

Summary: Adsorption refers to the accumulation process of a substance on the surface of a solid. The forces underlying this process can be physical (electrostatic interactions) or chemical (hydrogen bonds or covalent bonds). The adsorption process of pollutants on stormwater sediments is complex and is influenced by the physicochemical properties of the substance, the particles and the stormwater itself. Empirical adsorption isotherms relate the amount of sorbate bound to the surface at constant temperature to its concentration in solution. The simplified assumption of a linear relationship can be applied in this work, since there are relatively low pollutant concentrations and high solid concentrations.

2.3.1 Role of Particle Size

The studies in the previous Chapters 2.2.2 and 2.2.3 showed that different concentrations of pollutants are found on particles of different size fractions. In most cases, the highest pollutant concentrations could be attributed to the fine particles. This indicates that particle size, in addition to other properties (cf. Fig. 2.3), seems to have an influence on the adsorption of pollutants. This mainly can be attributed to the specific surface area (SSA) of the particles. In addition it also could be attributed to the surface charge of the particles, however the surface charge, besides of pH-value and ionic strength of the surrounding solution, is mainly determined by the chemical composition of the particles and not by their size (Hillebrand 2008). However, clay minerals as an example for charged particles naturally occur in sizes < 2 μm.

SSA is measured as the surface area per unit mass, assuming a constant particle density. The adsorption ability of particles increases with the increase of the specific surface area (SSA) due to the larger interface that is provided for sorptives to interact with the particle surface (White 2009). Tab. 2.7 lists the size range and the calculated SSA for three particle size classes (sand, silt and clay) under the assumption of spherical SiO_2 particles with a density of 2.65 mg m^{-3}. The highest SSA can be found for the smallest particle size class. Sansalone et al. (1997) studied rainfall and snowmelt solids from a heavily travelled urban roadway in Cincinnati and showed increasing SSA with decreasing particle size.

Tab. 2.7: Specific surface area of different sized spherical SiO_2 particles (particle-size classes: sand, silt and clay) with a density of 2.65 mg m^{-3} (Bleam 2017)

Particle Class	Diameter (mm)	Specific Surface Area (m² g^{-1})
Coarse sand	2.0000	1.13×10^{-3}
Medium sand	0.6300	3.50×10^{-3}
Fine sand	0.0200	1.13×10^{-2}
Coarse silt	0.0630	3.59×10^{-2}
Medium silt	0.0200	1.13×10^{-1}
Fine silt	0.0063	3.59×10^{-1}
Clay	0.0020	$1.13 \times 10^{+0}$

Summary: Particle size plays a significant role with respect to the adsorption of pollutants onto particles. With decreasing particle size, the specific surface area of the particles increases. Thus, a larger surface is generally available for the corresponding pollutants to interact with.

2.3.2 Role of Organic Content

Among the sorbents found in the environment, organic matter has a significant impact on the overall adsorption of pollutants (Schwarzenbach et al. 2002). Natural organic

matter in solids is mainly derived from plants and animals. It consists of a mixture of partially decomposed plants and animal remains that can be divided into a humic and a non humic fraction. The non humic fraction, also referred to as the humin fraction consists of compounds whose physico-chemical charachterisitcs are still recognisable. It includes fats, waxes, oils that are rapidly subject to microbial attack (Stevenson 1965). The humic compounds (humic acids and fluvic acids) are stable byproducts of microbial transformation containing numerous functional groups most commonly including carboxy-, phenoxy-, hydroxy-, amino- and carbonyl-substituents which are capable of binding cations (Hofstede 1994; Gunawardana et al. 2012).

Besides the natural organic matter present due to biogenesis and diagenesis, organic matter mostly of anthropogenic origin including combustion byproducts (soots and fly ash), plastics and rubbers, and nonaqueous-phase liquids are known to be potent sorbents as well (Kim et al. 1997; Severtson und Banerjee 1996; Schwarzenbach et al. 2002)

In addition to the high specific surface area, the high cation exchange capacity, attributed to the different functional groups of to the humic compounds, makes organic matter an important sorbent of plant macronutrients and micronutrients, metal cations, and organic micropollutants (Sparks 2003).

As organic matter can be present in a wide size range, also colloidal matter or dissolved organic carbon can have significant influence in the sorption process. The presence of DOC can affect the partitioning of pollutants between the dissolved and the particulate phase and may shift the ratio towards the dissolved phase (Katsoyiannis und Samara 2007; Barret et al. 2010).

In order to evaluate the ability of natural organic materials to adsorb pollutants, an organic carbon normalized sorption coefficient can be defined as:

$$K_{OC} = \frac{K_D}{f_{OC}} \qquad (2.4)$$

With f_{OC} being the mass fraction of organic carbon (see equation 2.5), knowing that actually the total organic mass (including carbon, hydrogen, oxygen etc.) acts as sorbent for the pollutants of interest. Due to the fact, that natural organic matter typically consists of 40 – 60 % carbon, f_{OM} equals approximately two times f_{OC} (Schwarzenbach et al. 2002).

$$f_{OC} = \frac{\text{mass of organic carbon}}{\text{total mass of sorbent}} \text{ (kg OC kg}^{-1} \text{ solids)} \qquad (2.5)$$

Generally each pollutant or chemical has its own organic carbon normalized solid-water partitioning coefficient, which is dependent on the physicochemical properties of the chemical. It can be calculated from the n-octanol/water partition coefficient (K_{OW}), which is known for many organic compounds, using empirical relationships (Förstner und Grathwohl 2007):

$$\log K_{OC} = 0.544 \log K_{OW} + 1.377 \qquad (2.6)$$

The n-octanol/water partition coefficient Kow is defined as the ratio of the concentration of a compound in n-octanol divided by its concentration in water at equilibrium at a specified temperature. This coefficient is an extremely important physical parameter to indicate the partitioning of a substance between water and lipophilic matter, e.g. lipids, sediments or soil organic matter (Staples et al. 1997). The higher K_{ow} the higher the concentration of a Substance in the organic phase and the higher the lipophilicity of this substance. In general, it can be stated that the lipophilicity correlates with the adsorption tendency of a substance, the higher the lipophilicity the higher the adsorption tendency (Chmiel et al. 2019).

Summary: Among the sorbents found in the environment, organic material has a significant impact on the overall adsorption of pollutants. This can be attributed to humic acids and fulvic acids that are formed by the decomposition of vegetation debris. These humic compounds contain numerous functional groups that are capable of binding cations. In addition, OM exhibits a large SSA, which, depending on the origin of the material, may be due to high porosity (e.g. OM from combustion processes). Furthermore dissolved organic matter, can also have a significant influence in the sorption process, as DOC can affect the partitioning of pollutants. To evaluate the ability of OM to adsorb pollutants, a sorption coefficient normalized to organic carbon can be used (K_{OC}). K_{OC} can be derived from empirical relationships with the n-octanol/water partition coefficient K_{OW}, which is known for a variety of organic compounds.

2.4 Research Gap

The quality of urban stormwater runoff has long been a subject of research. Contaminants present in urban stormwater were already investigated in the early 1970s and 1980s (Sartor und Boyd 1972; Nightingale 1975; Hoffman et al. 1984). However, those studies mainly focused on metals and PAHs. These early investigations were of utmost importance, as they formed the basis and showed the need for further investigations. As sampling techniques and laboratory analysis have become much more sophisticated and precise over the years, the issue of stormwater quality is still relevant today. Yet, the majority of studies in recent years still focused their investigation mainly on metals and PAHs and very often the pollutants were only analysed in one fraction (Lepom et al. 2009; Kayhanian et al. 2012; Petrie et al. 2015).

However, the distribution between the dissolved and the particulate fraction is particularly important for understanding the transport of pollutants, their removal ability and thus also understanding their bioavailability (Paulson und Amy 1993; Crabtree et al. 2008).

Compared to PAHs and metals, only few studies focused on the behaviour of other pollutants present in stormwater runoff (Eriksson et al. 2007). Investigating other contaminants (e.g. industrial chemicals like flame retardants or herbicides) provides a

comprehensive knowledge of stormwater pollutants and thereby contributes to improved stormwater management (Gunawardena et al. 2018).

Furthermore, the distribution of contaminants within the particulate fraction over different particle size fraction plays an important role as well. Especially with regards to the treatment of urban stormwater. In order to increase the efficiency of rainwater treatment, in-depth knowledge of these relationships is required (Hilliges et al. 2013; Maniquiz-Redillas und Kim 2014).

In general, consistently comprehensive measurement data is required to improve stormwater management. Stormwater quality models are frequently used but also show high uncertainties in their results (Dotto et al. 2010; Francey et al. 2010). In depth knowledge about relevant processes, gained through monitoring campaigns, represents an important element in strengthening these models (Leutnant 2018).

3 Objectives of the work

The starting point of this study was to further investigate the hypothesis that with the removal of total suspended solids a significant amount of particulate micropollutants can be removed as well. This hypothesis is strongly dependent on the characteristics of the particulate matter in urban stormwater runoff and their associated pollutants. If, as some literature suggests, the fine fraction of particulate matter is contaminated the most (Xanthopoulos und Hahn 1990; Evans et al. 1990; Sansalone und Buchberger 1997a), as well as the amount of fine particles in urban runoff is about 70 – 80 % of the total suspended solids (Fuchs et al. 2014; Kayhanian et al. 2012; Wu et al. 2015), the hypothesis is doubtful. Due to the overall better removal efficiency of coarse particles, the less polluted fraction would be removed and the major part of pollutants would reach the environment with the fine fraction.

Therefore, the objectives of this study were to:

- characterise the particle size distribution of particulate matter in urban storm-water, and quantify the content of organic micropollutants as well as metals in the total, the particulate and the dissolved fractions of urban stormwater

- investigate the composition of particulate matter in stormwater runoff in terms of physico-chemical parameters and to evaluate the association of particulate matter and pollutants with regard to these parameters

- elaborate the suitability of TSS or specific particle size fractions of TSS as a proxy for urban stormwater contamination with organic micropollutants and metals. In addition to the question whether the pollution load is sufficiently repre-sented, it is to be investigated if this also applies to the efficiency of treatment facilities in relation to organic micropollutants and metals

To achieve these objectives, an intensive long term monitoring campaign at a storm-water treatment facility in an industrial area was conducted. The stormwater samples were taken volume-proportional at the two outlets of the facility in order to be able to evaluate the event mean concentrations (EMC) of different parameters as well as the treatment efficiency for different substances. Physico-chemical characteristics as well as a total of 29 substances including industrial chemicals, PAHs, metals, and pesticides were analysed within different particle size fractions.

This study can contribute to a better understanding of pollutant transport in storm-water runoff in the future. Likewise, a better understanding of the composition of stormwater runoff can optimise treatment measures.

4 Materials and Methods

4.1 Monitoring Campaign

In order to answer the main research question outlined in the previous chapter, an intensive monitoring campaign was carried out at a central stormwater treatment facility in an industrial area in southern Germany. Samples were taken at the treatment facility from November 2015 to January 2019 as part of two research projects. In the first project (2015 – 2016), the occurrence of particulate matter in two size classes and the treatment efficiency of the plant in relation to the retention of particulate matter were investigated in particular. In the follow-up project (2017 – 2019), the measurement programme was expanded to four particle size classes and the analysis of organic micropollutants and metals.

4.1.1 Study Area

The monitored catchment area consists of the "Freiburg Haid" industrial park with an area of 110.3 ha. It is located in the city of "Freiburg im Breisgau" in the southwest of Germany. The area is enclosed by major roads in the north, east, and south. To the west, the area is bordered by forest and agricultural land. About 400 companies from various sectors are located in the industrial park. Worth mentioning is the presence of a gas station with an attached car wash. The main business areas are the automobile, health, and solar industries. The urban development is characterized by industrial and small commercial buildings, most of which are equipped with flat roofs. There are green surfaces between paved roads and built-up areas. The catchment area shows a low slope (<1%) and has a paved area of about 70.6 ha which corresponds to a degree of pavement of 0.7. The annual average daily traffic volume (AADT) is estimated to 9000–17,000 vehicles per day (Stadt Freiburg 2012). The entire catchment area is served by a separate drainage system. At the end of the stormwater sewer network (location of the treatment plant, also see Fig. 4.1) the sewer has a diameter of DN 2000 with a slope of 5‰ over a length of 1000 m and is part of the stormwater treatment facility. The treated stormwater runoff is drained into a stormwater retention basin before being discharged into the small surface water body "Schelmengraben".

The wastewater from the catchment area is discharged to the sewage treatment plant via a wastewater sewer system designed according to the generally recognised codes of practice. The volume retained by the stormwater treatment facility is discharged into the wastewater sewer.
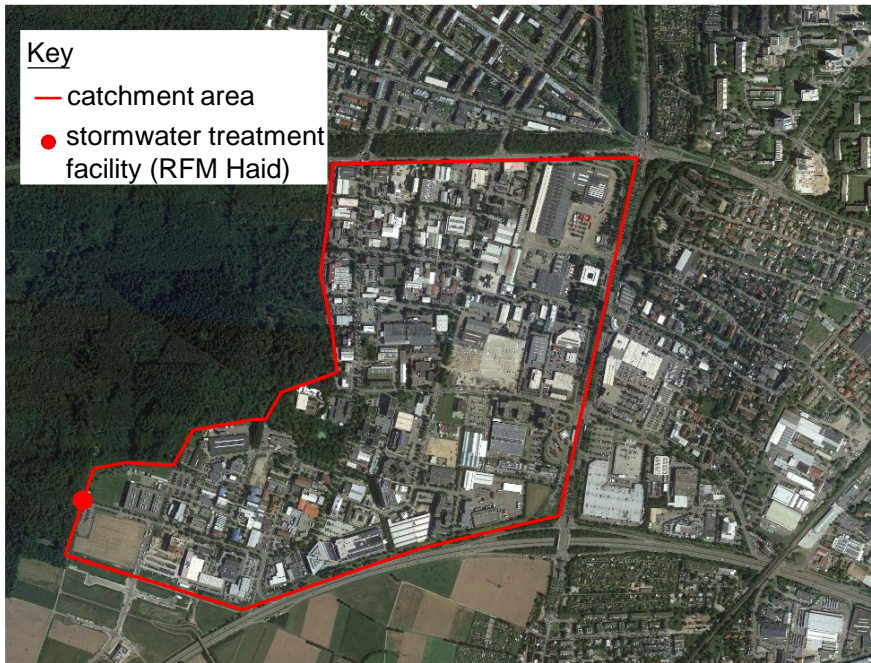
Fig. 4.1:   Catchment area of the monitored stormwater treatment facility. Industrial Park "Freiburg Haid".

4.1.2   Treatment Facility

The monitored stormwater treatment facility "RFM Haid" is a pilot plant of its type. It resembles a storage sewer with overflow. In contrast to a classic stormwater sedimentation tank, the RFM Haid uses the existing volume in the stormwater sewer. A weir (h = 2.2 m) is installed in the structure, which has a sluice gate (h = 1 m). This is the core element of the treatment facility and allows discharging treated stormwater into the receiving water body after the impoundment of the inflowing stormwater runoff and a certain sedimentation time (about six hours).

During dry weather conditions, the existing infiltration water is lead through a bypass with an integrated oil separator. At this location, the pH value is measured continuously and the water is checked for oil contamination with a special probe. The oil measurement was not functional during the investigation period.

About 400 m upstream of the treatment facility a manhole with an automated flushing device is located (see Fig. 4.2). At the beginning of a storm event the flushing device (h = 0.75 m) closes and a total volume of about 85 m³ of stormwater is impounded for flushing purposes. After a storm event and the complete discharge of the stormwater

sewer between both structures, the barrier is opened, and the retained water flushes the sewer as well as parts of the treatment facility. This water is also discharged into the foul sewer. There is another pH probe in front of the flushing device.

If the pH value at one of the two measuring points falls below 6.6 or rises above 8.6, an alarm is triggered. The same applies if oil contamination would be detected. In the event of an alert, the bypass to the receiving water body is closed immediately and the impounded volume is discharged into the wastewater sewer.

Fig. 4.2:   Aerial photograph showing the location of the treatment plant and the flushing device (aquadrat ingenieure 2014)

The following description of the functionality of the rainwater treatment facility as well as Fig. 4.3 to Fig. 4.8 are based on the operating instructions of the facility (aquadrat ingenieure 2014). In dry weather conditions all aggregates in the RFM-Haid are in the default position. The flushing device up-stream is open, in the treatment facility, the valves to the bypass are open and therefore the in-flowing infiltration water is led to the receiving water body (Fig. 4.3).
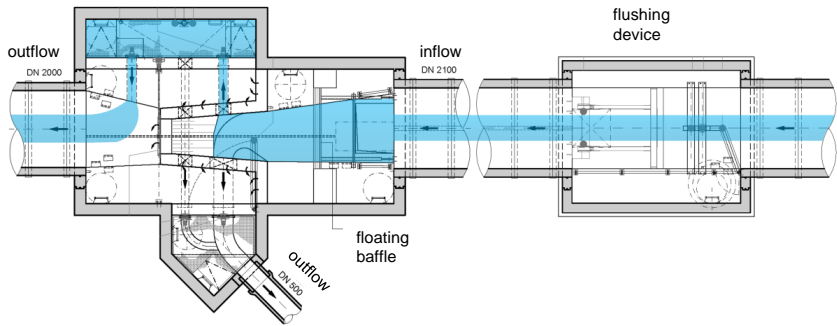
Fig. 4.3: Operating state of treatment facility: dry weather conditions (initial state). Adapted from aquadrat ingenieure (2014)

At the beginning of a storm event, the valves to the bypass in the stormwater treatment facility and the cut-off device upstream are closed. Storm events are detected by a rain sensor at the RFM Haid and additionally by a water level measurement in the inlet structure (water level >0.2 m for more than 30 s). At first the stormwater runoff is held back by the cut-off device (Fig. 4.4).
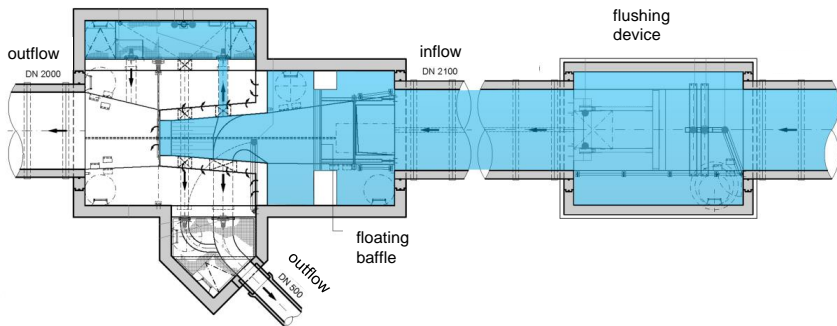
Fig. 4.4: Operating state of treatment facility: beginning of a rain event (impoundment). Adapted from aquadrat ingenieure (2014)

When it is overflowed (after approximately 85 m³), the stormwater is impounded in the treatment facility and in the stormwater sewer. If the stormwater runoff exceeds another approximately 1000 m³, the weir in the treatment facility is overflowed and the water is directly discharged to the receiving water body (overflow). Floating material is retained by a floating baffle.
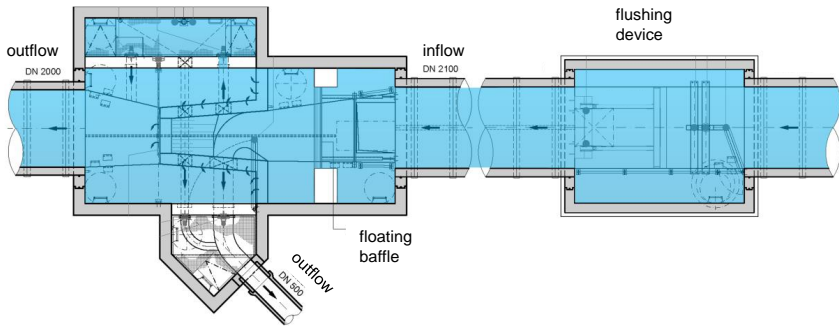
Fig. 4.5:   Operating state of treatment facility: overflow (exceeding max. impoundment volume). Adapted from aquadrat ingenieure (2014)

After the storm event, all aggregates remain in their position until the water level has lowered to the top level of the weir. After the sedimentation period of 6 h, the sluice gate is opened, and the treated stormwater is discharged towards the receiving water body (clear water discharge).
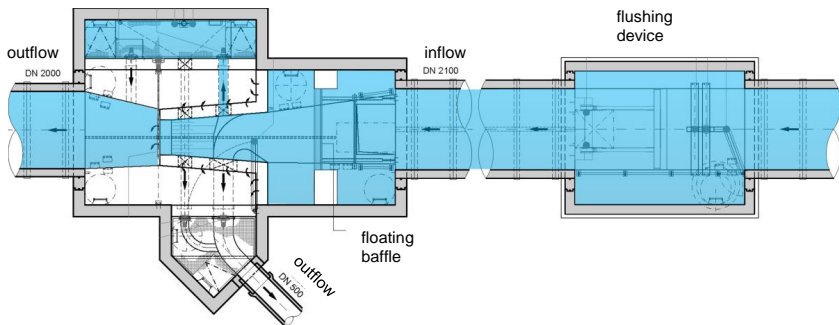
Fig. 4.6:   Operating state of treatment facility: clear water discharge (after sedimentation time). Adapted from aquadrat ingenieure (2014)

Subsequently, the valve to the foul sewer is opened to discharge the remaining water of approximately 245 m³ into the foul sewer (effluent)
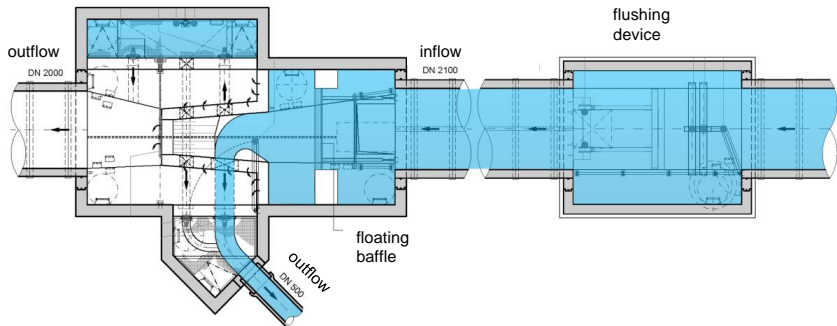
Fig. 4.7: Operating state of treatment facility: waste water discharge (effluent)

As soon as the water level falls below 0.3 m, the cut-off device upstream is opened and the storm sewer as well as parts of the treatment facility are flushed.
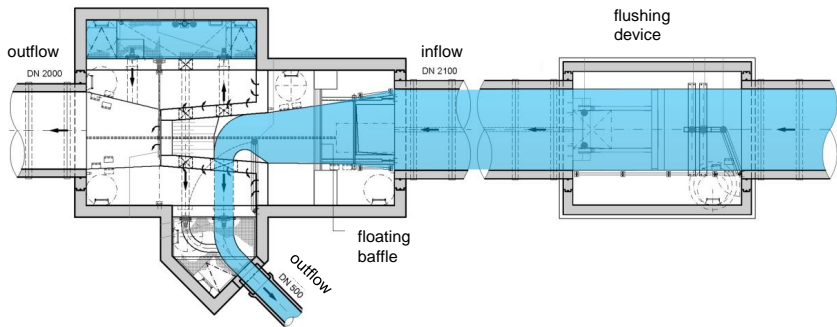
Fig. 4.8: Operating state of treatment facility: sewer flushing. Adapted from aquadrat ingenieure (2014)

After the completion of the treatment cycle described above, all aggregates are returned to their initial position (dry weather conditions).

4.1.3 Sampling Strategy

The objective was to sample individual rain events using large volume sampling tanks (LVST). Where possible separate and complete. Sampling was carried out throughout the year in order to take seasonal influences into account (Brezonik und Stadelmann 2002; Gustafsson et al. 2019). A continuous sampling of all rain events was not intended.

In this monitoring campaign the two, respectively three flows leaving the treatment facility were sampled using two submersible pumps. One pump was suspended in a floating position shortly before the weir crest in order to sample the overflow and the

clear water discharge as precisely as possible. The second pump was mounted on the bottom before the valve to the foul sewer to sample the effluent from the treatment facility (cf. Fig. 4.9).

Fig. 4.9:   Installed sampling pumps at the stormwater treatment facility RFM Haid, 1 over-flow, 2 effluent

In order to get samples representing the mean of the total rain event, sampling was performed volume proportional to the runoff and was realized by a pump controller, which integrates measured flows over time and activates the pumps when a certain volume has been discharged. A flow measurement system based on ultrasound cross correlation (OCM Pro by NIVUS GmbH with an air-ultrasonic sensor for water level measurement and a water-ultrasonic sensor including a pressure sensor for flow velocity and additional water level measurement) was installed behind the weir in the continuing stormwater sewer and its signal was transmitted to the pump controller. The sampling was performed in large-volume sampling tanks with a volume of 700–1000 litres. A total of four of these were used - two with a volume of approx. 1000 L for sampling the overflow and the clear water discharge and two with a volume of approx. 700 L for sampling the effluent. As higher concentrations of solids can be expected in the effluent, smaller sampling tanks are sufficient.

Fig. 4.10: Large volume sampling tanks used to sample the effluent (approx. 700 L)

4.1.4 Sampling Procedure

The initial setup of the sampling equipment required a manual change to empty sampling tanks in order to sample a following rain event separately after successfully sampling the precedent rain event. Due to the large distance between the institute and the rainwater treatment plant, this was not always possible. As a consequence, some rain events were sampled together in the same sampling tanks. Therefore, later on the term sampling event (SE) will also be used in the presentation of the results. The number of rain events within the respective SE will be indicated.

In mid-2017, the sampling was modified and further automated in order to sample both the overflow and the clear water discharge separately. For this purpose, a motor-controlled 3-way valve was installed, which diverts the inflow into a separate sampling tank at the beginning of the clear water discharge. Additionally, the controller was equipped with a GSM module in order to start or stop the sampling from a distance.

4.1.4.1 Sampling of Overflow and Clear Water Discharge

The pump control was configured that the floating pump is activated for a duration of 13 s (01/2018 to 01/2019), 16 s (01/2017 to 12/2017) and 20 s (11/2015 to 11/2016) after a discharged volume of 50 m³ (01/2018 to 01/2019), 36 m³ (01/2017 to 12/2017) and 87 m³ (11/2015 to 11/2016), respectively.

Fig. 4.11 shows the hydrograph during clear water discharge and the corresponding cumulative curve for one rain event as an example. The vertical lines mark the sampling times. The gap between the horizontal lines indicates the discharged volume in between the individual sub samples. Equal distances between the horizontal lines indicate that the sampling was carried out proportionally to the volume.
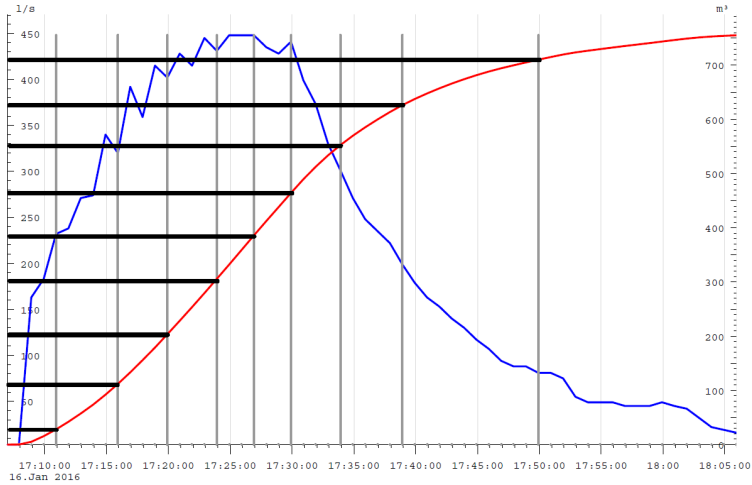
Fig. 4.11: Typical hydrograph for Clear Water discharge. Blue line: flow in l/s; red: corresponding cumulative volume in m³; vertical lines (grey): activision of sampling pump; horizontal lines (black): discharged volume in between sub samples

4.1.4.2 Sampling of Effluent

To sample the effluent volume proportionally, water levels were defined on the basis of a geometric model of the treatment plant (Schmiedgruber 2015), according to which a constant volume of approximately 40 m³ was discharged. The pump was then activated for 18 s (2018 – 2019) or 15 s (2015 – 2017) respectively and a subsample of about 32 L or 26 L was taken. It was ensured that the flushing of the facility was also covered by the sampling. Fig. 4.12 shows the sampling points in conjunction with the decreasing water level during the effluent discharge as well as the flushing. Since the volume is not linearly related to the water level, the vertical lines have different distances in between. It needs to be pointed out that the zero point of the ultrasound water level sensor of the facility is at the bottom level of the bypass and thus approx. 38 cm above the bottom level of the valve to the foul sewer. Therefore the pump is still able to take sample.
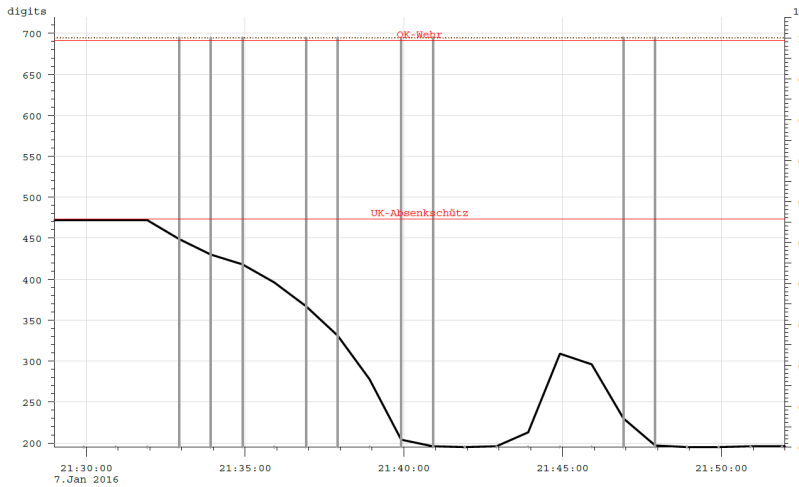
Fig. 4.12: Water level profil during emptying and flushing. Redlines indicating hights of the top edge weir and lower edge of weir or sluice gate. Vertical lines indicating the activision of the sampling pump.

4.1.4.3   Emptying of Sampling Tanks

Once the pumps filled the corresponding sampling tanks during a rain event, the solids were extracted after a sedimentation period of minimum one day (in 5 out of 36 times the period between sampling and empying was >10 days). Before the extraction of the solids, water level, temperature, pH value (GMH 5450, GHM Messtechnik GmbH), and electrical conductivity (EC) (GMH 3530, GHM Messtechnik GmbH) were measured. The volume in the sampling tanks was calculated from the water level. As a first step, the supernatant water was carefully drained from the containers until a residual volume of approximately 10 L was left. Representative sub-samples were taken from the drained supernatant water in order to determine the proportion of non-settable suspended solids contained in the supernatant water as well as its pollutant concentration. The suspended solids were later added to the < 63 µm fraction. In addition, 2 buckets of supernatant water (approx. 30 L) were taken from each of the sampling tanks for subsequent sample preparation. All settled solids in the remaining volume of the tank (approx. 10 – 15 L) were thoroughly remobilized and then collected in a smaller sampling container (SSC) by a thorough rinsing of the tank. This sample contains all particles from the sampling tank. The samples then were transported to the laboratory of the Institute for Sanitary Engineering, Water Quality, and Waste Management (ISWA) at the University of Stuttgart and examined.

4.2   Selection of Analysed Substances

The organic micropollutants and metals analysed were selected according to the following criteria:

- Regular occurrence in surface and municipal waters
- Comparability with other investigation programs
- Affiliation with specific application areas and input pathways
- Different physico-chemical properties as possible

The analysed organic micropollutants and their properties can be found Tab. 4.1 (structural formulas see Tab. B.1). The selected compounds represent typical pollution parameters of stormwater runoff to be expected for the investigated industrial area. They also include substances listed as priority substances in the Water Framework Directive (WFD) of the European Union. It was ensured that substances with a clear tendency towards particle adsorption due to their physico-chemical properties ($\log K_{OW} > 4.0$) were included as well as substances with high water solubility ($\log K_{OW} < 2.5$). The selection includes substances from the following substance groups: PAHs, household and industrial chemicals, biocides, flame retardants and plasticisers, pharmaceuticals and others. Carbamazepine, lidocaine and caffeine serve as indicator parameters for misconnections of foul sewers, as these substances are not necessarily to be expected in stormwater runoff.

The analyzed metals are chromium (Cr), copper (Cu), zinc (Zn), cadmium (Cd), and lead (Pb) as they are typical constituents derived from anthropogenic, in particular vehicular activities (see Tab. 2.6) and therefore typical expected constituents in stormwater runoff of an industrial area. Moreover, Cd and Pb are listed as priority substances in the Water Framework Directive (WFD) of the European Union. There are existing concentration values defined as environmental quality standards (EQS) which should not be exceeded in surface waters.

Tab. 4.1: List of 30 organic micorpollutants analysed in this study, their molecular formula and weight, their n-Octanol/Water Partition Coefficient and the abbrevations used in the text and figures. * Priority Substance of WFD, ** Identified as priority hazardous substance in WFD

Group	Substance	Abbr.	Molecular formula	Molecular weight (g/mol)	Log K_{OW}
Polycyclic aromatic hydrocarbons (PAHs)	Naphtalene*	NAP*	$C_{10}H_6$	128.2	3.33
	Acenaphthylene	ACY	$C_{12}H_8$	152.2	3.94
	Acenaphthene	ACN	$C_{12}H_{10}$	154.2	3.92
	Fluorene	FLE	$C_{13}H_{10}$	166.2	4.18
	Phenanthrene	PHE	$C_{14}H_{10}$	178.3	4.46
	Anthracene**	ANT**	$C_{14}H_{10}$	178.3	4.45
	Fluoranthene*	FLU*	$C_{16}H_{10}$	202.2	5.16
	Pyrene	PYR	$C_{16}H_{10}$	202.2	4.88
	Benz[a]anthracene	BaA	$C_{18}H_{12}$	228.3	5.79
	Chrysene	CHR	$C_{18}H_{12}$	228.3	5.73
	Benzo[b]fluoranthene**	BbF**	$C_{20}H_{12}$	252.3	5.78
	Benzo[k]fluoranthene**	BkF**	$C_{20}H_{12}$	252.3	6.11
	Benzo[a]pyrene**	BaP**	$C_{20}H_{12}$	252.3	6.13
	Indeno[1,2,3-cd]pyrene**	IND**	$C_{22}H_{12}$	267.3	6.76
	Benzo[ghi]perylene**	GHI**	$C_{22}H_{12}$	276.3	6.63
	Dibenz[ah]anthracene	DBA	$C_{22}H_{14}$	278.3	6.75
Household/ industrial chemicals	4-tert-octylphenol*	4tOP*	$C_{14}H_{22}O$	206.3	5.28
	4-nonylphenol**	4NP**	$C_{15}H_{24}O$	220.3	5.76
	1H-benzotriazole	BTR	$C_6H_5N_3$	119.1	1.44
	Benzothiazole	BT	C_7H_5NS	135.2	2.01
	2-methylthiobenzothiazole	MTBT	$C_8H_7NS_2$	181.2	3.22
Flame retardants and plasticisers	Tris(2-chloroethyl)phosphate	TCEP	$C_6H_{12}Cl_3O_4P$	285.5	1.42
	Tris(1-chloro-2-propyl)phosphate	TCPP	$C_9H_{18}Cl_3O_4P$	327.6	2.59
	Triphenylphosphate	TPP	$C_{18}H_{15}O_4P$	326.3	4.59
Biocides	Diethyltoluamid	DEET	$C_{12}H_{17}NO$	191.3	2.02
	Mecoprop	MCP	$C_{10}H_{11}ClO_3$	214.6	3.13
	Terbutryn*	TBY*	$C_{10}H_{19}N_5S$	241.3	3.74
Pharmaceuticals and others	Carbamazepine	CBZ	$C_{15}H_{12}N_2O$	236.3	2.45
	Lidocain	LID	$C_{14}H_{22}N_2O$	234.3	2.26
	Caffeine	CAF	$C_8H_{10}N_4O_2$	194.2	-0.07

4.3 Laboratory Analyses

A schematic overview of the laboratory analyses performed in this study is shown in Fig. 4.13. The sample preparation, i.e. the filtration of the supernatant water, the fractionation into the corresponding particle sizes and the division of the samples for further analyses in other laboratories of the institute, was done in own work with the support of student and research assistants.

The standard wastewater parameters were analysed according to the standards listed in Tab. 4.2. The analyses, except for TSS and LOI, were performed by the laboratory of the Department for Wastewater Technology. The analyses of organic micropollutants and metals were carried out by the laboratory of the Department of Hydrobiology and Organic Trace Compounds (BiOS).

A detailed description of the methods used for the analysis of solids, organic micropollutants and metals is given in the following subchapters.
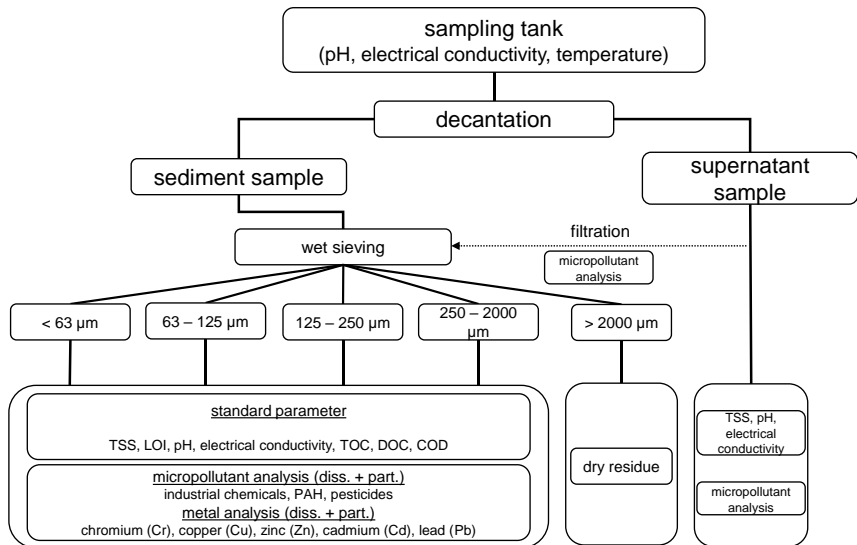
Fig. 4.13: Scheme of laboratory analysis

Tab. 4.2:   Analytical methods used for the determination of water and wastewater parameters

Parameter	Methode
TSS	DEV H2-3, DIN 38409-2: 1987
TSS<63	(Baum et al. 2018)
LOI	DEV H2-3, DIN 38409-2: 1987
TOC	DIN EN 1484 08/1997
DOC	DIN EN 1484 08/1997
COD	DIN 38409-41 12/1980
CODmf	Tube test by Macherey+Nagel in accordance with DIN ISO 15705 – H45

4.3.1   Particle Characteristics

Up to now, there has been no standardised procedure for the determination of the parameter TSS63 (TSS < 63 µm). The laboratory analysis of the new german indicator parameter proves to be challenging. The strong tendency of the fine particles to form flocs requires these flocs to be broken up again (dispersed) before the separation into < & > 63 µm. Failing to do this thoroughly will bias the measurement result (Welker et al. 2019). Within the two research projects, a lot of experience has been gained in this regard. Furthermore, collaborative experiments were initiated in cooperation with other universities and the experiencees gained were presented in at a scientific conference (Baum et al. 2018). The principles of the presented methodology were also applied in this study. However, in addition to TSS63, other particle size classes were investigated, as shown in Fig. 4.13. These steps are explained in the following.

As a first step, the volume of the samples was measured, then the coarse particles were separated by sieving (>2.0 mm). The separated coarse material was washed thoroughly to rinse off the smaller particles adhering to them. The rinsed particles were returned to the initial sample, the coarse material was dried to constant mass at 105 °C and weighed. The sample then was fractionated by wet sieving into the particle size classes <63 µm, 63–125 µm, 125–250 µm, and 250–2000 µm. In the first research project the samples were only divided in < 63 µm and > 63 µm after the separation of the coarse fraction. Until 2018 the sieving was performed manually and later with the use of a sieve shaker (vibratory sieve shaker AS 200 control, Retsch GmbH, Haan, Germany). Before each sieving, the sample was dispersed using a dissolver stirrer (IKA®-Werke GmbH, Staufen, Germany) for approximately 30 s. Membrane-filtered supernatant water from the corresponding sampling tanks was used for the wet sieving. This water was also used for thorough backwashing of the respective sieves. The resulting samples of different particle size classes (volume approximately 5–15 L) were then homogenized individually in a mixing reactor. Using a pump, identical samples were taken from the reactor. The volume of these subsamples were 1L of each particle size class for the analyses of organic micropollutants as well as for the metal analysis and 250 ml for

DOC, TOC and COD. If it was not possible to reliably split the samples due to a low amount of particulate matter, only TSS was analysed (this was mostly the case for the size fractions > 63 µm in CWD and Overflow samples). TSS concentrations were determined as average of five individual replicates, directly taken from the mixing reactor. If individual values of the five replicates deviate by more than 20 % from the mean TSS concentration, these values are dismissed and a new mean TSS concentration is calculated with the remaining values. The determination of the TSS concentration for the respective particle size fractions was carried out by vacuum filtration using 0.45 µm membrane filters (Sartorius). The filters were also dried to constant mass at 105 °C and weighted.

After the mass on the filters had been determined, they were incinerated at 550 °C in a muffle furnace to determine the loss on ignition. A duplicate determination was attempted for each sample. In order to obtain a reliable measurement, it was ensured that approx. 50 mg of dry mass were present in each combustion crucible.

4.3.2 Micropollutant Analysis

All substances were analysed in the in dissolved and homogenized (dissolved + particulate) phase for each sample of the different particle size fractions. The particulate fraction then was calculated from the difference between the two analyzed phases. For all substances the limit of quantification (LOQ) was 0.002 µg L^{-1}.

The respective sample was aliquoted first. Next, the Isotope labelled internal standard solutions were added. A double liquid/liquid extraction with dichloromethane followed before the sample was concentrated to 2 mL using a rotary evaporator. The sample then was dried anhydrous using sodium sulphate and further concentrated to 100 µL. After transferring the sample to GC vials, they were analysed in a GC-MS (Agilent 6890n; low-resolution Mass Selective Detector Agilant 5975; column: Varian VXms, length 30m, internal diammeter 0.25 mm, layer thickness 250 nm) using Single Ion Monitoring (SIM) method and quantified by isotope dilution method. The analysis of the dissolved phase followed the same methodology; however, the samples were filtered prior to the described analysis steps.

4.3.3 Metal Analysis

Metals were analyzed in dissolved and homogenized (dissolved + particulate) phase for each sample of the different particle size fractions. The homogenized samples (10 mL) were digested as triplicate determinations in two runs each with 5 mL HNO3 and 2 mL H2O2 (30%) in a microwave program (MLS Ethos, 1600W, 10 min heating, 20 min holding temperature at 210 °C) following DIN EN 16173 (2012) to analyze the acid soluble fraction of metals. The digest was filtered (2–4 µm, Macherey-Nagel MN 640 d, ash-free) and determined as concentration in mg L^{-1} in an inductively coupled plasma mass spectrometer (ICP-MS, Perkin Elmer Nexion 2000) (DIN EN ISO 17294-2 2017). The

instrument was matrix-matched calibrated before each measurement and a certified reference material (CRM BCR-723 "Road Dust" and NIST 1640a) was analyzed as quality control. The recovery rates of the elements were in the range of 90 to 110% (N = 16; percentual standard deviation 1.5–5.0%). Analytical results of CRMs used can be found in Tab. 4.3. The analysis of the dissolved phase followed the same methodology; however, the samples were filtered prior to the digestions.

The particulate concentration then was calculated from the difference between the two analyzed phases.

Tab. 4.3:   Average recovery rates of certified reference material (CRM BCR–723 "Road Dust" and NIST 1640a)

Element	Recovery rate (%)	Standard deviation (%)
Cr	100	2,9
Cu	99	3,4
Zn	111	3,6
Cd	104	5,0
Pb	92	1,5

4.4   Statistical Methods

Data from urban stormwater runoff investigations are usually not normally distributed (Mosley und Peake 2001). Therefore, samples with smaller sizes (n < 30) are examined with non-parametric tests (e.g. Spearman's rank correlation). For samples with n ≥ 30, parametric tests can be used, since based on the assumptions of the central limit theorem, the mean values of the data in a sampling distribution are approximately normally distributed, regardless of the distribution of the data (Field 2017).

4.4.1   Correlation

As a measure of linear correlation between two sets of data, the Pearson correlation coefficient (r) is used for samples with n ≥ 30 in this study. It is calculated according to Equation 4.1 and compares the empirical covariance to the root of the product of the standard deviations.

Pearson correlation coefficient (–):

$$r = \frac{\sum_{i=1}^{n}(x_i-\overline{x})(y_i-\overline{y})}{\sqrt{\sum_{i=1}^{n}(x_i-\overline{x})^2 \sum_{i=1}^{n}(y_i-\overline{y})^2}} \qquad (4.1)$$

where y represents the observation of variable y, x the observation of variable x, $\overline{y}$ and $\overline{x}$ are the mean of the variables x and y respectively.

For samples with n < 30 Spearman's rank correlation is used to determine the relationship between two variables.

Spearman's rank correlation coefficient (–):

$$r_s = r_{rg_x, rg_y} = \frac{cov\left(rg_x, rg_y\right)}{\sigma_{rg_x} \sigma_{rg_y}} \qquad (4.2)$$

with r as the usual Pearson correlation coefficient, but applied to the rank variables, $cov\left(rg_x, rg_y\right)$ is the covariance of the rank variables, σ_{rg_x} and σ_{rg_y} are the standard deviations of the rank variables.

In order to determine the significance of the correlations, p-values are determined using the two-tailed Student's t-distribution. The correlation is assumed significant if the calculated *p*-value is smaller than the level of significance of 0.05.

Fischer's z-tranformation can be used to find out whether the strength of two correlations differs significantly. For each correlation coefficient, a confidence interval is calculated. If these two confidence intervals do not overlap, the two correlation coefficients differ significantly.

$$\text{Fischer's z-tranformation: } z = 0{,}5 \times \left(\ln(1+r) - \ln(1-r)\right)$$
$$\text{95 \% confidence interval: } z \pm \frac{1}{\sqrt{n-3}} \qquad (4.3)$$

where r represents the correlation coefficient and n the respective sample size

4.4.2 Data presentation
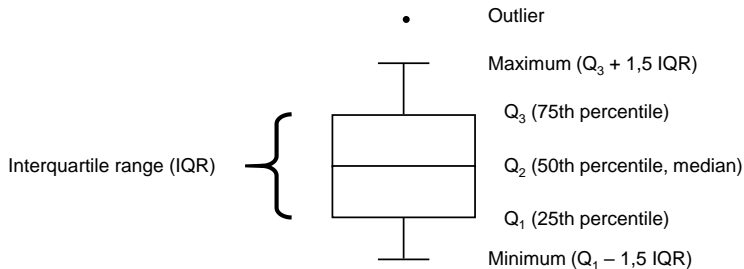
Fig. 4.14: Example of a boxplot with whisker and outlier

The presentation of the results as a boxplot diagram (Fig. 4.14) allows the values to be classified according to robust measures of location and dispersion. The box represents the 25th percentile (beginning of the box) and the 75th percentile (end of the box). The

bar within the box is the 50th percentile (median). The interquartile range (IQA) represents the range in which 50 % of the data are located. The whiskers signify the values in 1.5 times the interquartile range hence the range in which most of the data is found. Outliers beyond this are shown as individual dots (> 1.5 IQA).

4.5 Evaluation Methods

4.5.1 Event loads and Event Mean Concentration

Stormwater runoff events show significant variation in the constituent concentrations not only in between different stormwater runoff events, but also within the same runoff event. The first flush phenomenon for example is well known and often discussed (Bertrand-Krajewski et al. 1998; Deletic 1998). Due to that fact, a single index, the event mean concentration (EMC) is generally used to describe the constituent load transported by a stormwater runoff event (Sansalone und Buchberger 1997b). It is a flowweighted averaged concentration calculated as the total constituent load (mass) divided by the total volume of the stormwater runoff event (Huber 1997).

Due to sampling volume-proportional to the runoff in this study, the concentration in the LVST corresponds to the average concentration of the sampled runoff volume. The concentration in the LVST (c_{LVST}) is calculated from the concentration determined in the laboratory (c_{lab}) and the volume of the LVST (V_{LVST}) as well as the volume of the smaller sampling container (V_{SSC}) after emptying the LVST (see formula 4.4).

$$c_{EMC} = c_{LVST} = \frac{B_{TSS,SSC}}{V_{LVST}} = \frac{c_{lab}V_{SSC}}{V_{LVST}} \tag{4.4}$$

The event mean concentration of the influent ($c_{EMC,in}$) to the treatment facility is calculated by the sum of the loads of the individual flows (overflow (B_{over}), clear water discharge (B_{CWD}) and effluent (B_{eff})) divided by the influent volume (V_{in}) as shown in formula 4.5. By multiplaying the concentration with the volume of the respective flow its constituent load (constituent mass transported by the respective flow) can be estimated. This principle can be applied to TSS, organic micropollutants, metals and all other analysed parameters of this study. Fig. 4.15 gives an overview about the relevant flows of the treatment facility.

$$c_{EMC,in} = \frac{(B_{over} + B_{CWD} + B_{eff})}{V_{in}}$$
$$= \frac{(c_{EMC,over}V_{over} + c_{EMC,CWD}V_{CWD} + c_{EMC,eff}V_{eff})}{V_{in}} \tag{4.5}$$

where $c_{EMC,over}$ represents the event mean concentration in the overflow, V_{over} the volume of the overflow, $c_{EMC,CWD}$ the event mean concentration in the clear water

discharge, V_{CWD} the volume of the clear water discharge, $c_{EMC,eff}$ the event mean concentration in the effluent and V_{eff} the volume of the effluent.
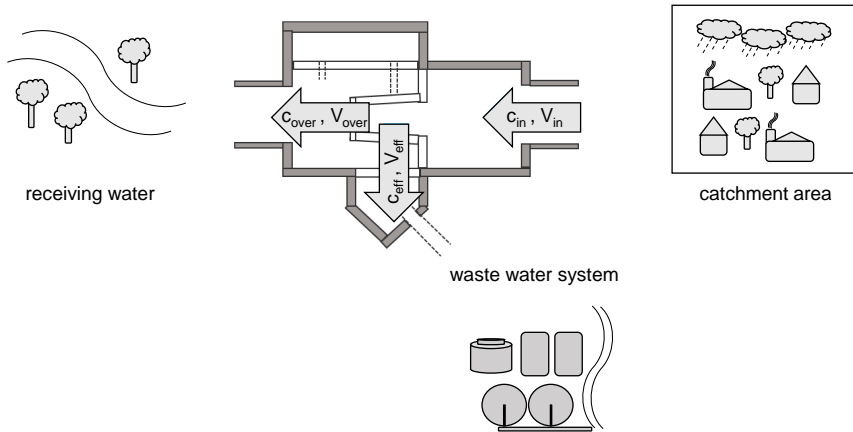
Fig. 4.15: Schematic of the monitored stormwater treatment facility and its relevant flows (inflow, overflow and effluent). The flow to the receiving water consists of overflow and clear water discharge.

The particulate event loads of organic micropollutants and metals were calculated using the particulate pollutant/metal concentrations in mg pollutant/metal kg TSS^{-1} of each individual sample multiplied by the respective event loads of TSS. The EMCs are derived by dividing the event pollutant/metal loads by the respective volume. In the case that a substance could be quantified in the homogenized phase, yet the dissolved phase was below the LOQ, a value of 0.5 × LOQ was asumed as a worst case scenerio for further calculation. To calculate the dissolved pollutant/metal load, the average of the event-specific dissolved concentrations over all particle size classes was formed and multiplied by the respective discharged volume. If analysis values of individual particle size fractions from specific sampled flows were missing because the initial bulk sample could not be completely divided due to insufficient solids (cf. 4.3.1), the mean of the corresponding particle size fraction over all sampled events and flows was assumed for the calculation of the respective event-specific loads. This was often the case for the particle size fractions > 63 μm of CWD and partly also of Overflow.

4.5.2 Treatment Efficiency

The definition of an efficiency enables the comparison of the inflowing pollutant load and the pollutant load in the overflow to the water body. In this way, different treatment facilities can be compared in terms of their treatment performance. In general, the load M results from the product of the determined concentration c and the respective volume V for a corresponding time period (also refer to the previous chapter). The

calculation of the total treatment efficiency related to the pollutant loads generally is as follows:

$$\eta_M = 1 - \frac{M_{over}}{M_{in}} = 1 - \frac{c_{over}V_{over}}{c_{in}V_{in}} \qquad (4.6)$$

where η_M is defined as the total treatment efficiency and M_{over} represents the total mass of a constituent reaching the receiving water and M_{in} the total mass of a constituent coming into the treatment facility. Respectively c_{over} is the constituent concentration flowing to the receiving water and V_{over} the according volume. c_{in} and V_{in} are the same but in the inlet to the facility.

Due to the sampling of the flows to the receiving water as well as the effluent in this study, the treatment efficiency for the monitored stormwater treatment facility is calculated as follows:

$$\eta_{M,RFM} = 1 - \frac{M_{over}}{M_{in}} = 1 - \frac{M_{over}}{(M_{eff}+M_{over})} = 1 - \frac{c_{over}V_{over}}{(c_{eff}V_{eff}+c_{over}V_{over})} \qquad (4.7)$$

where additionally to formula 4.6 M_{eff} stands for the total mass of a constituent in the effluent to the foul sewer and c_{eff} and V_{eff} for the respective constituent concentration and the volume of the effluent. Also see Fig. 4.15 for an overview of the relevant flows.

4.5.3   Partitioning of Pollutants

Partitioning typically results from sorption and desorption processes of a substance in a two phases system. In this study, the partitioning of organic micropollutants and metals results from the interaction between the dissolved fraction and the particulate-bound fraction, without consideration of the colloidal fraction. To evaluate the predominant phase the partitioning indices f_d and f_p, the dissolved fraction and the particulate fraction respectively, can be calculated as

$$f_d = \frac{c_d}{(c_d+c_p)} = \frac{M_d}{(M_d+M_p)} \qquad (4.8)$$

$$f_p = \frac{c_p}{(c_d+c_p)} = \frac{M_p}{(M_d+M_p)} \qquad (4.9)$$

$$f_d + f_p = 1 \qquad (4.10)$$

with c_d as the dissolved constituent concentration in (dissolved constituent mass/volume) and c_p as the particulate constituent concentration (particulate constituent mass/volume), M_d and M_p are the dissolved and particulate masses, respectively. Therefore, the partitioning indices are dimensionless. If f_p shows a value > 0.5, the tendency is towards the particulate metal fraction.

With the assumption of linear kinetics (cf. 2.3), the equilibrium partitioning coefficient K_d expresses the ratio between the constituent concentration "sorbed" to particulate matter (PM) and the dissolved concentration (Thomann und Mueller 1987). Therefore,

it can be used to evaluate the distribution between particulate and dissolved pollutants. K_d is calculated as follows:

$$K_d = \frac{c_s}{c_d} = \frac{c_p/m}{c_d} \tag{4.11}$$

with cs as "sorbed" concentration in (mass of constituent/mass of PM) and m as mass of PM. Typically cs is expressed in mg kg^{-1} as it is equal to a part per million. Hence, Kd is usually given as litre per kilogram. In formula 2.3 instead of c_d the more general term C_{eq} is used as it also applies to gaseous sorptives.

The adsorption coefficient for certain organic chemicals can vary considerably between different soils or sediments depending on the properties of the sorbent. The sorption coefficient for a large number of organic chemicals, especially for neutral hydrophobic organic compounds, is directly proportional to the amount of organic matter associated with the solid. Therefore, the partitioning coefficient K_{OC}, normalised to the organic carbon content f_{OC}, is commonly used to assess the extent to which an organic chemical is sorbed.

$$K_{OC} = \frac{K_D}{f_{OC}} \tag{4.12}$$

The normalised phase distirbution coefficient K_{OC} can be calculated on the basis of the octanol-water coefficient K_{OW} with empirical regression formulas. For example (Förstner und Grathwohl 2007):

$$\log K_{OC} = 0.544 \times \log K_{OW} + 1.377 \tag{4.13}$$

5 Results and Discussion

In the following, the results of the two measurement campaigns will be evaluated in order to address the research objectives outlined in chapter 3.

First, an overview of the rainfall and runoff patterns of the investigated catchment area is given. For this purpose, the measured rainfall data and the recorded runoff data of both research projects are used. Then the occurrence of solids and their retention by the rainwater treatment facility is examined in more detail. The data from both research projects will also be used for this. Next, the pollution of urban stormwater runoff will be evaluated and its distribution between the aqueous and particulate phases will be investigated. In this context, the role of OM in association of pollutants with particles will be further examined. It will also be investigated whether the parameter TSS fulfils a sufficient indicator function to represent the occurrence but also the treatability of organic micropollutants and metals. Mainly data from the second measurement campaign (2017–2019) will be used for this purpose.

5.1 Rain and Runoff Characteristics

5.1.1 Monitoring Period Nov. 2015 – Nov. 2016

During this study period, 91 runoff events occurred at the rainwater treatment facility. From the end of April to the beginning of June 2016 and from the end of July to August 2016, sampling had to be suspended due to an operational malfuntion at the plant. No data was recorded during this period. Out of the 91 runoff events, approximately 23 events were completely diverted to the wastewater treatment plant due to exceeding or falling below the pH limit. Since sampling these events was not useful for the research project's objective, the samples were discarded as far as they had been collected. A total of 30 sampling events were collected, of which 14 sampling events could be evaluated within the scope of this project, resulting in 20 rainfall events being sampled. The sampling events represented all seasons. The distribution was as follows: three sampling events in spring (March – May), seven in summer (June – August), two in autumn (September – November) and two in winter (December – Februrary).

During this monitoring period, a total of approx. 278,780 m³ water was discharged from the catchment area (180,913 m³ excluding the malfunctions). The sampled volume was 54,677 m³. With regard to the volume distribution within the treatment facility, it can be stated that 12 % of the discharged volume was directed to the wastewater treatment plant.

Fig. 5.1 gives an overview of the runoff volume and the rainfall depth as cumulative curves for this period. In the appendix an overview of the recorded events is given where it can be seen that the sampled events were distributed over the whole year (Fig. C.1). Therefore, possible seasonal influences were covered by the sampling. Details of the individual sampling events and the characteristics of the sampled rain events can also be found in the appendix (Tab. C.2 & Tab. C.3).

Temperature, pH and electrical conductivity (EC) were measured before the final solids removal from the sampling tanks. The results are shown in Tab. 5.1. The number of measurements varies because pH and EC were only measured starting in Feb. 2016. It can be seen that the water temperature showed large fluctuations. The seasonal change in outdoor temperatures can explain this variation. The pH value was largely stable over the entire sampling period. In the median, the pH value was the same in the overflow and in the effluent. At its maximum, the conductivity showed relatively high values. However, these come from only one event on 01.02.2016 and can therefore most likely be attributed to the use of road salt.

Tab. 5.1: On-site measurements in sampling tanks prior to solids extraction (monitoring period 2015 – 2016)

parameter	n	min.	median	max.	n	min.	median	max.
			overflow				effluent	
Temp (°C)	28	5.5	12.1	20.5	27	5.5	13.2	21.8
pH (-)	21	6.6	7.1	7.7	21	6.9	7.1	7.4
EC (µs/cm)	18	50	105	620	18	80	205	1650
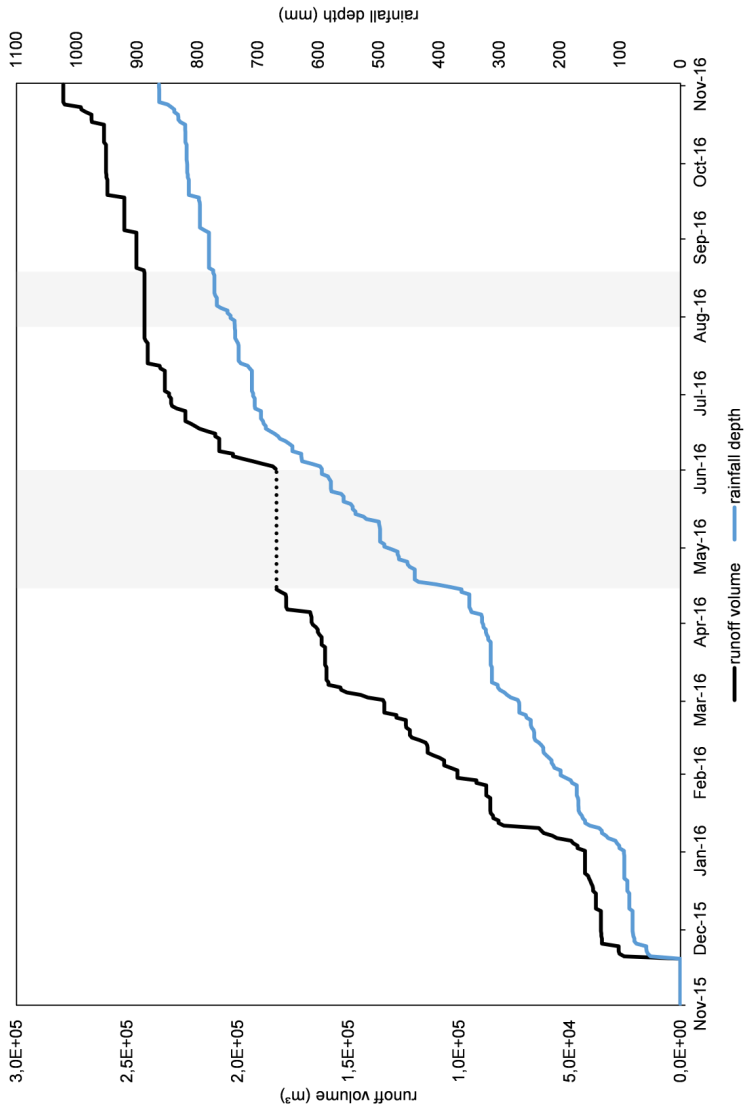
Fig. 5.1: Overview of runoff volume and rainfall depth for the monitoring period 2015 –2016. Gray area represents period with mal-function

5.1.2 Monitoring Period Jan. 2017 – Jan. 2019

In this investigation period, 178 runoff events were detected at the stromwater treatment facility. From mid-May 2017 until the end of February 2018, sampling operations had to be suspended due to extensive IT maintenance work by the treatment facility's operating company. Furthermore, no sampling operation could take place between the end of May and the end of June 2018 due to a defect in the flow measurement. Within 26 sampling events a total of 34 rain events were sampled. Due to errors in sample handling, 22 sampling events covering 31 rain events, could be used for evaluation. The sampling events represented all seasons. The distribution was as follows: nine sampling events in spring (March – May), two in summer (June – August), six in autumn (September – November) and five in winter (December – Februrary).

A total of approx. 714,433 m³ water was discharged from the catchment area (335,033 m³ excluding the malfunctions). The sampled volume was 86,481 m³. With regard to the volume distribution, it can be stated that 13 % of the discharged volume was directed to the wastewater treatment plant.

Fig. 5.2 gives an overview of the runoff volume and the rainfall depth as cumulative curves for this period. In the appendix an overview of the recorded events is given where it can be seen that the sampled events were distributed over the whole year (Fig. C.2). Therefore, possible seasonal influences were covered by the sampling. Details of the individual sampling events and the characteristics of the sampled rain events can also be found in the appendix (Tab. C.4 & Tab. C.5).
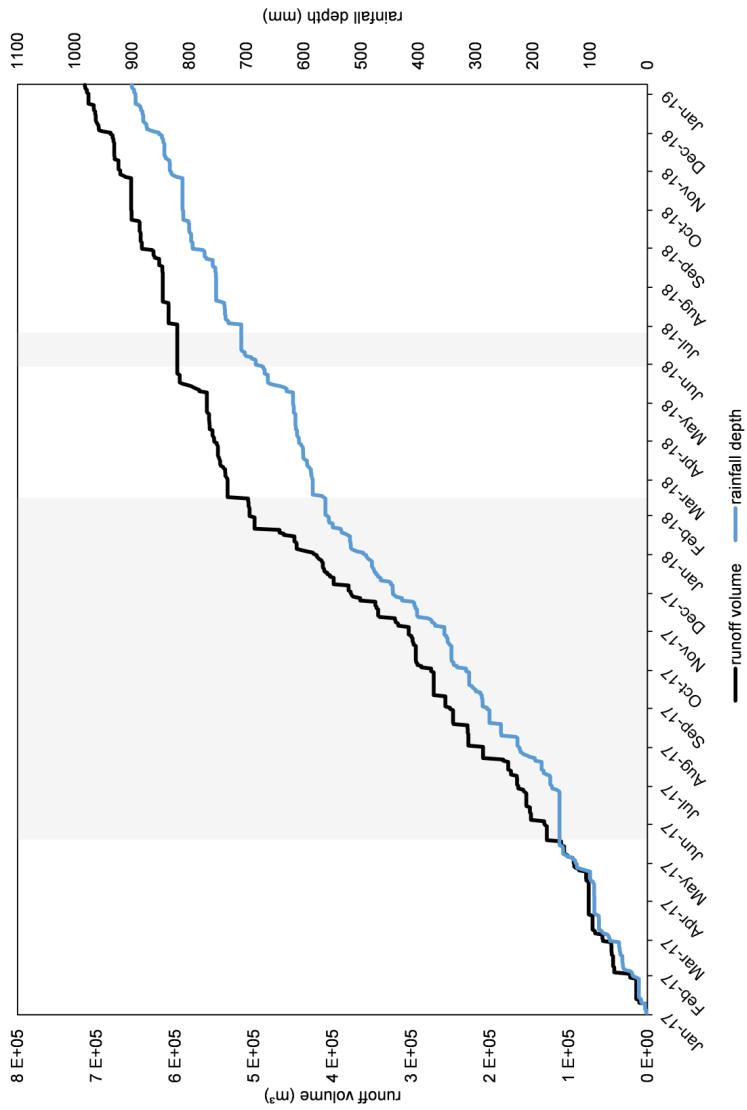
Fig. 5.2: Overview of runoff volume and rainfall depth for the monitoring period 2017 – 2019. Gray area represents period with malfunction

The on-site measurements of temperature, pH and EC laid within the same range as in the previous monitoring period (Tab. 5.2). The variations in temperature can also be attributed to the seasonal change in outdoor temperature. The pH values were also stable within the neutral range over the entire period. The extreme values for EC were measured for the events in winter 2018 and can therefore be attributed to road salt.

Tab. 5.2: On-site measurements in sampling tanks prior to solids extraction (monitoring period 2017 – 2019)

parameter	n	min.	me-dian	max.	n	min.	me-dian	max.	n	min.	me-dian	max.
	clear water discharge				overflow				effluent			
Temp (°C)	39	5.7	12.0	27.2	31	6.4	12.0	27.2	47	1.4	10.9	26.9
pH (-)	38	6.7	7.1	7.6	35	6.6	7.0	7.8	45	6.6	7.0	7.9
EC (µs/cm)	39	40	70	790	39	40	70	420	47	50	175	2260
Temp (°C)	39	5.7	12.0	27.2	31	6.4	12.0	27.2	47	1.4	10.9	26.9

5.2 Evaluation of Particulate Matter

5.2.1 Particle Size Distribution

The PSD was analysed for all 36 evaluated sampling events from 2015 to 2019 by sieving. In the first monitoring period (2015 – 2016), the particle sizes of 14 sampling events were distinguished between < 63 µm, <2000 µm and > 2000 µm. In the period from 2017 – 2019 the particle sizes of 22 sampling events were distinguished between < 63 µm, < 125 µm, < 250 µm, < 2000 µm and > 2000 µm. Since 2018, manual sieving was replaced by the usage of an automatic sieve shaker. Fig. 5.3 shows the PSD as accumulated percentage mass fractions of the sieve analyses as boxplots (left side) and the absolute mass fraction (right side). The total mass includes the fraction > 2000 µm. An overview of the grading curves of the individual events as well as the values of the absolute mass fractions can be found in the appendix (Fig. C.3 & Tab. C.6). In the median, the smallest fraction accounted for 64 % of the total particulate mass, 79 % was smaller than 125 µm, 83 % smaller than 250 µm and 90 % smaller than 2000 µm. The fine particles (< 63 µm) showed by far the greatest spread, with a range from a minimum of 15 % to a maximum of 92 %, compared to the spread of the other fractions. The calculation of the standard deviation (SD) of the absolute mass fractions showed the following values: 0.22 (< 63 µm), 0.03 (63 – 125 µm), 0.05 (125 – 250 µm) and 0.04 (250 – 2000 µm). To further investigate this observation the particle size distribution is differentiated by the sampled flows.
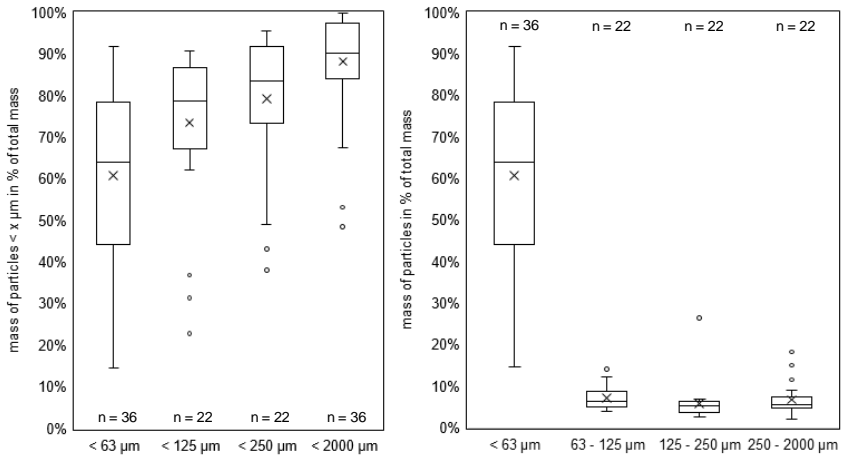
Fig. 5.3: Particle size distribution as boxplots of accumulated mass fractions (left), and as boxplots of the absolute mass fractions (right)

Starting 2018, Overflow, CWD and Effluent of the stormwater events was sampled separately, accounting in 17 sampling events for which the particle size distribution could be differentiated by these flows. Fig. 5.4 shows the PSD as accumulated and absolute mass fractions for the different flows. It can be seen that almost over all particle sizes the largest variations showed up in the Effluent, again the largest spread was found in the fraction < 63 µm. Only for 63 – 125 µm Overflow showed a higher SD (0.04) than Effluent (0.03). However, due to the relatively small sample size of the Overflow samples (n = 7) the significance is limited. The larger spread in the Effluent samples could be explained by the fact that depending of catchment, rainfall and runoff characteristics (rain duration and intensity as well as the flow velocities of the runoff) a certain proportion of coarse mineral particles already settled within the sewer network as well as during the impounding process in the stormwater treatment plant. In the study of Fuchs et al. (2013) similar observations were made. They monitored different centralised treatment facilities and found higher variations in the fine fraction than in the coarse particle fraction as well.

In Fig. 5.4 it can be seen that almost no coarse particles were found in Overflow and in CWD, while more than 90% of these flows consisted of the fine fraction. This could already indicate that the fine fraction has worse settling properties than the coarse particles. To gain clarity on this, the particle concentrations or loads in the outflow relative to those in the inflow need to be known. The treatment efficiency of the plant will be quantified in sections 5.2.5.

For comparison with international studies on particle size distribution in urban stormwater runoff, the mean values of the measurements in this study were plotted with the particle size distributions from the literature studies (Fig. 5.5). The grading curve of

the mean values (black dashed, grey area as standard deviation) lies in the range of the values found in the literature. The PSD of a catchment area is strongly dependent on its characteristics (use, traffic frequency, human activities, vegetation, surroundings, etc.). This comparison, however, shows that the study carried out did not reveal any particularly unusual results in terms of PSD. Attention should be paid to the comments made in Chapter 2.2.1.3 regarding the comparison of studies with different methods for determining the PSD.
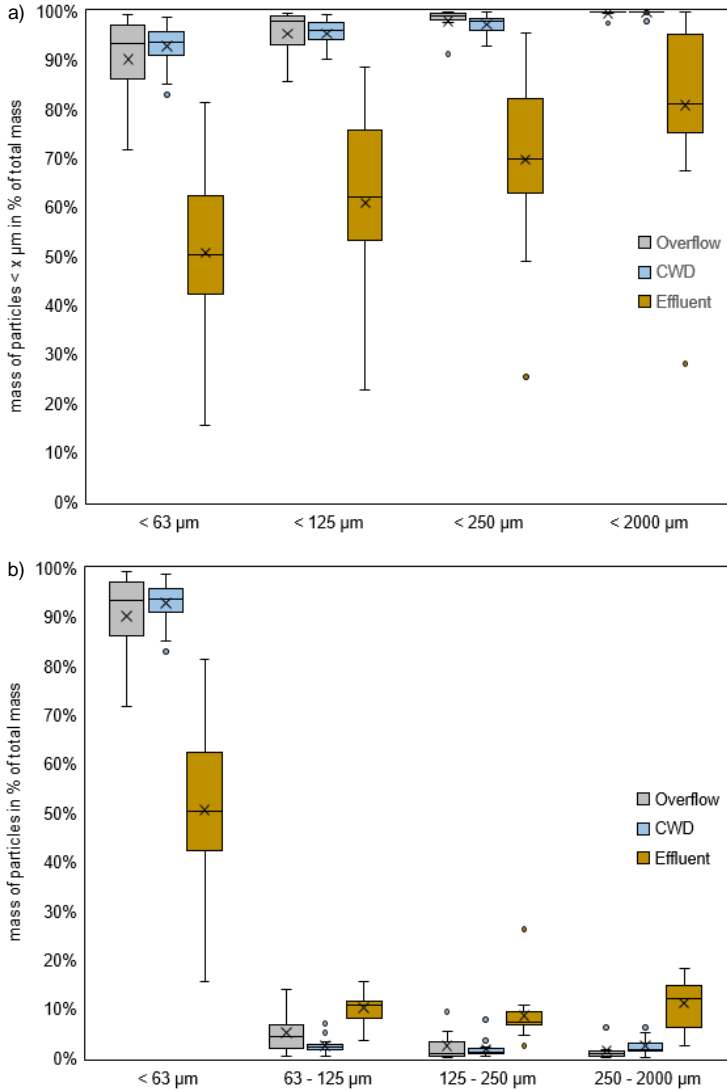
Fig. 5.4: Particle size distribution as boxplots of a) accumulated mass fractions and b) as boxplots of the absolute mass fractions both differentiated by sampled flows ($n_{Overflow}$ = 7, n_{CWD}= 16, $n_{Effluent}$ = 17)
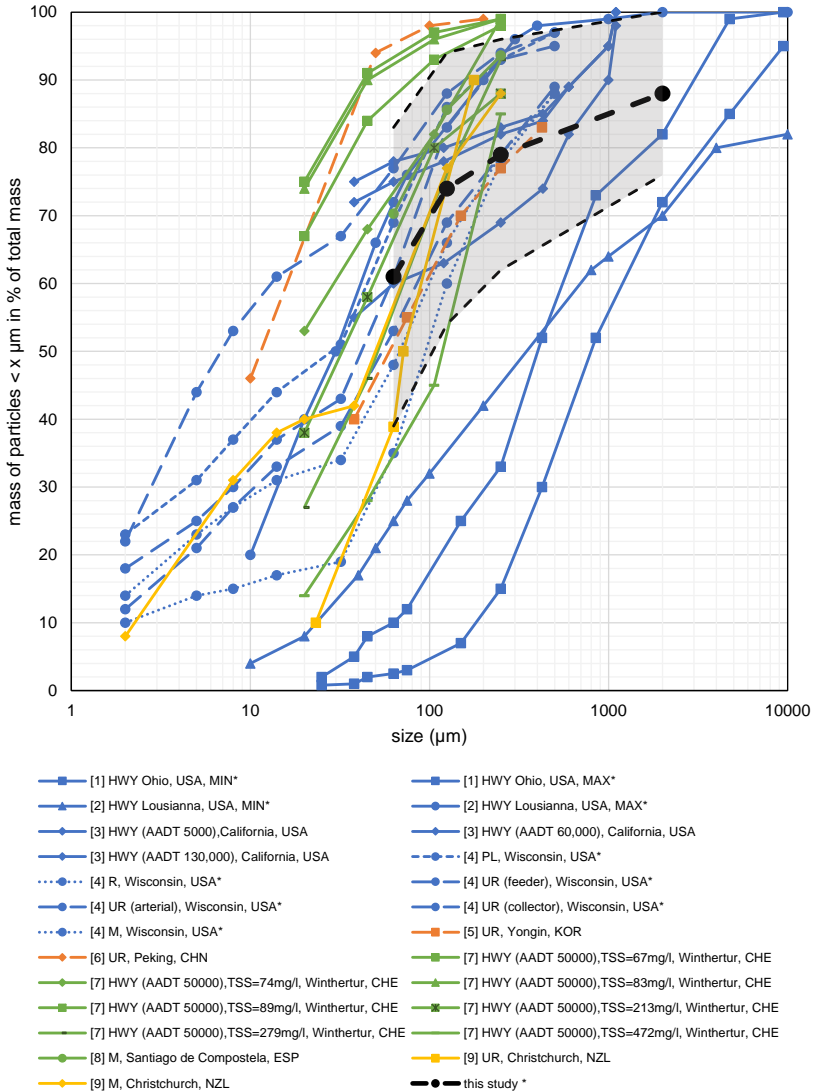
Fig. 5.5: Particle size distribution of this study (mean values, black dashed line, grey area as standard deviation, n = see Fig. 5.3) in comparison with international studies in literature. (Repetition of Fig. 2.1, details Tab. A.1)

5.2.2   Organic Content

During the entire period of the investigations (2015 – 2019), the organic content was determined by loss on ignition. For this purpose, the solids were burnt on the membrane filter used for TSS analysis at 550° Celsius in a muffle furnace. After combustion, the mineral content of the solids remains. Thus, the mass fraction lost through ignition corresponds to the organic fraction of the sample. Particles with a high organic content have an increased adsorption capacity (see chapter 2.2.1.5 & 2.3.2). Furthermore, solids with a high organic content tend to have lower settling velocities due to the relative low density of organic material compared with minerals (cf. 2.2.1.4). An additional reason for this could be the increased tendency to flocculate (Tisdall und Oades 1982; Droppo et al. 2002). However, it must also be mentioned that, depending on the size and density of the produced flocs, they could also have higher settling velocities. Fig. 5.6 shows the results for the measurements differentiated according to the respective particle size fractions that were analysed in the two monitoring periods. For the sampled events between 2017 and 2019, the loss on ignition of the < 63 μm fraction was the lowest at approx. 28 % (median). The loss on ignition increased with increasing particle size. In the largest fraction it was approx. 61 % (median). Combining the results of both monitoring campaigns (Fig. 5.6 b), the median loss on ignition for particles < 63 μm was about 31 % and for the coarse particles it was 46 %.
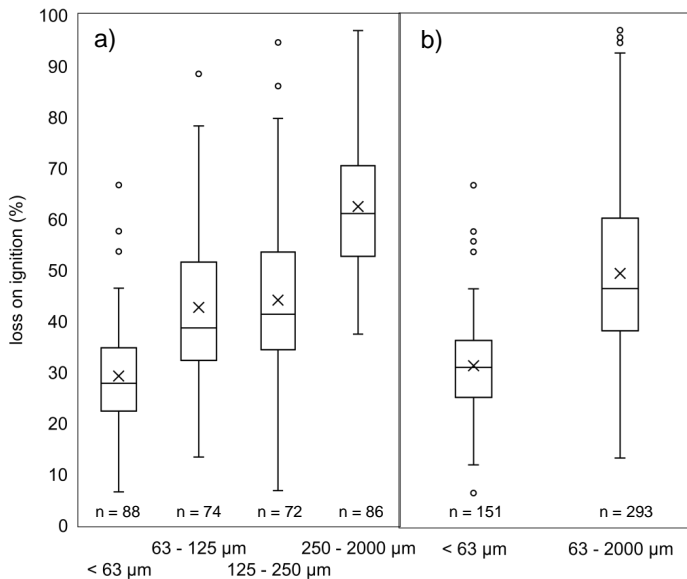
Fig. 5.6:   Loss on ignition of different particle size fractions. a) monitoring period 2017 – 2018 b) monitoring period 2015 – 2019

Gelhardt (2020) compiled a dataset from literature for the loss on ignition of particles from urban stormwater runoff consisting of seven studies with 151 individual measurements from eleven highways and one parking lot. In the compilation, care was taken to exclude values whose underlying sample volume or underlying solid mass on the filter was too low to reliably determine the residue on ignition. The median of the dataset is 26 % LOI.

In her own very extensive measurement campaign, the loss on ignition (n = 730) of RDS in different size classes was investigated. There was an even distribution across the particle size classes with a slight tendency of increasing LOI in the direction of the fine particles. In the size range < 1000 µm the median of 75 % of the values was below 18 % LOI with a few outliers.

When comparing the values determined in Freiburg Haid with the compiled data set of urban runoff, it must be noted that the latter is largely composed of runoff samples from highways. And there, for reasons of traffic safety, less trees are to be expected in the direct vicinity. Whereas in the samples of Freiburg a lot of leafs and twigs were present. Therefore, it is evident that fragmented plant parts in the particle fractions > 125 µm might be one of the reasons for the higher losses on ignition. The fact that the vegetation has a high influence on the organic content was clearly highlighted by Gelhardt (2020) in her own measurement campaign. However, the proportion of vegetation in the catchment area of the monitored rainwater treatment facility was not specifically recorded, so this assumption cannot be substantiated in this thesis.

Another explanation, which also covers the different distribution of LOI across the particle size fractions, might be the sedimentation process of coarse mineral particles already taking place in the sewer system leading to a higher organic content of these fractions in the analysed samples.

Fig. 5.7 shows the loss on ignition for the particle size fractions separated according to the sampled flow (Overflow, CWD, Effluent). It can be seen that the differences in LOI between the considered flows were smallest in the < 63 µm fraction. Larger differences can be seen in the remaining size classes. The lowest loss on ignition was found in the effluent. The lower LOI values in the effluent compared to overflow and CWD can be attributed to the fact that the samples there were taken after the sedimentation process in the treatment facility and therefore presumably contain more of the well-settling mineral particles. The largest difference between effluent and overflow or CWD is found in the size class of 63 – 250 µm. This size class corresponds to the general sizes found for fine sands, which have good settling properties due to their density.

The inverse relationship between density and loss on ignition in RDS, which was clearly highlighted by Gelhardt (2020), can also be seen here. In the particle size fractions > 63 µm, there was a very clear difference between the LOI in the CWD and in the Effluent. This can be explained by the fact that the mineral particles with a higher density settle during the sedimentation phase of the cleaning cycle and thus are found in the Effluent. Whereas the organic particles (high LOI) show a rather poor settleability probably due to a low density and were still found in the CWD after 6 h of sedimentation time.

This is different for solids < 63 µm, as these sometimes have higher densities but poor settling behaviour due to their very small size. According to the findings of Gelhardt (2020) the settleability of solids shows the following order: large, mineral particles >> large, organic particles ≈ fine, mineral particles > fine, organic particles.
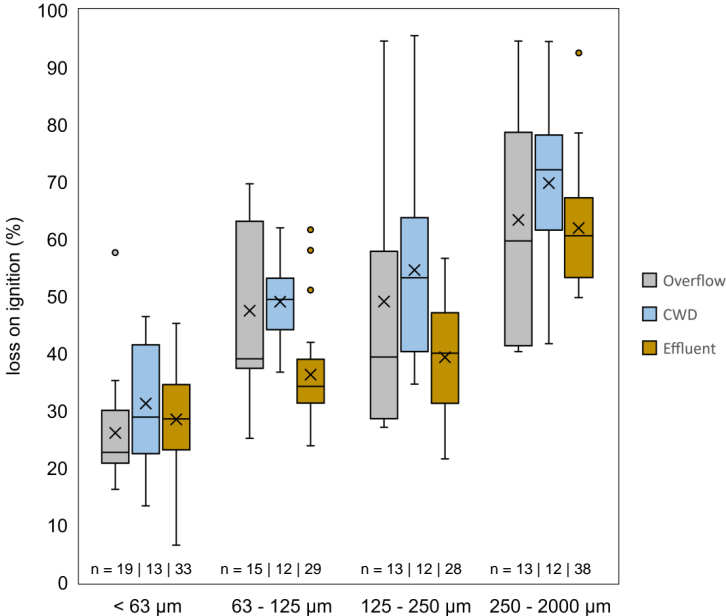
Fig. 5.7:   Loss on ignition of different particle size fractions differentiated by sampled flows

In addition to the loss on ignition, organic carbon was analysed in all samples wherever possible during the investigation period from 2017 to 2019. In the homogenised sample it was measured as total organic carbon (TOC) and in the filtered sample (< 0.45 µm) as dissolved organic carbon (DOC). The median DOC content measured for the individual particle size classes was 7.21 mg L^{-1} for < 63 µm, 5.81 mg L^{-1} for 63 –125 µm, 5.11 mg L^{-1} for 125 – 250 µm and 6.35 mg L^{-1} for 250 – 2000 µm. To deduce the particulate organic carbon, DOC was subtracted from TOC (POC = TOC –DOC).

Fig. 5.8 shows the POC values related to the solid mass in mg POC per kg TSS. There was an even distribution over the different particle size fractions. The median values were in the range of 139 – 151 mg kg TSS^{-1}. This distribution differed from the distribution of the loss on ignition. Most likely, this is due to the fact that for the most part samples of the Effluent were analysed in all particle size fractions for TOC and DOC (Effluent shows the lowest LOI). The samples of Overflow and CWD often had a very low particle concentration, except in the < 63 µm fraction. Therefore, it was not possible to reliably split the samples for further analysis besides TSS. This as well is the

reason for the reduced sample size (n) of the POC in the larger particle size classes. Compared to < 63 μm the sample size was only about half. Compared to the sample size of LOI (72 – 88) the sample size of the fractions > 63 μm was only about one third to one quarter. Another factor to consider when comparing LOI and POC is that the presence of clay minerals and carbonates in a sample leads to increased weight loss when determining LOI, as these can also release substances during combustion (e.g. crystal water or carbon dioxide). As a result, the organic content is slightly overestimated by the determination of the loss on ignition. Furthermore, it could even be that the determination of the LOI does not correctly represent the distribution of the organic content across the different size classes. If one assumes that the particle fraction < 63 μm presumably contains a larger share of clay minerals, the POC investigations indicate that the determination of the LOI in this size fraction leads to a systematic overestimation of the organic content. However, this cannot be pursued further, as the individual elemental composition of the particle size fractions in this study would have to be known.
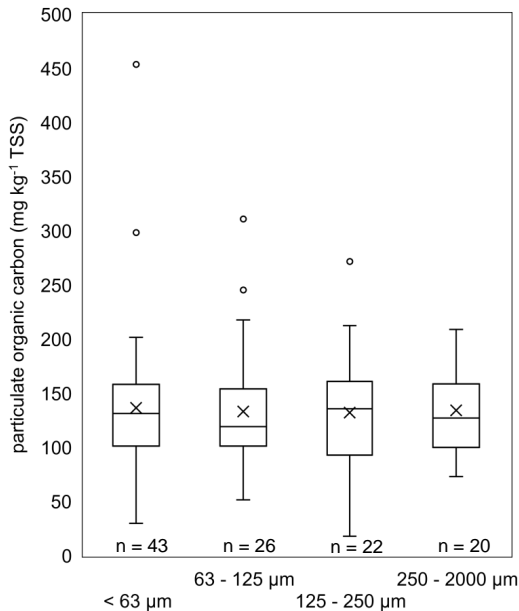
Fig. 5.8:   Particulate organic carbon of different particle size fractions related to solid mass

Fig. 5.9 shows the correlation analysis of POC and LOI as scatter plots for the different particle sizes to further investigate the relationship between LOI and POC. Visually, a correlation was recognisable. The Spearman correlation showed a mediocre dependency of the two variables for the first three particle size fractions. This correlation can

be considered significant and not random. The Spearman's rank correlation coefficient values were, in order of ascending particle size fraction: 0.678, 0.651, 0.554 and 0.085. There are probably several reasons for the only moderate dependency of the variables. Besides a certain inaccuracy of the laboratory results, e.g. the analysis of TOC turned out to be not easy for very inhomogeneous samples (mainly > 125 µm), there have been samples with very low solid mass, which made a reliable determination of the loss on ignition difficult. Yet another reason may be the rather small sample size as it can be seen that the values of the correlation coefficients decreased with decreasing sample size. A larger sample size would probably reduce the effects mentioned above.
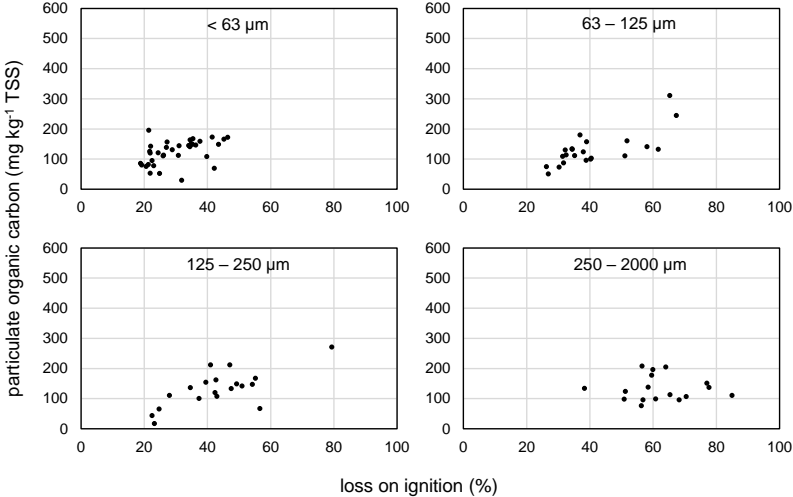
Fig. 5.9: Correlation analysis of particulate organic carbon mg kg^{-1} TSS and loss on ignition for different particle size fractions. $n_{<63\mu m}$ = 36, $n_{63 – 125\mu m}$ = 23, $n_{125 – 250\mu m}$ = 19, $n_{250 – 2000\mu m}$ = 17

5.2.3 Event Mean Concentration

Over the entire sampling period, the event mean concentration (EMC) in the influent to the plant was calculated using the TSS loads and the corresponding discharged volumes of Overflow, CWD and Effluent (cf. 4.5.1). Tab. 5.3 and Tab. 5.4 gives the minimum, maximum, mean, median, and standard deviation (SD) values of the EMC observed across the different particle size fraction as well as for the total TSS (0.45 µm to > 2000 µm). Additionally, Fig. 5.10 shows the calculated EMC as boxplots, differentiated by monitoring campaigns as well as combined. The highest concentrations could be found for the smallest particle fraction. The size fraction < 63 µm also showed the highest variations. In the monitoring campgaing of 2015 – 2016, slightly larger fluctuations were observed at 63 – 2000 µm.

Comparing to the concentrations shown by Brombach et al. (2005), who compiled a vast database for separate as well as combined sewer systems, the concentrations found in this study can be considered as low. For example, the median TSS concentration of separate systems and storm sewers is given as 141 mg L^{-1} whereas the median EMC in this study is 41 mg L^{-1}.

An overview about the single events can be found in the Appendix (Tab. C.7 & Tab. C.8)

Tab. 5.3: Event mean concentration of TSS in mg L^{-1} (monitoring period 2017 – 2019, n = 22)

Size fraction	min	max	mean	median	SD
total	8.95	332	87.1	45.4	100
< 63 µm	7.52	191	43.0	30.6	39.7
63 – 125 µm	0.54	32.8	6.58	3.12	8.4
125 – 250 µm	0.50	87.6	8.03	2.08	18.7
250 – 2000 µm	0.39	60.5	7.8	2.50	15.2
> 2000 µm	0.39	145	23.8	4.33	42.2

Tab. 5.4: Event mean concentration of TSS in mg L^{-1} (monitoring period 2015 – 2019, n = 36)

Size fraction	min	max	mean	median	SD
total	8.95	332	73.6	41.4	86.2
< 63 µm	7.08	191	34.0	22.4	34.2
63 – 2000 µm	0.39	103	14.9	4.32	24.4
> 2000 µm	0.11	145	16.7	3.78	33.7
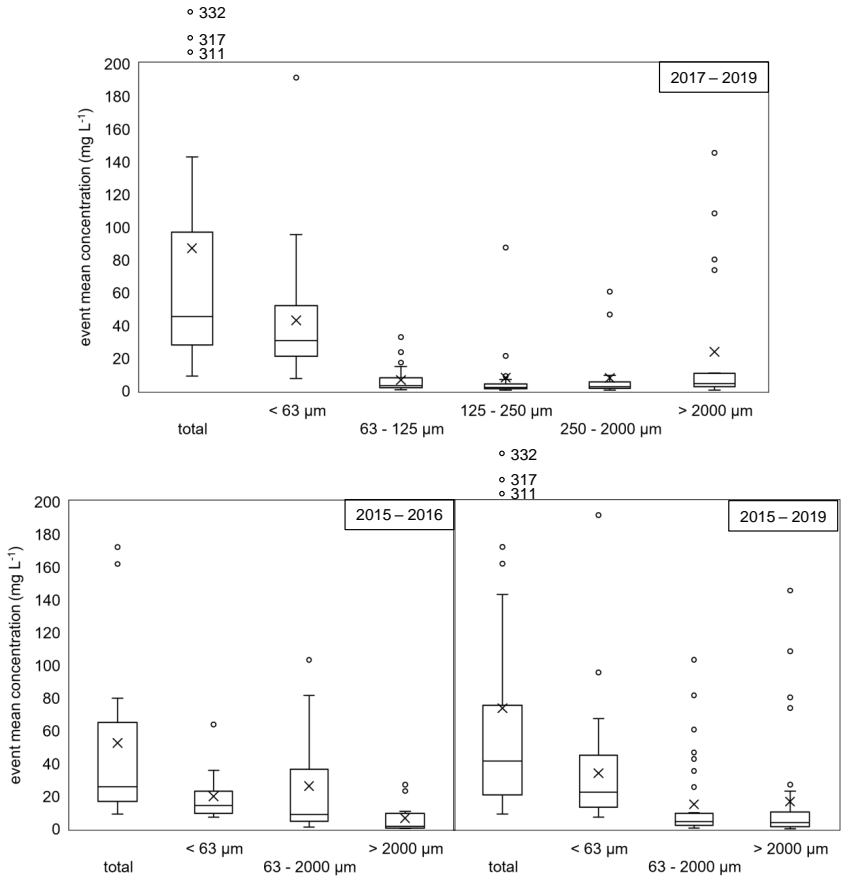
Fig. 5.10: Event mean concentrations as boxplots for the monitoring campaign 2017 – 2019 (n = 22), 2015 – 2016 (n = 14) and combined (n = 36).

5.2.4   Total Loads

The calculation of the load is based on the evaluation methods presented in chapter 4.5.1. The transported solid loads were calculated from the laboratory-determined event concentrations of the sampled flows with the corresponding discharged volumes. The sum of the loads results in the total inflow load.

In the same way as in the previous chapter, Tab. 5.5 and Tab. 5.6 show the minimum, maximum, mean, median and SD values of the event loads across the different particle size fraction as well as for the total TSS (0.45 µm to > 2000 µm) and Fig. 5.11 shows the

eventloads as boxplots. Consequently, the largest solid loads were found in the < 63 µm particle fraction.

Tab. 5.5: Event loads of TSS in kg (monitoring period 2017 – 2019, n = 22)

Size fraction	min	max	mean	median	SD
total	6.78	1131	260	102	330
< 63 µm	5.70	682	149	73.8	182
63 – 125 µm	0.41	111	19.8	10.1	29.0
125 – 250 µm	0.38	77.7	14.6	5.32	21.9
250 – 2000 µm	0.29	157	17.6	6.46	33.3
> 2000 µm	0.45	490	64.0	13.7	130

Tab. 5.6: Event loads of TSS in kg (monitoring period 2015 – 2019, n = 36)

Size fraction	min	max	mean	median	SD
total	6.78	1131	229	62.5	301
< 63 µm	3.94	682	119	45.0	152
63 – 2000 µm	1.08	581	66.3	20.5	116
> 2000 µm	0.00	490	43.8	7.10	101
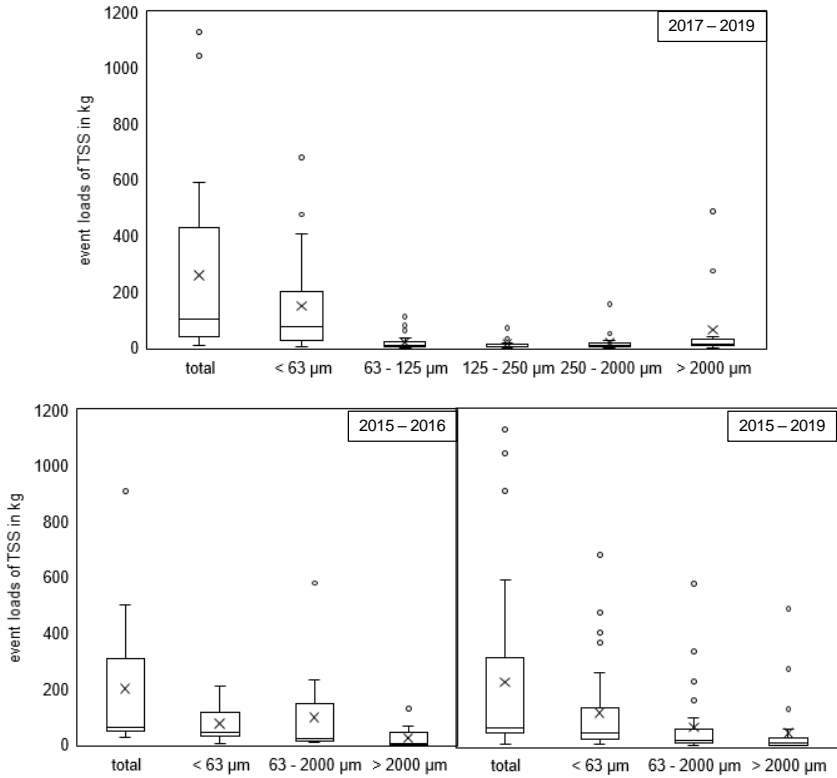
Fig. 5.11: Event loads of TSS in kg as boxplots for the monitoring campaign 2017 – 2019 (n = 22), 2015 – 2016 (n = 14) and combined (n = 36).

The distribution of the total solid loads (sum of 22 sampling events) across the particle size fraction and the relevant flows analysed in the investigation period 2017 – 2019 is shown in Fig. 5.12. The total load in the inlet to the stormwater treatment facility was composed of 57.6 % solids with a size smaller than 63 μm, 7.6 % solids with a particle size between 63 μm and 125 μm, 5.6 % solids with a particle size between 125 μm and 250 μm, 6.8 % solids with a particle size between 250 μm and 2000 μm and 22.4 % solids with a particle size larger than 2000 μm. The fine fraction < 63 μm was highest in CWD, accounting for almost 90 % of the total load. Followed by overflow with 83 % of the total load. The low proportion of coarse solids in the CWD and the increased proportion of these solids in the effluent illustrate the sedimentation process taking place in the treatment facility. The detailed treatment efficiency of the plant is quantified in the following chapter.
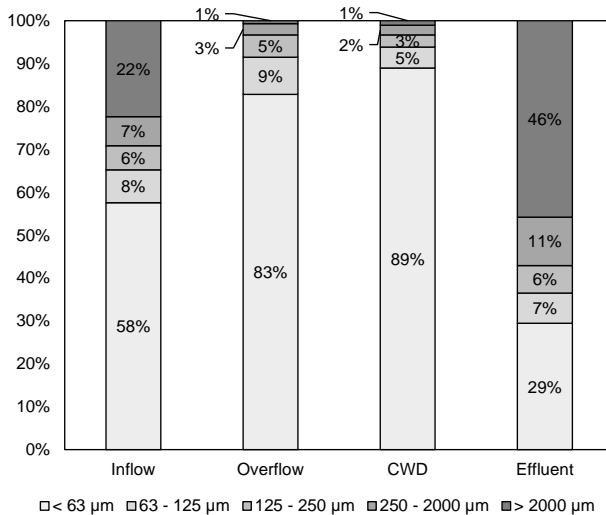
Fig. 5.12:   Distribution of the total load across the particle size fractions and the relevant flows (values rounded to whole numbers, monitoring period 2017 – 2019)

5.2.5   Treatment Efficiency

Subsequently, the treatment performance of the central stormwater treatment facility is evaluated. For this purpose, the solids load discharged into the water body was compared with the solids load in the inflow to the treatment facility, as described in 4.5.2. First, the efficiency for the monitoring period 2017 – 2019 and the analysed particle size fractions is quantified. The efficiency then is extended by the monitoring period 2015 – 2016.

Tab. 5.7 shows the accumulated loads of the sampled events, distinguished by sampled flows and analysed particle size fractions as well as the total TSS load removal efficiency of the treatment facility. It can be seen that a total of approx. 5.7 tonnes of solids were transported to the rainwater treatment facility as a result of the 22 sampled events during the 2017 – 2019 observation period. The discharge of solids into the water body was reduced by 48 % by the treatment plant. Just under 2.9 tonnes of solids were discharged to the water body and the remaining approx. 2.7 tonnes to the treatment plant. The reduction of the solids load, i.e. the treatment performance of the plant, decreased with decreasing particle sizes. The retention efficiency for coarse particles > 2.0 mm was 98 % and for < 63 µm it was 25 %. Additionally, Fig. 5.13 shows the load shares of the size fractions across the sampled flows in relation to the inflow. It can be clearly seen that for overflow and CWD the load shares decreased with increasing particle size. For the load shares in the Effluent which correspond to the removal

efficiency, the contrary is true, the load shares increased with increasing particle size, indicating the poorer settling properties of the finder particles.

Tab. 5.7: Accumulated loads of the sampled events, distinguished by sampled flows (inflow calculated) and analysed particle size fractions and the total TSS loads removal efficiency (monitoring period 2017 – 2019, n = 22)

Total TSS loads (kg)	total	< 63 µm	63 – 125 µm	125 – 250 µm	250 – 2000 µm	> 2000 µm
Inflow	5711	3288	437	320	387	1279
Overflow	2589	2143	225	134	68	18
CWD	377	335	18	11	9	4
Effluent	2745	809	193	175	311	1257
η_M	0.48	0.25	0.44	0.55	0.80	0.98

In Tab. 5.8 the minimum, maximum, mean, median and SD values of the individual treatment efficiencies of the sampled events is given. A comprehensive list can be found in the appendix (Tab. C.11 & Tab. C.12). It can be seen, that the respective efficiencies had a wide variation. The values of the standard deviation ranged from 0.09 for TSS > 2000 µm (2017 – 2019) to 0.26 for TSS 63 – 125 µm (2017 – 2019). The total treatment efficiency over the entire monitoring campaign had a SD of 0.25.
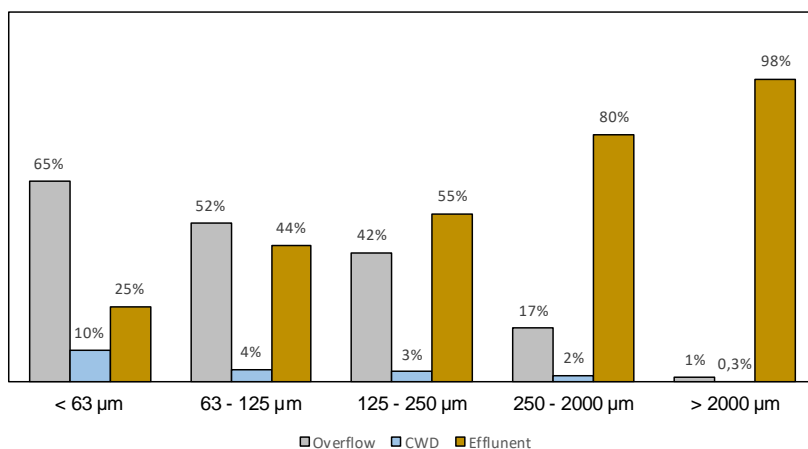
Fig. 5.13: Load shares of size fractions across sampled flows in relation to the inflow (monitoring period 2017 – 2019, n = 22)

The maximum efficiency of 100 % across all particle size fractions was caused by two single events (one in each investigation period) in which the entire discharged volume and thereby the total TSS load was directed to the wastewater treatment plant.

When considering the individual event efficiencies, it must be noted that there were sampling events in which up to 4 consecutive rain events were sampled (cf. 5.1). In the one case of 4 consecutive rain events, 3 of them were completely retained. The overall efficiency of this sampling event was therefore significantly higher than if the one "larger" event would have been sampled individually. The combined sampling of successive rainfall events, of which at least one was completely retained, was observed in 4 out of 36 samplings during the entire sampling period (2015 – 2019). This is one reason why the mean values of the individual treatment efficiencies were significantly higher than the treatment efficiency determined by the accumulation of the individual loads (Tab. 5.7 and Tab. 5.9)

Tab. 5.8: Descriptive statistics of individual treatment efficiencies of samples events (monitoring period 2017 – 2019, n = 22)

Size fraction	min	max	mean	median	SD
total	0.24	1.00	0.54	0.46	0.23
< 63 µm	0.11	1.00	0.41	0.31	0.25
63 – 125 µm	0.23	1.00	0.73	0.85	0.26
125 – 250 µm	0.13	1.00	0.80	0.87	0.22
250 – 2000 µm	0.43	1.00	0.85	0.92	0.16
> 2000 µm	0.70	1.00	0.95	1.00	0.09

If the 14 sampled events from the observation period 2015 – 2016 are included (see Tab. 5.9, Tab. 5.10, Fig. 5.14), the overall retention efficiency of the plant for total TSS increased slightly to 0.53 and for TSS < 63 µm the efficiency value increased to 0.26. While the coarse particle load could be reduced by up to 70 % by the rainwater treatment facility, the fine particle load was only reduced by less than a third (26 %). A poor treatment efficiency with regard to the fine particle fraction was also observed by different studies for different stormwater treatment systems (Fuchs et al. 2014; Charters et al. 2015; Lieske et al. 2021).

Tab. 5.9: Accumulated loads of the sampled events, distinguished by sampled flows (inflow calculated) and analysed particle size fractions and the total TSS loads removal efficiency (monitoring period 2015 – 2019, n = 36)

Total TSS loads (kg)	total	< 63 µm	63 – 2000 µm	> 2000 µm
Inflow	8526	4366	2525	1634
Overflow	3191	2564	600	27
CWD	839	661	166	12
Effluent	4496	1141	1759	1595
η_B	0.53	0.26	0.70	0.98
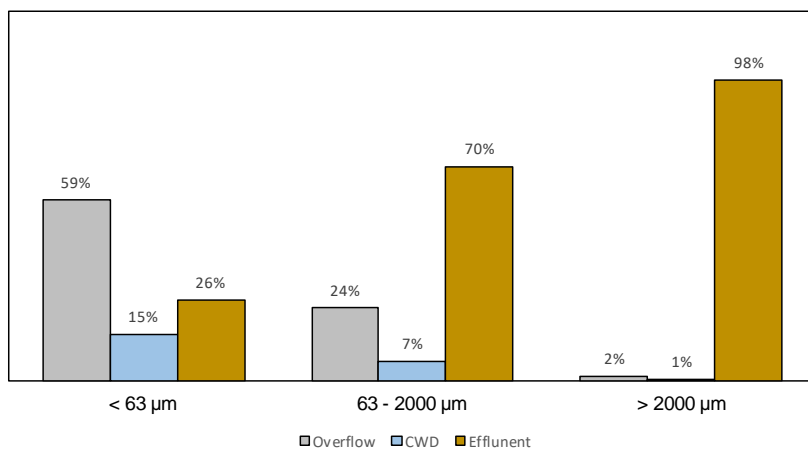
Fig. 5.14: Load shares of size fractions across sampled flows in relation to the inflow (monitoring period 2015 – 2019, n = 36)

Tab. 5.10: Descriptive statistics of individual treatment efficiencies of samples events (monitoring period 2015 – 2019, n = 36)

Size fraction	min	max	mean	median	SD
total	0.09	1.00	0.54	0.53	0.25
< 63 µm	0.05	1.00	0.39	0.33	0.25
63 – 2000 µm	0.21	1.00	0.76	0.86	0.23
> 2000 µm	0.43	1.00	0.93	0.99	0.12

5.2.6 Correlation Analysis

Tab. 5.11 shows the pearson correlation coefficients for TSS loads, TSS event mean concentrations, TSS removal efficiency, loss on ignition as well as the particulate and dissolved organic carbon load correlated with the ratio of $TSS_{<63}$ to TSS_{total} as well as several runoff and rainfall characteristics for the monitoring period 2015 – 2019. The correlations for which there are no values in the table were not carried out due to the dependency of the variables (e.g. EMC is calculated from the solid load).

Due to the fact that the calculation of TSS loads is based on the analysed mean concentrations of the sampled flows and their volume (cf. 4.3.1), the dependency shown in the table is comprehensible. Furthermore, there was a weak correlation between the duration of the rainfall and the total solids load. As shown in Tab. C.3 and Tab. C.5, the sampled rainfall events had comparatively low intensities. For this reason, the runoff volume correlated with the rain duration (peason correlation coefficient = 0.49). This also explains the correlation between total solids load and rainfall duration. Beyond this, no further correlations between loads or EMC with rainfall characteristics could be identified.

In terms of solids removal efficiency, it can be seen that this clearly depended on the proportion of fine particles. The larger the percentage of fine particles, the worse the efficiency of the treatment facility and vice versa. This was already clearly shown in the previous chapter and is once more underlined by the negative correlation between the TSS removal efficiencies and the the ratio of $TSS_{<63}$ to TSS_{total}. The equally clear negative correlation with the run-off volume illustrates that if the run-off volume exceeded the retention volume of the facility, the investigated rainwater treatment facility showed low TSS removal efficiencies. The weak negative correlation with rainfall depth should also be seen in this context.

No correlations were found between LOI and rainfall characteristics. However, there was a moderate correlation between the dissolved organic carbon load and the antecedent dry weather period, rainfall duration and rainfall depth.

Overall, the correlation analysis did not show any strong correlations. The results should be viewed with a certain caution due to the sample size.

Tab. 5.11: Pearson correlation coefficients for TSS loads ($B_{<63\mu m}$, B_{total}), TSS event mean concentrations ($EMC_{<63\mu m}$, EMC_{total}), and TSS removal efficiency ($\eta_{<63\mu m}$, η_{total}), loss on ignition ($LOI_{<63\mu m}$, LOI_{total}) as well as the particulate and dissolved organic carbon load (B_{POC}, B_{DOC}) correlated with the ratio of $TSS_{<63}$ to TSS_{total} ($f_{<63\mu m/total}$) as well as runoff and rainfall characteristics: runoff volume (V_{inflow}), antecedent dry weather period (ADWP), rainfall duration (D_p), mean rainfall intensities (I_{mean}) and rainfall depth (H_p). Bold values indicate correlation coefficients > 0.5 or < -0.5, * correlation is statistically significant at the significance level of 0.05 (two-tailed). n = 36 except n_{LOI} = 32 and n_{POC} = n_{DOC} = 22.

	$f_{<63\mu m/total}$	V_{inflow}	ADWP	D_P	I_{mean}	H_P
$B_{<63\mu m}$		**0.532***	0.147	0.275	0.210	0.209
B_{total}		0.421*	0.210	0.340*	0.162	0.201
$EMC_{<63\mu m}$		0.062	0.099	0.022	0.159	-0.151
EMC_{total}		-0.073	0.181	0.100	0.005	-0.182
$\eta_{<63\mu m}$	-0.474*	**-0.618***	0.054	-0.261	-0.239	-0.475*
η_{total}	**-0.689***	**-0.566***	0.118	-0.225	-0.160	-0.437*
$LOI_{<63\mu m}$	0.270	-0.238	-0.144	-0.021	-0.046	-0.099
LOI_{total}	0.323	-0.028	-0.082	-0.153	0.236	-0.090
B_{POC}	-0.218	**0.587***	0.111	0.404	0.313	0.190
B_{DOC}	0.106		**0.508***	**0.565***	0.180	**0.539***

5.3 Organic Micropollutants

Organic micropollutants have been analysed in dissolved and homogenised (dissolved + particulate) phase within samples of different particle sizes (cf. 4.3.2). The particulate amount of each particle size fraction was calculated by subtracting the homogenised phase and the dissolved phase. To evaluate the particle-bound pollutant concentrations (mass of pollutant per mass of particulate matter) the results of the subtraction were set in relation to the concentrations of TSS in the samples. For the calculation of the transported particulate pollutant loads, the particle bound pollutant concentrations were multiplied by the transported solid load. The dissolved loads were calculated with the average dissolved concentration across all particle size fraction and the respective runoff volume of the individual sampling events.

5.3.1 Event Mean Concentrations

The dissolved and particulate event mean concentration (EMC) in the influent to the treatment facility was calculated using the respective pollutant loads and the corresponding discharged volumes of Overflow, CWD and Effluent (cf. 4.5.1).

The distribution between particulate and dissolved EMC is shown in Fig. 5.15. A comprehensive list of all events and their descriptive statistical analysis can be found in the

appendix (Tab. C.13 & Tab. C.14). It can be seen that in the group of polycyclic aromatic hydrocarbons, the particulate concentrations exceeded the dissolved concentrations for almost all substances. The other substances, except for 4-nonylphenol (particulate and dissolved approximately equal), 4-tert-octylpenols, triphenylphosphates (particulate approx. half of dissolved), had much higher dissolved than particulate concentrations. Fig. 5.16 shows the distribution of particulate EMCs among the investigated particle size fraction for PAH, 4NP and TCPP as an example. All other substances showed the same distribution as PAH and 4NP. The concentrations were highest in the fraction < 63 µm. Only the organophosphates TCPP and TPP showed a different pattern. Here, the highest concentrations were found in the fractions 63 – 125 µm and 125 – 250 µm.
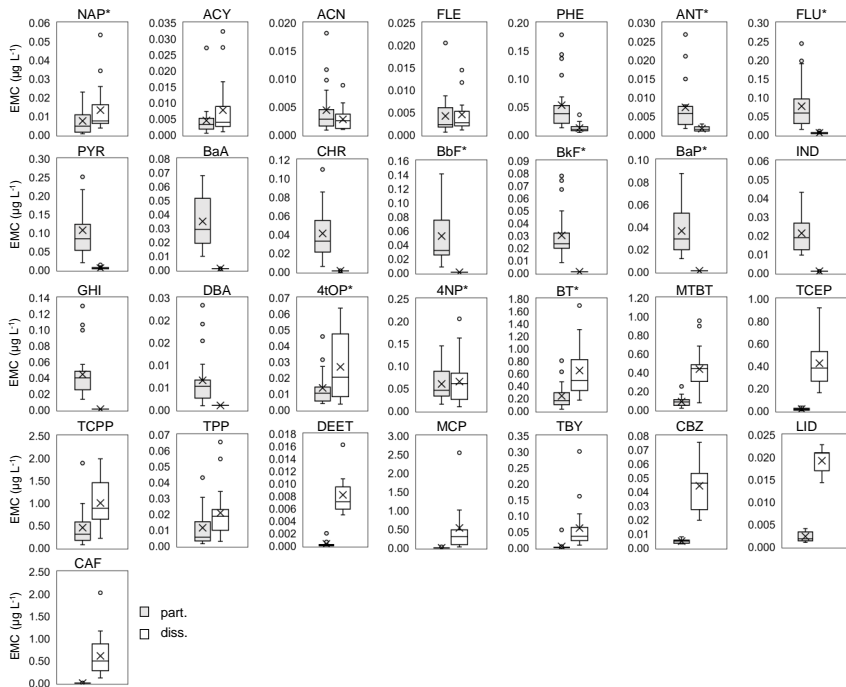
Fig. 5.15: Particulate and dissolved event mean concentrations of organic micropollutants analysed within the monitoring period 2017 – 2019 in µg L^{-1}. n = 22
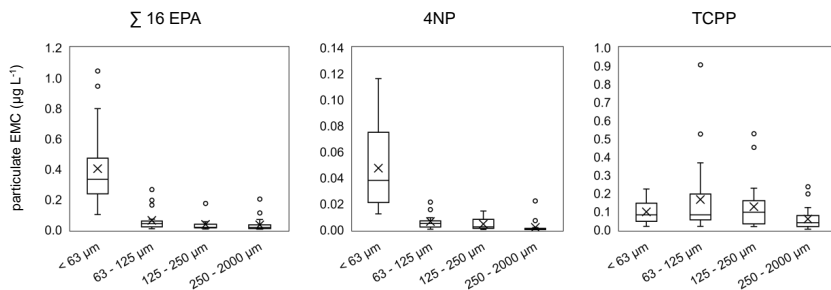
Fig. 5.16: Distribution of particulate event mean concentrations (EMC) across different particle size fraction in µg L^{-1}. n = 22

The highest concentrations (part. + diss.) were found in the group of organophosphates. Tris(1-chloro-2-propyl)phosphate (TCPP) showed the highest average EMC (mean: 1.45 µg L^{-1}, median: 1.26 µg L^{-1}) across all sampled events. Peak concentrations were up to 3.81 µg L^{-1}. These substances are used in large quantities as flame retardants in foam and insulation materials, plasticisers, and as additives in polyester resins in the construction industry and in coatings, among other things (Regnery und Puttmann 2010). Benzothiazole, which belongs to the group of industrial chemicals and primarily used as a vulcanisation accelerator, showed the second highest event mean concentrations (mean: 0.89 µg L^{-1}, median: 0.91 µg L^{-1}). In the group of the sixteen polycyclic aromatic hydrocarbons (16EPA), Pyrene showed the highest average concentrations (mean: 0.11 µg L^{-1}, median: 0.09 µg L^{-1}), followed by Fluoranthene (mean: 0.08 µg L^{-1}, median: 0.07 µg L^{-1}), which is classified as a priority substance by the EU Water Framework Directive (Directive 2000/60/EC). The order of PAHs with decreasing concentrations was as follows: PYR > FLU > PHE > BbF > GHI > CHR > BaP > BaA > BkF > IND > NAP > ACY > ANT > FLE > DBA > ACE. The substances benzo(b)fluoranthene, benzo(a)pyrene, benzo(k)fluoranthene, indeno[1,2,3-c,d]pyrene and benzo[g,h,i]perylene, which are also classified as priority substances, all exhibited concentrations that exceeded the annual average environmental quality standards (AA-EQS) of the EU Water Framework Directive, in some cases considerably. Occasionally, even the maximum allowable concentrations (MAC-EQS) were exceeded. Fig. 5.17 shows a direct comparison of the event mean concentrations in the outflow (Overflow + CWD) to the receiving waterbody of the priority substances analysed in this study with the environmental quality standards (Tab. 5.12) of the WFD. Depending on the size of the water body, a significant dilution of the discharge must be taken into account in the comparison. However, the median EMCs of the PAH BbF, BkF, BaP, IND and GHI exceeded the AA-EQS by factors of 10 – 100. It must be assumed that this resulted in a significant local impairment of the receiving water body.
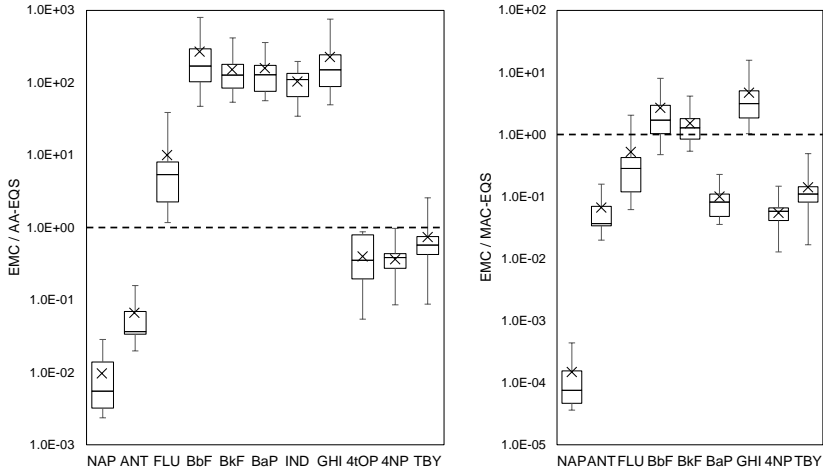
Fig. 5.17: Risk quotients from the event mean concentrations in the outflow (Overflow + CWD) to the receiving water body and the environmental quality standards of the EU WFD. AA-EQS: annual average environmental quality standard, MAC-EQS: maximum allowable concentration environmental quality standard. n = 22

Tab. 5.12: Environmental quality standards for priority substances according to the EU Water Framework Directive (Directive 2013/39/EU), given as annual average (AA-EQS) and maximum allowable concentration (MAC-EQS) in $\mu g\ L^{-1}$.

Priority substances	AA-EQS ($\mu g\ L^{-1}$)	MAC-EQS($\mu g\ L^{-1}$)
NAP	2.00	130
ANT	0.10	0.10
FLU	6.3×10^{-3}	0.12
BbF	1.7×10^{-4}	1.7×10^{-2}
BbK	1.7×10^{-4}	1.4×10^{-2}
BaP	1.7×10^{-4}	0.27
IND	1.7×10^{-4}	not applicable
GHI	1.7×10^{-4}	8.2×10^{-3}
4tOP	0.1	not applicable
4NP	0.3	2.0
TBY	6.5×10^{-2}	0.34

Although PAHs concentrations exceeded EQS, the levels are considered average compared to other studies. Zgheib et al. (2012) studied three urban catchments located in Paris and its suburbs. Across all study sites they found a median concentration for the 16 PAHs of about 1.6 $\mu g\ L^{-1}$. The composition pattern of the PAH showed a similar distribution to this study (dominated by Pyrene, followed by Fluoranthene, Phenanthrene and Chrysene). PAH with high molecular weight (HMW) indicate pyrolytic origin

for example from gasoline combustion of vehicles or from residential heating. This explains the much higher PAH contamination for Paris as it has a much higher density of combustion sources than the catchment in this area. The same applies to the values of a similar study in Berlin. Wicke et al. (2015) found mean values for the 16 EPA PAH of 1.17 µg L^{-1} dominated by Flouranthen and Pyren.

The study in Berlin also examined organophosphates as well as industrial chemicals. Yet, the determined concentrations for TCPP (mean: 0.47 µg L^{-1}) are significantly lower than those found in this study. Benzothiazole (BT) and 2-methylthiobenzothiazole (MTBT) from the industrial chemicals group, had mean values across all catchments of 0.54 and 0.17 µg L^{-1}. Compared to the concentrations of this study with 0.89 µg L^{-1} (BT, mean) and 0.53 µg L^{-1} (MTBT, mean) the values of the RFM Haid catchment seem significantly higher. These substances are used as vulcanisation accelerators in tyre production, for instance. They are released into the environment through tyre abrasion and get washed of by urban stormwater runoff. This association becomes apparent when looking at the measured concentrations of a sub-catchment area of the study in Berlin. Here, the street runoff of two heavily trafficked roads was sampled (15,000 – 22,500 vehicles per day). The mean BT concentrations was 1.14 µg L^{-1} (max. 3.5 µg L^{-1}).

Substances untypical of surface runoff, such as caffeine, lidocaine and carbamazepine, were also analysed in the samples. These were intended to provide information about possible misconnections of wastewater to the storm sewer. In all samples examined, caffeine (0.12 -2.03 µg L-1) was detected. In their study, Wicke et al. (2015) suggest that caffeine may also originate from discarded coffee cups washed out by the rain. However, since pharmaceutical residues of LID (min: 0.01 µg L-1, max.: 0.02 µg L-1) and CBZ (min: 0.02 µg L-1 max. 0.08 µg L-1) were also found in five samples, the possibility of misconnections cannot be completely ruled out. However, no further evidence of discharged wastewater such as toilet paper, food scraps or faeces were detected in the system. It is assumed that the investigation was not significantly affected by wastewater, as the discharged stormwater volume exceeds the volume of possible misconnections by far. In the further evaluation, these substances are partially included, but are not discussed any further.

5.3.2 Total Loads

In the previous chapter it has been pointed out that the urban stormwater runoff of the investigated catchment area showed increased contamination with organic micropollutants. The focus in this part lies on the distribution between the dissolved and the particulate fraction of the transported pollutant load on basis of the sampling events. Information on the distribution between particulate and dissolved fractions is particularly relevant with regard to the potential treatability of urban stormwater runoff and for the selection of the best management practises (BMPs). The absolute pollutant loads of the individual sampling events can be found in the Appendix (Tab. C.15). Furthermore, the distribution of the particulate pollutant loads among the investigated

particle size fractions will be discussed. Since the EMC are based on the loads covered in this section, the load distribution between particulate and dissolved fraction can also be related to the mean distribution of the EMC. Individual sampling events may deviate.

The distribution of the measured pollutant load between particulate and dissolved fractions correlated with the octanol-water coefficient of the individual substances. This distribution coefficient can serve as a measure for the relationship between hydrophilicity and lipophilicity of a substance and is known for a vast number of organic compounds. As can be roughly seen in Fig. 5.18, the particulate fraction increased with the log K_{OW}. The Spearman correlation resulted in a rank correlation coefficient of 0.869 with a p-value < 0.05. This relationship is more evident on sample basis, as depicted in Fig. 5.26 (cf. 5.4.4).
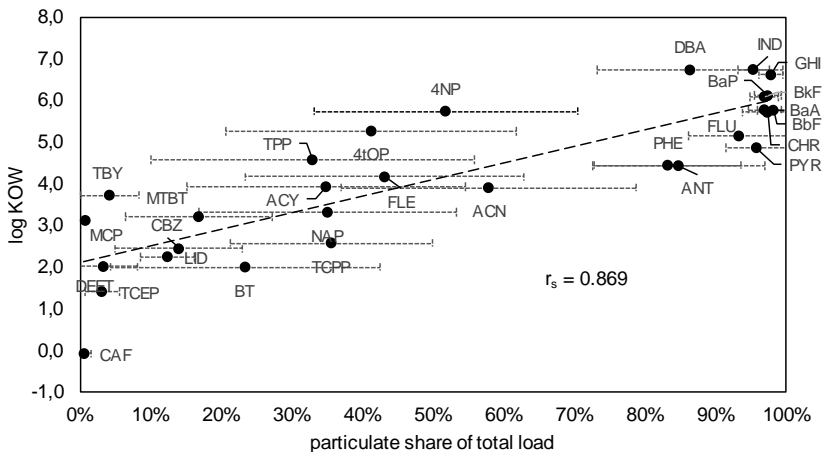
Fig. 5.18:   Correlation of log K_{OW} and the particulate fraction of the total pollutant load for all 29 investigated substances (error bars indiciatig standard deviation of individual event loads).

The particulate fraction of the HMW PAHs, which are composed of four or more aromatic rings (FLU, PYR, BaA, CHR, BbF, BkF, BaP, GHI, IND, DBA), was between 86 % (DBA) and 98 % (BbF, GHI). PHE and ANT, from the group of the low molecular weight (LMW) PAHs (composed of less than four aromatic rings (NAP, ACY, ACN, FLE, PHE, ANT)), also showed a high particulate fraction (83 % and 85 %), whereas for NAP, ACY, ACN and FLE the particulate fraction was between 35 % (NAP, ACY) and 58 % (ACN). It needs to be mentioned, that for BaA 78 % and for CHR 76 % of the values measured in the dissolved phase were below the LOQ, for BbF, BkF, BaP, GHI, IND, DBA all values were below the LOQ. Therefore, these PAHs are present exclusively in the particulate fraction. The dissolved fraction shown here is due to the worst-case approach (for

substances with quantifiable values in the homogenised phase and values below LOQ in the dissolved phase, a value of 0.5 times LOQ is used for the calculation (cf. 4.3.2, 4.5.1)). For most of the other substances, the total pollutant load transported by stormwater runoff was dominated by the dissolved fraction. The nonylphenols investigated showed the largest particulate fraction with 52 % (4NP) and 48 % (4tOP) followed by the organophophates TCPP (36%) and TPP (33%). The particulate fraction of TCEP was only 3 %. BT and its metabolite MTBT showed a particulate content of 23 % and 17 %, respectively. With a particulate content of 3 %, TBY, which is used as a biocide in roof and facade paints, wall protection agents and sealants, was mainly transported in dissolved form.
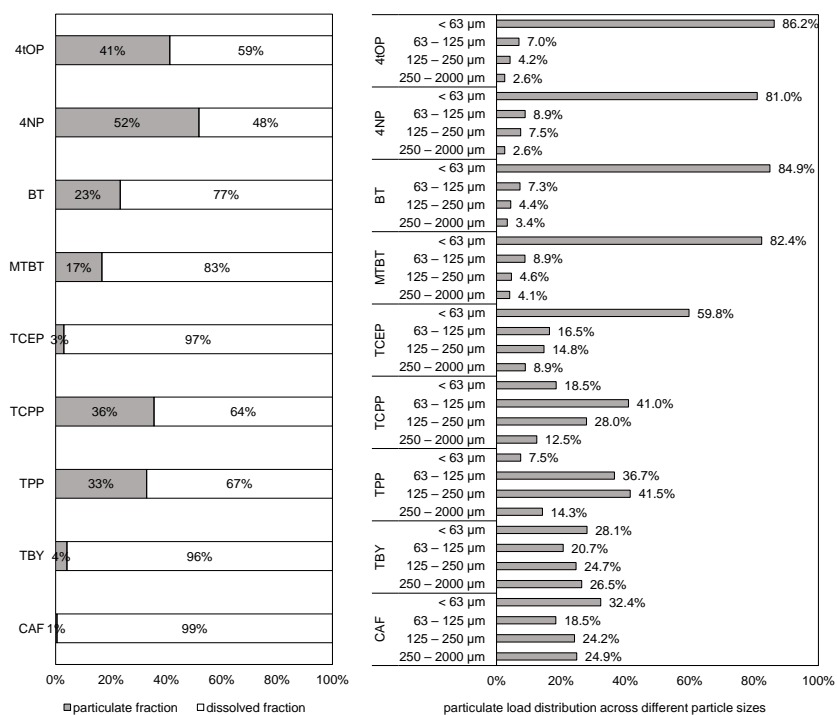
Fig. 5.19: Total pollutant load distribution for industrial chemicals, organophosphates, terbutryn (biocide) and caffeine of sampling events (n = 22).

Fig. 5.19 and Fig. 5.20 show the particulate transported pollutant load distributed over the investigated particle size classes (distribution over particle sizes mainly relevant for substances with high particulate fraction). The distribution was very similar for all PAHs. The proportion dominating the total load of pollutants was transported with particles < 63 μm (74 – 80 %). The load fractions decreased with increasing particle

size. In the particle size fraction 63 – 125 µm the proportion was between 10 % and 13 %, in the fraction 125 – 250 µm the proportion was between 6 % and 10 % and in the largest fraction of 250 – 2000 µm the proportion was only between 4 % and 7 %. This trend continued for the substances in the industrial chemicals group. The shares in the fraction < 63 µm were over 80 % and decreased continuously. In the size fraction 250 – 2000 µm, the proportion was about 2 – 4 %. The organophosphates TCPP and TPP showed a completely different distribution. The particle size fraction < 63 µm accounted for only 18.5 % (TCPP) and 7.5 % (TPP) of the total particulate pollutant load. The largest proportion for TCPP was in the size fraction 63 – 125 µm with 41 % and for TPP in the size fraction 125 – 250 µm with 42 %. A possible explanation for this would be that, since TCPP and TPP are used as flame retardants in, among other things, cleaning rags or sponges, they may have been transported directly from a car wash, for example, as sponge particles with sizes between 63 – 250 µm to the rainwater treatment plant. And thus, caused increased concentrations these particle size classes. The load distribution across the particle size fractions for TCEP and the biocide TBY will not be evaluated because the dissolved phase clearly dominates the pollutant load. Hence, the particulate distribution is negligible with regard to treatability by rainwater treatment facilities.

The results show that, of the substances investigated, PAHs are predominantly found in the solid phase, as has often been documented. Therefore, it is also known that the emitted loads can be reduced by retaining particulate matter in the urban runoff, e.g. in a stormwater treatment facility. This is not the case to the same extent for the remaining investigated substances. Even if some of the substances (e.g. 4NP, 4tOP) still have a significant particulate fraction, the dissolved part clearly predominates. The dissolved load cannot be significantly reduced purely by sedimentation, which is a common BMP in stormwater management. Furthermore, it becomes clear that especially the fine fraction of particles (< 63 µm) plays a significant role for the absolute pollutant load. This, in turn, is of particular importance with regard to treatability, as this particle fraction can also only be removed to a limited extent by means of sedimentation (Charters et al. 2015).

In order to further investigate the distribution of organic trace substances among solids of different particle sizes, the particulate fraction of the pollutants is compared to the amount of particulate matter (in TSS) on the basis of the analysed individual samples.
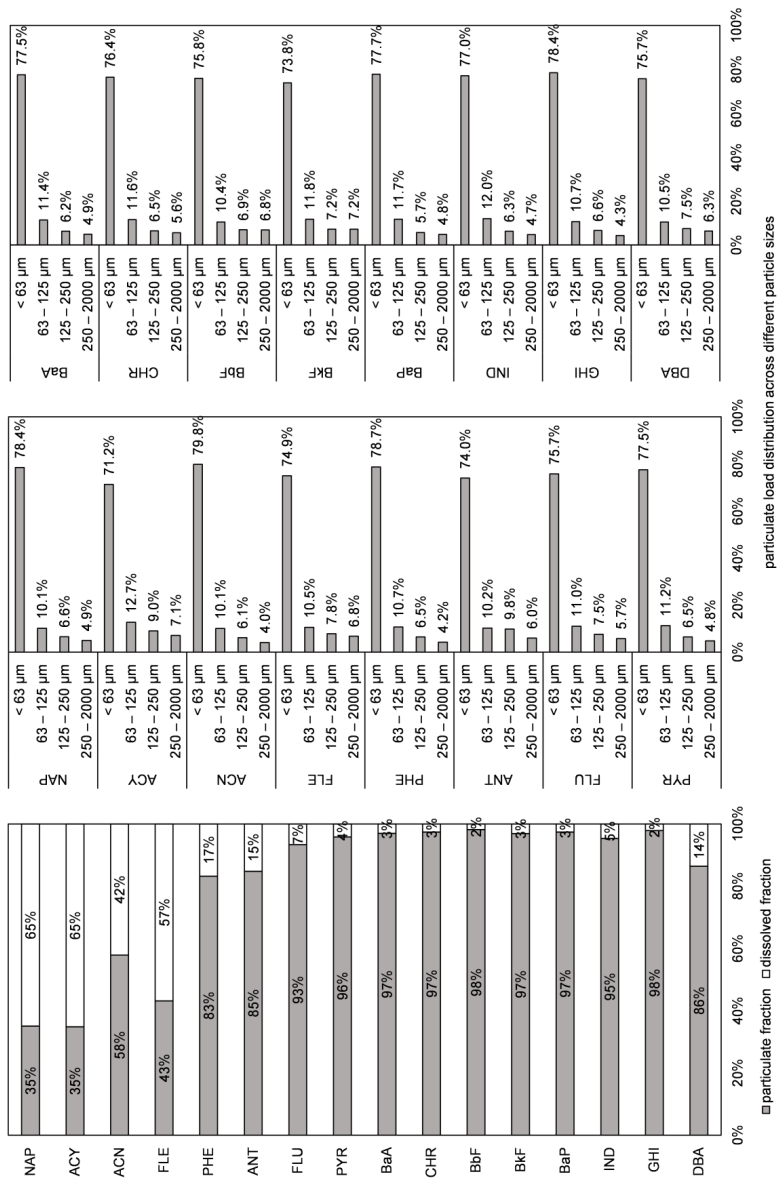
Fig. 5.20: Total pollutant load distribution for PAH of sampling events (n = 22).

5.3.3 Pollutant Concentrations across Different Particle Size Fractions

In the previous chapter, the distribution of particulate pollutant loads over different particle size fractions was shown based on the load of the sampling events. In this chapter, the particle-bound pollutant concentrations of the investigated substances are presented on the basis of the analysed individual samples across all sampled flows. For this purpose, the analysed particulate pollutant concentrations (homogenised phase minus dissolved phase) were divided by the TSS concentrations determined in the respective samples. An overview of the distribution of particle-bound pollutant concentrations across the particle size fractions investigated is given in Fig. 5.21 and Fig. 5.22.

For the LMW PAHs, a mostly equal loading of the particles was found across the particle size fractions. PHE showed a slightly higher concentration in the size fraction 63 – 125 µm. For HMW PAHs, a slight decrease in concentration with increasing particle size was seen. This trend seems to increase with the molecular weight of the substances. For FLU, PYR and BaA the mean concentrations in the size fractions < 63 µm and 63 – 125 µm were almost identical. From BbF onwards, the differences in the particle size fractions became larger. An even more pronounced decrease in concentration with increasing particle size was seen for alkyphenol 4tOP. Whereas the alkyphenol 4NP showed an almost equal average concentration in the size classes < 63 – 250 µm. Only the fraction 250 – 2000 µm showed significantly lower concentrations. The greatest differences between the concentrations of the particle size fractions as well as the highest particle-bound pollutant concentrations were detected for the organophosphate TCPP. The highest concentrations were found in the range 63 – 250 µm. TCPP also showed relatively wide variations in this size range. A similar distribution, but with lower concentrations and less variations, was found for TPP.
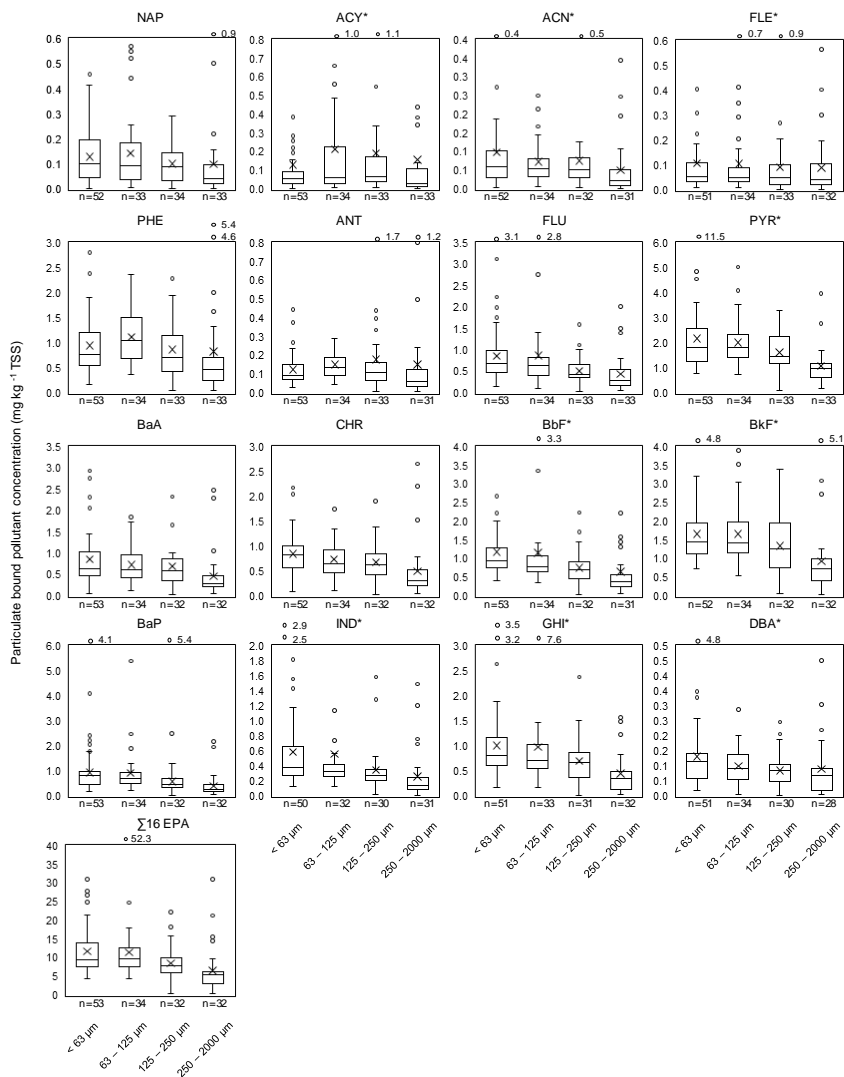
Fig. 5.21: Particle-bound pollutant concentrations for across different particle size fractions in mg kg^{-1} – part 1 (PAH)
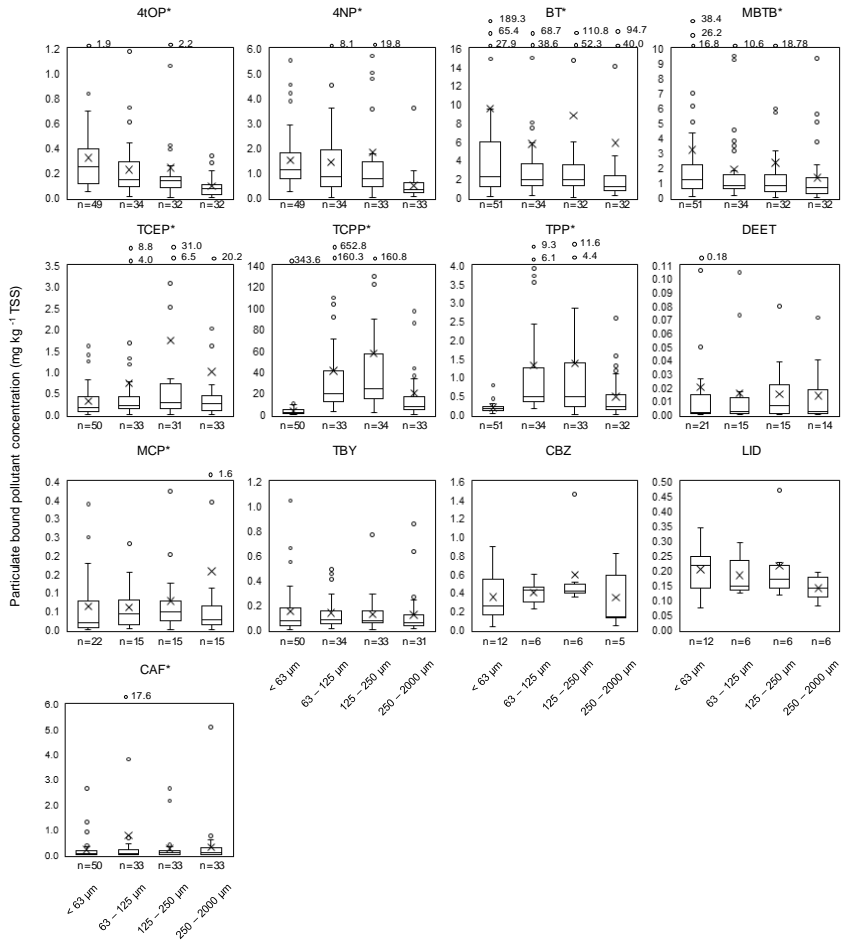
Fig. 5.22: Particle-bound pollutant concentrations across different particle size fractions in mg kg^{-1} – part 2 (other substances)

In terms of the PAHs the results are consistent with the findings of Herngren et al. (2010). In their study, the distribution of PAHs across different particle size classes (< 0.45 μm, 0.45 – 75 μm, 75 – 150 μm and > 150 μm) was investigated in urban stormwater runoff in Queensland, Australia. It was found that regardless of land use and rainfall characteristics, the highest PAH concentrations in the particles were between 0.45 μm and 150 μm. No studies were found on the distribution of particle-bound concentrations for alkylphenols and organophosphates in urban stormwater context. Björklund et al. (2009) investigated the occurrence of the alkyphenol 4NP in

sediments from a stormwater sedimentation chamber in Stockholm, Sweden. The determined concentrations were in the range of 0.75 – 1.5 µg g^{-1} dw (dry weight) and thus significantly lower than the particle-bound concentrations measured in Freiburg-Haid (mean values: < 63 µm: 1.5 µg g^{-1} TSS; 63 – 125 µm: 1.42 µg g^{-1} TSS, 125 – 250 µm: µg g^{-1}TSS, 250 – 2000 µm: 0.48 µg g^{-1} TSS, sum: 5.24 µg g^{-1} TSS). Strömvall et al. (2007) reported values in sediment from a stormwater pond of 4-NP with 3.1 µg g^{-1} dw.

The question arises as to how significant the results are for substances with only a low particulate content. The methods used in this study do not allow a substantiated answer to this question based on measurement data. However, it is assumed that the adsorption behaviour of these substances is more strongly influenced by other factors due to their physico-chemical properties (e.g. much stronger influence of dissolved organic matter) and thus the significance of these results also decreases with decreasing particulate content. With regard to practical conclusions, however, it must also be noted that for substances with a high dissolved fraction, the particle-bound concentration of different particle sizes is of secondary importance. To significantly reduce the load of these substances in urban stormwater runoff, more than just particle retention is needed. Moreover, as shown in the previous chapter, the largest pollutant load of the mainly particle-bound pollutants is transported in the size fraction < 63 µm. Therefore, if the treatment measure is optimised to reatin this size fraction, the remaining particle-borne fraction of the mainly dissolved pollutants will also be retained, regardless of whether the particle-bound concentration is highest e.g. between 125 – 250 µm.

5.3.4   Phase Distribution and Association with Organic Matter

In this section the phase distribution of the investigated pollutants will be evaluated on the basis of the analysed individual samples across all sampled flows. Therefore, the particulate fraction index f_p as well as the equilibrium partitioning coefficient K_D (cf. 4.5.3) were calculated. Their distribution is illustrated in Fig. 5.23 and Fig. 5.24 (Fig. 5.19 and Fig. 5.20 show the distribution of the total loads). Furthermore, the occurrence of pollutants in the particulate phase as well the dissolved phase and its association with organic matter in the respective samples will be investigated. Therefore, correlation analyses were carried out between the particulate concentrations of pollutants with the TOC concentrations in the individual samples. Respectively, the dissolved concentrations were compared with the content of DOC in every sample analysed.

As expected from literature (eg. Pitt et al. 1999, Bathi 2008) the investigated PAH in this study clearly tended to accumulate more in the particulate phase than in the dissolved phase due to their hydrophobic nature (high K_{OW}). This was most obvious for the HMW PAH. The mean particulate fraction indices across all particle size fraction ranged from 0.93 (DBA) to 0.99 (BaA, CHR, BbF, BaP, GHI).

The LMW PAH showed mean particulate fraction indices between 0.68 (NAP) and 0.94 (PHE). Naphthalene showed the highest variance followed by Flouren and Acenaphthen. This wide range indicates increased mobility of these substances in urban stormwater runoff, which is a major concern especially with regard to the toxicity of LMW PAHs to aquatic life (Smith et al. 1988).

The investigated nonylphenols showed mean particulate fraction indices of 0.71 (4NP) and 0.81 (4tOP) clearly showing their tendency towards the particulate fraction in this study. Yet, 4tOP showed a larger variability across all the samples. The phase distribution of the pollutants BT and MTBT also showed large variations. This is the reason why, although the mean phase distribution showed values for the particular fraction of 0.55 (MTBT) and 0.64 (BT) across all the samples, only 17 % of the total MTBT load and 23 % of the total BT load was transported adsorbed to particles when referring to the total loads transported by the sampled events (cf. 5.4.2). Similar large variations in phase distribution were seen with the organophosphates. Whereas TCEP showed a clear tendency towards the dissolved phase (mean particulate fraction indices of 0.26), TCPP and TPP tended towards the particulate phase (mean particulate fraction indices of 0.73 and 0.81).

In the case of biocides, in addition to Terbutryn, Diethyltoluamide (DEET) and Mecoprop (MCP) were also analysed for a certain period (the first ten events sampled) and detected in all samples. DEET is a very common active ingredient in insect repellents applied to the skin or to clothing, and Mecoprop is used in bituminous roof sealing membranes (Bucheli et al. 1998). However, due to the small amount of data compared to the other substances, these were not included in the previous evaluation. Yet it can be seen that both substances clearly showed a tendency towards the dissolved phase. Across all substances TBY showed the largest variability with a mean particulate fraction indices of 0.49.

The equilibrium partitioning coefficient K_d expresses the ratio between the constituent concentration "sorbed" to PM and the dissolved concentration. Its distribution shown in Fig. 5.24 follows the pattern of the distribution indices, thereby underlining the tendencies described beforehand.
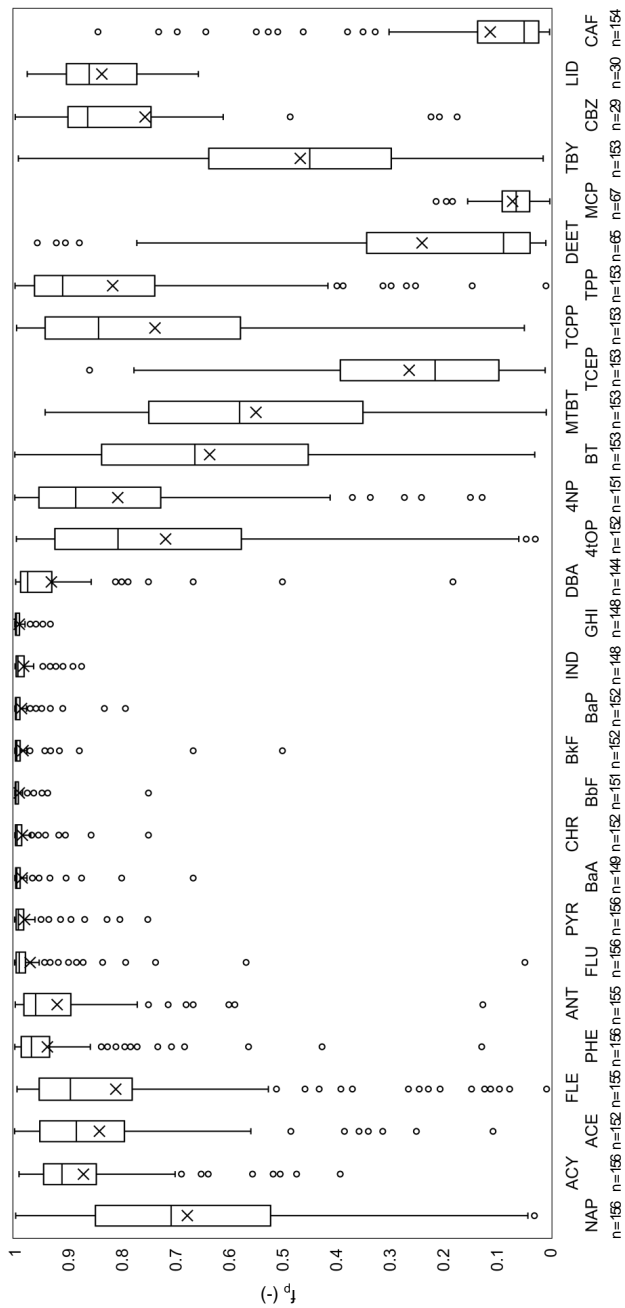
Fig. 5.23: Distribution of the particulate fraction, fp, of the analysed organic micropollutants on sample basis
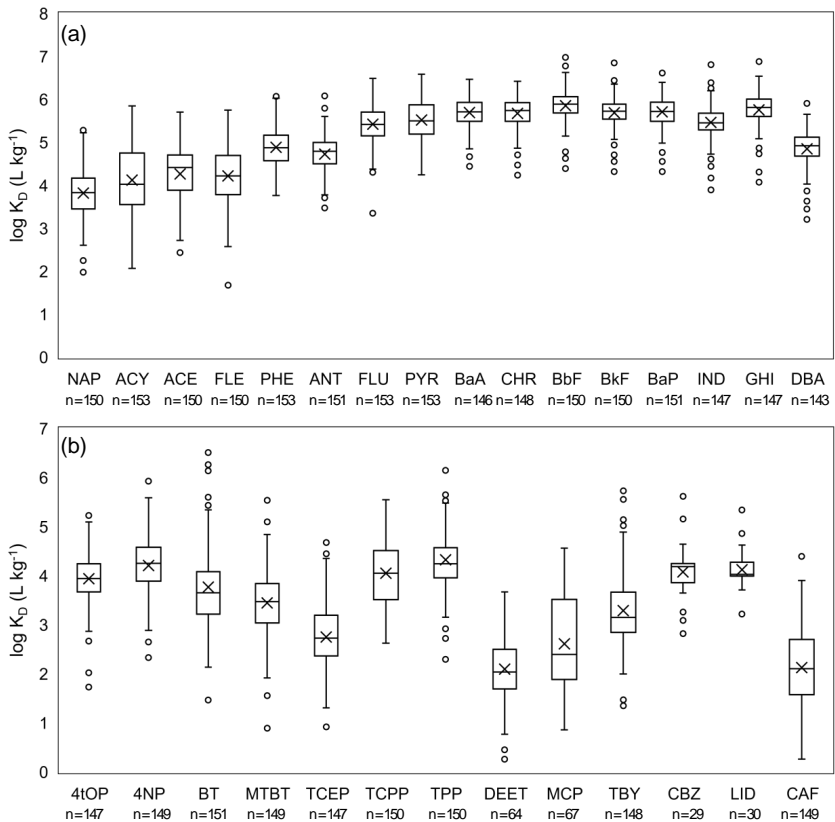
Fig. 5.24: Equilibrium partitioning coefficient, log K_D (L kg^{-1}) on sample basis. (a) PAHs and (b) other substances.

Fig. 5.25 shows the phase distribution of the substances across the particle size classes investigated. In the case of PAHs, the differences between the particle sizes decreased with increasing molecular weight. For both nonylpheonols, there was a recognisable trend towards more dissolved substances with increasing particle size. BT and MTBT were slightly more particle-bound in the particle size 63 – 125 µm. The organophos-phates showed a higher particulate occurrence in the size fractions 63 – 125 µm and 125 – 250 µm. Overall, it can be noted that the phase distribution of the substances across the different particle size classes depicts the distribution of the particle-bound concentrations of Fig. 5.21.
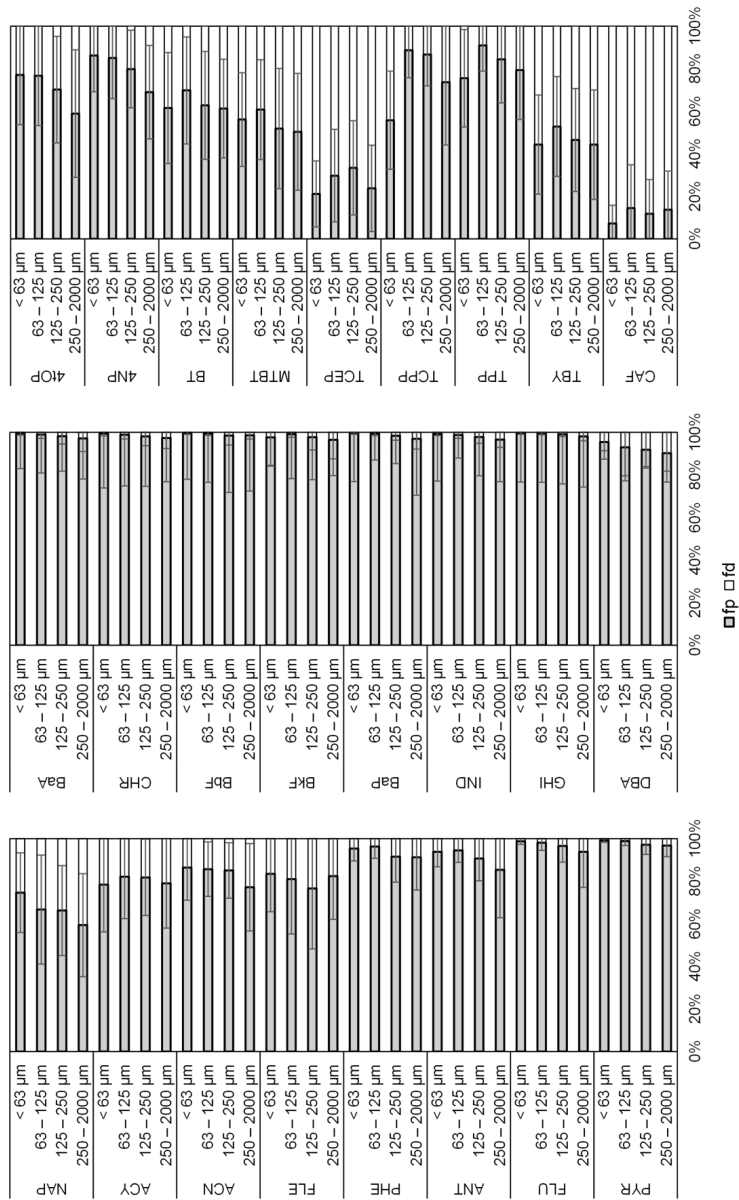
Fig. 5.25: Mean distribution of the particulate (fp) and dissolved (fd) fraction, in different particle size fractions. Error bars indicating standard deviation of values.

On average across all sampled flows and particle size classes, the phase distribution of the substances follows their octanol-water partition coefficients relatively well. The higher this value, the higher the particulate occurrence of this substance in urban stormwater runoff. In this study, a spearman rank correlation coefficient (r_s) of 0.838 (significant at the 0.05 level) was found for this relationship. Fig. 5.26 shows that K_{OC}, the distribution coefficient normalised to the organic content (particulate fraction of TOC used for the calculation, cf.4.5.3) is even better suited to describe the phase distribution of the substances (r_s of 0.993, significant at the 0.05 level). It can be clearly seen that the substances with similar particulate fraction but different log KOW values (data points lying on an imaginary horizontal line in the left diagram) are grouped together in the right diagram. For example, the HMW PAHs now form a clear cluster with the exception of DBA. This is not surprising, as the KOW values are empirical literature values that merely reflect the physico-chemical properties of the substances. The log KOC values, on the other hand, are based on the actual measurement results of this study and thus also reflect the individual boundary conditions of the catchment area or the sampling and analysis methodology, for example.
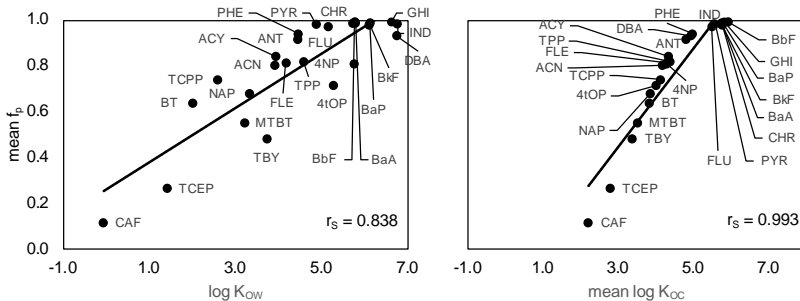
Fig. 5.26: Correlation of mean phase distribution, expressed as particulate fraction, f_p, with literature values of log K_{OW} and mean log K_{OC} of the investigated substances.

In the following, the association of the investigated substances with organic matter is further examined. It will be investigated whether the distribution of the particle-bound concentration across the different particle size fractions can be attributed to their organic content. Therefore, in a first step the particulate concentration was correlated with the respective particulate organic carbon (POC = TOC-DOC) concentration determined in each sample. Furthermore, the dissolved concentrations were correlated with the respective DOC concentrations. A comprehensive overview of the correlation analysis can be found in the appendix (Tab. C.17). Fig. 5.27 shows the scatter plots of the particular PAH concentrations (16EPA) with the POC concentrations across the analysed particle size fractions. There was a strong correlation for the particle size fractions < 63 μm – 2000 μm (r between 0.953 and 0.809). Similar observations for PAHs have been documented in the literature (e.g. Karickhoff et al. 1979, Evans et al. 1990, Herngren et al. 2010). A clear trend of decreasing strength of the correlation with

increasing particle size could be observed. In the particle size fraction 250 – 2000 μm, a moderate correlation, for some PAH like ACN or PHE, between dissolved concentration and DOC content (Kalmykova et al. 2013) could also be found. This could be one possible reason why the correlation strength decreased with increasing particle size. Similar patterns could be observed for other substances as well. BT and MTBT, for example, also showed strong/moderate correlations for their particulate concentrations with POC content especially in the sizes of 63 – 250 μm (r: 0.605 – 0.749) and a reduced correlation for the size fraction 250 – 2000 μm (r: 0.488 – 0.538). Yet both substances showed moderate/strong correlations in the largest particle size fraction between the dissolved concentration and the DOC content (BT r: 0.619, MTBT r: 0.887). It should also be noted that the decreasing correlation strength with increasing particle size may also be partly related to measurement uncertainties of TOC in the large particle size fraction due to difficult sample handling (cf. 5.2.2).
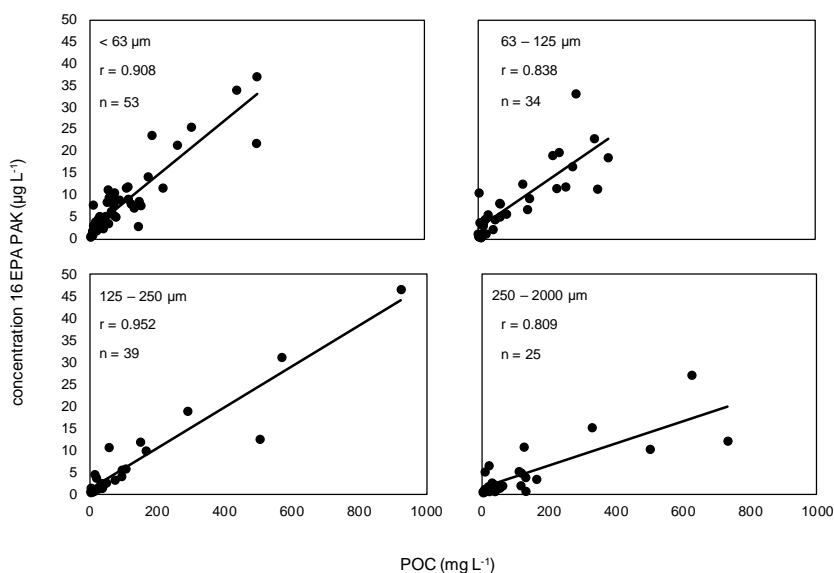
Fig. 5.27: Correlation of particulate PAH (16 EPA) concentration (μg L^{-1}) with the POC concentration (mg L^{-1}) across different particle size fractions on sample basis. r = Pearson correlation coefficient, correlation significant at the 0.05 level.

To further investigate the role of organic matter in the phase distribution of the investigated substances across the different particle size fraction, three reference substances, Naphthalene, Flouranthene and 4-Nonylphenol were chosen depending on their physico-chemical properties (cf. Tab. 5.13) and evaluated in more detail. Naphtalene is found both in dissolved and particulate form in this study (mean f_p = 0.68). Fluoranthene was found mainly particulate (mean f_p = 0.97) and 4NP has a similar log

K_{OW} as FLU but showed similar variations in the phase distribution as NAP (mean f_p = 0.81). It is assumed that samples with a higher particulate content (f_p) also have higher organic content. For the further investigation, the log K_{OC} values (distribution coefficient normalised to organic matter) were calculated on the basis of the individual samples (cf. 4.5.3) and compared with the phase distribution, expressed by f_p. In addition to log K_{OC}, POC calculated in each sample was compared with the phase distribution.

Tab. 5.13: Physico-chemical properties of the selected reference substances to further investigate the phase distribution and its association with organic content

	Literature		Log K_{OC} (median values, monitoring campaign)				
	Log K_{OW}	Log K_{OC}	total	< 63 μm	63 – 125 μm	125 – 250 μm	250 – 2000 μm
NAP	3.30	3.17	3.86	3.94	3.74	4.00	3.69
FLU	5.16	4.18	5.55	5.70	5.68	5.42	5.40
4NP	5.76	4.51	4.22	4.34	4.34	4.13	3.81

The correlations were evaluated using both the respective scatter plots (Fig. 5.28 and Fig. 5.29 for NAP; FLU and 4NP see appendix (Fig. C.4 – Fig. C.7) and Pearson correlation coefficients (Tab. 5.14). NAP and 4NP showed approximately the assumed correlations between f_p and log K_{OC}. With correlation coefficients of 0.558 NAP and 0.354 4NP (significant at the 0.05 level). Reasons for the poor correlation (large variations) cannot be clearly identified and will be further investigated in the following. In 39 of the 113 samples used for this evaluation, a high COD:TOC ratio was detected (> 5.3). TOC is the carbon content of an organic compound/substrate, and COD is the oxygen equivalent of the same compound/substrate, serving as electron donor during full oxidation. The COD/TOC ratio thus indicates the oxygen demand required for the oxidation of the carbon. The value thereby characterises the average degree of oxidation of the organic compounds contained in the samples. Values > 5.3 indicate the presence of strongly reduced compounds such as petroleum hydrocarbons. For this reason it is suspected that these 39 samples with high COD:TOC ratio are contaminated with mineral oil components. Previous investigations in the same catchment already detected mineral oil pollution (Stotz und Dittmer 2009). It is assumed that this had an influence on the phase distribution. Evidence could be obtained by comparing the correlations of f_p and log K_{OC} and of f_p and POC between the different samples. For this purpose, the correlation of the total data (all samples) is compared with the correlations of the samples with a COD:TOC ratio of less than and greater than 5.3, both for all particle sizes together and differentiated according to the particle size fractions.

Tab. 5.14: Pearson correlation coefficients of the correlations between phase distributions, expressed as fp, and the particulate organic carbon (POC = TOC-DOC) as well as log K_{OC} (distribution coefficient normalised to organic matter). *significant at the 0.05 level. Number of data can be found in scatter plott analysis in the appendix

		Total sample size				
		f_p - phase distribution				
		total	< 63 µm	63 – 125 µm	125 – 250 µm	250 – 2000 µm
NAP	POC	0.154	0.337*	0.514*	0.435*	-0.275*
	log K_{OC}	0.558*	0.443*	0.548*	0.373	0.693*
FLU	POC	0.273*	0.393	0.368	0.390	0.312
	log K_{OC}	0.285*	0.096*	0.210	0.146	0.402
4NP	POC	0.285*	0.317*	0.272	0.433*	0.493*
	log K_{OC}	0.354*	0.359*	0.154	0.347	0.150
		COD:TOC < 5,3				
NAP	POC	0.381*	0.360*	0.614*	0.493*	0.757
	log K_{OC}	0.402*	0.462*	0.129	0.372	0.505
FLU	POC	0.349*	0.410*	0.447	0.409	0.280
	log K_{OC}	0.137	0.102	0.247	0.098	-0.109
4NP	POC	0.265*	0.352*	0.356	0.419	-0.190
	log K_{OC}	0.344*	0.363*	0.170	0.008	0.407
		COD:TOC > 5,3				
NAP	POC	-0.152	0.360	0.614	0.493	0.757
	log K_{OC}	0.672*	0.462	0.129	0.372	0.505
FLU	POC	0.236*	0.508	0.585*	0.647	0.353
	log K_{OC}	0.443*	0.308	0.523	0.299	0.485
4NP	POC	0.316*	0.253	0.500	0.428	0.616*
	log K_{OC}	0.415*	0.342	0.198	0.531	-0.144

For NAP, it can be noted that the correlation of the population across all particle size classes for f_p and POC improved slightly from 0.154 to 0.381 when samples with reduced carbon compounds were excluded. For the correlation of f_p to log K_{OC} there was a slight deterioration of the correlation (from 0.558 to 0.402). For the samples with a high COD:TOC ratio, the correlation with POC was no longer statistically significant (p-value 0.35) and the correlation with log K_{OC} improved from 0.558 to 0.672 (p-value < 0.05). Differentiated by particle size classes, the correlations with POC partly improved more, partly less. However, only the particle size classes < 63 µm, 63 – 125 µm and 125 – 250 µm were found to be statistically significant at the 0.05 level. In the correlations with log K_{OC}, only the correlation at < 63 µm could still be considered statistically significant. However, the correlation coefficient only changed minimally here. For the correlations of samples with high COD:TOC ratios, the Pearson correlation coefficient could no longer be used for interpretation due to the very small number of samples (between 5 and 16 values). The scatter plots of f_p to log K_{OC} showed the anticipated correlation for particle sizes 63 – 125 µm and 250 – 2000 µm (f_p increases with log K_{OC}).

The relationship between f_p and POC can also be suspected for the fraction 63 – 125 µm. Regarding the remaining particle size classes no relationship could be recognised for the correlation of f_p to POC and for f_p to log K_{OC}.

In summary, it can be seen that when the data are divided according to COD:TOC ratio, the correlation of f_p (total data) with POC improved. The correlation of f_p with log K_{OC} deteriorated, but the expected correlation can still be seen in the scatter plot. This was similar for different particle sizes, but not consistent. Thus, it can be stated for NAP that the phase distribution is noticeably influenced by the COD:TOC ratio, but this influence cannot be described in more detail on basis of the evaluation carried out.

Presumably, further influencing factors on the phase distribution complicate the correlation of f_p with the organic content of the samples. In addition, the evaluation was carried out on all sampled flows, as a separation of the data according to individual flows would have led to an insufficient data volume. However, there are clear differences between the flows in terms of the organic content of the solids. Particles from CWD and overflow have a higher organic content (cf. 5.2.2). However, the samples of particle sizes 63 – 2000 µm, are mostly composed of samples from the effluent due to reasons already mentioned (insufficient solids in CWD and Overflow to split the samples).

Looking at the evaluation carried out for Flouranthene, almost no correlation between f_p and log K_{OC} or POC could be detected. FLU shows K_{OC} values two magnitudes higher than NAP and the dissolved concentrations were close to the limit of quantification. The evaluation of 4NP showed similarities with that of NAP. However, it also does not allow any clear conclusions on the influence of the COD:TOC ratio on the phase distribution.
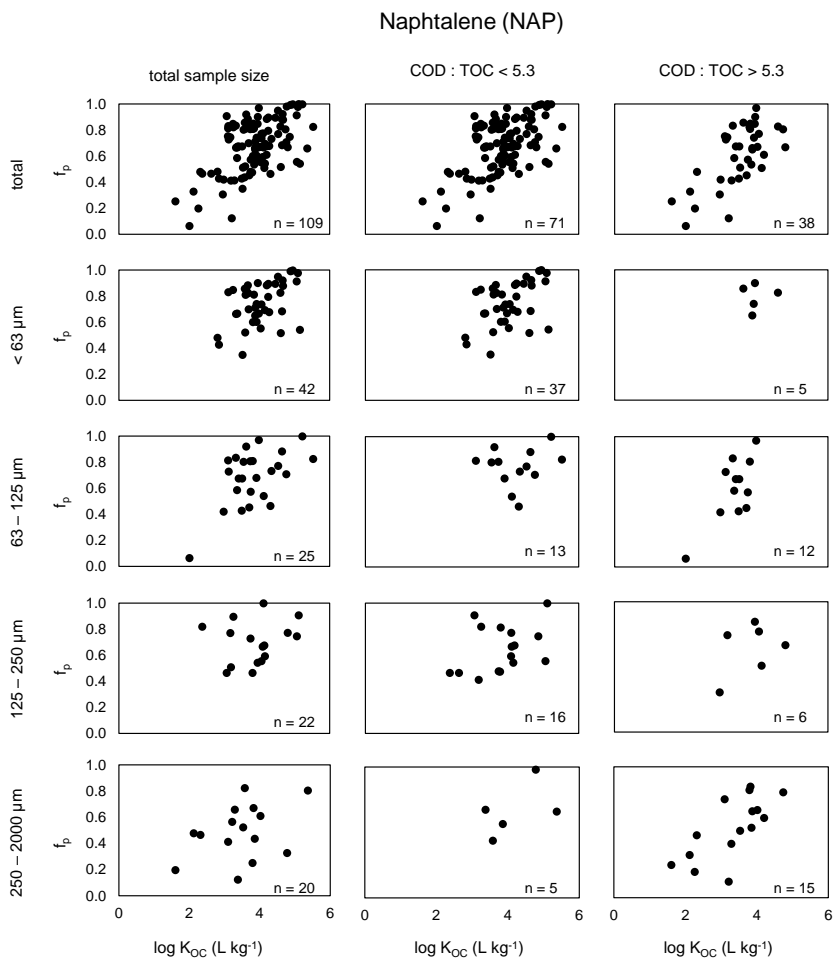
Fig. 5.28: Scatter plot for the correlation between the phase distribution of NAP as fp (particulate fraction), and log KOC (distribution coefficient normalised to organic matter).

Naphtalene (NAP)
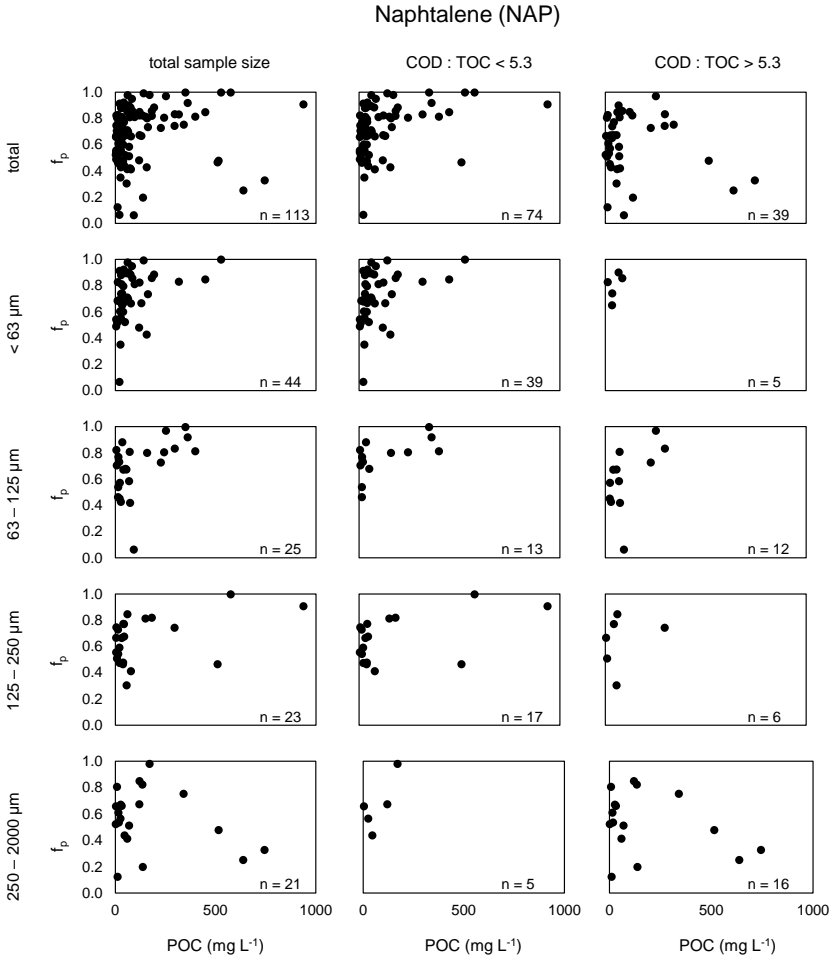
Fig. 5.29: Scatter plot for the correlation between the phase distribution of NAP as fp (particulate fraction), and the organic content of the particles (POC = TOC-DOC).

5.3.5   Treatment efficiency

This chapter gives an overview of the load-related removal efficiencies for the organic micropollutants investigated during the study period of 2017 – 2019. The values were determined as described in 4.5.2. Fig. 5.30 shows the distribution of the treatment efficiencies for the sum of the 16 EPA PAHs (mean particulate load approx. 87 %), 4NP (mean particulate load approx. 52 %), BT (mean particulate load approx. 23 %) and TBY

(mean particulate load approx. 4 %) as an example. These substances represent the spectrum between high particulate and high dissolved fraction of the total pollutant load. An overview of the treatment efficiencies for all substances can be found in the appendix (Tab. C.19).
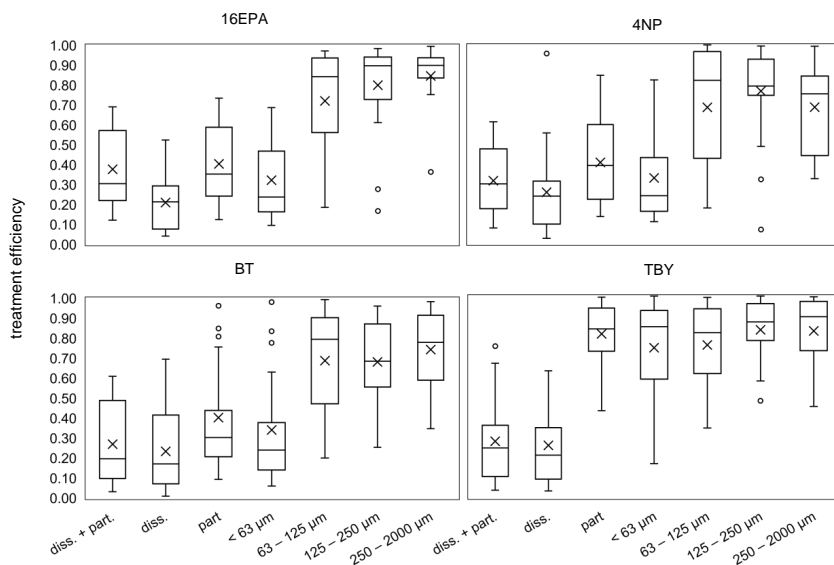
Fig. 5.30: Distribution of pollutant removal efficiencies across different phases and particle size fractions. Substances depicted: 16 EPA PAH, 4-Nonylphenol, Benzothiazole and Terbutryn. n = 21, sampling event 2018_0720 not included.

For the depicted substances the difference of the total treatment efficiency (part. + diss.) to the dissolved treatment efficiency became smaller with increasing proportion of dissolved pollutant loads.

Looking at the treatment efficiencies of the size specific particulate pollutant fractions, it can be clearly seen that there were very large differences between the particle size class < 63 μm and 63 – 2000 μm. This can be attributed to the poor settling properties of the particulate fine fraction. The 16 EPA PAHs showed a clear trend that the cleaning performance decreases with decreasing particle size. When considering the particulate fractions of TBY, it must be noted that the particulate load of this substance was very low and this low particulate fraction was well retained by the treatment plant. Comparing the total treatment efficiencies for TBY with the dissolved treatment efficiencies, it becomes clear that the high particulate treatment efficiencies for this substance did not have a significant influence on the total treatment efficiencies.

The rainwater treatment facility showed a mean removal rate of the substance-specific total load (diss. + part.) for the investigated organic micropollutants between 0.28

(MTBT) and 0.49 (FLU). The mean removal rate of the dissolved load was between 0.22 (FLU) and 0.28 (ANT). As expected, the investigated stormwater treatment facility does not show a good treatment efficiency for dissolved loads. The fact that there is any retention of dissolved loads at all is due to the volume retention of the facility.

The results (Tab. C.19) show that although the pollutant load of some substances was reduced by almost 50 % (FLU), the concentrations after treatment still exceeded the EQS of the WFD in some cases very significantly (cf. Fig. 5.17). This was especially the case for mainly particulate transported substances (HMW PAH). Thus, it is not the poor treatment efficiency for dissolved substances that is responsible for this, but the reduced retention capacity of fine particles.

In order to achieve a more effective treatment of organic micropollutants in urban stormwater runoff, especially in heavily polluted catchment areas (e.g. industrial areas), a combination of various decentralised systems and centralised treatment systems is required. For example systems with longer residence time or treatment systems with a filtration/adsorption step, in order to enable increased sedimentation of fine particles and the retention of dissolved substances (Hvitved-Jacobsen et al. 1994; Charters et al. 2015; Lieske et al. 2021).

5.3.6 Suitability of TSS as a Proxy for Contamination with Organic Micropollutants

In order to elaborate the suitability of TSS or specific particle size fractions of TSS as a proxy for urban stormwater contamination with organic micropollutants the investigated particle size specific TSS sampling event loads are compared with the substance-specific total load (dissolved + particulate) of the investigated organic micropollutants. Furthermore, it will be examined whether the treatment efficiency of the investigated rainwater treatment facility for organic micropollutants is sufficiently represented by the retention capacity of TSS and TSS < 63 µm.Fig. 5.31 shows the comparison of Spearmans rank correlation coefficients for the correlation between TSS loads and total organic micropollutant load (diss. + part.) across different particle size fractions and depicted substance on sampling event basis. The correlations were significant at the 0.05 level for all particle size fraction and substances except for CAF. The values for TSS < 63 µm are sorted in descending order. The rest are sorted according to the resulting substance order of TSS < 63 µm. Based on this figure, it can be estimated how well the total pollutant load (dissolved + particulate) of a substance is represented by the solid load of different particle size fractions.

TSS		TSS$_{<63\,\mu m}$		TSS$_{63-125\,\mu m}$		TSS$_{125-250\,\mu m}$		TSS$_{250-2000\,\mu m}$	
PHE	0.913	PHE	0.958	PHE	0.825	PHE	0.724	PHE	0.778
GHI	0.907	GHI	0.936	GHI	0.805	GHI	0.726	GHI	0.775
ANT*	0.889	ANT*	0.931	ANT*	0.836	ANT*	0.738	ANT*	0.800
∑16 EPA	0.895	∑16 EPA	0.920	∑16 EPA	0.832	∑16 EPA	0.727	∑16 EPA	0.788
PYR	0.901	PYR	0.916	PYR	0.834	PYR	0.748	PYR	0.809
BaP*	0.894	BaP*	0.914	BaP*	0.875	BaP*	0.739	BaP*	0.794
BkF*	0.851	BkF*	0.905	BkF*	0.765	BkF*	0.669	BkF*	0.722
BbF*	0.841	BbF*	0.904	BbF*	0.745	BbF*	0.678	BbF*	0.704
IND	0.874	IND	0.902	IND	0.810	IND	0.684	IND	0.741
BaA	0.877	BaA	0.901	BaA	0.833	BaA	0.713	BaA	0.774
DBA	0.858	DBA	0.885	DBA	0.780	DBA	0.720	DBA	0.761
FlU*	0.850	FlU*	0.872	FlU*	0.810	FlU*	0.727	FlU*	0.749
NAP*	0.827	NAP*	0.864	NAP*	0.727	NAP*	0.661	NAP*	0.766
CHR	0.802	CHR	0.852	CHR	0.700	CHR	0.600	CHR	0.634
TPP	0.824	TPP	0.839	TPP	0.813	TPP	0.675	TPP	0.718
4NP*	0.770	4NP*	0.831	4NP*	0.706	4NP*	0.577	4NP*	0.609
BT	0.764	BT	0.792	BT	0.671	BT	0.518	BT	0.628
ACN	0.776	ACN	0.791	ACN	0.768	ACN	0.635	ACN	0.705
FLE	0.774	FLE	0.788	FLE	0.732	FLE	0.578	FLE	0.648
TCEP	0.726	TCEP	0.787	TCEP	0.665	TCEP	0.547	TCEP	0.598
TCPP	0.719	TCPP	0.765	TCPP	0.691	TCPP	0.530	TCPP	0.565
MTBT	0.743	MTBT	0.745	MTBT	0.746	MTBT	0.597	MTBT	0.676
4tOP*	0.587	4tOP*	0.700	4tOP*	0.490	4tOP*	0.378	4tOP*	0.379
ACY	0.647	ACY	0.651	ACY	0.650	ACY	0.542	ACY	0.654
TBY	0.675	TBY	0.626	TBY	0.735	TBY	0.651	TBY	0.680
CAF	0.374	CAF	0.403	CAF	0.274	CAF	0.179	CAF	0.251

Fig. 5.31: Spearmans rank correlation coefficients for correlation between TSS load and total organic micropollutant load (diss. + part.) across different particle size fractions and depicted substances. Correlations are significant at the 0.05 level except for CAF. TSS represents 0.45 – 2000 µm. The values for TSS < 63 µm are sorted in descending order. The rest are sorted according to the resulting substance order of TSS < 63 µm. * *Priority Substance of WFD,* n = 22

The correlation coefficients (without CAF) ranged for TSS between 0.587 and 0.918, for TSS < 63µm between 0.626 and 0.958, for TSS 63 – 125 µm between 0.490 and 0.875, for TSS 125 – 250 µm between 0.378 and 0.791 and for TSS 250 – 2000 µm between 0.379 and 0.813. This already shows that the load of some substances correlates very well with the TSS load. Overall, TSS < 63 µm showed the best correlation across all substances except for TBY and TPP. The load of these two substances was represented best by the solid load in the particle size 63 – 125 µm. As expected, the mostly particulate transported substances correlate best with TSS < 63 µm. This is illustrated in Fig. 5.32 by comparing the correlation coefficients with the mean phase distribution of the substances (f_p) observed in this study.
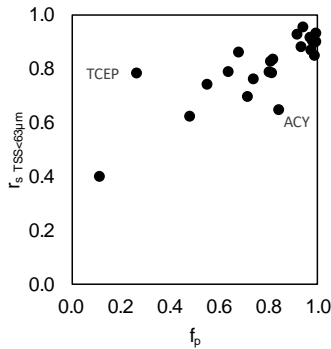
Fig. 5.32: Scatter plot for the correlation between Spearman's rank correlation coefficients and the mean phase distribution of the investigated organic micropollutants (f_p).

The correlation coefficients increased with increasing particulate fraction. The data points that stand out are the organophosphate TCEP and the LMW PAH ACY. TCEP is relatively well represented by the TSS < 63 µm load despite the large dissolved load. With ACY it is rather the other way around. This can be attributed to the fact that in the case of TCEP, approx. 60 % of the particulate load is caused by TSS < 63 µm (cf.Fig. 5.19), while ACY shows the lowest particulate load of all the PAHs investigated in the particle size class < 63 µm (cf. Fig. 5.20). Using Fisher's z-transformation, it was statistically tested whether the correlation coefficients of the different particle size classes differ significantly (Myers und Sirois 2006). For this purpose, a confidence interval was calculated for each correlation coefficient. If these do not overlap, the correlation coefficients differ significantly. However, this was not the case for any correlation (cf. Tab. C.20). Thus, it can be stated that TSS< 63 represents the organic trace substance load best, but the differences to TSS were not statistically significant. It is therefore questionable whether the additional laboratory work required to determine the particulate fine fraction is recommendable in this context. Since the occurrence of solids, as well as their composition, is strongly dependent on location, usage, human activities, etc., these conclusions are difficult to transfer to other sites. Furthermore, if, for example, increased amounts of sand and gravel were to enter the runoff in a catchment over a period of time due to temporary construction site activities, the TSS load would not represent the load of organic micropollutants very well, but the load of TSS < 63 µm would still be a good estimate.

Fig. 5.33 shows the correlation of the treatment efficiencies. The drawn line in each scatter plot represents the bisector. The Spearman's rank correlation coefficients were almost all above 0.6, which suggests a medium to strong association between the two variables. Only TPP and TBY showed values below 0.4. There was a marginal difference between TSS and TSS< 63 µm. Yet, for most substances, the removal efficiency was overestimated by both TSS and TSS < 63 µm.

Concluding, it can be stated that on the basis of the investigations carried out, TSS provides a sufficiently good representation of organic micropollutants in relation to the transported load. The fine fraction of TSS seems to be even more suitable. However, its broad applicability is questionable with regard to the high demand on laboratory analysis and sampling campaigns (Baum et al. 2018). With regard to treatment efficiency, TSS or TSS < 63 μm seems to overestimate the removal efficiency of organic micropollutants for the most part and therefore is less suitable as a surrogate parameter.

It should be pointed out again that in this study the total treatment efficiency was considered. It is composed of the load retention due to actual sedimentation and the load retention due to volume retention of the runoff. Because of the sampling methodology used in this study (sampling of all outflows and no sampling in the inflow) in combination with the treatment process of the plant, the pure sedimentation efficiency could not be quantified. However, it would be interesting to see the distribution of the two components for different substances with different particulate and dissolved fractions. Since the sedimentation efficiency must be lower than the total treatment efficiency, the removal of the pollutant load would probably be less overestimated and therefore the retention of organic pollutants would possibly be better represented by the sedimentation efficiency.
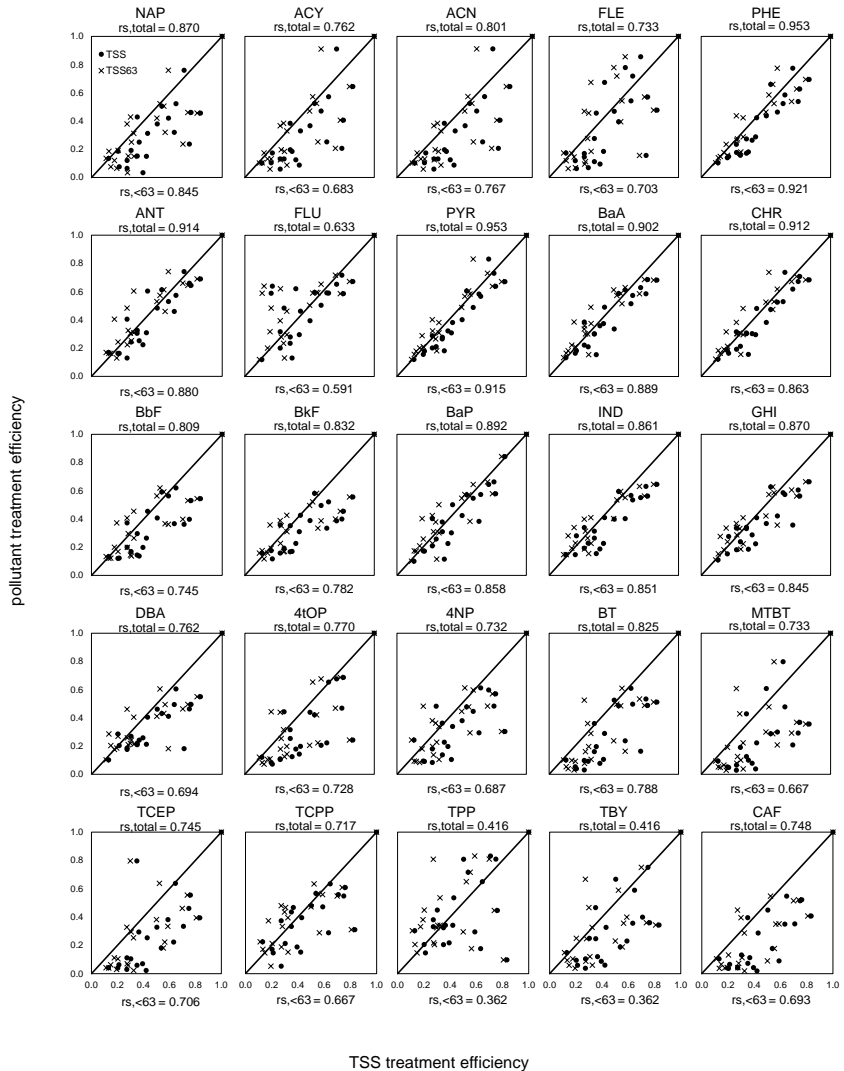
Fig. 5.33: Scatter plots for the correlation of pollutant treatment efficiencies and TSS as well as TSS < 63 µm treatment efficiencies. Drawn line represents bisector. rs = Spearman's rank correlation coefficients (above plot for TSS below for TSS < 63 µm). n = 22

5.4 Metals[1]

Metals were analyzed in dissolved and homogenized (dissolved + particulate) phase as described in Chapter 4.3.3. Chromium (Cr), Copper (Cu), Zinc (Zn), Cadmium (Cd) and Lead (Pb) were analysed for seventeen sampling events in 2018/2019. The following results are partially published

5.4.1 Event Mean Concentrations

Tab. 5.15 summarizes the EMC values for the total fraction (dissolved and particulate-bound), the dissolved fraction and the particulate fraction for the analysed particle size fractions.

For all metals the highest concentrations can be found in the smallest size fraction. Yet, this fraction also shows the highest variation. It needs to be mentioned that Cd and Pb were very often not quantifiable in the dissolved fraction. About 70% of the analyzed samples were lower than 0.1 µg L^{-1} (limit of quantification). For Cr, about 7% of the dissolved values were not quantifiable. However, for calculating the EMC, the total load, and the removal efficiency respectively, 0.5 times LOQ was used. The sampling event specific EMC data can be found in the appendix (Tab. C.21).

Cadmium and Pb are listed as priority substances in the Water Framework Directive (WFD) of the European Union (Directive 2013/39/EU). Therefore, there are existing concentration values defined as environmental quality standards (EQS) which should not be exceeded in surface waters. Those EQS values are given as annual average (AA-EQS) or as maximum allowable concentration (MAC-EQS). For Cd, the MAC-EQS of 0.45 µg L^{-1} was exceeded two times and the AA-EQS of 0.08 µg L^{-1} was exceeded by each sampled event. For Pb, the MAC-EQS of 14 µg L^{-1} was exceeded three times and the AA-EQS of 1.2 µg L^{-1} was exceeded within 16 of 17 sampling events. Although Pb content in surface runoff has shown a decreasing trend since the use of unleaded petrol (Huber et al. 2016), elevated concentrations can still be found in some areas. Lead in runoff originates mainly from geogenic sources, but due to the past use of Pb in petrol and the resulting increased emissions, there are still many persisting Pb compounds that can enter surface runoff, e.g., through dust drifts from the soil (Jayarathne et al. 2017). Cadmium comes from brake and especially tyre wear (Welker 2005). Depending on the traffic load, this can lead to high concentrations in urban runoff. It needs to be mentioned that a direct comparison of the substance concentrations with the EQS values should take into account that, depending on the size of the water body, a significant dilution may occur.

---

[1] This chapter is partly composed of paragraphs from Baum et al. 2021.

Tab. 5.15: Descriptive statistics of metal event mean concentrations in different particle size fractions for samples collected in 2018 (n = 17). "Total" includes the dissolved and the particulate-bound fraction, SD as Standard Deviation

Cr (μg L^{-1})					
	min	max	mean	median	SD
total	1.60	41.9	13.4	8.82	12.2
dissolved	<0.1	3.19	0.61	0.28	0.73
< 63 μm	1.19	27.2	9.47	6.52	7.76
63 – 125 μm	<0.1	7.56	1.49	0.56	2.18
125 – 250 μm	<0.1	5.57	0.98	0.31	3.70
250 – 2000 μm	<0.1	9.05	0.90	0.30	2.06

Cu (μg L^{-1})					
	min	max	mean	median	SD
total	14.3	108	36.3	26.3	26.6
dissolved	3.00	19.1	10.8	10.7	3.97
< 63 μm	1.75	65.4	17.9	13.2	15.2
63 – 125 μm	0.16	19.2	3.48	1.33	5.33
125 – 250 μm	<0.1	13.0	2.00	0.81	3.70
250 – 2000 μm	<0.1	18.2	2.18	0.81	4.12

Zn (μg L^{-1})					
	min	max	mean	median	SD
total	157	835	350	276	180
dissolved	71.3	399	217	212	87.6
< 63 μm	14.7	323	92.9	61.1	83.7
63 – 125 μm	1.40	131	18.0	8.07	32.4
125 – 250 μm	1.24	63.7	9.13	4.35	14.8
250 – 2000 μm	0.96	105	13.1	4.95	24.0

Cd (μg L^{-1})					
	min	max	mean	median	SD
total	<0.1	0.58	0.18	0.12	0.14
dissolved	<0.1	0.21	<0.1	<0.1	<0.1
< 63 μm	<0.1	0.21	<0.1	<0.1	<0.1
63 – 125 μm	<0.1	<0.1	<0.1	<0.1	<0.1
125 – 250 μm	<0.1	<0.1	<0.1	<0.1	<0.1
250 – 2000 μm	<0.1	<0.1	<0.1	<0.1	<0.1

Tab. 5.15: continued

	Pb (µg L^{-1})				
	min	max	mean	median	SD
total	0.88	31.5	7.27	4.03	8.82
dissolved	<0.1	1.28	0.15	<0.1	0.29
< 63 µm	0.20	18.7	4.64	3.11	4.69
63 – 125 µm	<0.1	6.64	0.99	0.37	1.72
125 – 250 µm	<0.1	3.90	0.57	0.19	1.03
250 – 2000 µm	<0.1	11.3	0.92	0.18	2.61

Fig. 5.34 shows the distribution of particulate-bound (grey boxplots) and dissolved (white boxplots) event mean concentrations for the examined metals. These results show that for Cr, Cu and Pb the particulate phase is significantly higher than the aqueous phase in which Cu shows the highest values of the three metals. Zinc shows the highest concentrations overall, but contrary to the other metals the dissolved concentrations exceed the particulate one significantly. For Cd the distribution between particulate and aqueous phase is more equal. However, the significance of this comparison must be viewed critically, as a large proportion of the values are not measured but calculated, as mentioned before. Zinc also shows the widest interquartile range of all analysed metals for both the particulate and dissolved phase. The particulate EMC shows a minimum of 21 µg L^{-1} and a maximum of 175 µg L^{-1}, for the dissolved EMC the values range from 71 µg L^{-1} to 399 µg L^{-1}. This behaviour indicates a high variability in the partitioning process shown in the next section. Huber et al. (2016) also found a high variability of Zn in urban runoff from traffic areas compared to other metals. Gnecco et al. (2019) investigates the fate of Zn, Cu and Pb in urban runoff from paved source areas with different usage. In their study, Zn showed an even higher variability. In the particulate fraction, the values ranged within three orders of magnitude over the different catchments. While TSS concentrations vary considerably at the investigated areas, the metals associated with storm runoff show significant concentrations across the different sites. They raise the question whether TSS is sufficient as the single index parameter to represent the total metal loads, including dissolved and particulate-bound fractions.
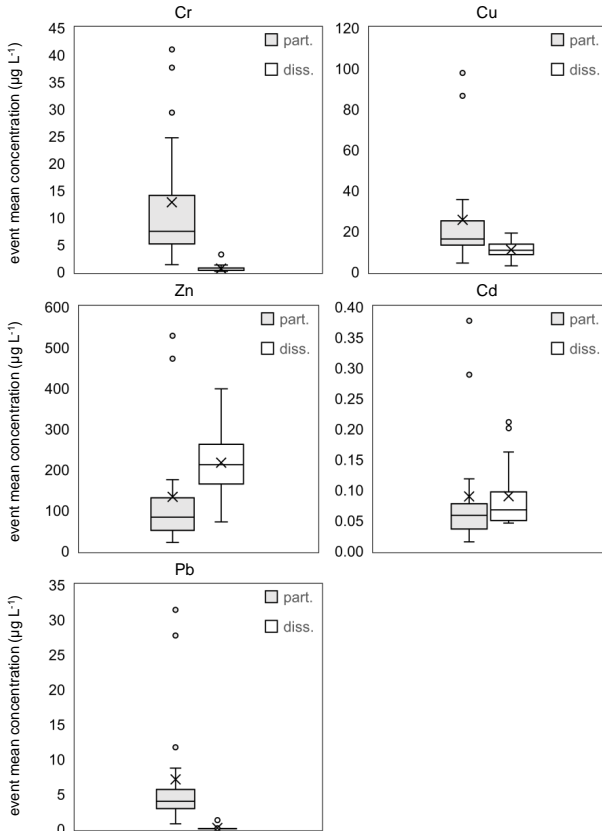
Fig. 5.34: Distribution of metal event mean concentrations on an event basis (n = 17) distin-guished be-tween particulate-bound and dissolved fraction.

5.4.2 Total Loads

Fig. 5.35 shows the distribution between particulate and dissolved fraction of the total metal load for the sampled events. In addition, the distribution of the particulate frac-tion across the investigated particle size classes is shown.

For Cr and Pb, the recorded load was almost exclusively transported in particulate form. The dissolved fraction of the total load only accounted for three percent. In the case of Cu, almost two thirds were transported in particulate form. For Zn and Cd, on the other hand, the dissolved fraction was more than half. For Zn it was 64 % and for Cd 52 %. Looking at the distribution of the particulate fraction across the particle size classes investigated, it can be seen that for all metals more than 70 % of the particulate

load was transported with particles < 63 μm. Furthermore, it can be seen that the transported proportion of the total load decreases with increasing particle size.

The phase distribution of the investigated metals will be further investigated and discussed chapter 5.4.4.
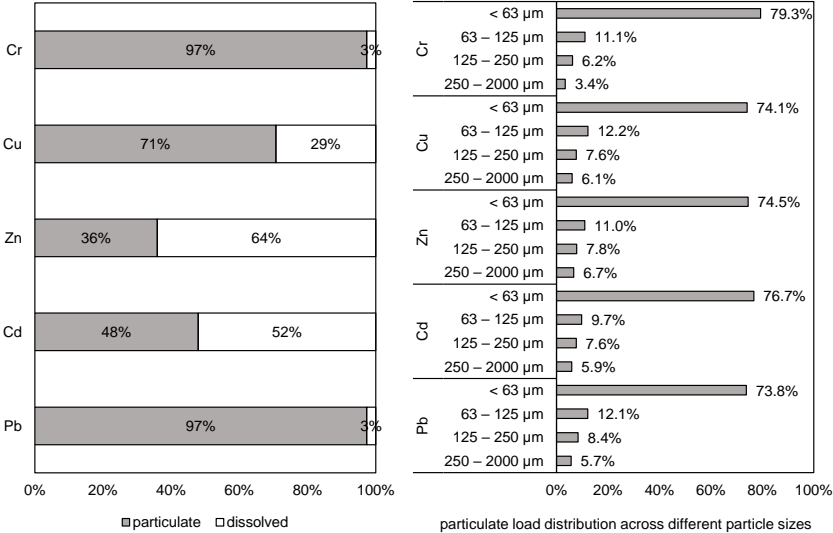
Fig. 5.35: Total metal load distribution for chromium (Cr), copper (Cu), zinc (Zn), cadmium (Cd), and lead (Pb) of sampling events (n = 17).

5.4.3 Pollutant Concentrations across Different Particle Size Fractions

In literature, it is often suggested that the smallest particles are contaminated the most (Sartor et al. 1974; Xanthopoulos und Hahn 1990). As already shown in Tab. 5.15, in this study the highest event mean concentrations for all of the investigated metals can be found in the size fraction 0.45 – 63 μm. However, TSS also shows the highest concentrations in this particle size fraction. Therefore, the particulate bound metal concentration as mass of metal per mass of particulate matter was further investigated on a sample basis. The results can be seen in Fig. 5.36. Contrary to the common understanding, that the fine fraction is loaded disproportionally high with pollutants, the particulate matter in this study shows rather uniform particulate bound metal concentrations over the first three particle size fractions. The median concentration in the largest particle size fraction shows lower values. However, this fraction is by far the widest. Chromium is the sole metal that clearly shows an inverse relation between metal concentration and particle size, when referring to the median values. Copper has similar concentrations for <63 μm and 63 – 125 μm and slightly lower concentrations

in the fraction 125 – 250 µm and 250 – 2000 µm. A similar trend can be seen for Cd. Zinc and Pb both show higher concentrations in the fraction of 125 – 250 µm. Across all particle size fractions, the metal concentrations are in the following order: Zn > Cu > Cr > Pb > Cd. A most recent similar study in China on metals associated with road dust, shows comparable uniform results over the particle size fraction of <75 µm, 75–125 µm, and 125–250 µm but with a different order: Cr > Zn > Cu > Pb > Cd (Niu et al. 2020). Interestingly, Pb and Cu change their positions in the 500 – 1000 µm size class. The different order can possibly be explained by the catchment. Zn is often used in building materials (e.g., for roofs) and paints (e.g. for facades) (Welker 2005) and therefore it is more likely to be found in the stormwater runoff of the catchment in this study than in road dust.

The shown distribution of particulate bound metal concentration over different particle size fractions could be explained by the organic content of the PM. In Fig. 5.6 it can be seen that the organic content increase with the particle size. Therefore it could be assumed that the particle size fraction <63 µm has a high adsorption potential due to its relatively large specific surface area (Andral et al. 1999), whereas the pollutants adsorb to the larger particle size fractions to an equal extent due to the higher organic content (Charlesworth und Lees 1999; Lair et al. 2007).The association with organic matter will be further investigated in chapter 5.4.4. Niu et al. (2020) also mention that the size fraction content changed depending on element and land use. For example, in industrial areas the investigated metals tend to be more associated with coarser particles. Although the particle size fractions investigated in this study, show a uniform distribution of particulate bound metal concentration, the highest metal load comes with the particle size fraction <63 µm (highest EMC and highest amount of particles, see Tab. 5.15 and Fig. 5.3).
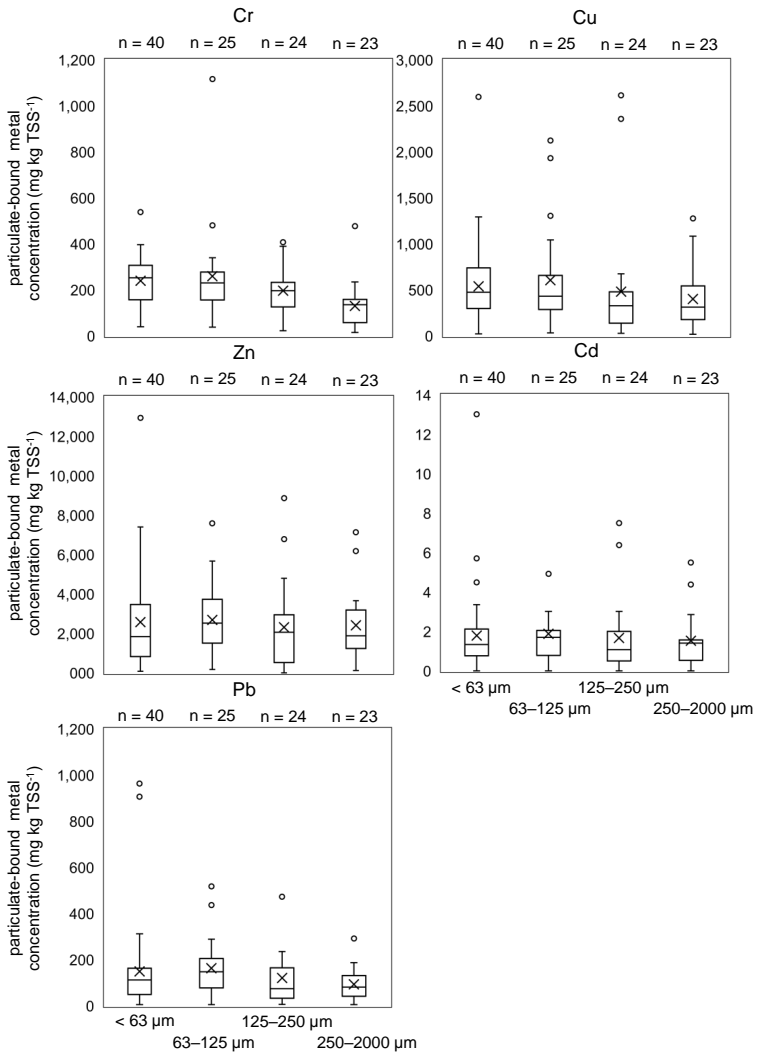
Fig. 5.36: Distribution of particulate-bound metal concentrations in (mg "metal" kg TSS^{-1}) per sample for the metals chromium (Cr), copper (Cu), zinc (Zn), cadmium (Cd) and lead (Pb) in four different particle size fractions (< 63 µm, 63 – 125 µm, 125 – 250 µm, 250 – 2000 µm).

5.4.4   Phase Distribution and Association with Organic Matter

Studies on the transport behaviour of metals in surface runoff highlight the relevance of metal partitioning in the mass transport (e.g. Maniquiz-Redillas und Kim 2014; Gunawardana et al. 2015; Gnecco et al. 2019). Furthermore knowledge about the partitioning of metals is crucial for the planning and design of adequate stormwater treatment measures (Hilliges et al. 2013). Therefore, in the conducted monitoring campaign all collected samples were analysed in the dissolved and homogenized (diss. + part.) phase, which allowed getting the particulate-bound phase, by subtraction. In general, the partitioning of metals in stormwater can be influenced by different factors. Predominantly by the pH value of the rainfall or the runoff matrix, the type and quantity of PM, the solubility of the metal as well as the pavement residence time (Sansalone und Buchberger 1997b). The larger the catchment, the higher the residence time therefore the tendency toward the particulate phase is increased due to the longer contact time between metals and PM. Fig. 5.37 shows the distribution of the particulate fraction index f_p for the investigated metals on event basis. It clearly can be seen, that Pb shows the highest affinity for particulate-bound fraction with fp values between 0.80 and 0.99 and an average of 0.97 followed by Cr with an average of 0.93. Copper as well shows an affinity towards particulate-bound transport. However, in 5 out of the 17 events the partitioning index is lower than 0.5. In these events, the tendency was towards the aqueous phase. For all sampled events, the pH was in the neutral range between 6.8 and 7.6 (cf. Tab. C.21). Therefore, the shift of Cu towards the dissolved fraction cannot be explained with an acidic runoff matrix. It could rather be due to the comparatively low TSS concentrations (9 – 27.7 mg L^{-1}) of these sampling events (Gnecco et al. 2019). Cadmium shows a median value of 0.46 therefore no clear partitioning tendency can be deduced. A clear trend for the aqueous phase is shown by Zn. The values range from 0.18 to 0.65 and therefore Zn also shows the biggest interquartile range which can be interpreted that Zn has a high mobility. Jayarathne et al. (2017) studied the mobility of metals using sequential extraction. They found a similar trend for metals even from different land uses. The order was as follows in relation to the exchangeable geochemical fraction (also referred to as effective bioavailable or mobile fraction): Cd > Zn > Cu > Pb > Cr. For industrial land use the position of Cd and Zn are changed.
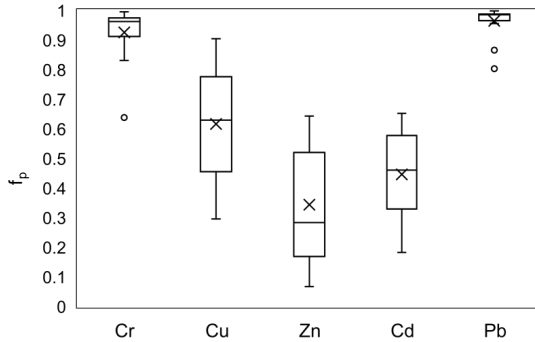
Fig. 5.37: Distribution of the particulate fraction, f_p, for chromium (Cr), copper (Cu), zinc (Zn), cadmium (Cd), and lead (Pb) on event basis (n = 17).

Fig. 5.38 shows the distribution of the corresponding equilibrium partitioning coefficients. Here as well the highest values can be seen for Pb and Cr that supports their high affinity for the particulate-bound phase as it is often documented in the literature. A large dataset of heavy metal contamination in traffic areas examined by Huber et al. (2016) highlights that Pb is mostly transported particulate-bound whereas Cu and Zn show a more intermediate behaviour. This is also applicable to the results of this study, as can be seen from the K_D values for Cu and Zn. Cadmium could be added to this list as it shows similar values as Cu and shows a high mobility in stormwater runoff even at low concentrations (Jayarathne et al. 2017). The order of metals in relation to the highest affinity for particulate phase in this study is: Pb > Cr > Cu > Cd > Zn. This is almost the opposite to the before mentioned order of highest metal mobility.
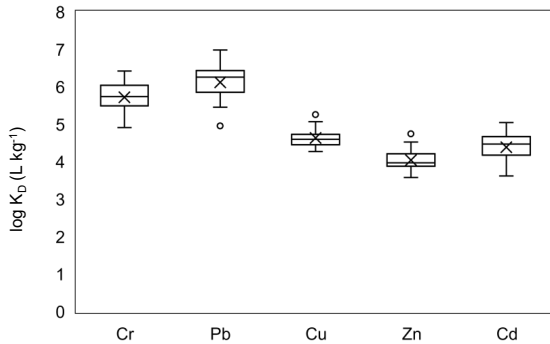
Fig. 5.38: Equilibrium partitioning coefficient log K_D (L kg-1) for chromium (Cr), copper (Cu), zinc (Zn), cadmium (Cd) and Lead (Pb) on event basis (n = 17).

In order to further investigate the previously established hypothesis that the uniform particle loading of the different size classes is related to the respective organic content, the correlation between the determined particulate metal concentration and the measured particulate organic carbon (TOC - DOC) across all particle size classes is shown in Fig. 5.39. The Pearson correlation coefficients range between 0.645 (Pb) and 0.797 (Cr) indicating a moderate relation between particulate metal concentration and particulate organic carbon. The diagrams showed a stronger scatter at higher organic concentrations. However, the trend of higher metal concentrations at higher organic concentrations is recognisable. A possible reason for the strong scatter could be the already mentioned problems with the determination of TOC in the larger particle size classes (cf. 5.2.2).

The results of this investigation show, that metals in urban runoff are transported particulate bound as well as in the dissolved fraction. If the monitored treatment facility is capable of removing both fractions sufficiently will be investigated in the following part. Furthermore, the documented association of metals with organic matter in the literature was also recognisable in the samples of this study. This supports the hypothesis of the equally loaded particles due to higher organic content of the coarse particle size fractions.
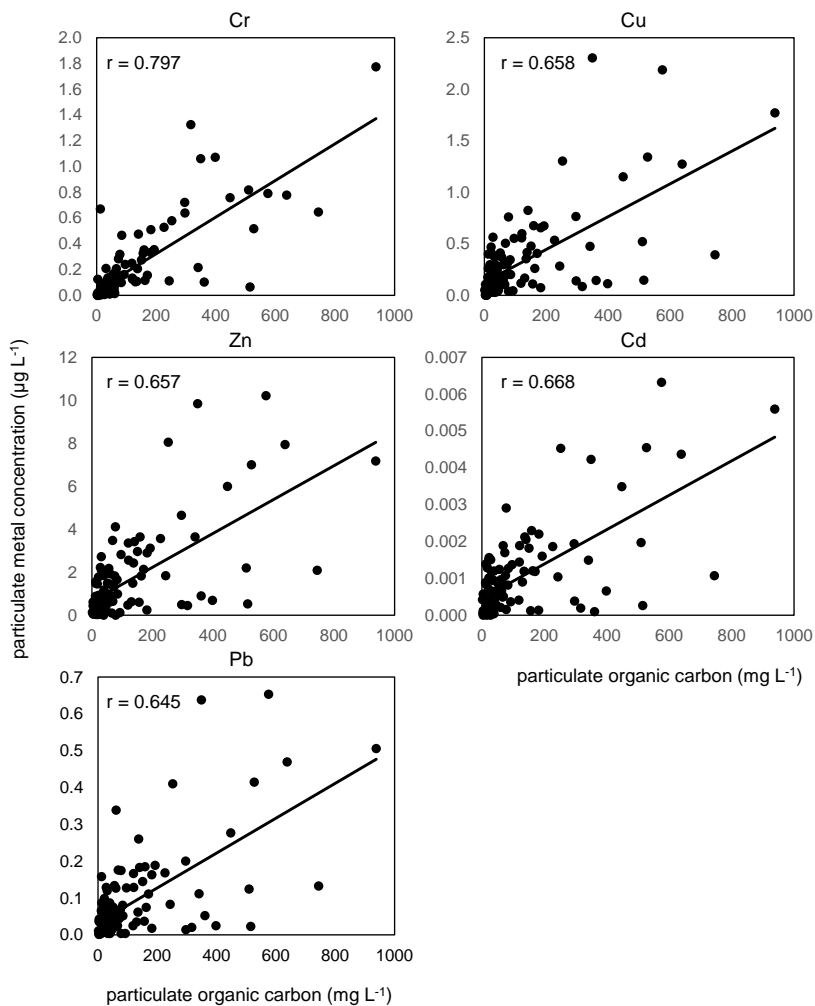
Fig. 5.39: Correlation between particulate metal concentration (µg L⁻¹) and particulate or-
ganic carbon (TOC-DOC in mg L⁻¹) for chromium (Cr), copper (Cu), zinc (Zn), cad-
mium (Cd) and Lead (Pb) on sample basis (n = 110). r as Pearson correlation coeffi-
cient. Correlations significant at the 0.05 level for all metals.

5.4.5   Treatment Efficiency

This chapter gives an overview of the load-related removal efficiencies for the metals
analysed during the study period of 2018/2019. The values were determined as

described in 4.5.2. Fig. 5.40 shows the distribution of the treatment efficiencies for the total (diss. + part.), the dissolved, the particulate fraction as well as the respective investigated particle size classes of the particulate fraction. The sampling event 2018_0720 is not included since this event was completely discharged to the wastewater treatment plant because of its small volume. The calculated efficiency of this sampling event therefore is 100 %. However, this would bias the overall assessment of the treatmen effciencies.
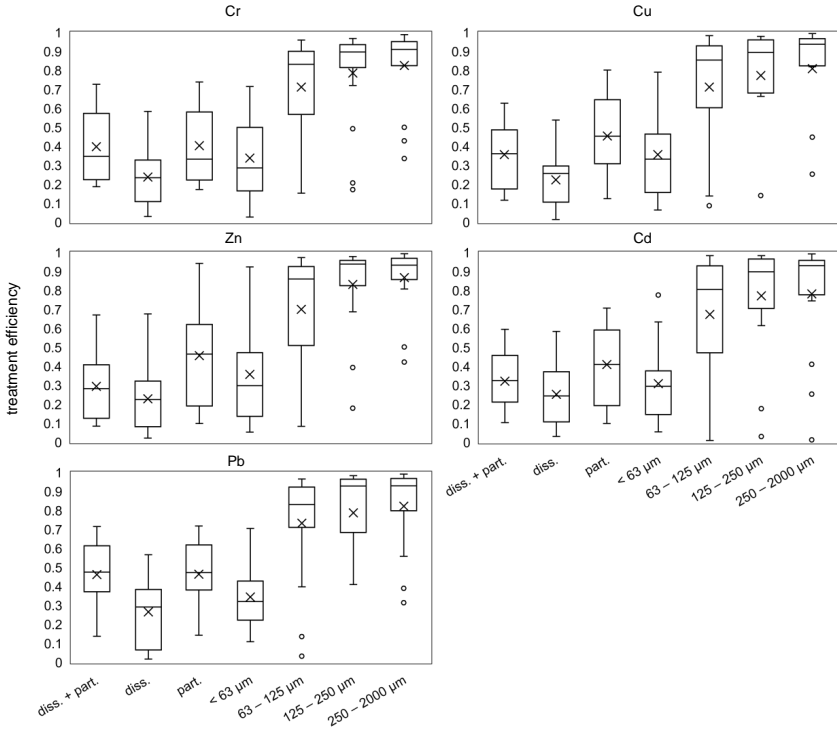
Fig. 5.40: Distribution of pollutant removal efficiencies across different phases and particle size fractions for chromium (Cr), copper (Cu), zinc (Zn), cadmium (Cd) and Lead (Pb) on event basis n = 16, sampling event 2018_0720 not included.

The mean total treatment efficiencies ranged between 0.29 (Zn) and 0.46 (Pb), meaning about one third of the total zinc load and about half of the lead load was removed by the investigated stormwater treatment facility. As expected for a sedimentation-based treatment facility, the removal efficiencies of the particulate fraction were higher than of the dissolved fraction, for all metals. The efficienicies for the dissolved fraction ranged between 0.22 (Cu) and 0.27 (Pb). Looking at the treatment efficiencies of the size specific particulate metal fractions, it could be clearly seen that there were

very large differences between the fine particles (< 63 µm) and the coarser particles. This can be attributed to the poor settling properties of the particulate fine fraction. The metals showed a clear trend that the treatment efficiency decreases with decreasing particle size.

The results show that the particulate metal load can be retained to a certain extent. However, the dissolved part (in the case of Zn, this accounts for about two-thirds of the total load) can only be removed to a small extent by the treatment plant and thus a large proportion of the dissolved metals end up in the receiving water. Therefore, an extensive stormwater treatment requires a combination of sedimentation or filtration for the particulate-bound fraction as well as an adsorption step for the dissolved fraction.

5.4.6   Suitability of TSS as a Proxy for Contamination with Metals

Metal contamination in urban stormwater runoff is mostly transported by PM washed off from different surfaces (Gromaire et al. 1999; Huber et al. 2016). It is therefore obvious to use the particulate matter parameter TSS as a substitute for particulate-bound contamination in urban stormwater runoff. The correlations of the metal loads (dissolved + particulate) with the particulate matter loads in Fig. 5.41 are also supporting this approach. However, in view of the partitioning of different metals between the aqueous and solid phases, which is heavily dependent on site-specific conditions (see Chapter 3.5), the question arises as to whether the assumption, that with the removal of TSS a significant amount of particulate pollutants can be removed as well, is generally correct. Hence, the assumption should also apply to the effectiveness of treatment plants, since it depends on these how much of the pollution of the urban runoff ultimately reaches the aquatic environment. Here in particular, the distribution of metals in different particle size fractions is of particular importance. Classical sedimentation-based treatment plants show a rather poor treatment performance with regard to small solids. In this case, the metal contamination actually released into the environment would be underestimated if the solids were used in their entire particle size distribution as a substitute parameter. However, the limitation of a substitute parameter to the fine fraction is accompanied by the issue that the analysis of this fraction is extremely complex and can already be influenced by many factors during sampling as well as during the analysis steps in the laboratory (Baum et al. 2018)

In the following, the data collected in this study at the investigated stormwater treatment plant will be used to further elaborate the suitability of TSS as a substitute for metal contamination. Fig. 5.41 compares the already mentioned positive correlation of metal load and particulate matter load with the respective correlation of the treatment efficiency. On the right side of the figures, the y-axis shows the event-based retention efficiency of the plant for the entire metal load (dissolved + particulate). This is compared to the retention efficiency of the particulate fraction shown on the x-axis. The particle size fractions 0.45–2000 µm (total TSS) and <63 µm (TSS < 63 µm) are shown. Spearmans rank correlation coefficient (r_s) is also shown as evaluation

criterion. The particle size class <63 µm was selected because according to current guidelines in Germany the quantity of this fraction determines whether stormwater runoff requires treatment (DWA 2020).

As already mentioned, the metal load correlates well with the load of PM for almost all metals investigated. Spearmans rank correlation coefficient (r_s) ranging from 0.81 to 0.94. In particular higher r_s values are obtained for the <63 µm size fraction, underlining the German decision. For Cr, the correlation with total TSS is slightly better. However, it needs to be mentioned that as for the correlation shown in the left site of the figures, the differences between total TSS and TSS < 63 µm are minor. Zn, as was to be expected due to its documented tendency towards the aqueous phase, shows the worst correlation. The correlation is significant at the 0.05 level.

If looking at the correlations in the right section of the figures, a slightly different picture emerges. Spearmans rank correlation coefficients ranging from 0.51 to 0.87 (all correlations significant at 0.05 level except Pb). It can be seen that although the metal load is closely related to the solid load, the retention efficiency of the metal load is significantly different from the retention efficiency of the solid load. The drawn line represents the bisector, making it more obvious that the removal efficiency of the total metal load is overestimated by both total TSS and TSS < 63 µm. This effect can be explained due to a certain proportion of the metals being transported in the aqueous phase.

In summary, on basis of the conducted research, it can be noted that TSS provides a sufficiently good representation of metals in terms of transported load. The limitation to the fine fraction of TSS could be even more appropriate, but in terms of the practicability with regard to sampling campaigns, it might be questionable. However, the representation of metals by TSS in terms of treatment efficiency is not sufficient. Moreover, in order to fully understand these relationships, due to the different impacts on partitioning, further data from different catchment areas with different treatment facilities is needed.

Cd

metal load (diss. + part.) (g)

rs= 0.880

rs= 0.821

▲ TSS < 63 μm
■ total TSS
⋯⋯ Linear (TSS < 63 μm)
--- Linear (total TSS)

TSS load (kg)

Cd

metal removal efficiency (diss. + part.)

▲ TSS < 63 μm
■ TSS total

rs= 0.758

rs= 0.782

Pb

metal load (diss. + part.) (g)

rs= 0.831

rs= 0.875

TSS load (kg)

Pb

metal removal efficiency (diss. + part.)

rs= 0.517

rs= 0.532

TSS removal efficiency
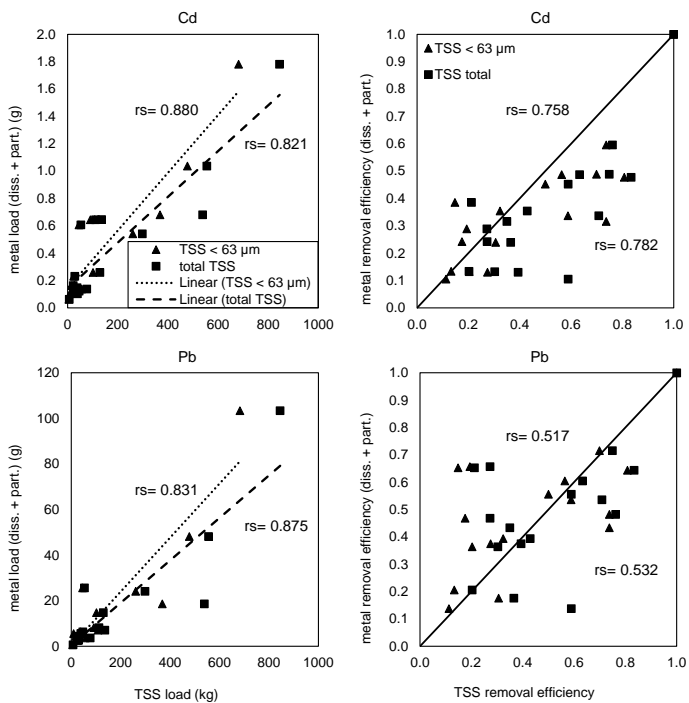
Fig. 5.41: see next caption.
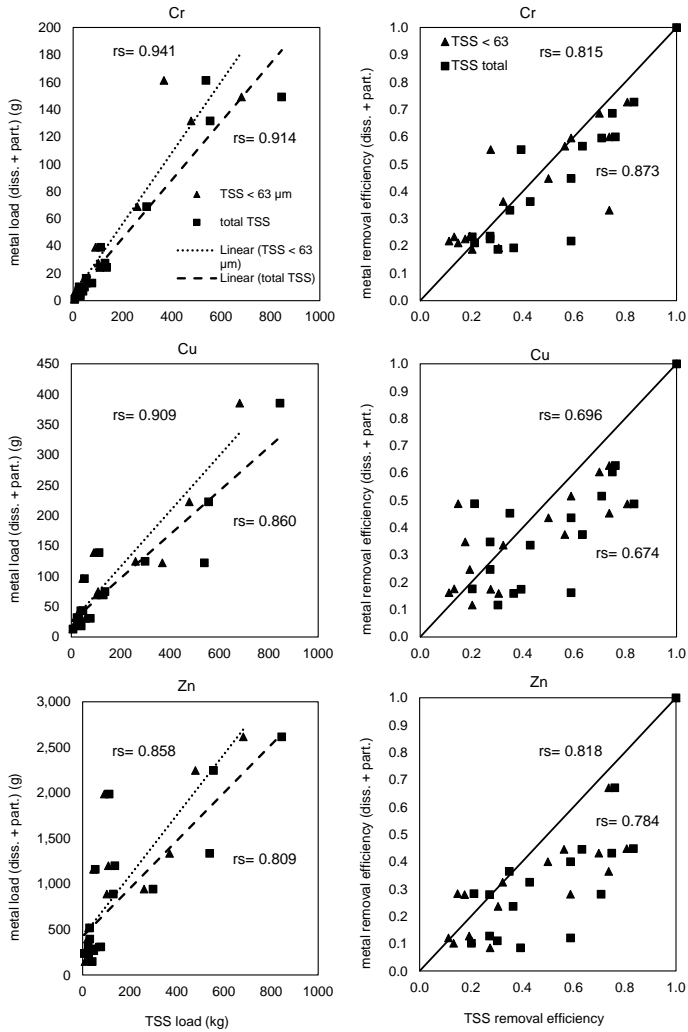
Fig. 5.41: Left: Correlation between total metal load (y-axis) and TSS load (x-axis) for < 63 μm and totaloTSS (see key in first diagram). Right: Correlation between metal removal efficieny (y-axis) and TSS removal efficiency for < 63 μm and total TSS. Line represents bisector, r values < 63 μm top, r values total TSS bottom both for chromium (Cr), copper (Cu), zinc (Zn).

6 Conclusion and Recommendations for Future Research

In this study an intensive long term monitoring campaign at a stormwater treatment facility in an industrial area was conducted. The stormwater samples were taken volume-proportional at the two outlets of the facility. The solids contained in urban stormwater runoff were analysed for their particle size distribution. For this purpose, the samples were divided into four different particle size fractions by wet sieving and further analysed. The particle size classes were: 0.45 – 63 μm, 63 – 125 μm, 125 – 250 μm and 250 – 2000 μm. In addition to the loss on ignition and the amount of organic carbon, the load of organic micropollutants and heavy metals was measured in the size-specific samples. The focus was on the one hand on the phase distribution of the substances between particulate and dissolved phase and on the other hand on the distribution of the particulate transported fraction of the substances across the investigated particle size classes. Furthermore, the association of the investigated substances with the organic content of the samples was examined and the treatability of the substances in the rainwater treatment facility was investigated.

6.1 Characterisation of Particulate Matter, Occurrence of Organic Micropollutants and Metals

Within the scope of this study, over a period of almost 2.5 years, a total of 36 sampling events were recorded and investigated within two sampling periods (2015 – 2016 and 2017 – 2019) at the rainwater treatment facility in Freiburg Haid. The occurrence of organic micropollutants was determined in 22 of these events and the occurrence of metals in 17. The evaluation of the event mean concentration (EMC) of TSS resulted in a mean of 73.6 mg L^{-1} (median: 41.4 mg L^{-1}). For TSS < 63 μm, the mean EMC (determined over 36 sampling events) was 34 mg L^{-1} (median: 22.4 mg L^{-1}). The particle sizes 63 - 2000 μm showed a mean EMC of 14.9 mg L^{-1} (median: 4.32 mg L^{-1}). The results clearly show that the fine fraction of the solids is of particular importance, as it shows an EMC more than twice as high as the coarser particle fraction. From 2017 to 2019, the events were investigated in four particle size classes. The results of this evaluation emphasise this more clearly. TSS < 63 μm showed a mean EMC (over 22 sampling events) of 43 mg L^{-1} (median: 30.6 mg L^{-1}), TSS 63 – 125 μm of 6.58 mg L^{-1} (median: 3.12 mg L^{-1}), TSS 125 – 250 μm of 8.03 mg L^{-1} (median: 2.08 mg L^{-1}) and TSS 250 – 2000 μm showed a mean EMC of 7.8 mg L^{-1} (median: 2.50 mg L^{-1}). The differences between the two sampling periods can be attributed on the one hand to construction activities in the vicinity of the treatment plant and on the other hand to the laboratory improvements in the analysis of solids over the years. Due to the strong tendency towards flocculation, the analysis of the fine fraction proves to be particularly challenging, as

elaborated in Baum et al. (2018). It can be assumed that the fine fraction was not always completely separated in the period 2015 – 2016 and partly remained in the coarse fraction, resulting in an overall underestimation of the fine fraction.

Regarding the occurrence of TSS in terms of the transported solid load, the solids < 63 µm accounted for a mean proportion of 61 % (median: 64 %), the fraction 63 – 125 µm for 13 % (median: 15 %), the fraction 125 – 250 µm for 6 % (median: 5 %), and the fraction 250 – 2000 µm for 9 % (median: 7 %). As mentioned before, the fine fraction is rather underestimated and could be higher in reality. Looking at the separately sampled flows of the plant, it could be seen that the coarser particles were hardly to be found in the overflow and in the clear water discharge (CWD). In the period 2017 – 2019, particles < 63 µm accounted for 83 % of the total solid load in the overflow and 89 % in the CWD, and only 29 % in the effluent. On the one hand, this was due to the fact that coarser particles may have already partially settled in the sewer system on their way to the treatment plant. On the other hand, it also showed that coarser particles settle better during the sedimentation period of the treatment cycle.

The organic content of solids is often closely associated with the settling properties of particles and their adsorption properties. In this study, the organic content was determined on the one hand by determining the loss on ignition, and on the other hand, the proportion of organic carbon in the form of the parameters TOC and DOC was also determined in the particle size-specific samples from 2017 onwards. The results of the loss on ignition investigation showed a clear increase of the organic content with increasing particle size. The loss on ignition of the particles < 63 µm was 28 % in median and increased steadily up to 61 % (median) for the particle size fraction 250 – 2000 µm. When considering the loss on ignition over the sampled flows separately, it could be seen that the differences between the flows in the size class < 63 µm were much smaller than in the other two. One reason for this is that the effluent contains more easily settleable mineral particles, while the particles with a high organic content and presumably lower density can still be found in the clear water discharge after 6 hours of sedimentation.

The examination of the TOC content of the particle sizes showed a uniform distribution deviating from the loss on ignition. The particulate fraction (POC = TOC - DOC) was considered. The mean values were in the range of 139 – 151 mg kg TSS^{-1}. The differences are due to the fact that the particle sizes > 63 µm are dominated by effluent samples in this study that have a higher mineral content according to LOI. However, it was also pointed out that the LOI could systematically overestimate the OC of particles < 63 µm if the content of clay minerals is very high. A correlation between LOI and POC was shown for the individual particle size classes.

As in the case of solids, the highest concentrations of the organic trace substances and metals investigated were found in the particle size fraction < 63 µm. This again illustrates the significance of this particle size fraction for stormwater management in urban catchments. The investigated substances were detected in the homogenised phase (dissolved + particulate) for all samples. However, this was not always the case

in the dissolved phase, especially for high molecular weight (HMW) PAHs and for the metals cadmium and lead. The substances caffeine and pharmaceutical residues of lidocaine and carbamazepine were detected as non-typical substances in stormwater runoff. This suggests existing misconnections to the storm sewer. However, the volume of potential wastewater discharge is likely to be very small compared to the stormwater runoff. Therefore, this issue was not investigated further.

Among the organic micropollutants, the highest concentrations were found for Tris(1-chloro-2-propyl)phosphate (TCPP) from the group of organophosphates. The mean EMC was 1.45 µg L^{-1} (median: 1.26 µg L^{-1}) with peak concentrations up to 3.81 µg L^{-1}. TCPP showed significantly higher EMCs in the dissolved phase. On average over the 22 sampled events it was 1.0 µg L^{-1} in the dissolved phase and 0.45 µg L^{-1} in the particulate phase. Benzothiazole, which belongs to the group of industrial chemicals and is mainly used as a vulcanisation accelerator, showed the second highest event mean concentration of 0.89 µg L^{-1} on average (median: 0.91 µg L^{-1}). BT and its metabolite MTBT showed significantly higher EMCs in the dissolved phase. Both are very likely traffic-related and originate, for example, from tyre and brake abrasion (Wicke et al. 2015). The occurrence of PAHs is also traffic-related and, to a lesser extent, geogenic. In this study, the HMW PAHs in particular showed almost exclusively particulate EMCs, while the other investigated micropollutants showed higher EMCs in the dissolved phase. Among the PAHs, the highest mean EMC was measured for Pyrene with 0.11 µg L^{-1} (median: 0.09 µg L^{-1}) followed by Fluoranthene with 0.08 µg L^{-1} (median: 0.07 µg L^{-1}). The order of the PAHs in descending order was: PYR > FLU > PHE > BbF > GHI > CHR > BaP > BaA > BkF > IND > NAP > ACY > ANT > FLE > DBA > ACE. In some cases, significant exceedances of the environmental quality standards were found, especially for the high-molecular-weight PAHs (BbF, BkF, BaP, IND, GHI), which are classified as priority substances under the European Water Framework Directive (WFD). Even when considering a possible dilution in the receiving water body, the limit values were sometimes exceeded by a factor of 10 to 100, which may have led to local impairments of flora and fauna. EQS were also exceeded for the priority metals cadmium and lead.

Among the metals, zinc showed the highest EMCs, but also the largest interquartile range for both the particulate and dissolved phases. This indicates a very high variability in the phase distribution of this metal and thus a high mobility. Looking at the phase distributions of the investigated metals in this study, the following order of highest affinity to the particulate phase was found: Pb > Cr > Cu > Cd > Zn. This corresponds very well with the high mobility of zinc. A purely particulate transported metal ion is not as mobile as one that is also partially dissolved or even exclusively dissolved. With regard to rainwater treatment, this requires further treatment measures besides sedimentation, for example combined filtration and adsorption stages, in order to effectively remove highly mobile substances or substances with a highly variable phase distribution.

The same applies with regard to organic micropollutants. With the exception of the HMW PAHs, all other substances also have relevant dissolved fractions and a partly

large variability in the phase distribution. For MTBT, for example, the interquartile range of the particulate fraction f_p, ranges from 35 – 75 %. The dissolved load fraction of the alkyphenols 4tOP and 4NP is 59 % and 48 %, respectively. The dissolved load fractions of the organophosphates TCEP, TCPP and TPP are 97 %, 64 % and 67 %, respectively. The load distribution of the particulate fraction over different particle sizes showed a consistent pattern. With the exception of the organophosphates and the biocide terbutryn, which is almost exclusively dissolved, over 70 % of the load is transported with particles < 63 µm. Since the dissolved load cannot be reduced by sedimentation plants, and the particle fraction < 63 µm has rather poor settling properties, an advanced treatment stage or a combination of different centralised and decentralised rainwater treatment strategies are required, especially for catchments where pollution of stormwater runoff is generally higher.

The results of this work show that the individual pollutants can differ significantly in their fate as well as their transport and removal behaviour in urban stormwater runoff. General statements about the occurrence and phase distribution of organic micropollutants as well as metals can therefore be misleading.

6.2 Association of Organic Micropollutants and Metals to different Particle Size Fractions and to Organic Matter

For the metals as well as for most of the organic micropollutants investigated, the fine fraction of the particles accounted for the greatest load. This is consistent with the statement often found in the literature that the fine particles are the most loaded with pollutants. However, in this study, the highest TSS concentrations respectively the largest TSS loads were also found in the particle size fraction 0.45 – 63 µm. Therefore, the particle loading with organic micropollutants or metals respectively the particle-bound micropollutant/metal concentration was calculated on the basis of the individual samples. For most substances, a rather equal distribution over the smallest three particle size fractions was found, deviating from the literature. In the case of PAHs, the substances with a low molecular weight showed a relatively uniform distribution. Starting with Fluoranthene, an inverse relationship between loading and particle size became increasingly clear as the molecular weight increased. The alkyphenol 4tOP showed a similar distribution. 4NP, on the other hand, showed a similar particle-bound concentration across the smallest three particle size classes. The organophosphates TCPP and TPP showed a considerably higher particle-bound concentration in the particle sizes 63 – 250 µm than in the smallest and largest particle size fraction. Among the metals, Chromium showed a slightly decreasing particle loading with increasing particle size. Copper had a slightly lower particle-bound concentration in the particle sizes 125 – 2000 µm and Lead and Zinc showed a slightly higher particle-bound concentration in the fraction 63 – 125 µm than in the remaining particle size classes.

A possible explanation for the distribution across the particle size fractions is that the smallest particles 0.45 – 63 µm have a large adsorption potential for organic micropollutants and metals due to their relatively large specific surface area, but that these substances adsorb just as much to the larger particle fractions due to the higher organic content of these particles. To further investigate this hypothesis, the association of the investigated organic micropollutants and metals with the organic content was examined.

The phase distribution or the particulate phase index f_p, correlated very well with the octanol-water partition coefficient of the investigated organic micropollutants and even better with the partition coefficient K_{OC} (or log K_{OC}) normalised to the organic content. This already gives a first indication of a correlation between adsorption to particles and organic content. The strong correlation (Pearson correlation coefficient r: 0.952 – 0.809) between the particulate fraction of the 16 EPA PAHs and the POC content of the samples also highlights this correlation. For BT and MTBT a moderate to strong correlation (r: 0.589 – 0.773) could also be shown in the particle sizes 63 – 250 µm. For both substances, a correlation between the dissolved concentration and the DOC content could also be shown. The same was shown for some other PAHs, e.g. ACN or PHE. This illustrates the influence of dissolved or colloidal substances on the adsorption of the substances and thus on the phase distribution of the substances. In the case of metals, a recognisable correlation between particulate metal concentration and particulate organic carbon could also be shown across all particle size classes (Spearman's correlation coefficient rs: 0.645 – 0.797). However, the correlation showed a large scattering of the values, especially in the higher concentration ranges.

A direct correlation of the phase distribution, expressed by the particulate phase index, with the particulate organic carbon and the log KOC was also tested for the substances Naphthalene, Fluoranthene and 4 Nonylphenol. The correlation for NAP and 4NP with log K_{OC} was significant at the 0.05 level, but showed strong scatter (r: 0.558 NAP and 0.354 4NP). The correlation of f_p with particulate organic carbon could not be shown. 39 of the 113 samples used for this evaluation showed a very high COD:TOC ratio. This gives a possible indication of a contamination of the samples with mineral oil. It is therefore assumed that this has an influence on the phase distribution of the substances. It could also be shown that the distribution was influenced by this, but the influence could not be specified more precisely.

Reasons for no better correlation could be that the influence of the organics on adsorption was probably superimposed by other factors such as the influence of the particle concentration or the surface charge of the particles. Other possible influencing factors could be the matrix of the rainfall runoff, as the pH was mostly in the neutral range, it could rather be the adsorption competition by other dissolved or colloidal substances (as suggested by the correlation of the dissolved concentration with the DOC content for some substances).

A certain correlation of the organic content with the occurrence of organic micropollutants and metals could be shown, so it can be assumed that the particle-bound

concentration is certainly influenced by this. However, it was found that despite the partly uniform loading of particles, the fine fraction represents the relevant particle size in urban stormwater runoff. Due to the large fraction of the total solid load, the largest particle-bound pollutant loads are transported with particles < 63 μm.

6.3 Treatment Efficiencies for Organic Micropollutants and Metals, Suitability of TSS for Representing the Occurrence and Treatability

This study showed that the majority of PAHs and the metals Cr, Cu, Cd and Pb are largely transported particle-bound. Many of the other substances were also detected in particle-bound form. It is therefore obvious to use the solid parameter TSS as a sub-stitute for particle-bound pollution in urban stormwater runoff. This is also supported by the correlations carried out between solid load and pollutant load (organic mi-cropollutants and metals). However, the correlations also showed that logically, the correlation decreased with increasing dissolved fraction of the investigated sub-stances. Especially with regard to the site-specific distribution of substances between the particulate and dissolved phase, the question arises whether the assumption, that with the removal of TSS a significant proportion of pollutants can also be removed, is generally true. Since the amount of pollution released into the environment ultimately depends on the stormwater treatment facilities, this assumption should also apply to the efficiency of the treatment facilities. Especially in this context, the distribution of pollutants over different particle sizes is of particular importance. Classical sedimenta-tion-based stormwater treatment facilities show a rather poor treatment performance with respect to fine solids. The plant investigated in this study was able to reduce the load of fine particles by only a quarter. The larger particle size classes were reduced by far more than half in most cases. If TSS in its entire particle size range were used as a proxy, the pollutant load actually released into the environment would be underesti-mated. However, limiting TSS to the fine fraction is accompanied by the issue that the analysis of this fraction is extremely complex and can be influenced by many factors already during sampling as well as during the analysis steps in the laboratory. There-fore, the data of this study were used to investigate how well the retention of solids (TSS, TSS < 63 μm) reflects the retention of the total pollutant load (dissolved + partic-ulate). However, the comparison showed that even for substances with a high ten-dency to adsorb onto particles (e.g., Cr, Cu, IND, GHI), the cleaning performance was overestimated by TSS as well as TSS < 63 μm. This was even more evident for sub-stances with a larger dissolved fraction. Furthermore, this study refers to the overall treatment efficiency and does not distinguish between sedimentation efficiency and volume retention. However, this approach could provide further insights and should be considered in future studies realted to this topic.

TSS seems to provide a sufficiently good representation of the pollutant load. The fine fraction is even slightly better. Yet the above-mentioned issues with analytics and sam-pling must be taken into account. However, TSS/TSS < 63 μm does not adequately

represent the retention capacity of pollutants. It must be emphasised though, that due to the various influences on the phase distribution, further data from different catchments with different treatment facilities are required for a comprehensive understanding of this relationship.

6.4 Recommendations for Future Research

One possible starting point for future research would be to investigate whether the distribution of substances across the particle size fractions is significantly influenced by their origin or application. This means, for example, whether substances from brake abrasion are found predominantly in one specific particle size and the same substances from other sources are found in other particle size classes. This would help to gain further insights into the adsorption of substances onto particles of specific sizes fractions. Furthermore, since metals can be present for example as solid metallic abrasions or as metal ions adsorbed to other particles, it is important to determine the species in which they occur.

In this study, the phase distribution was only investigated in total composite samples over complete runoff events. Sampling at a higher temporal resolution would allow to investigate whether phase distribution can also vary significantly within a single runoff event. This could provide further information on the adsorption behaviour of the individual substances.

An investigation of different catchments and sub-catchments could provide further useful information for improved stormwater treatment strategies in the future. For example, if PAHs in road runoff show a different phase distribution in heavily vegetated residential areas (e.g. due to higher dissolved organic content) compared to runoff from highways, treatment strategies adapted to the respective sub-catchment could be applied.

In this study, a certain correlation between the phase distribution of the substances and the organic content of the particles was shown. However, not to the quality required to estimate the particulate concentration based on the physico-chemical properties of the substances and on the measured dissolved concentration. Further investigations should be carried out in this regard in the future. As online measurement methods become better and better, it would then be possible to estimate the amount of pollutants in-situ with a minimum of measurement effort. For example, this could make stormwater management more efficient in the future through specific and automated control of the sewer system or treatment facilities.

References

Adachi, Kouji; Tainosho, Yoshiaki (2004): Characterization of heavy metal particles embedded in tire dust. In: *Environment International* 30 (8), S. 1009–1017. DOI: 10.1016/j.envint.2004.04.004.

Aiguier, Emmanuelle; Chebbo, Ghassan; Bertrand-Krajewski, Jean-Luc; Hedgest, Peter; Tyack, Naomi (1996): Method s for determining the settling velocity profiles of solids in storm sewage. In: *Water Sci Technol* 33 (9), S. 117–125. DOI: 10.1016/0273-1223(96)00377-0.

Andral, M. C.; Roger, S.; Montréjaud-Vignoles, M.; Herremans, L. (1999): Particle Size Distribution and Hydrodynamic Characteristics of Solid Matter Carried by Runoff from Motorways. In: *Water Environ Res* 71 (4), S. 398–407.

aquadrat ingenieure (2014): Betriebsanweisung: Regenwasserbehandlungsanlage RFM-Haid. Stand: August 2014 (Vorabzug).

Bäckström M. (2002): Sediment transport in grassed swales during simulated runoff events. In: *Water Sci Technol* 45 (7), S. 41–49, zuletzt geprüft am 03.11.2017.

Badin, Anne-Laure; Faure, Pierre; Bedell, Jean-Philippe; Delolme, Cecile (2008): Distribution of organic pollutants and natural organic matter in urban storm water sediments as a function of grain size. In: *The Science of the Total Environment* 403 (1-3), S. 178–187. DOI: 10.1016/j.scitotenv.2008.05.022.

Badin, Anne-Laure; Méderel, Guillaume; Béchet, Béatrice; Borschneck, Daniel; Delolme, Cécile (2009): Study of the aggregation of the surface layer of Technosols from stormwater infiltration basins using grain size analyses with laser diffractometry. In: *Geoderma* 153 (1-2), S. 163–171. DOI: 10.1016/j.geoderma.2009.07.022.

Ball, James E.; Abustan, Ismail (1995): An Investigation of Particle Size Distribution during Storm Events from an Urban Catchment. In: The Second International Symposium on Urban Stormwater Management 1995. Integrated management of urban environments: preprints of papers. Barton, A.C.T.: Institution of Engineers, Australia, zuletzt geprüft am 27.01.2018.

Banerjee, Sulagno; Mandal, Aritra; Rooby, Jessy (2016): Studies on Mechanical Properties of Tyre Rubber Concret. In: *IJCE* 3 (7), S. 18–21. DOI: 10.14445/23488352/IJCE-V3I7P103.

Bannerman, Roger T.; Owens, D. W.; Dodds, R. B.; Hornewer, N. J. (1993): Sources of pollutants in Wisconsin stormwater. In: *Water Science & Technology* (Volume: 28 Issue: 3-5), S. 241–259.

Barret, Maialen; Carrère, Hélène; Latrille, Eric; Wisniewski, Christelle; Patureau, Dominique (2010): Micropollutant and sludge characterization for modeling sorption equilibria. In: *Environ Sci Technol* 44 (3), S. 1100–1106. DOI: 10.1021/es902575d.

Bash, J.; Bernman, C. (2001): Effects of turbidity and suspended solids on salmonids. Washington State Department of Transportation.

Bathi, Jejal Reddy (2008): Associations of Polycyclic Aromatic Hydrocarbons (PAHs) with Particulates in the Environment. Dissertation. University of Alabama, Tuscaloosa.

Baum, Philipp; Benisch, Jakob; Blumensaat, Frank; Dierschke, Martina; Dittmer, Ulrich; Gelhardt, Laura et al. (2018): AFS63 – Harmonisierungsbedarf und Empfehlungen für die labortechnische Bestimmung des neuen Parameters. In: Regenwasser in urbanen Räumen. Aqua Urbanica trifft RegenwasserTage. Landau in der Pfalz, 18.-19.06.2018 (Schriftenreihe wasser infrastruktur ressourcen der Universität Kaiserslautern, 1).

Baum, Philipp; Kuch, Bertram; Dittmer, Ulrich (2021): Adsorption of Metals to Particles in Urban Stormwater Runoff—Does Size Really Matter? In: *Water* 13 (3), S. 309. DOI: 10.3390/w13030309.

Beckwith, P. R.; Ellis, J. Bryan; Revitt, D. M.; Oldfield, F. (1986): Heavy metal and magnetic relationships for urban source sediments. In: *Physics of the Earth and Planetary Interiors* 42 (1-2), S. 67–75. DOI: 10.1016/S0031-9201(86)80009-7.

Becouze-Lareure, C.; Dembélé, A.; Coquery, M.; Cren-Olivé, C.; Bertrand-Krajewski, J-L (2019): Assessment of 34 dissolved and particulate organic and metallic micropollutants discharged at the outlet of two contrasted urban catchments. In: *The Science of the Total Environment* 651 (Pt 2), S. 1810–1818. DOI: 10.1016/j.scitotenv.2018.10.042.

Becouze-Lareure, Céline; Dembélé, A.; Coquery, M.; Cren-Olivé, C.; Barillon, B.; Bertrand-Krajewski, Jean-Luc (2015): Source characterisation and loads of metals and pesticides in urban wet weather discharges. In: *Urban Water Journal* 13 (6), S. 600–617. DOI: 10.1080/1573062X.2015.1011670.

Bertrand-Krajewski, Jean-Luc; Chebbo, Ghassan; Saget, Agnes (1998): Distribution of pollutant mass vs volume in stormwater discharges and the first flush phenomenon. In: *Water Res* 32 (8), S. 2341–2356. DOI: 10.1016/S0043-1354(97)00420-X.

Bian, Bo; Zhu, Wei (2009): Particle size distribution and pollutants in road-deposited sediments in different areas of Zhenjiang, China. In: *Environmental Geochemistry and Health* 31 (4), S. 511–520. DOI: 10.1007/s10653-008-9203-8.

Biggins, P. D.; Harrison, R. M. (1980): Chemical speciation of lead compounds in street dusts. In: *Environmental science & technology* 14 (3), S. 336–339. DOI: 10.1021/es60163a005.

Bilotta, G. S.; Brazier, R. E. (2008): Understanding the influence of suspended solids on water quality and aquatic biota. In: *Water Res* 42 (12), S. 2849–2861. DOI: 10.1016/j.watres.2008.03.018.

Birch, G. F.; Scollen, A. (2003): Heavy metals in road dust, gully pots and parkland soils in a highly urbanised sub-catchment of Port Jackson, Australia. In: *Soil Res.* 41 (7), S. 1329. DOI: 10.1071/SR02147.

Birch, H.; Mikkelsen, P. S.; Jensen, J. K.; Lutzhoft, H-C Holten (2011): Micropollutants in stormwater runoff and combined sewer overflow in the Copenhagen area, Denmark. In: *Water Sci Technol* 64 (2), S. 485–493.

Björklund, K. (2010): Substance flow analyses of phthalates and nonylphenols in stormwater. In: *Water Sci Technol* 62 (5), S. 1154–1160. DOI: 10.2166/wst.2010.923.

Björklund, Karin (2011): Sources and fluxes of organic contaminants in urban runoff. Zugl.: Göteborg, Univ., Diss., 2011. Göteborg: Chalmers Univ. of Technology (Doktorsavhandlingar vid Chalmers Tekniska Högskola, N.S., 3161), zuletzt geprüft am 23.11.2017.

Björklund, Karin; Cousins, Anna Palm; Strömvall, Ann-Margret; Malmqvist, Per-Arne (2009): Phthalates and nonylphenols in urban runoff. Occurrence, distribution and area emission factors. In: *The Science of the Total Environment* 407 (16), S. 4665–4672. DOI: 10.1016/j.scitotenv.2009.04.040.

Bleam, W. F. (2017): Soil and environmental chemistry. Second edition. Amsterdam: Elsevier/Academic Press.

Bollmann, Ulla E.; Vollertsen, Jes; Carmeliet, Jan; Bester, Kai (2014): Dynamics of biocide emissions from buildings in a suburban stormwater catchment - concentrations, mass loads and emission processes. In: *Water Res* 56, S. 66–76. DOI: 10.1016/j.watres.2014.02.033.

Bradford, Wesley L. (1977): Urban Stormwater Pollutant Loadings: A Statistical Summary through 1972. In: *Journal (Water Pollution Control Federation)* 49 (4), S. 613–622. Online verfügbar unter http://www.jstor.org/stable/25039320.

Bradl, Heike B. (2004): Adsorption of heavy metal ions on soils and soils constituents. In: *Journal of colloid and interface science* 277 (1), S. 1–18. DOI: 10.1016/j.jcis.2004.04.005.

Brauer, H.; Thiele, H. (1973): Bewegung von Partikelschwärmen. In: *Chemie Ingenieur Technik* 45 (13), S. 909–912. DOI: 10.1002/cite.330451317.

Brezonik, Patrick L.; Stadelmann, Teresa H. (2002): Analysis and predictive models of stormwater runoff volumes, loads, and pollutant concentrations from watersheds in the Twin Cities metropolitan area, Minnesota, USA. In: *Water Res* 36 (7), S. 1743–1757. DOI: 10.1016/S0043-1354(01)00375-X.

Brombach, H.; Weiss, G.; Fuchs, S. (2005): A new database on urban runoff pollution: comparison of separate and combined sewer systems. In: *Water Sci Technol* 51 (2), S. 119–128. DOI: 10.2166/wst.2005.0039.

Brown, Jeffrey N.; Peake, Barrie M. (2003): Determination of colloidally-associated polycyclic aromatic hydrocarbons (PAHs) in fresh water using C18 solid phase extraction disks. In: *Analytica Chimica Acta* 486 (2), S. 159–169. DOI: 10.1016/S0003-2670(03)00472-0.

Bryan Ellis, J.; Revitt, D. Michael (1982): Incidence of heavy metals in street surface sediments. Solubility and grain size studies. In: *Water, Air, and Soil Pollution* 17 (1), S. 87–100. DOI: 10.1007/BF00164094.

Bucheli, Thomas D.; Müller, Stephan R.; Voegelin, Andreas; Schwarzenbach, René P. (1998): Bituminous Roof Sealing Membranes as Major Sources of the Herbicide (R, S)-Mecoprop in Roof Runoff Waters: Potential Contamination of Groundwater and Surface Waters. In: *Environ Sci Technol* 32 (22), S. 3465–3471. DOI: 10.1021/es980318f.

Burkhardt, M.; Zuleeg, S.; Vonbank, R.; Schmid, P.; Hean, S.; Lamani, X. et al. (2011): Leaching of additives from construction materials to urban storm water runoff. In: *Water Sci Technol* 63 (9), S. 1974–1982. DOI: 10.2166/wst.2011.128.

Burton, G. Allen; Pitt, Robert E. (2001): Stormwater effects handbook. A toolbox for watershed managers, scientists, and engineers. Boca Raton: Lewis Publishers.

Butler, D.; Thedchanamoorthy, S.; Payne, J. A. (1992): Aspects of Surface Sediment Characteristics on an Urban Catchment in London. In: *Water Sci Technol* 25 (8), S. 13–19. Online verfügbar unter http://wst.iwaponline.com/content/25/8/13.

Čabanová, Kristina; Hrabovská, Kamila; Matějková, Petra; Dědková, Kateřina; Tomášek, Vladimír; Dvořáčková, Jana; Kukutschová, Jana (2019): Settled iron-based road dust and its characteristics and possible association with detection in human tissues. In: *Env Sci Poll Res Int* 26 (3), S. 2950–2959. DOI: 10.1007/s11356-018-3841-x.

Carpenter, Kurt D.; Kuivila, Kathryn M.; Hladik, Michelle L.; Haluska, Tana; Cole, Michael B. (2016): Storm-event-transport of urban-use pesticides to streams likely impairs invertebrate assemblages. In: *Environmental monitoring and assessment* 188 (6), S. 345. DOI: 10.1007/s10661-016-5215-5.

Charlesworth, S. M.; Lees, J. A. (1999): The distribution of heavy metals in deposited urban dusts and sediments, Coventry, England. In: *Environmental Geochemistry and Health* 21 (2), S. 97–115. DOI: 10.1023/A:1006694400288.

Charters, Frances J.; Cochrane, Thomas A.; O'Sullivan, Aisling D. (2015): Particle size distribution variance in untreated urban runoff and its implication on treatment selection. In: *Water Res* 85, S. 337–345. DOI: 10.1016/j.watres.2015.08.029.

Chebbo, Ghassan (1992): Solides des rejets pluviaux urbains: caractérisation et traitabilité (Suspended-solids in urban wet weather discharges: Characteristics and treatability). Dissertation. Ecole Nationale des Ponts et Chaussées. Online verfügbar unter https://pastel.archives-ouvertes.fr/pastel-00569043.

Chebbo, Ghassan; Gromaire, M.-C. (2009): VICAS—An Operating Protocol to Measure the Distributions of Suspended Solid Settling Velocities within Urban Drainage Samples. In: *J Environ Eng* 135 (9), S. 768–775. DOI: 10.1061/(ASCE)0733-9372(2009)135:9(768).

Chiou, Cary T.; McGroddy, Susan E.; Kile, Daniel E. (1998): Partition Characteristics of Polycyclic Aromatic Hydrocarbons on Soils and Sediments. In: *Environ. Sci. Technol.* 32 (2), S. 264–269. DOI: 10.1021/es970614c.

Chmiel, Tomasz; Mieszkowska, Anna; Kempińska-Kupczyk, Dagmara; Kot-Wasik, Agata; Namieśnik, Jacek; Mazerska, Zofia (2019): The impact of lipophilicity on environmental processes, drug delivery and bioavailability of food components. In: *Microchemical Journal* 146, S. 393–406. DOI: 10.1016/j.microc.2019.01.030.

Choi, W. W.; Chen, K. Y. (1976): Associations of chlorinated hydrocarbons with fine particles and humic substances in nearshore surficial sediments. In: *Environ Sci Technol* 10 (8), S. 782–786. DOI: 10.1021/es60119a004.

Cladière, Mathieu; Gasperi, Johnny; Lorgeoux, Catherine; Bonhomme, Céline; Rocher, Vincent; Tassin, Bruno (2013): Alkylphenolic compounds and bisphenol A contamination within a heavily urbanized area. Case study of Paris. In: *Environmental Science and Pollution Research International* 20 (5), S. 2973–2983. DOI: 10.1007/s11356-012-1220-6.

Councell, Terry B.; Duckenfield, Kea U.; Landa, Edward R.; Callender, Edward (2004): Tire-wear particles as a source of zinc to the environment. In: *Environ Sci Technol* 38 (15), S. 4206–4214. DOI: 10.1021/es034631f.

Crabtree, B.; Dempsey, P.; Johnson, I.; Whitehead, M. (2008): The development of a risk-based approach to managing the ecological impact of pollutants in highway runoff. In: *Water Sci Technol* 57 (10), S. 1595–1600. DOI: 10.2166/wst.2008.269.

Craig, Robert F. (2004): Craig's soil mechanics. 7th ed. London: Taylor & Francis. Online verfügbar unter http://www.loc.gov/catdir/enhancements/fy0651/2003061302-d.html.

Cristina, Chad; Tramonte, Jarrod; Sansalone, John J. (2002): A Granulometry-Based Selection Methodology for Separation of Traffic-Generated Particles in Urban Highway Snowmelt Runoff. In: *Water Air Soil Pollut* 136 (1/4), S. 33–53. DOI: 10.1023/A:1015239831619.

Davis, Allen P.; Shokouhian, Mohammad; Ni, Shubei (2001): Loading estimates of lead, copper, cadmium, and zinc in urban runoff from specific sources. In: *Chemosphere* 44 (5), S. 997–1009. DOI: 10.1016/S0045-6535(00)00561-0.

Deletic, Ana (1998): The first flush load of urban surface runoff. In: *Water Res* 32 (8), S. 2462–2470. DOI: 10.1016/S0043-1354(97)00470-3.

Dierkes, Carsten; Lucke, Terry; Helmreich, Brigitte (2015): General Technical Approvals for Decentralised Sustainable Urban Drainage Systems (SUDS)—The Current Situation in Germany. In: *Sustainability* 7 (12), S. 3031–3051. DOI: 10.3390/su7033031.

Dierschke, M. (2014): Methodischer Ansatz zur Quantifizierung von Feinpartikeln (PM63) in Niederschlagsabflüssen in Abhängigkeit von der Herkunftsfläche. Dissertation. TU Kaiserslautern, Kaiserslautern.

Dietrich, William E. (1982): Settling velocity of natural particles. In: *Water Resour. Res.* 18 (6), S. 1615–1626. DOI: 10.1029/WR018i006p01615.

Directive 2000/60/EC: Directive 2000/60/EC of the European Parliament and of the Council of 23 October 2000 establishing a framework for Community action in the field of water policy.

Directive 2013/39/EU: Directive 2013/39/EU of the European Parliament and of the Council of 12 August 2013 amending Directives 2000/60/EC and 2008/105/EC as regards priority substances in the field of water policy Text with EEA relevance.

Donald I. Bleiwas (2006): Stocks and flows of lead-based wheel weights in the United States. In: *Open-File Report* (2006-1111). DOI: 10.3133/ofr20061111UR.

Dotto, C. B. S.; Kleidorfer, M.; Deletic, A.; Fletcher, T. D.; McCarthy, D. T.; Rauch, W. (2010): Stormwater quality models: performance and sensitivity analysis. In: *Water Sci Technol* 62 (4), S. 837–843. DOI: 10.2166/wst.2010.325.

Drapper, Darren; Tomlinson, Rodger; Williams, Philip (2000): Pollutant Concentrations in Road Runoff. Southeast Queensland Case Study. In: *J Environ Eng* 126 (4), S. 313–320. DOI: 10.1061/(ASCE)0733-9372(2000)126:4(313).

Droppo, I. G.; Irvine, K. N.; Jaskot, C. (2002): Flocculation/aggregation of cohesive sediments in the urban continuum: implications for stormwater management. In: *Environmental Technology* 23 (1), S. 27–41. DOI: 10.1080/09593332508618433.

Duong, Trang T. T.; Lee, Byeong-Kyu (2011): Determining contamination level of heavy metals in road dust from busy traffic areas with different characteristics. In: *Journal of Environmental Management* 92 (3), S. 554–562. DOI: 10.1016/j.jenvman.2010.09.010.

DWA (2020): Arbeitsblatt DWA-A 102. Grundsätze zur Bewirtschaftung und Behandlung von Regenwetterabflüssen zur Einleitung in Oberflächengewässer. Hennef: Deutsche Vereinigung für Wasserwirtschaft Abwasser und Abfall (DWA-Regelwerk, A 102).

El-Mufleh, Amelene; Bechet, Beatrice; Basile-Doelsch, Isabelle; Geffroy-Rodier, Claude; Gaudin, Anne; Ruban, Veronique (2014a): Distribution of PAHs and trace metals in urban stormwater sediments: combination of density fractionation, mineralogy and microanalysis. In: *Environmental Science and Pollution Research International* 21 (16), S. 9764–9776. DOI: 10.1007/s11356-014-2850-7.

El-Mufleh, Amelene; Bechet, Beatrice; Ruban, Veronique; Legret, Michel; Clozel, Blandine; Barraud, Sylvie et al. (2014b): Review on physical and chemical characterizations of contaminated sediments from urban stormwater infiltration basins within the framework of the French observatory for urban hydrology (SOERE URBIS). In: *Environmental Science and Pollution Research International* 21 (8), S. 5329–5346. DOI: 10.1007/s11356-013-2490-3.

El-Mufleh, Amelène; Béchet, Béatrice; Grasset, Laurent; Rodier, Claude; Gaudin, Anne; Ruban, Véronique (2013): Distribution of PAH residues in humic and mineral fractions of sediments from stormwater infiltration basins. In: *J Soils Sediments* 13 (3), S. 531–542. DOI: 10.1007/s11368-012-0586-x.

Eriksson, E.; Baun, A.; Scholes, L.; Ledin, A.; Ahlman, S.; Revitt, M. et al. (2007): Selected stormwater priority pollutants: a European perspective. In: *The Science of the Total Environment* 383 (1-3), S. 41–51. DOI: 10.1016/j.scitotenv.2007.05.028.

Evans, K. M.; Gill, R. A.; Robotham, P. W. J. (1990): The PAH and organic content of sediment particle size fractions. In: *Water, Air, and Soil Pollution* 51 (1), S. 13–31. DOI: 10.1007/BF00211500.

Everett, D. H. (1988): Basic principles of colloid science. London: Royal Society of Chemistry.

Fedotov, Petr S.; Ermolin, Mikhail S.; Karandashev, Vasily K.; Ladonin, Dmitry V. (2014): Characterization of size, morphology and elemental composition of nano-, submicron, and micron particles of street dust separated using field-flow fractionation in a rotating coiled column. In: *Talanta* 130, S. 1–7. DOI: 10.1016/j.talanta.2014.06.040.

Field, Andy (2017): Discovering Statistics Using IBM SPSS Statistics. 5th edition. London, England: SAGE Publications.

Förstner, Ulrich; Grathwohl, Peter (2007): Ingenieurgeochemie. Technische Geochemie - Konzepte und Praxis. 2., neu bearbeitete Auflage. Berlin, Heidelberg: Springer Berlin Heidelberg, zuletzt geprüft am 27.03.2020.

Francey, Matt; Fletcher, Tim D.; Deletic, Ana; Duncan, Hugh (2010): New Insights into the Quality of Urban Storm Water in South Eastern Australia. In: *J Environ Eng* 136 (4), S. 381–390. DOI: 10.1061/(ASCE)EE.1943-7870.0000038.

Fuchs, Stephan; Eyckmanns-Wolters, Rebecca; Maus, C.; Sommer, M.; Voßwinkel, N.; Mohn, R. (2013): Reduktion des Feststoffeintrages durch Niederschlagseinleitungen - Abschlussbericht der Phase 1. beauftragt vom MKULNV NRW. Hg. v. DWA. Hennef, zuletzt geprüft am 02.02.2017.

Fuchs, Stephan; Mayer, Ingo; Haller, Bernd; Roth, Hartmut (2014): Lamella settlers for storm water treatment - performance and design recommendations. In: *Water Sci Technol* 69 (2), S. 278–285. DOI: 10.2166/wst.2013.698.

Gasperi, J.; Sebastian, Christel; Ruban, V.; Delamain, M.; Percot, S.; Wiest, L. et al. (2014): Micropollutants in urban stormwater: occurrence, concentrations, and atmospheric contributions for a wide range of contaminants in three French catchments. In: *Environ Sci Pollut Res* 21 (8), S. 5267–5281. DOI: 10.1007/s11356-013-2396-0.

Gasperi, Johnny; Garnaud, Stephane; Rocher, Vincent; Moilleron, Regis (2009): Priority pollutants in surface waters and settleable particles within a densely urbanized area: case study of Paris (France). In: *The Science of the Total Environment* 407 (8), S. 2900–2908. DOI: 10.1016/j.scitotenv.2009.01.024.

Gelhardt, Laura (2020): Charakterisierung von Feststoffen auf urbanen Verkehrsflächen als potenzielle Schadstoffträger im Niederschlagsabfluss. PhD Thesis. TU Kaiserslautern, Kaiserslautern. Online verfügbar unter https://kluedo.ub.uni-kl.de/frontdoor/index/index/searchtype/authorsearch/author/%22Gelhardt%2C+Laura%22/docId/6156/start/0/rows/1.

Gelhardt, Laura; Huber, Maximilian; Welker, Antje (2017): Development of a Laboratory Method for the Comparison of Settling Processes of Road-Deposited Sediments with Artificial Test Material. In: *Water Air Soil Pollut* 228 (12), S. 849. DOI: 10.1007/s11270-017-3650-8.

German, J.; Svensson, G. (2002): Metal content and particle size distribution of street sediments and street sweeping waste. In: *Water Sci Technol* 46 (6-7), S. 191–198.

Gnecco, I.; Palla, A.; Sansalone, J. J. (2019): Partitioning of zinc, copper and lead in urban drainage from paved source area catchments. In: *J Hydrol* 578, S. 124128. DOI: 10.1016/j.jhydrol.2019.124128.

Göbel, P.; Dierkes, C.; Coldewey, W. G. (2007): Storm water runoff concentration matrix for urban areas. In: *Journal of Contaminant Hydrology* 91 (1-2), S. 26–42. DOI: 10.1016/j.jconhyd.2006.08.008.

Goonetilleke, Ashantha; Thomas, Evan; Ginn, Simon; Gilbert, Dale (2005): Understanding the role of land use in urban stormwater quality management. In: *Journal of Environmental Management* 74 (1), S. 31–42. DOI: 10.1016/j.jenvman.2004.08.006.

Gosset, Antoine; Durrieu, Claude; Orias, Frédéric; Bayard, Rémy; Perrodin, Yves (2017): Identification and assessment of ecotoxicological hazards attributable to pollutants in urban wet weather discharges. In: *Environmental Science. Processes & Impacts* 19 (9), S. 1150–1168. DOI: 10.1039/c7em00159b.

Grant S.B.; Rekhi N.V.; Pise N.R.; Reeves R.L.; Matsumoto M.; Wistrom A. et al. (2003): A review of the contaminants and toxicity associated with particles in stormwater runoff. Hg. v. California Departement of Transport.

Gromaire, M. C.; Garnaud, S.; Gonzalez, A.; Chebbo, Ghassan (1999): Charecterisation of urban runoff pollution in Paris. In: *Water Sci Technol* 39 (2), S. 1–8, zuletzt geprüft am 20.12.2016.

Gromaire, M. C.; van de Voorde, A.; Lorgeoux, C.; Chebbo, G. (2015): Benzalkonium runoff from roofs treated with biocide products - In situ pilot-scale study. In: *Water research* 81, S. 279–287. DOI: 10.1016/j.watres.2015.05.060.

Grout, Hélène; Wiesner, Mark R.; Bottero, Jean-Yves (1999): Analysis of Colloidal Phases in Urban Stormwater Runoff. In: *Environ. Sci. Technol.* 33 (6), S. 831–839. DOI: 10.1021/es980195z.

Gunawardana, Chandima; Egodawatta, Prasanna; Goonetilleke, Ashantha (2014): Role of particle size and composition in metal adsorption by solids deposited on urban road surfaces. In: *Environmental pollution (Barking, Essex : 1987)* 184, S. 44–53. DOI: 10.1016/j.envpol.2013.08.010.

Gunawardana, Chandima; Egodawatta, Prasanna; Goonetilleke, Ashantha (2015): Adsorption and mobility of metals in build-up on road surfaces. In: *Chemosphere* 119, S. 1391–1398. DOI: 10.1016/j.chemosphere.2014.02.048.

Gunawardana, Chandima; Goonetilleke, Ashantha; Egodawatta, Prasanna; Dawes, Les; Kokot, Serge (2012): Source characterisation of road dust based on chemical and mineralogical composition. In: *Chemosphere* 87 (2), S. 163–170. DOI: 10.1016/j.chemosphere.2011.12.012.

Gunawardena, Janaka M.A.; Liu, An; Egodawatta, Prasanna; Ayoko, Godwin A.; Goonetilleke, Ashantha (2018): Influence of Traffic and Land Use on Urban Stormwater Quality. Singapore: Springer Singapore.

Gupta, M. K.; Agnew, R. W.; Kobriger, N. P.; Envirex, Inc. (1981): Constituents of Highway Runoff: Volume I, State-of-the-Art Report. United States. Federal Highway Administration. Offices of Research and DevelopmentUR - https://rosap.ntl.bts.gov/view/dot/29955 (FCP 33E3-014).

Gustafsson, Mats; Blomqvist, Göran; Järlskog, Ida; Lundberg, Joacim; Janhäll, Sara; Elmgren, Max et al. (2019): Road dust load dynamics and influencing factors for six winter seasons in Stockholm, Sweden. In: *Atmospheric Environment: X* 2, S. 100014. DOI: 10.1016/j.aeaoa.2019.100014.

Hallermeier, Robert J. (1981): Terminal settling velocity of commonly occurring sand grains. In: *Sedimentology* 28 (6), S. 859–865. DOI: 10.1111/j.1365-3091.1981.tb01948.x.

Hamilton, R. S.; Revitt, D. M.; Warren, R. S. (1984): Levels and physico-chemical associations of Cd, Cu, Pb and Zn in road sediments. In: *Science of The Total Environment* 33 (1-4), S. 59–74. DOI: 10.1016/0048-9697(84)90381-4.

Herngren, Lars; Goonetilleke, Ashantha; Ayoko, Godwin A. (2005): Understanding heavy metal and suspended solids relationships in urban stormwater using simulated rainfall. In: *Journal of Environmental Management* 76 (2), S. 149–158. DOI: 10.1016/j.jenvman.2005.01.013.

Herngren, Lars; Goonetilleke, Ashantha; Ayoko, Godwin A. (2006): Analysis of heavy metals in road-deposited sediments. In: *Analytica Chimica Acta* 571 (2), S. 270–278. DOI: 10.1016/j.aca.2006.04.064.

Herngren, Lars; Goonetilleke, Ashantha; Ayoko, Godwin A.; Mostert, Maria M. M. (2010): Distribution of polycyclic aromatic hydrocarbons in urban stormwater in Queensland, Australia. In: *Environmental pollution (Barking, Essex : 1987)* 158 (9), S. 2848–2856. DOI: 10.1016/j.envpol.2010.06.015.

Hillebrand, Gudrun (2008): Transportverhalten kohäsiver Sedimente in turbulenten Strömungen - Untersuchungen im offenen Kreisgerinne.

Hilliges, Rita; Schriewer, Alexander; Helmreich, Brigitte (2013): A three-stage treatment system for highly polluted urban road runoff. In: *Journal of Environmental Management* 128, S. 306–312. DOI: 10.1016/j.jenvman.2013.05.024.

Hoffman, Eva J.; Mills, Gary L.; Latimer, James S.; Quinn, James G. (1984): Urban runoff as a source of polycyclic aromatic hydrocarbons to coastal waters. In: *Environ. Sci. Technol.* 18 (8), S. 580–587. DOI: 10.1021/es00126a003.

Hofstede, Henricus Theodorus (1994): Use of bauxite refining residue to reduce the mobility of heavy metals in municipal waste compost. PhD Thesis. Murdoch University, Australia. School of Biological and Environmental Sciences. Online verfügbar unter https://researchrepository.murdoch.edu.au/id/eprint/101/.

Holleman, Arnold F.; Wiberg, Nils; Wiberg, Egon (2007): Lehrbuch der Anorganischen Chemie. 102. Aufl. Berlin: Walter de Gruyter.

Holten Lützhøft, Hans-Christian; Eriksson, Eva; Donner, Erica; Wickman, Tonie; Banovec, Primož; Mikkelsen, Peter Steen; Ledin, Anna (2009): Quantifying Releases of Priority Pollutants from Urban Sources. In: *proc water environ fed* 2009 (10), S. 5873–5891. DOI: 10.2175/193864709793952567.

Hong, Yi; Bonhomme, Celine; Le, Minh-Hoang; Chebbo, Ghassan (2016): New insights into the urban washoff process with detailed physical modelling. In: *The Science of the Total Environment* 573, S. 924–936. DOI: 10.1016/j.scitotenv.2016.08.193.

Huber, Maximilian; Welker, Antje; Helmreich, Brigitte (2016): Critical review of heavy metal pollution of traffic area runoff: Occurrence, influencing factors, and partitioning. In: *The Science of the Total Environment* 541, S. 895–919. DOI: 10.1016/j.scitotenv.2015.09.033.

Huber, Wayne Charles (1997): Contaminant transport in surface water. In: David R. Maidment (Hg.): Handbook of hydrology. 6th print. New York, N.Y., [etc.]: McGraw-Hill.

Hvitved-Jacobsen, T.; Johansen, N. B.; Yousef, Y. A. (1994): Treatment systems for urban and highway run-off in Denmark. In: *Science of The Total Environment* 146-147, S. 499–506. DOI: 10.1016/0048-9697(94)90275-5.

Hvitved-Jacobsen, Thorkild; Vollertsen, Jes; Nielsen, Asbjørn Haaning (2010): Urban and highway stormwater pollution. Concepts and engineering. Boca Raton, FL: CRC Press/Taylor & Francis.

ISO 14688-1:2017 (2017): Geotechnical investigation and testing - identification and classification of soil. Part 1: Identification and description.

Jacopin, Ch; Bertrand-Krajewski, Jean-Luc; Desbordes, M. (1999): Characterisation and settling of solids in an open, grassed, stormwater sewer network detention basin. In: *Water Sci Technol* 39 (2), S. 135–144. DOI: 10.1016/S0273-1223(99)00017-7.

Jayarathne, Ayomi; Egodawatta, Prasanna; Ayoko, Godwin A.; Goonetilleke, Ashantha (2017): Geochemical phase and particle size relationships of metals in urban road dust. In: *Environmental pollution (Barking, Essex : 1987)* 230, S. 218–226. DOI: 10.1016/j.envpol.2017.06.059.

Jiang, Weiying; Luo, Yuzhou; Conkle, Jeremy L.; Li, Juying; Gan, Jay (2016): Pesticides on residential outdoor surfaces: environmental impacts and aquatic toxicity. In: *Pest management science* 72 (7), S. 1411–1420. DOI: 10.1002/ps.4168.

Kalmykova, Yuliya; Björklund, Karin; Strömvall, Ann-Margret; Blom, Lena (2013): Partitioning of polycyclic aromatic hydrocarbons, alkylphenols, bisphenol A and phthalates in landfill leachates and stormwater. In: *Water Res* 47 (3), S. 1317–1328. DOI: 10.1016/j.watres.2012.11.054.

Karickhoff, Samuel W.; Brown, David S.; Scott, Trudy A. (1979): Sorption of hydrophobic pollutants on natural sediments. In: *Water Res* 13 (3), S. 241–248. DOI: 10.1016/0043-1354(79)90201-X.

Kaskas, A.-A. (1970): Schwarmgeschwindigkeiten in Mehrkornsuspensionen am Beispiel der Sedimentation. Dissertation. TU Berlin.

Katsoyiannis, Athanasios; Samara, Constantini (2007): The fate of dissolved organic carbon (DOC) in the wastewater treatment process and its importance in the removal of wastewater contaminants. In: *Environmental Science and Pollution Research International* 14 (5), S. 284–292. DOI: 10.1065/espr2006.05.302.

Kayhanian, Masoud (2012): Trend and concentrations of legacy lead (Pb) in highway runoff. In: *Environmental pollution (Barking, Essex : 1987)* 160 (1), S. 169–177. DOI: 10.1016/j.envpol.2011.09.009.

Kayhanian, Masoud; Fruchtman, Boaz D.; Gulliver, John S.; Montanaro, Comasia; Ranieri, Ezio; Wuertz, Stefan (2012): Review of highway runoff characteristics. Comparative analysis and universal implications. In: *Water research* 46 (20), S. 6609–6624. DOI: 10.1016/j.watres.2012.07.026.

Kim, Jae Y.; Park, Jae K.; Edil, Tuncer B. (1997): Sorption of Organic Compounds in the Aqueous Phase onto Tire Rubber. In: *J Environ Eng* 123 (9), S. 827–835. DOI: 10.1061/(ASCE)0733-9372(1997)123:9(827).

Kloepfer, Achim; Jekel, Martin; Reemtsma, Thorsten (2005): Occurrence, Sources, and Fate of Benzothiazoles in Municipal Wastewater Treatment Plants. In: *Environ Sci Technol* 39 (10), S. 3792–3798. DOI: 10.1021/es048141e.

Koglin, Bernd (1971): Statistische Verteilung der Sedimentationsgeschwindigkeit in niedrig konzentrierten Suspensionen. In: *Chemie Ingenieur Technik* 43 (13), S. 761–764. DOI: 10.1002/cite.330431306.

Kreider, Marisa L.; Panko, Julie M.; McAtee, Britt L.; Sweet, Leonard I.; Finley, Brent L. (2010): Physical and chemical characterization of tire-related particles: comparison of particles generated using different methodologies. In: *The Science of the Total Environment* 408 (3), S. 652–659. DOI: 10.1016/j.scitotenv.2009.10.016.

Lair, G. J.; Gerzabek, M. H.; Haberhauer, G. (2007): Sorption of heavy metals on organic and inorganic soil constituents. In: *Environ Chem Lett* 5 (1), S. 23–27. DOI: 10.1007/s10311-006-0059-9.

Larsen, Tove A.; Hoffmann, Sabine; Lüthi, Christoph; Truffer, Bernhard; Maurer, Max (2016): Emerging solutions to the water challenges of an urbanizing world. In: *Science (New York, N.Y.)* 352 (6288), S. 928–933. DOI: 10.1126/science.aad8641.

Lau, Sim-Lin; Stenstrom, Michael K. (2005): Metals and PAHs adsorbed to street particles. In: *Water Res* 39 (17), S. 4083–4092. DOI: 10.1016/j.watres.2005.08.002.

Launay, Marie Alexandra (2017): Organic Micropollutants in Urband Wastewater Systems during Dry and Wet Weather - Occurence, Spatio-Temporal Distribution and Emissions to Surface Waters. Dissertation. University of Stuttgart.

Lead J. R.; Davison W.; Hamilton-Taylor J.; Buffle J. (1997): Characterizing Colloidal Material in Natural Waters. In: *Aquatic Geochemistry* 3, S. 213–232, zuletzt geprüft am 03.11.2017.

Legret, M.; Pagotto, C. (1999): Evaluation of pollutant loadings in the runoff waters from a major rural highway. In: *Sci Total Environ* 235 (1), S. 143–150. DOI: 10.1016/S0048-9697(99)00207-7.

Lepom, Peter; Brown, Bruce; Hanke, Georg; Loos, Robert; Quevauviller, Philippe; Wollgast, Jan (2009): Needs for reliable analytical methods for monitoring chemical pollutants in surface water under the European Water Framework Directive. In: *Journal of chromatography. A* 1216 (3), S. 302–315. DOI: 10.1016/j.chroma.2008.06.017.

Leutnant, Dominik (2018): Monitoring, Analysis and Modelling of Urban Stormwater Quality. Dissertation. Technische Universität Graz. Institut für Siedlungswasserwirtschaft und Landschaftswasserbau.

Li, Haiyan; Shi, Anbang; Zhang, Xiaoran (2015): Particle size distribution and characteristics of heavy metals in road-deposited sediments from Beijing Olympic Park. In: *Journal of environmental sciences (China)* 32, S. 228–237. DOI: 10.1016/j.jes.2014.11.014.

Li, Yingxia; Lau, Sim-Lin; Masoud Kayhanian; Michael K. Stenstrom (2006): Dynamic Characteristics of Particle Size Distribution in Highway Runoff: Implications for Settling Tank Design. In: *J. Environ. Eng.* 132 (8), S. 852–861.

Lieske, Christian; Leutnant, Dominik; Uhl, Mathias (2021): Assessing the TSS Removal Efficiency of Decentralized Stormwater Treatment Systems by Long-Term In-Situ Monitoring. In: *Water* 13 (7), S. 908. DOI: 10.3390/w13070908.

Lin, Hong (2003): Granulometry, chemistry and physical interactions of non-colloidal particulate matter transported by urban storm water. Dissertation. Louisiana State University.

Loganathan, Paripurnanda; Vigneswaran, Saravanamuthu; Kandasamy, Jaya (2013): Road-Deposited Sediment Pollutants: A Critical Review of their Characteristics, Source Apportionment, and Management. In: *Critical Reviews in Environmental Science and Technology* 43 (13), S. 1315–1348. DOI: 10.1080/10643389.2011.644222.

Lucas-Aiguier, Emanuelle; Chebbo, Ghassan; Bertrand-Krajewski, Jean-Luc; Gagné, Benoit; Hedges, Peter (1998): Analysis of the Methods for Determining the Settling Characteristics of Sewage and Stormwater Solids. In: *Water Sci Technol* 37 (1), S. 53–60, zuletzt geprüft am 23.11.2017.

Luo, Yunlong; Guo, Wenshan; Ngo, Huu Hao; Nghiem, Long Duc; Hai, Faisal Ibney; Zhang, Jian et al. (2014): A review on the occurrence of micropollutants in the aquatic environment and their fate and removal during wastewater treatment. In: *The Science of the Total Environment* 473-474, S. 619–641. DOI: 10.1016/j.scitotenv.2013.12.065.

Lygren, E.; Gjessing, E.; Berglind, L. (1984): Pollution transport from a highway. In: *Sci Total Environ* 33 (1-4), S. 147–159. DOI: 10.1016/0048-9697(84)90389-9.

MacKenzie, Moira J.; Hunter, Joseph V. (1979): Sources and fates of aromatic compounds in urban stormwater runoff. In: *Environ Sci Technol* 13 (2), S. 179–183. DOI: 10.1021/es60150a011.

Makepeace, David K.; Smith, Daniel W.; Stanley, Stephen J. (1995): Urban stormwater quality. Summary of contaminant data. In: *Critical Reviews in Environmental Science and Technology* 25 (2), S. 93–139. DOI: 10.1080/10643389509388476.

Maniquiz-Redillas, Marla; Kim, Lee-Hyung (2014): Fractionation of heavy metals in runoff and discharge of a stormwater management system and its implications for treatment. In: *Journal of Environmental Sciences* 26 (6), S. 1214–1222. DOI: 10.1016/S1001-0742(13)60591-4.

Margot, Jonas (2015): Micropollutant removal from municipal wastewater – From conventional treatments to advanced biological processes. Dissertation. Ecole Polytechnique Fédérale de Lausanne, Lausanne.

Markiewicz, Anna; Björklund, Karin; Eriksson, Eva; Kalmykova, Yuliya; Strömvall, Ann-Margret; Siopi, Anna (2017): Emissions of organic pollutants from traffic and roads. Priority pollutants selection and substance flow analysis. In: *The Science of the Total Environment* 580, S. 1162–1174. DOI: 10.1016/j.scitotenv.2016.12.074.

Marsalek, Jiri; Jiménez-Cisneros B.E.; Malmqvist, Per-Arne; Karamouz M.; Goldenfum J.; Chocat B. (2008): Urban water cycle processes and interactions. Paris, France, Leiden, The Netherlands: Taylor & Francis (Urban water series - UNESCO-IHP, v. 2). Online verfügbar unter http://gbv.eblib.com/patron/FullRecord.aspx?p=325560.

Marsalek, Jiri; Marsalek, P. M. (1997): Characteristics of sediments from a stormwater management pond. In: *Water Sci Technol* 36 (8-9), S. 117–122. Online verfügbar unter http://wst.iwaponline.com/content/36/8-9/117.

McKenzie, Erica R.; Money, Jon E.; Green, Peter G.; Young, Thomas M. (2009): Metals associated with stormwater-relevant brake and tire samples. In: *The Science of the Total Environment* 407 (22), S. 5855–5860. DOI: 10.1016/j.scitotenv.2009.07.018.

Meland, Sondre; Borgstrøm, Reidar; Heier, Lene Sørlie; Rosseland, Bjørn Olav; Lindholm, Oddvar; Salbu, Brit (2010): Chemical and ecological effects of contaminated tunnel wash water runoff to a small Norwegian stream. In: *The Science of the Total Environment* 408 (19), S. 4107–4117. DOI: 10.1016/j.scitotenv.2010.05.034.

Michelbach, S.; Wöhrle, C. (1993): Settleable Solids in a Combined Sewer System, Settling Characteristics, Heavy Metals, Efficiency of Stormwater Tanks. In: *Water Sci Technol* 27 (5-6), S. 153–164.

Morquecho, Renee E.; Pitt, Robert E. (2003): Stormwater Heavy Metal Particulate Associations. In: *proc water environ fed* 2003 (12), S. 774–803. DOI: 10.2175/193864703784755247.

Morrison, Gregory M.; Revitt, D. Michael; Ellis, J. Bryan; Svensson, Gilbert; Balmer, Peter (1988): Transport mechanisms and processes for metal species in a gullypot system. In: *Water Res* 22 (11), S. 1417–1427. DOI: 10.1016/0043-1354(88)90099-1.

Mosley, Luke M.; Peake, Barrie M. (2001): Partitioning of metals (Fe, Pb, Cu, Zn) in urban run-off from the Kaikorai Valley, Dunedin, New Zealand. In: *New Zealand Journal of Marine and Freshwater Research* 35 (3), S. 615–624. DOI: 10.1080/00288330.2001.9517027.

Müller, Alexandra; Österlund, Heléne; Marsalek, Jiri; Viklander, Maria (2020): The pollution conveyed by urban runoff: A review of sources. In: *The Science of the Total Environment* 709, S. 136125. DOI: 10.1016/j.scitotenv.2019.136125.

Muschack, Werner (1990): Pollution of street run-off by traffic and local conditions. In: *Sci Total Environ* 93, S. 419–431. DOI: 10.1016/0048-9697(90)90133-F.

Myers, Leann; Sirois, Maria J. (2006): Spearman Correlation Coefficients, Differences between. In: Samuel Kotz, Campbell B. Read, N. Balakrishnan, Brani Vidakovic und Norman L. Johnson (Hg.): Encyclopedia of statistical sciences. 2nd ed. [Hoboken, N.ew Jersey]: Wiley.

Nightingale, Harry I. (1975): Lead, Zinc and Copper in Soils of Urban Storm-Runoff Retention Basins. In: *Journal - Amercican Water Works Association* 67 (8), S. 443–446.

Niu, Siping; Song, Xiaolong; Yu, Jianghua; Wang, Xuan; Liana, Jianjun (2020): Particle Size Dependent Heavy Metals in Road Dusts from Maanshan City, China. In: *KSCE J Civ Eng* 24 (5), S. 1411–1423. DOI: 10.1007/s12205-020-2193-5.

Paulson, C.; Amy, Gary (1993): Regulating metal toxicity in stormwater. In: *Water Environment & Technology* 5 (7), 44-49UR - https://pascal-francis.inist.fr/vibad/index.php?action=getRecordDetail&idt=4930737.

Petrie, Bruce; Barden, Ruth; Kasprzyk-Hordern, Barbara (2015): A review on emerging contaminants in wastewaters and the environment: current knowledge, understudied areas and recommendations for future monitoring. In: *Water Res* 72, S. 3–27. DOI: 10.1016/j.watres.2014.08.053.

Petrucci, Guido; Gromaire, Marie-Christine; Shorshani, Masoud Fallah; Chebbo, Ghassan (2014): Non-point source pollution of urban stormwater runoff. A methodology for source analysis. In: *Environmental Science and Pollution Research International* 21 (17), S. 10225–10242. DOI: 10.1007/s11356-014-2845-4.

Pisano, William C. (1996): Summary: United States 'sewer solids" settling characterization methods, results, uses and perspective. In: *Water Sci Technol* 33 (9), S. 109–115. DOI: 10.1016/0273-1223(96)00376-9.

Pisano, William C.; Brombach, Hans (1996): Solids Settling Curves. In: *Water Environment & Technology* 8 (4), S. 27–33. Online verfügbar unter http://www.jstor.org/stable/24665449.

Pitt, Robert E.; B. Peterson; P. Barron; A. Ayyoubi; S. Clark (1999): Stormwater treatment at critical areas: The multi-chambered treatment train (MCTT). Final report. Online verfügbar unter https://www.semanticscholar.org/paper/Stormwater-treatment-at-critical-areas%3A-The-train-Pitt-Peterson/0b9071f9e24e7a23c6647063dc6bcfe18bb4e0ed.

Preciado, Humberto F.; Li, Loretta Y. (2006): Evaluation of Metal Loadings and Bioavailability in Air, Water and Soil Along Two Highways of British Columbia, Canada. In: *Water, Air, and Soil Pollution* 172 (1-4), S. 81–108. DOI: 10.1007/s11270-005-9063-0.

Qian, Peng; Zheng, Xiangmin; Zhou, Limin; Jiang, Qingfeng; Zhang, Guoyu; Yang, Jian'er (2011): Magnetic Properties as Indicator of Heavy Metal Contaminations in Roadside Soil and Dust Along G312 Highways. In: *Procedia Environmental Sciences* 10, S. 1370–1375. DOI: 10.1016/j.proenv.2011.09.219.

Raudkivi, Arved J. (1982): Kohäsive Sedimente. In: Arved J. Raudkivi (Hg.): Grundlagen des Sedimenttransports. Berlin, Heidelberg: Springer Berlin Heidelberg, S. 127–165.

Readman, J. W.; Mantoura, R. F. C.; Rhead, M. M. (1984): The physico-chemical speciation of polycyclic aromatic hydrocarbons (PAH) in aquatic systems. In: *Fresenius' Zeitschrift für analytische Chemie* 319 (2), S. 126. DOI: 10.1007/BF00584673.

Reddy, C. M.; Quinn, J. G. (1997): Environmental Chemistry of Benzothiazoles Derived from Rubber. In: *Environ Sci Technol* 31, S. 2847–2853.

Regnery, Julia; Puttmann, Wilhelm (2010): Seasonal fluctuations of organophosphate concentrations in precipitation and storm water runoff. In: *Chemosphere* 78 (8), S. 958–964. DOI: 10.1016/j.chemosphere.2009.12.027.

Regnery, Julia; Püttmann, Wilhelm (2009): Organophosphorus Flame Retardants and Plasticizers in Rain and Snow from Middle Germany. In: *Clean Soil Air Water* 37 (4-5), S. 334–342. DOI: 10.1002/clen.200900050.

Revitt, D. M.; Hamilton R. S.; Warren R. S. (1990): The transport of heavy metals within a small urban catchment. In: *The Science of the Total Environment* (93), S. 359–373, zuletzt geprüft am 03.11.2017.

Robertson, D.J; Taylor, K.G; Hoon, S.R (2003): Geochemical and mineral magnetic characterisation of urban sediment particulates, Manchester, UK. In: *Appl Geochem* 18 (2), S. 269–282. DOI: 10.1016/S0883-2927(02)00125-7.

Roger, S.; Montrejaud-Vignoles, M.; Andral, M.C; Herremans, L.; Fortune, J.P (1998): Mineral, physical and chemical analysis of the solid matter carried by motorway runoff water. In: *Water research* 32 (4), S. 1119–1125. DOI: 10.1016/S0043-1354(97)00262-5.

Rogge, Wolfgang F.; Hildemann, Lynn M.; Mazurek, Monica A.; Cass, Glen R.; Simoneit, Bernd R. T. (1993): Sources of fine organic aerosol. 3. Road dust, tire debris, and organometallic brake lining dust. Roads as sources and sinks. In: *Environ. Sci. Technol.* 27 (9), S. 1892–1904. DOI: 10.1021/es00046a019.

Root, R. A. (2000): Lead loading of urban streets by motor vehicle wheel weights. In: *Environmental Health Perspectives* 108 (10), S. 937–940. DOI: 10.1289/ehp.00108937.

Sabin, Lisa D.; Lim, Jeong Hee; Stolzenbach, Keith D.; Schiff, Kenneth C. (2005): Contribution of trace metals from atmospheric deposition to stormwater runoff in a small impervious urban catchment. In: *Water Res* 39 (16), S. 3929–3937. DOI: 10.1016/j.watres.2005.07.003.

Sabin, Lisa D.; Lim, Jeong Hee; Venezia, Maria Teresa; Winer, Arthur M.; Schiff, Kenneth C.; Stolzenbach, Keith D. (2006): Dry deposition and resuspension of particle-associated metals near a freeway in Los Angeles. In: *Atmospheric Environment* 40 (39), S. 7528–7538. DOI: 10.1016/j.atmosenv.2006.07.004.

Sample, David J.; Grizzard, Thomas J.; Sansalone, John; Davis, Allen P.; Roseen, Robert M.; Walker, Jane (2012): Assessing performance of manufactured treatment devices for the removal of phosphorus from urban stormwater. In: *Journal of Environmental Management* 113, S. 279–291. DOI: 10.1016/j.jenvman.2012.08.039.

Sansalone, John; Tribouillard, Thierry (1999): Variation in Characteristics of Abraded Roadway Particles as a Function of Particle Size. Implications for Water Quality and Drainage. In: *Transportation Research Record: Journal of the Transportation Research Board* 1690, S. 153–163. DOI: 10.3141/1690-18.

Sansalone, John J.; Buchberger, Steven G. (1997a): Characterization of solid and metal element distributions in urban highway stormwater. In: *Water Sci Technol* 36 (8-9), S. 155–160. Online verfügbar unter http://wst.iwaponline.com/content/36/8-9/155.

Sansalone, John J.; Buchberger, Steven G. (1997b): Partitioning and First Flush of Metals in Urban Roadway Storm Water. In: *J. Environ. Eng.* 123 (2), S. 134–143. DOI: 10.1061/(ASCE)0733-9372(1997)123:2(134).

Sansalone, John J.; Buchberger, Steven G.; Koran, Joseph M.; Smithson, Joseph A. (1997): Relationship Between Particle Size Distribution and Specific Surface Area of Urban Roadway Stormwater Solids. In: *Transportation Research Record: Journal of the Transportation Research Board* 1601 (1), S. 95–108. DOI: 10.3141/1601-15.

Sansalone, John J.; Koran, Joseph M.; Smithson, Joseph A.; Buchberger, Steven G. (1998): Physical Characteristics of Urban Roadway Solids Transported during Rain Events. In: *J. Environ. Eng.* 124 (5), S. 427–440. DOI: 10.1061/(ASCE)0733-9372(1998)124:5(427).

Sartor, James D.; Boyd, Gail B. (1972): Water pollution aspects of street surface contaminants. U.S. Environmental Protection Agency (EPA-R2-72-081).

Sartor, James D.; Boyd, Gail B.; Agardy, Franklin J. (1974): Water Pollution Aspects of Street Surface Contaminants. In: *Journal (Water Pollution Control Federation)* 46 (3), S. 458–467. Online verfügbar unter http://www.jstor.org/stable/25038149.

Sartorius AG (1999): Manual of Weighing Applications -Part 1 Density. Online verfügbar unter http://www.dcu.ie/sites/default/files/mechanical_engineering/pdfs/manuals/DensityDeterminationManual.pdf, zuletzt geprüft am 05.02.2018.

Saulais, M.; Bedell, J. P.; Delolme, C. (2011): Cd, Cu and Zn mobility in contaminated sediments from an infiltration basin colonized by wild plants. The case of Phalaris arundinacea and Typha latifolia. In: *Water Science & Technology* 64 (1), S. 255. DOI: 10.2166/wst.2011.161.

Schmiedgruber, Michael (2015): Erstellung eines Bilanzmodells für eine Regenwasserbehandlunsanlage. Bachelorarbeit. Universität Stuttgart, Stuttgart. Institut für Siedlungswasserbau, Wassergüte- und Abfallwirtschaft.

Schwarzenbach, Rene P.; Gschwend, Philip M.; Imboden, Dieter M. (2002): Environmental Organic Chemistry. Hoboken, NJ, USA: John Wiley & Sons, Inc.

Severtson, Steven J.; Banerjee, Sujit (1996): Sorption of Chlorophenols to Wood Pulp. In: *Environ Sci Technol* 30 (6), S. 1961–1969. DOI: 10.1021/es950649h.

Shea, Damian. (1988): Developing national sediment quality criteria. In: *Environ. Sci. Technol.* 22 (11), S. 1256–1261. DOI: 10.1021/es00176a002.

Simpson, C. D.; Harrington, C. F.; Cullen, W. R. (1998): Polycyclic aromatic hydrocarbon contamination in marine sediments near Kitimat, British Columbia. In: *Environ. Sci. Technol.* 32 (21), S. 3266–3272. Online verfügbar unter <Go to ISI>://000076850200022.

Smith, James A.; Witkowski, P. J.; Fusillo, Thomas V. (1988): Manmade organic compounds in the surface waters of the United States; a review of current understanding: US Geological Survey (Circular).

Sörme, L.; Bergbäck, B.; Lohm, U. (2001): Goods in the Anthroposphere as a Metal Emission Source A Case Study of Stockholm, Sweden. In: *Water, Air, & Soil Pollution: Focus* 1 (3/4), S. 213–227. DOI: 10.1023/A:1017516523915.

Sparks, Donald L. (2003): Environmental soil chemistry. 2nd ed. Amsterdam, Boston: Academic Press. Online verfügbar unter http://www.loc.gov/catdir/description/els051/2002104258.html.

Stadt Freiburg (2012): Radverkehrskonzept Freiburg 2020. Anhang 3 - Maßnahmenbeschreibungen. Hg. v. Stadt Freiburg. Online verfügbar unter https://www.freiburg.de/pb/site/Freiburg/get/params_E-1121863396/431691/08b_Beschreibungen.pdf, zuletzt geprüft am 15.12.2020.

Staples, Charles A.; Peterson, Dennis R.; Parkerton, Thomas F.; Adams, William J. (1997): The environmental fate of phthalate esters: A literature review. In: *Chemosphere* 35 (4), S. 667–749. DOI: 10.1016/S0045-6535(97)00195-1.

Stevenson, F. J. (1965): Amino Acids. In: C. A. Black (Hg.): Methods of soil analysis. Madison, Wis.: American Society of Agronomy (Agronomy, no. 9), S. 1437–1451.

Stone, M.; Marsalek, Jiri (1996): Trace metal composition and speciation in street sediment. Sault Ste. Marie, Canada. In: *Water Air Soil Pollut* 87 (1-4), S. 149–169. DOI: 10.1007/BF00696834.

Stotz, Gebhard; Dittmer, Ulrich (2009): Erhebungen zur Verschmutzung der Abflüsse aus dem Industriegebiet Haid der Stadt Freiburg als Grundlage für den Ausbau der Regenwasserbehandlung. Schlussbericht zum Untersuchungsauftrag der Abwasser Freiburg GmbH (Auftraggeber). Institut für Siedlungswasserbau, Wassergüte- und Abfallwirtschaft.

Strömvall, Ann-Margret; Norin, Malin; Pettersson, Thomas (2007): Organic contaminants in urban sediments and vertical leaching in road ditches. In: Gregory M. Morrison und Sébastien Rauch (Hg.): Highway and urban environment. Proceedings of the 8th Highway and Urban Environment Symposium, Bd. 12. Dordrecht, the Netherlands: SPRINGER (Alliance For Global Sustainability Bookseries, volume 12), S. 235–247.

Sutherland, Ross A. (2003): Lead in grain size fractions of road-deposited sediment. In: *Environ Pollut* 121 (2), S. 229–237. DOI: 10.1016/S0269-7491(02)00219-1.

Thomann, Robert V.; Mueller, John H. (1987): Principles of surface water quality modeling and control. New York: Harper & Row, Publishers.

Tisdall, J. M.; Oades, J. M. (1982): Organic matter and water-stable aggregates in soils. In: *Journal of Soil Science* 33 (2), S. 141–163. DOI: 10.1111/j.1365-2389.1982.tb01755.x.

Tyack, J. Naomi; Hedges, Peter D.; Smisson, Robert P. M. (1996): The relationship between settling velocity grading and the characteristics of the contributing catchment. In: *Water Sci Technol* 33 (9), S. 135–142. DOI: 10.1016/0273-1223(96)00379-4.

United Nations General Assembly (2010): The human right to water and sanitation. A/RES/64/292.

van Leussen, Wim (1994): Estuarine macroflocs and their role in fine-grained sediment transport. Universiy of Utrecht, Den Haag.

Vaze, J.; Chiew, Francis H.S (2002): Experimental study of pollutant accumulation on an urban road surface. In: *Urban Water* 4 (4), S. 379–389. DOI: 10.1016/S1462-0758(02)00027-4.

Wakeham, Stuart G. (1977): A Characterization of the Sources of Petroleum Hydrocarbons in Lake Washington. In: *Journal (Water Pollution Control Federation)* 49 (7), S. 1680–1687. Online verfügbar unter http://www.jstor.org/stable/25039760.

Walling, D. E.; Woodward, J. C. (1993): Use of a field-based water elutriation system for monitoring the in situ particle size characteristics of fluvial suspended sediment. In: *Water Res* 27 (9), S. 1413–1421. DOI: 10.1016/0043-1354(93)90021-9.

Wang, Qing; Liu, Min; Li, Ye; Liu, Yankun; Li, Shuwen; Ge, Rongrong (2016): Dry and wet deposition of polycyclic aromatic hydrocarbons and comparison with typical media in urban system of Shanghai, China. In: *Atmospheric Environment* 144, S. 175–181. DOI: 10.1016/j.atmosenv.2016.08.079.

Ward, Neil I. (1990): Multielement contamination of British motorway environments. In: *Sci Total Environ* 93, S. 393–401. DOI: 10.1016/0048-9697(90)90130-M.

Weber, W. (2001): Contaminant interactions with geosorbent organic matter. Insights drawn from polymer sciences. In: *Water Res* 35 (4), S. 853–868. DOI: 10.1016/S0043-1354(00)00339-0.

Welker, A. (2005): Schadstoffströme im urbanen Wasserkreislauf - Aufkommen und Verteilung, insbesondere in den Abwasserentsorgungssystemen. Habilitation. TU Kaiserslautern, Kaiserslautern.

Welker, Antje; Dierschke, Martina; Gelhardt, Laura (2019): Methodische Untersuchungen zur Bestimmung von AFS63 (Feine Abfiltrierbare Stoffe) in Verkehrsflächenabflüssen. In: *Das Gas- und Wasserfach* 160 (4), S. 79–88.

Welker, Antje; Dittmer, Ulrich (2005): Belastung von Verkehrsflächenabflüssen mit Schwermetallen und PAK. Ergebnisse einer Literaturstudie. In: *gwf Wasser - Abwasser* 146 (4), S. 320–332.

White, Robert Edwin (2009): Principles and practice of soil science. The soil as a natural resource. 4. ed., Nachdr. Malden, Mass.: Blackwell.

Wicke, D.; Matzinger, A.; Rouault, Pascale (2015): Relevanz organischer Spurenstoffe im Regenwasserabfluss Berlins - OgRe. Abschlussbericht. Kompetenzzentrum Wasser Berlin.

Wilber, William G.; Hunter, Joseph V. (1979): Distribution of Metals in Street Sweepings, Stormwater Solids, and Urban Aquatic Sediments. In: *Journal (Water Pollution Control Federation)* 51 (12), S. 2810–2822. Online verfügbar unter http://www.jstor.org/stable/25040508.

Wium-Andersen, Tove; Nielsen, Asbjørn H.; Hvitved-Jacobsen, Thorkild; Kristensen, Niels Krogh; Brix, Hans; Arias, Carlos; Vollertsen, Jes (2012): Sorption media for stormwater treatment--a laboratory evaluation of five low-cost media for their ability to remove metals and phosphorus from artificial stormwater. In: *Water Environ Res* 84 (7), S. 605–616. DOI: 10.2175/106143012x13373550426832.

Wu, Junliang; Ren, Yufen; Wang, Xuemei; Wang, Xiaoke; Chen, Liding; Liu, Gangcai (2015): Nitrogen and phosphorus associating with different size suspended solids in roof and road runoff in Beijing, China. In: *Environmental Science and Pollution Research International* 22 (20), S. 15788–15795. DOI: 10.1007/s11356-015-4743-9.

Wu, Weiming; Perera, Chamil; Smith, Jarrell; Sanchez, Alejandro (2018): Critical shear stress for erosion of sand and mud mixtures. In: *J Hydraul Res* 56 (1), S. 96–110. DOI: 10.1080/00221686.2017.1300195.

Xanthopoulos, C.; Hahn, H. H. (1990): Pollutants attached to particles from drainage areas. In: *Science of The Total Environment* 93, S. 441–448. DOI: 10.1016/0048-9697(90)90135-H.

Xie, Shanju; Dearing, John A.; Bloemendal, Jan; Boyle, John F. (1999): Association between the organic matter content and magnetic properties in street dust, Liverpool, UK. In: *Sci Total Environ* 241 (1-3), S. 205–214. DOI: 10.1016/S0048-9697(99)00346-0.

Zanders, J. M. (2005): Road sediment. Characterization and implications for the performance of vegetated strips for treating road run-off. In: *The Science of the Total Environment* 339 (1-3), S. 41–47. DOI: 10.1016/j.scitotenv.2004.07.023.

Zeng, Eddy Y.; Tran, Kim; Young, Diana (2004): Evaluation of potential molecular markers for urban stormwater runoff. In: *Environ Monit Assess* 90, S. 23–43, zuletzt geprüft am 18.11.2016.

Zgheib, Sally; Moilleron, Regis; Chebbo, Ghassan (2012): Priority pollutants in urban stormwater: part 1 - case of separate storm sewers. In: *Water Res* 46 (20), S. 6683–6692. DOI: 10.1016/j.watres.2011.12.012.

Zgheib, Sally; Moilleron, Regis; Saad, Mohamed; Chebbo, Ghassan (2011): Partition of pollution between dissolved and particulate phases: what about emerging substances in urban stormwater catchments? In: *Water Res* 45 (2), S. 913–925. DOI: 10.1016/j.watres.2010.09.032.

Zhang, Hua; Wang, Zhaofeng; Zhang, Yili; Ding, Mingjun; Li, Lanhui (2015): Identification of traffic-related metals and the effects of different environments on their enrichment in roadside soils along the Qinghai-Tibet highway. In: *The Science of the Total Environment* 521-522, S. 160–172. DOI: 10.1016/j.scitotenv.2015.03.054.

Zhao, Hongtao; Li, Xuyong (2013): Understanding the relationship between heavy metals in road-deposited sediments and washoff particles in urban stormwater using simulated rainfall. In: *J Hazard Mater* 246-247, S. 267–276. DOI: 10.1016/j.jhazmat.2012.12.035.

Zuofeng, Luan (1987): Characteristics of organic geochemistry of sediments in the northern part of the South Huanghai Sea. In: *Chinese Journal of Oceanology and Limnology* 5 (1), S. 59–66. DOI: 10.1007/BF02848523.

Appendix

Tab. A.1: Comparison of particle size distribution in urban stormwater runoff

#	Country	catchment	Sampling method	drying	Smallest mesh size (µm)	Largest mesh size (µm)	PSD-Method	study
1	USA	HWY, Cincinnati (AADT: 150,000), Q1-Q4*	solid collection tank	110 °C	25	9,000	DS/LD	Sansalone et al. 1998
2	USA	HWY, Baton Rouge (AADT:140,000), Q2-Q3*	solid collection tank	40 °C	75	24,500	DS/LD (< 75 µm)	Kim and Sansalone 2008a
3	USA	HWY, California (AADT: 5,000 – 30,000)	Grab samples	N/A	38	1,000	WS/LD	Kayhanian et al. 2012b
4	USA	PL, UR, R, M Madison, Q1-Q3*	Flow proportional composite	105 °C	32	500	WS/CC	Selbig et al. 2016
5	South Korea	UR, Yongin, Q2-Q3*	Time proportional	N/A	38	425	WS	Yun et al. 2010
6	China	UR, Peking (AADT: > 20,000), Q2*	Flow proportional composite	N/A	38	200	WS, Filtration (< 10 µm)	Wu et al. 2015
7	Switzerland	HWY, Winterthur (AADT: 50,000), Q3	Volume proportional	N/A	20	250	WS	Furumai et al. 2002
8	Spain	M, Santiago de Compostela	Time proportional	N/A	0.375	2,000	CC	Anta et al. 2006
9	New Zealand	UR, M, Christchurch	Grab + auto sampling	N/A	0.01	3,000	LD	Charters et al. 2015

Tab. A.1: continued
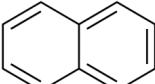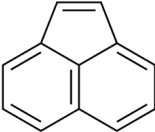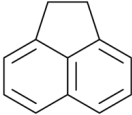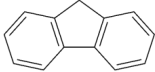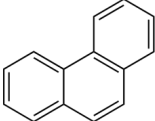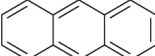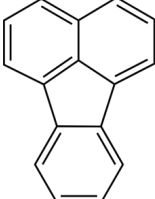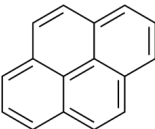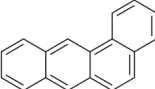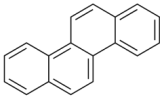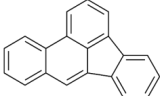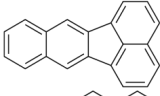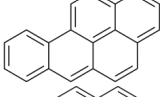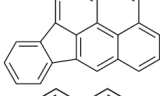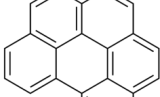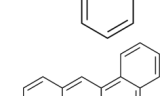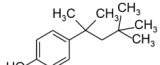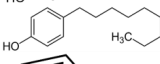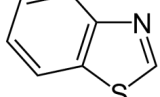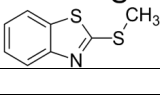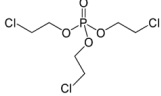
No.	Country	Location	Sampling method	Temperature		PSD-Method	Reference
10	USA	UR, Baltimore, Milwaukee, Bucyrus, Tulsa, Atlanta*	V,S, dry	< 37.8 °C	43	WS,DS,E	Sartor and Boyd 1972
11	USA	UR (I, C, R), Santa Monica, Q1	V, dry	air drying	43	DS	Lau and Stenstrom 2005
12	USA	HWY, Cincinnati (AADT: 150,000), Q4	V, dry	air drying	15	DS	Sansalone and Tribouillard 1999
13	China	UR (I, C, R), Shengzen	V, S, dry	air drying	75	DS	Zhao et al. 2017
14	Malaysia	UR (I, R) Singapore, Q3	S, dry	105 °C	63	DS	Yuen et al. 2012
15	Japan	UR, Kobe (AADT: 70,000), Q1*	V,S,dry	105 °C	50	DS	Adachi and Tainosho 2005
16	Serbia	PL, Belgrade University, Q2-Q3*	V,wet	50 °C	63	DS	Djukic et al. 2016
17	Austria	UR, Lienz	N/A	air drying	63	WS,E	Haile et al. 2016
18	Germany	UR, Dresden (DRV: 12,600), Q1	S, dry	N/A	63	DS	Zhang et al. 2016
19	Germany	UR, Hildesheim (AADT: 22,000), Q2-Q3*	V, dry	N/A	25	DS	Grottker 1987
20	England	UR, London*	V,S,dry	105 °C	63	DS	Butler et al. 1992
21	Australia	UR, Melbourne*	V,S,dry	100 °C	38	DS	Vaze and Chiew 2002
22	New Zealand	UR, Auckland, Hamilton, Christchurch, Q3*	SM, dry	40 °C	63	DS	Depree 2008

Sampling method: V = vacuum cleaner, S = street sweeping, SM = sweeping machine, N/A = no information given
PSD-Method: DS = dry sieving, WS = wet sieving, E = Elutriation, LD = Laser diffraction, CC = Coulter counter
Catchment: HWY = highway, UR = urban road, PL = parking lot, R = residential, M = mixed catchment, I = industrial, C = commercial
Season: Q1 = spring (march-may), Q2 = summer (june-august), Q3 = autumn (september-november), Q4 = winter (december-february)
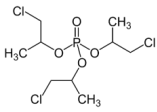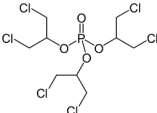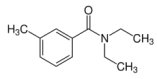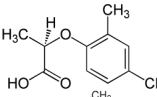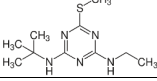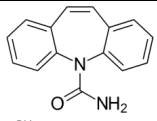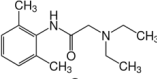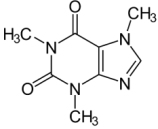
B   Materials and Methods

Tab. B.1:   Chemical structures of organic micropollutants analysed in this study

Compound	Molecular formula	Structure
Polycyclic aromatic hydrocarbons (PAHs)		
Naphtalene	$C_{10}H_6$	
Acenaphthylene	$C_{12}H_8$	
Acenaphthene	$C_{12}H_{10}$	
Fluorene	$C_{13}H_{10}$	
Phenanthrene	$C_{14}H_{10}$	
Anthracene	$C_{14}H_{10}$	
Fluoranthene	$C_{16}H_{10}$	
Pyrene	$C_{16}H_{10}$	
Benz[a]anthracene	$C_{18}H_{12}$	

Chrysene	C$_{18}$H$_{12}$	
Benzo[b]fluoranthene	C$_{20}$H$_{12}$	
Benzo[k]fluoranthene	C$_{20}$H$_{12}$	
Benzo[a]pyrene	C$_{20}$H$_{12}$	
Indeno[1,2,3-cd]py-rene	C$_{22}$H$_{12}$	
Benzo[ghi]perylene	C$_{22}$H$_{12}$	
Dibenzo[ah]anthra-cene	C$_{22}$H$_{14}$	

Household/ industrial chemicals		
4-tert-octylphenol	C$_{14}$H$_{22}$O	
4-nonylphenol	C$_{15}$H$_{24}$O	
Benzothiazole	C$_7$H$_5$NS	
2-methylthiobenzothi-azole	C$_8$H$_7$NS$_2$	

Flameretardants and plasticisers		
Tris(2-chlorethyl)phos-phate	C$_6$H$_{12}$Cl$_3$O$_4$P	

Tris(1-chloro-2-propyl)phosphate	$C_9H_{18}Cl_3O_4P$	
Tris(1,3-dichlorisopropyl)phosphate	$C_9H_{15}Cl_6O_4P$	

Biocides

Diethyltoluamid	$C_{12}H_{17}NO$	
Mecoprop	$C_{10}H_{11}ClO_3$	
Terbutryn	$C_{10}H_{19}N_5S$	

Pharmaceuticals and others

Carbamazepine	$C_{15}H_{12}N_2O$	
Lidocain	$C_{14}H_{22}N_2O$	
Caffeine	$C_8H_{10}N_4O_2$	

C   Results and Discussion
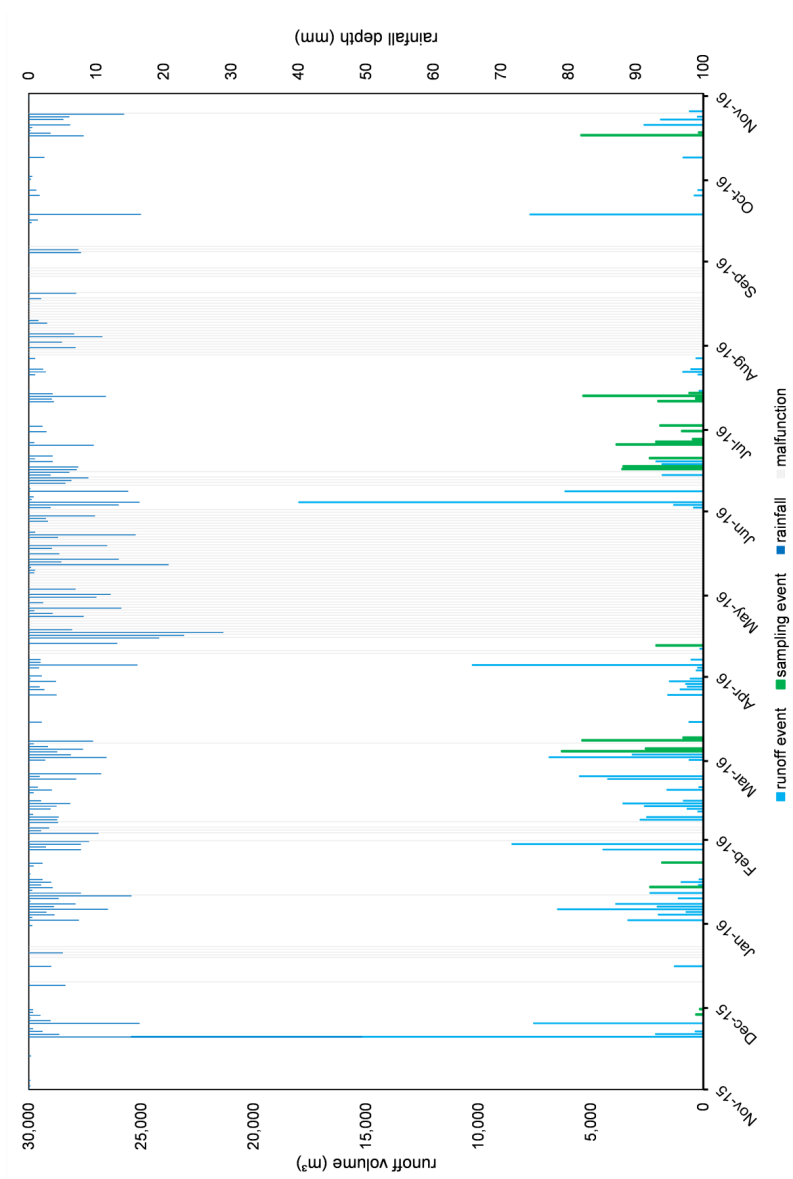
Fig. C.1:   Overview of recorded runoff events and sampling events for the monitoring period 2015 –2016

Tab. C.2:   Runoff characteristics of sampling events (monitoring period 2015-2016)

Sample	$n_{rain\ events}$	Date of rain event	V_{over} (m³)	V_{CWD} (m³)	V_{eff} (m³)	$\sum V$ (m³)	$Q_{max,over}$ (l/s)	$Q_{max,CWD}$ (l/s)
2015_1130	2	28/11/2015	0	0	321	321	0	0
		29/11/2015	0	0	156	156	0	0
2016_0118	1	14/01/2016	1278	757	332	2367	281	314
2016_0201	1	22/01/2016	738	760	332	1830	96	323
2016_0307	2	04/03/2016	5208	757	332	6297	325	324
		05/03/2016	1436	788	332	2556	144	328
2016_0331	1	07/03/2016	1248	3803	332	5383	85	343
2016_0415	1	13/04/2016	1096	660	332	2088	260	273
2016_0620	1	16/06/2016	2224	1054	332	3610	278	370
2016_0620	1	16/06/2016	0	3229	332	3561	0	389
2016_0627	1	20/06/2016	1150	899	332	2381	132	348
		25/06/2016	2498	1035	332	3865	447	390
2016_0627	3	25/06/2016	838	933	332	2103	85	362
		26/06/2016	0	132	332	464	0	105
2016_0707	2	30/06/2016	0	625	332	957	0	321
		02/07/2016	704	878	332	1914	85	354
2016_0715	1	11/07/2016	472	1205	332	2009	85	383
		12/07/2016	0	0	332	332	0	0
2016_0715	3	13/07/2016	2885	2122	322	5339	1220	866
		14/07/2016	0	287	332	619	0	206
2018_1028	1	17/10/2016	4210	890	332	5432	1220	866

Tab. C.3:   Characteristics of the sampled rainfall events (2015 – 2016). Recording interval of rain gauge: 2 h

Rain event	Rainfall depth (mm)	Start	Duration (hh:mm)	Mean intensity (mm/h)	Antecedent dry period
28/11/2015	1.70	06:00	08:00	0.2	1 day, 16 hours
29/11/2015	1.20	16:00	08:00	0.2	1 day, 2 hours
14/01/2016	4.60	16:00	10:00	0.5	1 day, 14 hours
22/01/2016	2.70	22:00	02:00	1.4	5 days, 6 hours
04/03/2016	10.6	12:00	18:00	0.6	16 hours
05/03/2016	4.40	18:00	10:00	0.4	12 hours
07/03/2016	10.2	18:00	24:00	0.4	1 day, 14 hours
13/04/2016	13.1	08:00	04:00	3.3	5 days, 21 hours
16/06/2016	5.90	04:00	06:00	1.0	16 hours
16/06/2016	8.50	18:00	22:00	0.4	8 hours
20/06/2016	4.40	22:00	06:00	0.7	1 day, 8 hours
25/06/2016	6.90	00:00	04:00	1.7	3 days, 20 hours
25/06/2016	2.70	18:00	02:00	1.4	14 hours
26/06/2016	0.80	20:00	02:00	0.4	1 day
30/06/2016	2.60	02:00	04:00	0.7	3 day, 4 hours
02/07/2016	1.90	02:00	02:00	1.0	1 day, 20 hours
11/07/2016	6.10	16:00	18:00	0.3	9 days, 12 hours
12/07/2016	1.00	20:00	02:00	0.5	10 hours
13/07/2016	12.6	08:00	16:00	0.8	10 hours
14/07/2016	1.90	18:00	02:00	1.0	18 hours
17/10/2016	11.3	14:00	24:00	0.5	8 days
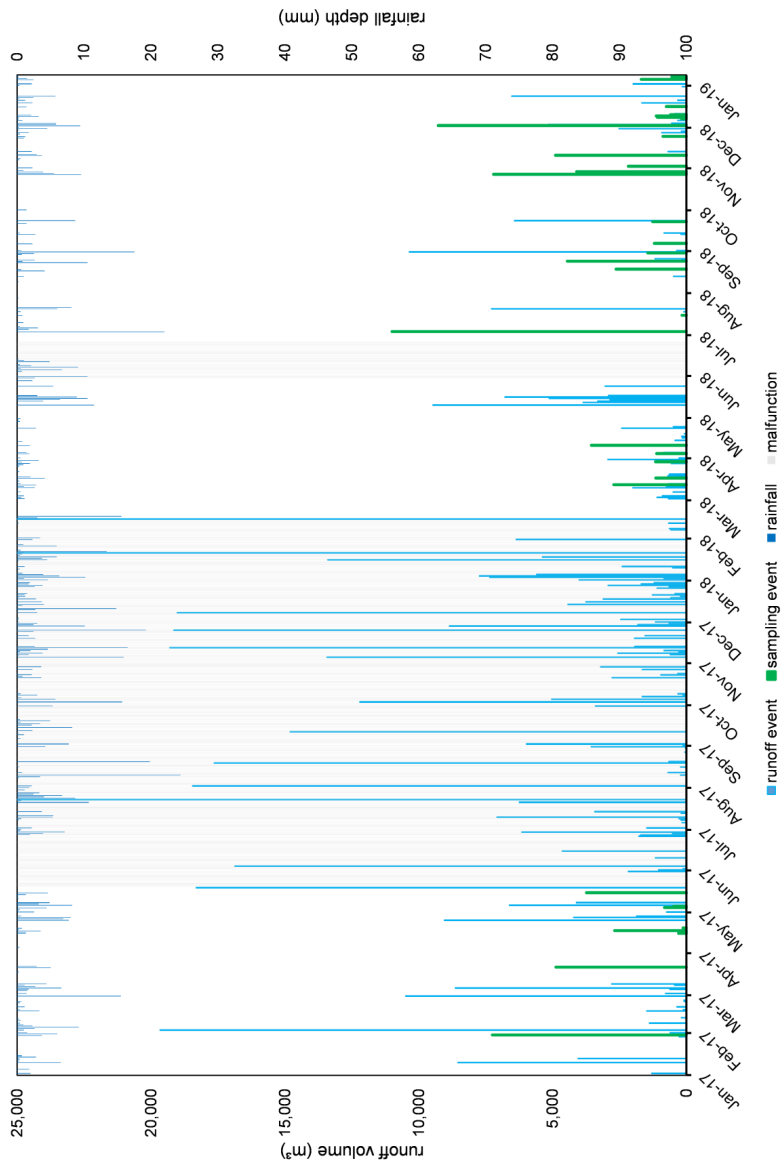
Fig. C.2: Overview of recorded runoff events and sampling events for the monitoring period 2017 – 2019

Tab. C.4: Runoff characteristics of sampling events (monitoring period 2017 – 2019)

Sample	$n_{rain\ events}$	Date of rain event	V_{over} (m³)	V_{CWD} (m³)	V_{eff} (m³)	$\sum V$ (m³)	$Q_{max,over}$ (l/s)	$Q_{max,CWD}$ (l/s)
2017_0206	1	30/01/2017	5236	1686	322	7254	312	343
2017_0331	1	21/03/2017	3804	745	332	4881	153	313
		15/04/2017	0	0	295	295	0	0
2017_0502	4	16/04/2017	0	0	247	247	0	0
		17/04/2017	2188	242	332	2762	476	274
		19/04/2017	0	0	135	135	0	0
2017_0505	2	04/05/2017	0	498	332	830	0	258
		04/05/2017	0	146	332	478	0	133
2017_0519	1	14/05/2017	2614	795	332	3741	507	331
2018_0314	1	12/03/2018	2725	1484	909	322	308	350
2018_0323	1	18/03/2018	0	824	322	1156	0	354
2018_0404	1	28/03/2018	0	827	332	1159	0	181
2018_0406	1	04/04/2018	0	787	322	1119	0	355
2018_0412	1	10/04/2018	2298	933	332	3563	1443	362
2018_0720	1	15/07/2018	0	0	178	178	0	0
2018_0828	1	24/08/2018	4145	995	332	5472	4454	325
2018_0914	1	06/09/2018	0	775	332	1107	0	305
2018_0928	1	21/09/2018	0	825	332	1157	0	305
2018_1030	1	27/10/2018	6041	837	332	7210	190	342
2018_1107	1	02/11/2018	1057	793	332	2182	318	327
2018_1114	1	10/11/2018	3763	806	332	4901	541	271
2018_1127	1	24/11/2018	0	548	332	880	0	300
2018_1205	1	02/12/2018	8132	815	332	9279	891	330
		07/12/2018	0	0	192	192	0	0
2018_1213	4	09/12/2018	0	753	332	1085	0	320
		09/12/2018	0	807	332	1139	0	328
		10/12/2018	0	269	332	601	0	189
2018_1220	1	16/12/2018	0	425	332	757	0	223
		05/01/2019	378	716	332	1426	49	288
2019_0108	3	06/01/2019	0	0	251	251	0	0
		06/01/2019	0	180	332	512	0	149

Tab. C.5: Characteristics of the sampled rainfall events (monitoring period 2017 – 2019). Recording interval of rain gauge: 10 min

Rain event	Rainfall depth (mm)	Start	Duration (hh:mm)	Mean intensity (mm/h)	Antecedent dry period
30/01/2017	11.2	10:40	48:10	0.23	14 days, 9 hours
21/03/2017	7.90	16:10	15:00	0.53	2 days, 16 hours
15/04/2017	1.30	12:50	07:40	0.17	10 days, 11 hours
16/04/2017	0.90	05:10	02:20	0.39	9 hours
17/04/2017	3.50	12:00	08:20	0.42	1 day, 4 hours
19/04/2017	0.70	12:00	07:30	0.01	1 day, 16 hours
04/05/2017	2.80	07:20	05:00	0.56	1 day, 5 hours
04/05/2017	1.60	21:40	01:20	1.20	9 hours
14/05/2017	5.90	13:00	15:40	0.38	1 day, 6 hours
12/03/2018	3.00	06:50	18:30	0.16	14 hours
18/03/2018	1.00	13:00	01:20	0.75	9 hours
28/03/2018	1.70	14:10	20:20	0.08	12 hours
04/04/2018	1.80	16:00	06:40	0.27	3 days, 6 hours
10/04/2018	1.90	14:10	01:00	1.90	4 days, 18 hours
15/07/2018	0.90	18:40	05:20	0.17	4 days, 23 hours
23/08/2018	11.0	20:10	05:20	2.06	5 days, 10 hours
06/09/2018	2.40	18:50	09:00	0.27	5 days, 10 hours
21/09/2018	1.50	19:00	09:10	0.16	6 days, 3 hours
27/10/2018	14.4	02:30	10:20	0.42	25 days, 5 hours
01/11/2018	2.30	18:20	01:50	1.25	2 days, 7 hours
10/11/2018	6.60	20:00	11:20	0.58	2 days, 15 hours
23/11/2018	2.20	23:10	03:40	0.60	8 days, 13 hours
02/12/2018	11.2	05:20	22:20	0.50	1 day, 1 hour
07/12/2018	1.30	22:00	02:00	0.65	1 day, 14 hours
09/12/2018	2.30	05:40	01:50	0.65	2 days, 20 hours
09/12/2018	3.20	15:20	05:40	0.35	8 hours
10/12/2018	1.60	05:00	02:40	0.38	8 hours
16/12/2018	2.10	04:00	06:00	0.35	5 days, 6 hours
05/01/2019	2.4	09:00	12:40	0.19	3 days, 4 hours
06/01/2019	0.6	03:50	03:30	0.17	6 hours
06/01/2019	1.1	13:40	10:30	0.10	6 hours
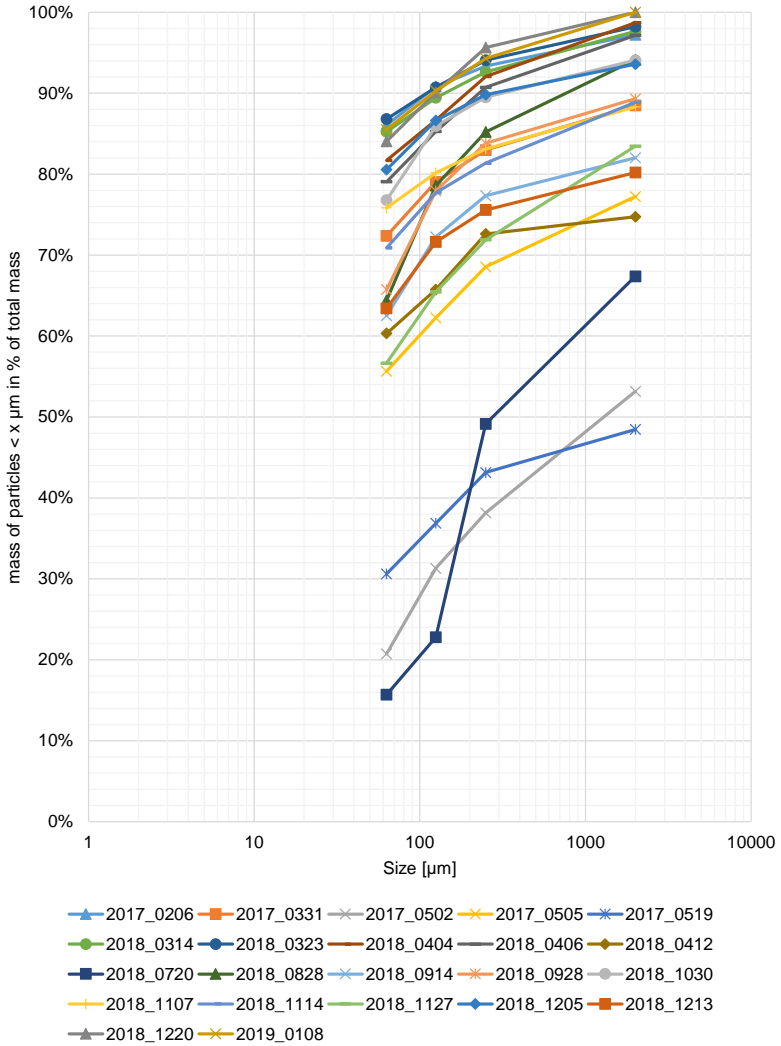
Fig. C.3: Particle size distributionl of the individual sampling events of this study (monitoring period: 2017 – 2019)

Tab. C.6: Particle size distribution as absolute mass fractions for the individual sampling events of this study

sample	< 63 μm		63 – 2000 μm		> 2000 μm
2015_1130	15%		75%		10%
2016_0118	61%		30%		9%
2016_0201	77%		21%		2%
2016_0307	92%		7%		1%
2016_0331	78%		20%		1%
2016_0415	57%		38%		5%
2016_0620_I	71%		26%		4%
2016_0620_II	61%		37%		1%
2016_0627_I	45%		45%		10%
2016_0627_II	34%		47%		19%
2016_0707	36%		52%		12%
2016_0715_I	37%		47%		16%
2016_0715_II	42%		46%		12%
2016_1028	22%		64%		14%
sample	< 63 μm	63 – 125 μm	125 – 250 μm	250 – 2000 μm	> 2000 μm
2017_0206	86%	5%	3%	4%	3%
2017_0331	72%	7%	4%	6%	11%
2017_0502	21%	11%	7%	15%	47%
2017_0505	56%	7%	6%	9%	23%
2017_0519	31%	6%	6%	5%	52%
2018_0314	85%	4%	3%	5%	2%
2018_0323	87%	4%	3%	4%	2%
2018_0404	82%	5%	5%	7%	1%
2018_0406	79%	6%	5%	6%	3%
2018_0412	60%	5%	7%	2%	25%
2018_0720	16%	7%	26%	18%	33%
2018_0828	64%	14%	7%	9%	6%
2018_0914	63%	10%	5%	5%	18%
2018_0928	66%	12%	6%	6%	11%
2018_1030	77%	9%	4%	5%	6%
2018_1107	76%	4%	3%	5%	12%
2018_1114	71%	7%	4%	7%	11%
2018_1127	57%	9%	6%	12%	17%
2018_1205	81%	6%	3%	4%	6%
2018_1213	63%	8%	4%	5%	20%
2018_1220	84%	6%	6%	4%	0%
2019_0108	86%	5%	4%	6%	0%

Tab. C.7: Sample specific TSS event mean concentrations, sampling period: 2015 – 2016 (pH, electrical conducivity and temperature mean values measured in sampling container)

sample	pH	EC (ms cm^{-1})	T (°C)	TSS (mg L^{-1})			
				total	< 63 μm	63 – 2000 μm	> 2000 μm
2015_1130	N/A	N/A	11.9	56.5	8.24	42.6	5.65
2016_0118	N/A	N/a	9.00	14.6	8.92	4.39	1.26
2016_0201	6.90	1.14	10.5	25.3	19.5	5.39	0.44
2016_0307	7.43	N/A	7.85	14.4	13.2	1.08	0.11
2016_0331	7.25	0.17	11.6	9.05	7.08	1.84	0.13
2016_0415	6.93	0.11	12.3	26.2	15.0	9.82	1.37
2016_0620_I	7.14	0.15	16.3	16.4	11.6	4.26	0.58
2016_0620_II	7.14	0.15	16.0	17.4	10.7	6.51	0.26
2016_0627_I	7.38	0.17	19.3	17.3	7.78	7.87	1.67
2016_0627_II	6.83	0.16	19.3	54.5	18.3	25.6	10.6
2016_0707	7.10	0.17	20.8	67.8	24.2	35.3	8.39
2016_0715_I	6.82	0.14	15.8	172	63.8	81.4	27.0
2016_0715_II	6.93	0.11	16.6	79.9	33.4	36.8	9.6
2016_1028	7.24	N/A	9.90	162	35.6	103	23.1

Tab. C.8: Sample specific TSS event mean concentrations, sampling period: 2017 – 2019 (pH, electrical conductivity and temperature mean values measured in sampling container)

sample	pH	EC (ms cm^{-1})	T (°C)	TSS (mg L^{-1}) total	< 63 µm	63 – 125 µm	125 – 250 µm	250 – 2000 µm	> 2000 µm
2017_0206	7.61	0.36	6.00	65.0	56.0	3.07	1.65	2.52	1.80
2017_0331	7.42	0.15	14.0	29.9	21.6	1.99	1.17	1.65	3.43
2017_0502	7.35	0.17	11.8	311	64.4	32.8	21.2	46.6	145
2017_0505	7.28	0.15	12.0	48.0	26.7	3.170	3.01	4.17	10.9
2017_0519	6.95	0.15	17.3	143	43.8	8.934	8.97	7.61	73.7
2018_0314	7.55	0.19	9.90	112	95.5	4.700	3.56	5.65	2.63
2018_0323	7.37	0.25	8.10	21.7	18.9	0.849	0.73	0.90	0.39
2018_0404	7.12	0.18	12.7	33.6	27.4	1.673	1.81	2.23	0.43
2018_0406	6.89	0.18	9.40	42.8	33.8	2.659	2.33	2.75	1.22
2018_0412	7.11	0.13	13.4	317	191	17.2	21.8	6.70	80.2
2018_0720	6.65	0.15	21.4	332	52.1	23.6	87.6	60.5	108
2018_0828	6.72	0.06	18.5	105	67.3	14.8	6.93	9.33	6.13
2018_0914	6.77	0.12	19.1	25.4	15.9	2.461	1.29	1.19	4.56
2018_0928	6.82	0.09	16.2	74.0	48.7	9.032	4.35	4.08	7.91
2018_1030	7.12	0.07	9.90	16.5	12.7	1.508	0.59	0.76	0.97
2018_1107	6.96	0.06	9.47	27.5	20.8	1.193	0.80	1.43	3.21
2018_1114	7.02	0.06	10.2	31.2	22.1	2.127	1.14	2.34	3.47
2018_1127	6.86	0.12	7.80	40.0	22.6	3.516	2.57	4.62	6.61
2018_1205	7.21	0.06	10.2	63.9	51.5	3.873	2.05	2.41	4.10
2018_1213	6.91	0.06	5.78	53.4	33.9	4.382	2.11	2.47	10.6
2018_1220	6.86	1.53	8.50	8.95	7.52	0.542	0.50	0.39	N/A
2018_0108	7.23	0.14	7.80	14.1	12.1	0.672	0.57	0.81	N/A

Tab. C.9:   Sample specific TSS event loads, sampling period: 2015 – 2016

TSS load (kg)

sample	total	< 63 µm	63 – 2000 µm	> 2000 µm
2015_1130	27	4	20	3
2016_0118	34	21	10	3
2016_0201	46	36	10	1
2016_0307	128	117	10	1
2016_0331	57	44	12	1
2016_0415	55	31	21	3
2016_0620_I	59	42	15	2
2016_0620_II	62	38	23	1
2016_0627_I	41	19	19	4
2016_0627_II	54	18	26	11
2016_0707	195	69	101	24
2016_0715_I	346	128	164	54
2016_0715_II	502	210	231	61
2016_1028	912	201	581	130

Tab. C.10: Sample specific TSS event loads, sampling period: 2017 – 2019

TSS (kg)

sample	total	< 63 µm	63 – 125 µm	125 – 250 µm	250 – 2000 µm	> 2000 µm
2017_0206	472	406	22	12	18	13
2017_0331	146	105	10	6	8	17
2017_0502	1046	217	111	72	157	490
2017_0505	63	35	4	4	5	14
2017_0519	535	164	33	34	28	276
2018_0314	305	260	13	10	15	7
2018_0323	25	22	1	1	1	0.4
2018_0404	39	32	2	2	3	1
2018_0406	48	38	3	3	3	1
2018_0412	1131	682	61	78	24	286
2018_0720	59	9	4	16	11	19

Tab. C.10: continued

| | TSS (kg) | | | | | |
sample	total	< 63 µm	63 – 125 µm	125 – 250 µm	250 – 2000 µm	> 2000 µm
2018_0828	572	368	81	38	51	34
2018_0914	28	18	3	1	1	5
2018_0928	86	56	10	5	5	9
2018_1030	119	91	11	4	5	7
2018_1107	60	45	3	2	3	7
2018_1114	153	108	10	6	11	17
2018_1127	35	20	3	2	4	6
2018_1205	593	478	36	19	22	38
2018_1213	161	102	13	6	7	32
2018_1220	7	6	0.4	0.4	0.3	N/A
2019_0108	29	25	1	1	2	N/A

Tab. C.11: Sample specific TSS removal efficiencies, sampling period: 2015 – 2016

| | $\eta_{M, TSS}$ (-) | | | |
sample	total	< 63 µm	63 – 2000 µm	> 2000 µm
2015_1130	1.00	1.00	1.00	1.00
2016_0118	0.51	0.25	0.91	0.99
2016_0201	0.60	0.50	0.94	1.00
2016_0307	0.09	0.05	0.54	0.43
2016_0331	0.12	0.06	0.30	0.70
2016_0415	0.50	0.35	0.68	0.85
2016_0620_I	0.20	0.08	0.40	0.97
2016_0620_II	0.21	0.10	0.36	0.77
2016_0627_I	0.56	0.33	0.70	0.93
2016_0627_II	0.74	0.43	0.85	0.99
2016_0707	0.74	0.47	0.88	0.95
2016_0715_I	0.75	0.46	0.91	0.97
2016_0715_II	502	210	231	61
2016_1028	912	201	581	130

Tab. C.12: Sample specific TSS removal efficiencies, sampling period: 2017 – 2019

$\eta_{M, TSS}$ (-)

sample	total	< 63 µm	63 – 125 µm	125 – 250 µm	250 – 2000 µm	> 2000 µm
2017_0206	0.36	0.28	0.86	0.88	0.92	0.74
2017_0331	0.47	0.32	0.79	0.87	0.91	0.82
2017_0502	0.74	0.27	0.26	0.67	0.91	1.00
2017_0505	0.69	0.52	0.94	0.97	0.97	0.84
2017_0519	0.78	0.55	0.48	0.45	0.61	1.00
2018_0314	0.29	0.18	0.95	0.94	0.94	1.00
2018_0323	0.38	0.31	0.79	0.82	0.82	1.00
2018_0404	0.44	0.32	0.95	0.87	0.98	1.00
2018_0406	0.60	0.50	0.97	0.97	0.99	0.97
2018_0412	0.35	0.11	0.23	0.13	0.43	0.99
2018_0720	1.00	1.00	1.00	1.00	1.00	1.00
2018_0828	0.24	0.15	0.26	0.38	0.47	0.70
2018_0914	0.70	0.56	0.84	0.87	0.88	1.00
2018_0928	0.85	0.81	0.93	0.80	0.96	1.00
2018_1030	0.32	0.19	0.47	0.81	0.79	1.00
2018_1107	0.38	0.20	0.88	0.93	0.92	1.00
2018_1114	0.46	0.27	0.75	0.91	0.95	1.00
2018_1127	0.76	0.59	0.95	0.97	0.96	1.00
2018_1205	0.25	0.13	0.46	0.75	0.82	0.98
2018_1213	0.80	0.70	0.94	0.95	0.93	1.00
2018_1220	0.76	0.74	0.92	0.94	0.78	
2019_0108	0.35	0.30	0.54	0.64	0.75	

Tab. C.13: Event specific micropollutant event mean concentration (µg L^{-1}) for particular and dissolved phase. Limit of quantification (LOQ) = 0.002 µg L^{-1}

sample	NAP part.	NAP diss.	ACY part.	ACY diss.	ACN part.	ACN diss.	FLE part.	FLE diss.	PHE part.	PHE diss.
2017_0206	0.023	0.023	0.005	0.003	0.008	0.004	0.006	0.015	0.136	0.011
2017_0331	0.004	0.008	0.002	0.004	0.002	0.004	<LOQ	0.002	0.014	0.010
2017_0502	0.021	0.017	0.006	0.009	0.010	0.003	0.008	0.004	0.107	0.008
2017_0505	0.012	0.026	0.005	0.032	0.005	0.004	0.002	0.005	0.037	0.013
2017_0519	0.013	0.007	0.002	0.017	0.004	<LOQ	0.002	0.002	0.039	0.004
2018_0314	0.019	0.034	0.005	0.027	0.012	0.009	0.009	0.014	0.179	0.021
2018_0323	0.004	0.015	<LOQ	0.009	0.003	<LOQ	0.002	0.002	0.020	0.009
2018_0404	0.006	0.012	0.002	0.007	0.003	<LOQ	0.002	0.002	0.032	0.015
2018_0406	0.008	0.006	<LOQ	<LOQ	0.003	<LOQ	<LOQ	0.003	0.036	0.007
2018_0412	0.022	0.006	0.004	0.002	0.010	<LOQ	0.007	<LOQ	0.144	0.036
2018_0720	0.005	0.011	0.007	0.012	0.004	0.002	0.003	0.003	0.045	0.007
2018_0828	0.005	0.023	0.003	0.002	0.002	0.003	0.005	0.002	0.053	0.020
2018_0914	0.004	0.006	0.005	0.003	0.002	0.006	0.004	0.002	0.019	0.010
2018_0928	0.002	0.007	0.005	0.004	0.002	0.003	0.007	0.006	0.043	0.013
2018_1030	0.002	0.004	0.002	0.004	<LOQ	0.004	0.002	0.002	0.016	0.006
2018_1107	<LOQ	0.005	0.002	0.002	<LOQ	0.002	0.002	0.007	0.023	0.012
2018_1114	<LOQ	0.054	0.002	0.002	<LOQ	0.003	<LOQ	0.004	0.020	0.008
2018_1127	0.007	0.009	0.027	0.011	0.018	0.003	0.021	0.003	0.042	0.005
2018_1205	<LOQ	0.006	<LOQ	0.004	<LOQ	<LOQ	<LOQ	0.002	0.068	0.009
2018_1213	<LOQ	0.007	0.003	0.008	0.004	0.004	0.002	0.012	0.052	0.024
2018_1220	<LOQ	0.004	0.005	0.006	<LOQ	<LOQ	0.002	0.002	0.013	0.004
2019_0108	<LOQ	0.004	0.005	0.003	0.002	0.002	0.003	0.005	0.030	0.017

sample	ANT part.	ANT diss.	FLU part.	FLU diss.	PYR part.	PYR diss.	BaA part.	BaA diss.	CHR part.	CHR diss.
2017_0206	0.027	<LOQ	0.162	0.005	0.192	0.006	0.038	0.002	0.073	0.002
2017_0331	0.005	0.002	0.032	0.015	0.045	0.008	0.015	<LOQ	0.028	<LOQ
2017_0502	0.016	0.002	0.198	0.004	0.217	0.003	0.068	<LOQ	0.111	<LOQ
2017_0505	0.005	0.002	0.066	0.006	0.083	0.007	0.021	<LOQ	0.009	<LOQ
2017_0519	0.007	<LOQ	0.072	0.004	0.079	0.005	0.019	<LOQ	0.006	<LOQ
2018_0314	0.021	0.002	0.191	0.005	0.252	0.006	0.051	<LOQ	0.086	0.003
2018_0323	0.002	<LOQ	0.048	0.004	0.078	0.005	0.022	<LOQ	0.034	<LOQ
2018_0404	0.005	<LOQ	0.057	0.008	0.087	0.014	0.020	<LOQ	0.032	<LOQ
2018_0406	0.003	<LOQ	0.068	0.004	0.085	0.008	0.014	<LOQ	0.026	<LOQ
2018_0412	0.015	<LOQ	0.245	0.008	0.260	0.009	0.065	<LOQ	0.110	<LOQ
2018_0720	0.006	0.002	0.105	0.004	0.114	0.004	0.056	<LOQ	0.060	<LOQ
2018_0828	0.008	0.003	0.030	0.004	0.125	0.004	0.063	<LOQ	0.072	<LOQ
2018_0914	0.003	0.003	0.031	0.005	0.033	0.006	0.019	<LOQ	0.020	<LOQ
2018_0928	0.007	0.003	0.060	0.010	0.063	0.011	0.036	<LOQ	0.039	0.002
2018_1030	0.002	<LOQ	0.029	0.004	0.035	0.003	0.017	0.002	0.015	0.002
2018_1107	0.002	<LOQ	0.017	0.003	0.053	0.003	0.022	<LOQ	0.023	<LOQ
2018_1114	0.002	0.002	0.015	0.003	0.041	0.002	0.018	<LOQ	0.013	<LOQ
2018_1127	0.006	0.002	0.066	0.010	0.217	0.007	0.060	<LOQ	0.039	0.002
2018_1205	0.008	0.002	0.024	0.006	0.117	0.005	0.049	<LOQ	0.036	<LOQ
2018_1213	0.007	0.002	0.106	0.003	0.116	0.003	0.052	<LOQ	0.040	<LOQ

| 2018_1220 | 0.002 | <LOQ | 0.017 | 0.003 | 0.020 | 0.002 | 0.010 | <LOQ | 0.009 | <LOQ |
| 2019_0108 | 0.004 | <LOQ | 0.054 | 0.003 | 0.054 | 0.003 | 0.036 | <LOQ | 0.026 | <LOQ |

	BbF		BkF		BaP		IND		GHI	
sample	part.	diss.	part.	diss.	part.	diss.	part.	diss.	part.	diss.
2017_0206	0.069	<LOQ	0.033	<LOQ	0.035	<LOQ	0.021	<LOQ	0.057	<LOQ
2017_0331	0.027	<LOQ	0.016	<LOQ	0.018	<LOQ	0.011	<LOQ	0.026	<LOQ
2017_0502	0.121	<LOQ	0.050	<LOQ	0.065	<LOQ	0.043	<LOQ	0.106	<LOQ
2017_0505	0.027	<LOQ	0.014	<LOQ	0.029	<LOQ	0.011	<LOQ	0.038	<LOQ
2017_0519	0.034	<LOQ	0.020	<LOQ	0.030	<LOQ	0.012	<LOQ	0.036	<LOQ
2018_0314	0.119	<LOQ	0.028	<LOQ	0.046	<LOQ	0.027	<LOQ	0.100	<LOQ
2018_0323	0.091	<LOQ	0.026	<LOQ	0.023	<LOQ	0.018	<LOQ	0.043	<LOQ
2018_0404	0.058	<LOQ	0.025	<LOQ	0.018	<LOQ	0.012	<LOQ	0.042	<LOQ
2018_0406	0.046	<LOQ	0.021	<LOQ	0.015	<LOQ	0.026	<LOQ	0.042	<LOQ
2018_0412	0.141	<LOQ	0.067	<LOQ	0.061	<LOQ	0.035	<LOQ	0.130	<LOQ
2018_0720	0.101	<LOQ	0.078	<LOQ	0.088	<LOQ	0.039	<LOQ	0.049	<LOQ
2018_0828	0.078	<LOQ	0.074	<LOQ	0.068	<LOQ	0.024	<LOQ	0.031	<LOQ
2018_0914	0.025	<LOQ	0.022	<LOQ	0.025	<LOQ	0.010	<LOQ	0.013	<LOQ
2018_0928	0.026	<LOQ	0.022	<LOQ	0.057	<LOQ	0.020	<LOQ	0.025	<LOQ
2018_1030	0.021	<LOQ	0.016	<LOQ	0.019	<LOQ	0.010	<LOQ	0.017	<LOQ
2018_1107	0.019	<LOQ	0.027	<LOQ	0.022	<LOQ	0.015	<LOQ	0.028	<LOQ
2018_1114	0.016	<LOQ	0.015	<LOQ	0.014	<LOQ	0.014	<LOQ	0.019	<LOQ
2018_1127	0.030	<LOQ	0.024	<LOQ	0.043	<LOQ	0.038	<LOQ	0.046	<LOQ
2018_1205	0.054	<LOQ	0.035	<LOQ	0.055	<LOQ	0.023	<LOQ	0.046	<LOQ
2018_1213	0.027	<LOQ	0.020	<LOQ	0.038	<LOQ	0.030	<LOQ	0.050	<LOQ
2018_1220	0.009	<LOQ	0.008	<LOQ	0.012	<LOQ	0.013	<LOQ	0.016	<LOQ
2019_0108	0.023	<LOQ	0.023	<LOQ	0.025	<LOQ	0.018	<LOQ	0.018	<LOQ

	DBA		4tOP		4NP		BT		MTBT	
sample	part.	diss.	part.	diss.	part.	diss.	part.	diss.	part.	diss.
2017_0206	0.006	<LOQ	0.046	0.004	0.107	0.009	0.141	0.348	0.034	0.077
2017_0331	0.005	<LOQ	0.004	0.005	0.016	0.018	0.071	0.231	0.019	0.106
2017_0502	0.019	<LOQ	0.013	0.007	0.105	0.018	0.245	0.687	0.113	0.452
2017_0505	0.005	<LOQ	0.009	0.006	0.035	0.022	0.112	1.309	0.136	0.654
2017_0519	0.006	<LOQ	0.004	0.004	0.033	0.012	0.100	0.386	0.104	0.473
2018_0314	0.015	<LOQ	0.031	0.052	0.082	0.163	0.213	0.728	0.097	0.412
2018_0323	0.006	<LOQ	0.010	0.053	0.023	0.086	0.095	0.420	0.252	0.454
2018_0404	0.005	<LOQ	0.013	0.057	0.048	0.054	0.090	0.264	0.044	0.268
2018_0406	0.007	<LOQ	0.014	0.064	0.057	0.054	0.113	0.534	0.058	0.381
2018_0412	0.023	<LOQ	0.027	0.063	0.145	0.206	0.306	0.441	0.131	0.685
2018_0720	0.010	<LOQ	0.013	0.012	0.100	0.069	0.248	0.174	0.127	0.459
2018_0828	0.003	<LOQ	0.008	0.012	0.037	0.037	0.225	0.792	0.074	0.955
2018_0914	<LOQ	<LOQ	0.004	0.016	0.026	0.055	0.032	0.217	0.032	0.437
2018_0928	0.002	<LOQ	0.008	0.026	0.044	0.080	0.632	0.836	0.088	0.488
2018_1030	0.002	<LOQ	0.005	0.021	0.036	0.086	0.129	1.694	0.039	0.396
2018_1107	0.003	<LOQ	0.007	0.004	0.034	0.018	0.191	0.768	0.073	0.295
2018_1114	0.002	<LOQ	0.011	0.011	0.089	0.064	0.028	1.282	0.025	0.447
2018_1127	0.009	<LOQ	0.032	0.030	0.088	0.091	0.105	1.253	0.082	0.898
2018_1205	0.004	<LOQ	0.018	0.028	0.085	0.071	0.468	0.967	0.169	0.333
2018_1213	0.007	<LOQ	0.014	0.035	0.090	0.089	0.317	0.323	0.083	0.632
2018_1220	<LOQ	<LOQ	0.004	0.020	0.015	0.059	0.629	0.255	0.100	0.119

sample										
2019_0108	0.004	<LOQ	0.004	0.060	0.026	0.075	0.808	0.351	0.091	0.192

	TCEP		TCPP		TPP		DEET		MCP**	
sample	part.	diss.	part.	diss.	part.	diss.	part.	diss.	part.	diss.
2017_0206	0.002	0.162	0.137	0.215	0.002	0.012	<LOQ	0.005	<LOQ	0.026
2017_0331	0.009	0.739	0.071	0.383	0.004	0.009	<LOQ	0.005	<LOQ	0.413
2017_0502	0.025	0.390	0.381	0.463	0.031	0.009	<LOQ	0.010	0.030	2.548
2017_0505	0.037	0.277	0.110	0.434	0.008	0.009	<LOQ	0.007	0.002	0.506
2017_0519	0.007	0.222	0.361	0.280	0.015	0.003	<LOQ	0.006	0.002	1.013
2018_0314	0.020	0.629	0.550	0.804	0.006	0.015	0.002	0.011	<LOQ	0.054
2018_0323	0.016	0.427	0.291	0.625	0.002	0.034	<LOQ	0.009	<LOQ	0.080
2018_0404	0.014	0.346	0.253	0.686	0.003	0.021	<LOQ	0.006	<LOQ	0.113
2018_0406	0.007	0.425	0.319	0.763	0.002	0.013	<LOQ	0.008	<LOQ	0.308
2018_0412	0.030	0.921	0.991	1.323	0.010	0.031	<LOQ	0.016	<LOQ	0.290
2018_0720	0.043	0.642	0.737	1.004	0.043	0.021				
2018_0828	0.024	0.524	0.972	0.944	0.016	0.023				
2018_0914	0.017	0.466	0.156	1.501	<LOQ	0.022				
2018_0928	0.015	0.261	0.321	1.692	0.003	0.055				
2018_1030	0.006	0.700	0.123	1.989	0.003	0.009				
2018_1107	0.006	0.230	0.207	0.828	0.006	0.008				
2018_1114	0.004	0.214	0.278	0.704	0.004	0.020				
2018_1127	0.029	0.532	0.817	1.526	0.043	0.025				
2018_1205	0.019	0.375	1.894	1.911	0.026	0.066				
2018_1213	0.003	0.310	0.590	1.249	0.016	0.016				
2018_1220	0.009	0.307	0.153	1.004	0.005	0.022				
2019_0108	0.015	0.259	0.229	1.731	0.004	0.018				

	TBY		CBZ		LID		CAF	
sample	part.	diss.	part.	diss.	part.	diss.	part.	diss.
2017_0206	<LOQ	0.009	0.006	0.027	0.004	0.023	0.002	0.117
2017_0331	<LOQ	0.024	0.003	0.075	<LOQ	0.017	<LOQ	0.526
2017_0502	0.012	0.081	0.005	0.053	0.002	0.014	0.024	0.470
2017_0505	0.002	0.068	0.003	0.046	<LOQ	0.021	0.011	1.170
2017_0519	<LOQ	0.050	0.008	0.020	0.003	0.021	<LOQ	0.178
2018_0314	<LOQ	0.036					0.003	0.966
2018_0323	<LOQ	0.022					<LOQ	0.807
2018_0404	0.003	0.035					<LOQ	0.356
2018_0406	<LOQ	0.044					<LOQ	0.884
2018_0412	<LOQ	0.042					<LOQ	0.523
2018_0720	0.056	0.301					0.002	0.145
2018_0828	0.006	0.162					<LOQ	0.212
2018_0914	0.002	0.106					<LOQ	0.261
2018_0928	0.002	0.167					<LOQ	0.394
2018_1030	<LOQ	0.054					<LOQ	0.877
2018_1107	<LOQ	0.031					<LOQ	0.337
2018_1114	<LOQ	0.037					<LOQ	0.410
2018_1127	0.004	0.036					0.006	1.161
2018_1205	<LOQ	0.012					<LOQ	0.118
2018_1213	<LOQ	0.013					<LOQ	0.587
2018_1220	<LOQ	0.021					0.008	2.031
2019_0108	<LOQ	0.016					<LOQ	0.915

Tab. C.14: Descriptive statistics of micropollutant event mean concentration distribution n = 22, except for DEET,MCP n = 10 and CBZ,LID n = 5

Substance	particulate (µg L^{-1})					dissolved (µg L^{-1})				
	min	max	mean	median	SD	min	max	mean	median	SD
NAP	< LOQ	0.023	0.007	0.005	0.008	< LOQ	0.023	0.007	0.005	0.008
ACY	< LOQ	0.027	0.005	0.003	0.005	< LOQ	0.032	0.008	0.004	0.008
ACN	< LOQ	0.018	0.004	0.003	0.004	< LOQ	0.009	0.003	0.003	< 0.002
FLE	< LOQ	0.021	0.004	0.002	0.004	< LOQ	0.015	0.005	0.003	0.004
PHE	< LOQ	0.179	0.053	0.038	0.046	0.004	0.036	0.012	0.010	0.008
ANT	< LOQ	0.027	0.007	0.006	0.007	< LOQ	0.003	< LOQ	< LOQ	< LOQ
FlU	0.015	0.245	0.077	0.058	0.065	0.003	0.015	0.006	0.004	0.003
PYR	0.020	0.260	0.108	0.084	0.073	< LOQ	0.014	0.006	0.005	0.003
BaA	0.010	0.068	0.035	0.029	0.019	< LOQ	< LOQ	< LOQ	< LOQ	< LOQ
CHR	0.006	0.111	0.041	0.033	0.031	< LOQ	< LOQ	< LOQ	< LOQ	< LOQ
BbF	0.009	0.141	0.053	0.032	0.039	< LOQ	< LOQ	< LOQ	< LOQ	< LOQ
BkF	0.008	0.078	0.030	0.024	0.019	< LOQ	< LOQ	< LOQ	< LOQ	< LOQ
BaP	0.012	0.088	0.037	0.029	0.021	< LOQ	< LOQ	< LOQ	< LOQ	< LOQ
IND	0.010	0.043	0.021	0.019	0.010	< LOQ	< LOQ	< LOQ	< LOQ	< LOQ
GHI	0.013	0.130	0.044	0.040	0.031	< LOQ	< LOQ	< LOQ	< LOQ	< LOQ
DBA	< LOQ	0.023	0.007	0.005	0.006	< LOQ	< LOQ	< LOQ	< LOQ	< LOQ
4tOP	0.004	0.046	0.014	0.010	0.011	0.004	0.064	0.027	0.020	0.022
4NP	0.015	0.145	0.060	0.046	0.036	0.009	0.206	0.065	0.061	0.048
BT	0.028	0.808	0.241	0.166	0.212	0.174	1.694	0.648	0.488	0.427
MTBT	0.019	0.252	0.090	0.085	0.054	0.077	0.955	0.437	0.442	0.229
TCEP	< LOQ	0.043	0.016	0.015	0.011	0.162	0.921	0.425	0.383	0.200
TCPP	0.071	1.894	0.452	0.305	0.424	0.215	1.989	1.003	0.886	0.539
TPP	< LOQ	0.043	0.011	0.006	0.013	0.003	0.066	0.021	0.019	0.015
DEET	< LOQ	0.002	< LOQ	< LOQ	< LOQ	0.005	0.016	0.008	0.007	0.003
MCP	< LOQ	0.030	0.004	< LOQ	0.009	0.026	2.548	0.535	0.299	0.766
TBY	< LOQ	0.056	0.004	< LOQ	0.012	0.009	0.301	0.062	0.036	0.069
CBZ	0.003	0.008	0.005	0.005	< LOQ	0.020	0.075	0.044	0.046	0.022
LID	< LOQ	0.004	0.002	< LOQ	< LOQ	0.014	0.023	0.019	0.021	0.003
CAF	< LOQ	0.024	0.003	< LOQ	0.005	0.117	2.031	0.611	0.496	0.461

Tab. C.15: Event specific micropollutant loads in all analysed fractions

			NAP (mg)				
				particular			
sample	part. + diss.	diss.	total	< 63 µm	63 – 125 µm	125 – 250 µm	250 – 2000 µm
2017_0206	332	165	166	160	2.49	1.90	1.99
2017_0331	56.8	37.1	19.7	17.5	0.35	0.34	1.50
2017_0502	127	55.7	71.8	33.5	19.2	10.3	8.73
2017_0505	49.1	33.9	15.2	7.55	2.20	0.57	4.93
2017_0519	75.8	27.3	48.5	32.4	8.66	4.75	2.62
2018_0314	146	93.6	52.0	48.4	1.07	1.75	0.85
2018_0323	22.1	17.3	4.80	4.51	0.14	0.12	0.03
2018_0404	20.6	13.8	6.80	6.03	0.37	0.22	0.18

sample	part. + diss.	diss.	total	< 63 µm	63 – 125 µm	125 – 250 µm	250 – 2000 µm
2018_0406	16.2	7.19	9.04	8.19	0.58	0.18	0.09
2018_0412	101	22.2	78.9	57.6	9.49	10.1	1.77
2018_0720	2.83	1.88	0.95	0.76	0.10	0.06	0.02
2018_0828	155	126	28.9	20.4	3.93	3.50	1.04
2018_0914	10.5	6.20	4.32	3.41	0.65	0.13	0.13
2018_0928	10.4	7.66	2.73	1.66	0.57	0.31	0.19
2018_1030	41.5	30.5	11.0	9.7	0.93	0.19	0.25
2018_1107	14.7	11.6	3.10	2.81	0.14	0.05	0.09
2018_1114	269	263	6.19	4.27	1.34	0.09	0.49
2018_1127	13.8	7.73	6.05	5.66	0.16	0.09	0.14
2018_1205	63.0	57.3	5.68	1.32	2.17	0.65	1.54
2018_1213	23.4	20.6	2.80	1.87	0.57	0.28	0.08
2018_1220	4.05	3.03	1.02	0.64	0.22	0.11	0.06
2019_0108	9.21	7.44	1.77	1.21	0.17	0.21	0.18

ACY (mg)

sample	part. + diss.	diss.	particular				
			total	< 63 µm	63 – 125 µm	125 – 250 µm	250 – 2000 µm
2017_0206	55.9	19.6	36.3	33.0	1.78	0.83	0.68
2017_0331	28.0	19.2	8.84	5.36	1.64	0.62	1.21
2017_0502	49.2	28.8	20.4	9.86	3.23	3.14	4.16
2017_0505	48.4	42.3	6.08	2.65	1.96	0.88	0.58
2017_0519	68.9	62.3	6.68	3.91	1.24	0.81	0.73
2018_0314	88.7	74.4	14.3	12.8	0.27	0.68	0.51
2018_0323	11.0	10.4	0.63	0.51	0.05	0.04	0.03
2018_0404	9.55	7.54	2.01	0.80	0.13	0.11	0.97
2018_0406	2.75	1.12	1.63	1.23	0.18	0.13	0.09
2018_0412	21.3	8.10	13.2	8.38	1.37	3.01	0.43
2018_0720	3.36	2.06	1.30	1.02	0.03	0.20	0.05
2018_0828	24.6	10.2	14.5	7.71	3.39	2.24	1.15
2018_0914	8.23	2.91	5.32	3.65	1.37	0.23	0.07
2018_0928	9.54	4.13	5.41	3.37	1.40	0.58	0.06
2018_1030	41.9	26.5	15.4	12.0	2.02	0.67	0.71
2018_1107	9.24	5.17	4.07	3.40	0.21	0.26	0.20
2018_1114	19.4	10.5	8.85	5.91	0.91	1.81	0.22
2018_1127	33.9	10.0	23.9	19.1	3.01	0.39	1.36
2018_1205	47.9	36.7	11.2	7.65	1.57	1.22	0.71
2018_1213	34.2	25.6	8.63	5.74	1.22	0.67	0.99
2018_1220	8.28	4.31	3.96	2.27	0.71	0.65	0.33
2019_0108	17.4	6.55	10.8	8.71	0.62	0.88	0.60

ACN (mg)

sample	part. + diss.	diss.	total	particular < 63 µm	63 – 125 µm	125 – 250 µm	250 – 2000 µm
2017_0206	84.2	26.1	58.1	54.1	1.93	0.87	1.19
2017_0331	26.9	18.3	8.57	7.53	0.51	0.25	0.27
2017_0502	43.5	9.45	34.0	14.8	9.27	5.35	4.66
2017_0505	11.0	5.02	5.95	4.42	0.60	0.34	0.58
2017_0519	20.4	3.73	16.6	9.92	3.35	2.17	1.20
2018_0314	55.9	24.2	31.7	30.0	0.62	0.62	0.49
2018_0323	4.66	1.16	3.50	3.36	0.06	0.04	0.04
2018_0404	4.18	1.16	3.02	2.69	0.12	0.13	0.07
2018_0406	4.57	1.12	3.45	3.15	0.10	0.10	0.10
2018_0412	38.4	3.56	34.9	27.3	3.55	3.21	0.83
2018_0720	1.04	0.40	0.64	0.54	0.03	0.04	0.02
2018_0828	24.9	14.9	10.0	5.66	2.44	1.45	0.47
2018_0914	8.47	6.34	2.13	1.60	0.41	0.08	0.03
2018_0928	5.71	2.98	2.73	1.68	0.85	0.17	0.03
2018_1030	41.4	31.8	9.57	8.48	0.74	0.18	0.17
2018_1107	7.54	5.44	2.10	1.90	0.06	0.08	0.06
2018_1114	16.8	12.6	4.19	3.33	0.57	0.25	0.04
2018_1127	18.2	2.21	16.0	15.2	0.21	0.28	0.28
2018_1205	18.6	10.3	8.22	6.60	1.09	0.36	0.17
2018_1213	22.2	11.52	10.7	10.2	0.36	0.02	0.06
2018_1220	1.81	0.92	0.89	0.66	0.08	0.09	0.06
2019_0108	6.74	3.61	3.14	2.43	0.21	0.40	0.10

FLE (mg)

sample	part. + diss.	diss.	total	particular < 63 µm	63 – 125 µm	125 – 250 µm	250 – 2000 µm
2017_0206	153	106	46.5	42.0	2.01	1.11	1.31
2017_0331	17.0	9.74	7.25	6.08	0.32	0.26	0.60
2017_0502	40.8	14.6	26.2	8.62	6.45	4.81	6.29
2017_0505	8.97	6.71	2.27	1.23	0.05	0.41	0.57
2017_0519	15.0	8.18	6.78	4.35	0.93	0.97	0.53
2018_0314	63.2	39.4	23.8	22.3	0.58	0.45	0.49
2018_0323	4.76	2.21	2.54	2.41	0.03	0.02	0.09
2018_0404	4.92	2.31	2.61	1.06	0.07	0.03	1.44
2018_0406	3.64	2.95	0.69	0.54	0.08	0.04	0.03
2018_0412	29.4	3.94	25.5	16.9	2.59	5.29	0.72
2018_0720	1.12	0.58	0.54	0.08	0.26	0.17	0.03
2018_0828	36.4	8.66	27.8	18.9	4.42	2.59	1.90
2018_0914	6.63	2.38	4.25	2.69	0.98	0.21	0.36
2018_0928	15.4	7.35	8.06	5.59	2.14	0.31	0.02
2018_1030	27.9	16.5	11.3	9.09	1.08	0.72	0.46
2018_1107	19.3	14.6	4.76	4.20	0.18	0.18	0.20
2018_1114	25.1	18.0	7.12	5.93	0.85	0.16	0.19
2018_1127	20.6	2.51	18.1	16.7	0.51	0.46	0.43
2018_1205	25.4	14.7	10.7	8.04	1.53	0.42	0.73

sample	part. + diss.	diss.	total	< 63 µm	63 – 125 µm	125 – 250 µm	250 – 2000 µm
2018_1213	40.9	35.3	5.61	4.58	0.54	0.25	0.25
2018_1220	3.40	1.60	1.81	1.11	0.28	0.32	0.10
2019_0108	16.3	10.8	5.52	4.74	0.32	0.24	0.21

PHE (mg)

sample	part. + diss.	diss.		particular			
			total	< 63 µm	63 – 125 µm	125 – 250 µm	250 – 2000 µm
2017_0206	1071	82.3	989	897	41.5	21.3	29.1
2017_0331	119	50.1	69.3	52.8	6.37	6.00	4.15
2017_0502	386	27.2	359	153	85.5	56.4	64.5
2017_0505	64.5	16.4	48.1	34.8	8.53	1.75	3.05
2017_0519	163	15.9	147	92.1	23.4	20.7	10.6
2018_0314	545	57.3	487	450	9.72	16.7	10.8
2018_0323	33.4	10.7	22.7	21	0.68	0.33	0.37
2018_0404	55.5	17.9	37.6	23.1	1.75	1.01	11.8
2018_0406	48.3	7.86	40.4	36.0	2.20	1.59	0.66
2018_0412	640	128	512	364	62.7	73.3	11.8
2018_0720	9.28	1.32	7.96	4.44	1.68	1.39	0.45
2018_0828	398	109	289	155	85.2	32.4	16.9
2018_0914	32.6	11.2	21.4	15.0	5.27	0.82	0.33
2018_0928	64.9	14.8	50.1	31.5	15.6	2.14	0.93
2018_1030	155	42.7	112	92.7	11.8	5.86	1.68
2018_1107	77.5	27.2	50.3	46.2	1.67	1.75	0.70
2018_1114	137	38.8	98.4	81.5	10.8	3.64	2.37
2018_1127	41.3	4.27	37.0	28.5	6.28	1.44	0.79
2018_1205	710	81.1	629	555	49.9	19.3	4.70
2018_1213	230	72.3	158	133	18.8	4.39	1.63
2018_1220	12.9	3.37	9.55	7.70	0.93	0.83	0.09
2019_0108	96.4	34.5	61.9	58.8	1.52	0.99	0.55

ANT (mg)

sample	part. + diss.	diss.		particular			
			total	< 63 µm	63 – 125 µm	125 – 250 µm	250 – 2000 µm
2017_0206	203	8.35	195	173	8.84	4.41	8.58
2017_0331	32.8	7.77	25.0	20.4	1.60	2.26	0.72
2017_0502	57.4	5.07	52.3	24.3	10.5	8.76	8.68
2017_0505	8.80	2.91	5.89	4.16	1.04	0.26	0.44
2017_0519	29.7	4.87	24.8	14.2	3.98	2.80	3.87
2018_0314	63.8	6.41	57.4	39.0	1.34	15.9	1.15
2018_0323	4.04	1.16	2.88	2.58	0.08	0.06	0.17
2018_0404	7.51	1.16	6.35	2.86	0.25	0.17	3.07
2018_0406	4.66	1.12	3.54	2.74	0.15	0.15	0.50
2018_0412	56.9	3.56	53.3	28.2	9.13	14.0	1.92
2018_0720	1.33	0.27	1.06	0.59	0.25	0.16	0.06
2018_0828	58.6	14.6	44.1	25.1	10.4	6.51	2.09
2018_0914	6.12	3.15	2.96	1.75	0.73	0.19	0.30
2018_0928	11.8	3.39	8.43	5.04	2.93	0.37	0.08
2018_1030	19.6	7.29	12.3	10.2	1.12	0.42	0.59

sample	part. + diss.	diss.	total	< 63 µm	63 – 125 µm	125 – 250 µm	250 – 2000 µm
2018_1107	6.29	2.27	4.03	3.55	0.22	0.13	0.13
2018_1114	19.9	8.83	11.03	8.96	1.17	0.56	0.34
2018_1127	7.18	1.76	5.42	3.43	0.79	0.23	0.96
2018_1205	87.6	16.2	71.4	60.2	6.09	2.63	2.55
2018_1213	28.2	7.22	21.0	17.7	2.29	0.65	0.34
2018_1220	2.37	1.01	1.36	1.05	0.07	0.05	0.19
2019_0108	11.2	2.72	8.45	7.87	0.26	0.20	0.13

FLU (mg)

sample	part. + diss.	diss.	total	particular			
				< 63 µm	63 – 125 µm	125 – 250 µm	250 – 2000 µm
2017_0206	1210	38.1	1172	1055	48.0	22.8	46.7
2017_0331	228	72.3	156	121.4	17.4	11.3	6.02
2017_0502	682	14.2	668	300	151	100	117
2017_0505	94.7	8.37	86.4	66.5	14.1	2.49	3.36
2017_0519	287	16.3	271	180	42.9	26.8	20.7
2018_0314	533	13.4	520	470	12.5	23.2	13.5
2018_0323	59.7	4.11	55.6	54.0	0.75	0.50	0.37
2018_0404	75.5	9.32	66.1	48.6	2.77	1.83	12.9
2018_0406	80.7	4.69	76.0	68.3	3.48	3.02	1.26
2018_0412	900	27.3	872	618	114	121	19.7
2018_0720	19.3	0.67	18.6	10.7	5.23	1.82	0.83
2018_0828	187	21.3	165	93.4	44.1	16.2	11.8
2018_0914	39.6	5.09	34.5	23.6	7.70	1.80	1.44
2018_0928	80.9	11.7	69.2	54.3	9.40	4.40	1.17
2018_1030	237	27.5	210	161	21.2	12.7	14.3
2018_1107	43.7	7.26	36.4	27.1	3.44	3.75	2.17
2018_1114	89.0	16.9	72.0	51.4	11.2	5.58	3.93
2018_1127	67.3	9.07	58.3	46.2	5.43	2.67	3.97
2018_1205	277	52.9	224	149	32.1	27.2	15.3
2018_1213	328	9.10	319	277	31.0	7.16	4.49
2018_1220	14.7	2.11	12.6	9.86	1.52	0.87	0.35
2019_0108	117	6.30	110	106	1.77	0.82	1.43

PYR (mg)

sample	part. + diss.	diss.	total	particular			
				< 63 µm	63 – 125 µm	125 – 250 µm	250 – 2000 µm
2017_0206	1433	41.3	1392	1260	57.5	26.7	47.8
2017_0331	259	39.9	219	178	20.8	12.6	8.05
2017_0502	741	11.4	730	324	165	109	131
2017_0505	118	8.66	109	84.8	16.3	3.06	4.88
2017_0519	312	17.0	295	195	45.8	30.8	23.6
2018_0314	702	16.1	685	626	16.8	24.7	18.2
2018_0323	96.4	5.91	90.5	86.7	1.69	1.23	0.83
2018_0404	117	15.9	101	83.7	4.26	2.97	10.1
2018_0406	104	8.47	95.6	85.2	4.80	3.77	1.86
2018_0412	958	31.2	927	646	120	137	23.9
2018_0720	21.0	0.71	20.3	11.3	5.38	1.88	1.68

sample	part. + diss.	diss.	total	< 63 µm	63 – 125 µm	125 – 250 µm	250 – 2000 µm
2018_0828	706	21.0	685	390	194	64.0	37.8
2018_0914	43.0	6.19	36.8	24.9	8.39	1.98	1.52
2018_0928	85.6	12.8	72.7	55.5	10.0	5.10	2.20
2018_1030	273	20.5	253	203	23.6	12.5	13.3
2018_1107	122	6.15	116	104	4.77	4.10	3.38
2018_1114	207	7.65	200	171	18.2	6.33	4.35
2018_1127	197	5.96	191	162	15.1	6.59	6.79
2018_1205	1136	46.2	1090	930	99.4	39.7	21.0
2018_1213	357	7.86	350	295	37.8	9.15	7.29
2018_1220	16.8	1.68	15.2	12.7	1.13	0.99	0.37
2019_0108	116	6.71	109	105	2.16	1.02	1.25

BaA (mg)

sample	part. + diss.	diss.	total	< 63 µm	63 – 125 µm	125 – 250 µm	250 – 2000 µm
				particular			
2017_0206	287	12.2	275	236	12.3	8.07	18.4
2017_0331	76.0	4.88	71.2	57.1	6.59	5.15	2.36
2017_0502	232	3.37	229	130	38.1	27.6	33.1
2017_0505	28.2	1.31	26.9	21.6	3.62	0.77	0.93
2017_0519	75.5	3.51	72.0	48.3	11.2	7.88	4.60
2018_0314	142	2.73	139	122	3.55	8.78	4.90
2018_0323	27.0	1.16	25.9	24.0	0.75	0.62	0.49
2018_0404	23.8	1.16	22.7	15.4	0.82	0.62	5.84
2018_0406	17.1	1.12	16.0	14.8	0.45	0.59	0.21
2018_0412	235	3.56	232	156	34.2	37.2	4.38
2018_0720	10.1	0.18	9.90	4.7	4.22	0.44	0.51
2018_0828	351	5.47	346	217	92.9	16.6	19.8
2018_0914	22.6	1.11	21.5	15.7	3.96	0.92	0.91
2018_0928	43.1	1.24	41.9	33.1	4.78	2.93	1.13
2018_1030	134	13.3	120	87.1	13.6	8.49	11.2
2018_1107	50.1	2.18	47.9	41.8	1.88	2.93	1.26
2018_1114	92.9	4.90	88.0	76.1	6.55	2.78	2.54
2018_1127	53.5	0.96	52.5	43.7	3.27	3.71	1.87
2018_1205	462	9.36	453	399	29.9	16.1	7.49
2018_1213	159	3.31	156	137	12.6	4.17	2.27
2018_1220	8.3	0.76	7.50	6.35	0.67	0.36	0.12
2019_0108	75.1	2.03	73.0	70.6	1.22	0.73	0.49

CHR (mg)

sample	part. + diss.	diss.	total	< 63 µm	63 – 125 µm	125 – 250 µm	250 – 2000 µm
				particular			
2017_0206	540	12.6	527	468	20.1	12.7	26.2
2017_0331	144	4.88	139	116	10.7	7.48	4.38
2017_0502	378	3.37	375	171	86.7	52.3	65.2
2017_0505	12.90	1.31	11.6	7.51	2.53	0.92	0.63
2017_0519	25.83	3.74	22.1	14.7	3.14	2.45	1.80
2018_0314	236	2.73	234	209	4.85	13.1	6.50
2018_0323	40.41	1.16	39.3	37.8	0.37	0.58	0.53

2018_0404	38.17	1.16	37.010	27.8	1.41	1.01	6.75
2018_0406	30.13	1.46	29	25.2	1.33	1.44	0.68
2018_0412	395	3.56	391	277	51.3	56.2	7.14
2018_0720	10.88	0.18	10.7	5.35	4.33	0.47	0.56
2018_0828	402	5.47	396	257	98.6	18.2	22.0
2018_0914	23.76	1.19	22.6	16.4	4.28	0.89	0.97
2018_0928	46.78	2.23	44.6	35.0	5.01	3.40	1.08
2018_1030	118	13.3	105	78.6	8.85	7.03	10.1
2018_1107	53.40	2.18	51.2	47.5	1.22	1.43	1.11
2018_1114	70.91	4.98	65.9	55.3	6.18	2.55	1.92
2018_1127	36.12	1.51	34.6	29.1	2.80	1.55	1.21
2018_1205	340	9.36	330	283	26.9	11.9	8.12
2018_1213	124	3.31	121	108	10.1	0.61	1.95
2018_1220	7.683	0.76	6.93	5.77	0.70	0.34	0.11
2019_0108	54.36	2.03	52.3	50.5	0.65	0.70	0.51

BbF (mg)

| sample | part. + diss. | diss. | total | particular | | | |
				< 63 µm	63 – 125 µm	125 – 250 µm	250 – 2000 µm
2017_0206	506	7.25	498	439	22.9	11.1	25.1
2017_0331	136	4.88	131	112	8.26	7.38	3.65
2017_0502	410	3.37	406	179	89.2	60.2	77.8
2017_0505	36.1	1.31	34.8	27.1	5.16	1.07	1.41
2017_0519	133	3.74	129	89.3	19.0	12.3	8.41
2018_0314	327	2.73	324	291	6.62	16.1	10.8
2018_0323	106	1.16	105	103	1.02	0.78	0.45
2018_0404	68.1	1.16	66.9	51.6	2.74	1.75	10.8
2018_0406	52.2	1.12	51.1	46.2	2.08	1.99	0.78
2018_0412	507	3.56	504	353	68.3	72.2	9.92
2018_0720	18.1	0.18	18.0	7.86	3.25	0.67	6.19
2018_0828	430	5.47	425	266	86.3	30.6	42.0
2018_0914	29.3	1.11	28.1	19.9	3.38	4.32	0.58
2018_0928	31.8	1.16	30.7	14.7	7.00	3.31	5.59
2018_1030	161	7.21	154	126	18.0	4.70	5.72
2018_1107	43.2	2.18	41.0	35.9	2.30	1.10	1.75
2018_1114	81.6	4.90	76.7	63.5	5.09	2.83	5.33
2018_1127	27.0	0.88	26.2	17.1	2.76	1.60	4.69
2018_1205	509	9.28	500	445	22.1	12.7	20.2
2018_1213	85.8	3.02	82.8	63.7	8.25	4.10	6.74
2018_1220	7.27	0.76	6.51	2.89	0.09	3.36	0.16
2019_0108	48.9	2.03	46.9	41.5	1.12	0.79	3.53

BkF (mg)

| sample | part. + diss. | diss. | total | particular | | | |
				< 63 µm	63 – 125 µm	125 – 250 µm	250 – 2000 µm
2017_0206	250	7.25	243	213	8.35	8.71	12.8
2017_0331	81.3	4.88	76.4	63.5	6.83	3.38	2.68
2017_0502	172	3.37	168	79.6	36.6	25.4	26.6

sample	part. + diss.	diss.	total	< 63 µm	63 – 125 µm	125 – 250 µm	250 – 2000 µm
2017_0505	19.0	1.31	17.7	13.5	3.20	0.46	0.54
2017_0519	77.9	3.74	74.2	51.6	10.9	7.84	3.85
2018_0314	79.4	2.73	76.7	69.8	1.68	3.11	2.13
2018_0323	31.1	1.16	30.0	28.3	0.68	0.49	0.54
2018_0404	30.1	1.16	29.0	22.6	1.50	1.33	3.56
2018_0406	24.6	1.12	23.5	19.2	1.70	1.51	1.07
2018_0412	243	3.56	239	163	28.2	37.7	10.4
2018_0720	14.1	0.18	13.9	6.6	2.72	0.56	4.00
2018_0828	412	5.47	407	256	83.4	27.8	39.1
2018_0914	25.3	1.11	24.2	17.6	2.61	3.54	0.51
2018_0928	26.6	1.16	25.4	12.1	6.05	2.46	4.80
2018_1030	121	7.21	114	91.5	13.1	5.17	4.03
2018_1107	61.7	2.18	59.5	54.0	2.57	1.00	1.98
2018_1114	78.8	4.90	73.9	59.6	4.86	4.12	5.34
2018_1127	22.2	0.88	21.3	13.6	1.16	1.13	5.40
2018_1205	332	9.28	322	264	31.4	10.5	16.2
2018_1213	64.1	3.02	61.0	45.4	4.35	5.34	5.94
2018_1220	7.12	0.76	6.36	3.63	0.06	2.50	0.16
2019_0108	48.5	2.03	46.5	40.6	1.04	0.83	4.02

BaP (mg)

sample	part. + diss.	diss.	total	particular < 63 µm	63 – 125 µm	125 – 250 µm	250 – 2000 µm
2017_0206	260	7.25	252.9	221	16.2	8.07	7.64
2017_0331	90.8	4.88	85.9	71.6	7.50	4.37	2.44
2017_0502	223	3.37	219	94.0	53.2	34.4	37.5
2017_0505	39.5	1.31	38.2	30.6	5.18	1.15	1.30
2017_0519	115	3.74	111	77.8	15.8	10.2	7.34
2018_0314	129	2.73	126	112	3.07	6.97	4.02
2018_0323	27.6	1.16	26.4	25.5	0.43	0.26	0.19
2018_0404	22.2	1.16	21.1	14.4	1.05	0.74	4.95
2018_0406	18.1	1.12	17.0	15.2	0.75	0.82	0.22
2018_0412	220	3.56	216	154	31.5	27.7	3.40
2018_0720	15.8	0.18	15.6	7.78	2.99	0.56	4.32
2018_0828	375	5.47	370	245	79.8	19.1	26.2
2018_0914	29.3	1.11	28.2	21.0	6.02	0.87	0.36
2018_0928	67.4	1.16	66.2	54.1	8.49	3.37	0.29
2018_1030	145	7.21	138	104	14.8	8.95	9.73
2018_1107	50.2	2.18	48.0	42.6	2.30	1.77	1.41
2018_1114	73.4	4.90	68.5	58.3	5.34	2.70	2.08
2018_1127	38.7	0.88	37.8	33.8	2.98	0.75	0.29
2018_1205	516	9.28	506	455	32.0	10.8	8.86
2018_1213	119	3.02	116	104	8.99	2.02	1.35
2018_1220	9.69	0.76	8.94	6.21	2.06	0.46	0.21
2019_0108	51.8	2.03	49.8	48.0	1.04	0.44	0.32

IND (mg)

sample	part. + diss.	diss.	total	particular < 63 µm	63 – 125 µm	125 – 250 µm	250 – 2000 µm
2017_0206	161	7.25	154	135	7.37	4.99	6.53
2017_0331	56.3	4.88	51.5	44.5	3.51	2.01	1.46
2017_0502	149	3.37	146	58.7	36.0	23.1	27.9
2017_0505	15.8	1.31	14.5	11.8	1.72	0.33	0.64
2017_0519	49.2	3.74	45.5	30.1	6.90	5.36	3.17
2018_0314	76.3	2.73	73.6	64.9	4.69	1.28	2.68
2018_0323	22.4	1.16	21.2	20.5	0.33	0.25	0.16
2018_0404	15.3	1.16	14.2	11.0	0.65	0.60	1.93
2018_0406	29.9	1.12	28.8	25.1	1.89	0.98	0.79
2018_0412	127	3.56	123	89.8	15.2	16.0	2.38
2018_0720	7.06	0.18	6.88	5.02	1.53	0.24	0.09
2018_0828	135	5.47	129	69.1	41.5	15.6	2.92
2018_0914	11.7	1.11	10.6	7.03	2.84	0.53	0.22
2018_0928	23.8	1.16	22.6	18.6	2.47	1.30	0.21
2018_1030	82.6	7.21	75.3	57.0	7.05	4.66	6.69
2018_1107	35.6	2.18	33.4	30.8	0.82	0.80	0.96
2018_1114	72.0	4.90	67.1	60.8	3.29	1.37	1.57
2018_1127	34.7	0.88	33.8	31.6	1.40	0.58	0.25
2018_1205	220	9.28	211	179	21.4	5.79	4.15
2018_1213	93.8	3.02	90.7	85.2	4.17	0.94	0.45
2018_1220	10.9	0.76	10.1	6.81	2.44	0.57	0.29
2019_0108	38.7	2.03	36.6	35.1	0.95	0.38	0.25

GHI (mg)

sample	part. + diss.	diss.	total	particular < 63 µm	63 – 125 µm	125 – 250 µm	250 – 2000 µm
2017_0206	420	7.25	413	362	22.8	12.5	14.9
2017_0331	130	4.88	125	109	8.40	3.96	3.50
2017_0502	361	3.37	358	161	87.4	51.6	57.5
2017_0505	51.5	1.31	50.1	39.7	6.02	2.12	2.27
2017_0519	138	3.74	135	92.5	20.0	13.2	8.89
2018_0314	274	2.73	271	248	5.93	10.7	7.10
2018_0323	50.5	1.16	49.3	47.0	0.99	0.84	0.51
2018_0404	49.5	1.16	48.3	39.9	2.39	2.07	3.93
2018_0406	48.6	1.12	47.5	41.3	3.05	1.86	1.29
2018_0412	467	3.56	463	350	49.0	55.3	8.13
2018_0720	8.90	0.18	8.72	5.81	2.43	0.33	0.15
2018_0828	173	5.47	167	88.5	54.0	20.6	4.38
2018_0914	15.8	1.11	14.7	9.66	3.70	1.02	0.35
2018_0928	30.0	1.16	28.8	23.2	3.26	2.08	0.32
2018_1030	132	7.21	124	100	12.7	5.67	5.80
2018_1107	62.5	2.18	60.4	56.0	1.54	1.38	1.47
2018_1114	98.5	4.90	93.6	80.3	7.02	3.71	2.49
2018_1127	41.6	0.88	40.7	37.7	1.96	0.64	0.35

sample	part. + diss.	diss.	total	< 63 µm	63 – 125 µm	125 – 250 µm	250 – 2000 µm
2018_1205	437	9.28	427	374	30.4	12.1	10.4
2018_1213	153	3.02	150.4	142	5.78	1.98	0.89
2018_1220	13.0	0.76	12.2	8.11	2.89	0.86	0.37
2019_0108	38.5	2.03	36.5	34.3	1.31	0.58	0.35

DBA (mg)

sample	part. + diss.	diss.	total	< 63 µm	63 – 125 µm	125 – 250 µm	250 – 2000 µm
					particular		
2017_0206	54.3	7.25	47.0	42.6	1.87	1.03	1.58
2017_0331	30.4	4.88	25.6	22.4	1.48	0.89	0.83
2017_0502	67.9	3.37	64.6	24.1	16.3	11.4	12.7
2017_0505	7.44	1.31	6.13	4.74	0.87	0.27	0.25
2017_0519	27.1	3.74	23.4	13.9	3.55	1.94	4.01
2018_0314	44.7	2.73	42.0	37.8	0.98	1.95	1.33
2018_0323	7.83	1.16	6.68	6.35	0.10	0.10	0.12
2018_0404	7.28	1.16	6.12	4.76	0.30	0.27	0.79
2018_0406	8.62	1.12	7.50	6.78	0.27	0.23	0.22
2018_0412	86.8	3.56	83.2	63.7	8.75	9.00	1.75
2018_0720	1.99	0.18	1.82	0.70	0.28	0.05	0.78
2018_0828	22.1	5.47	16.7	10.6	3.59	2.06	0.45
2018_0914	2.17	1.11	1.06	0.57	0.34	0.12	0.03
2018_0928	3.76	1.16	2.60	1.44	0.49	0.32	0.35
2018_1030	21.4	7.21	14.2	12.2	1.19	0.42	0.41
2018_1107	7.65	2.18	5.47	5.06	0.15	0.14	0.12
2018_1114	12.7	4.90	7.81	6.24	0.76	0.58	0.24
2018_1127	8.79	0.88	7.91	7.62	0.24	0.04	0.01
2018_1205	45.6	9.28	36.3	30.9	2.84	1.47	1.15
2018_1213	22.8	3.02	19.8	18.7	0.84	0.10	0.15
2018_1220	1.46	0.76	0.70	0.50	0.11	0.05	0.03
2019_0108	9.50	2.03	7.47	7.13	0.20	0.08	0.05

4tOP (mg)

sample	part. + diss.	diss.	total	< 63 µm	63 – 125 µm	125 – 250 µm	250 – 2000 µm
					particular		
2017_0206	360	26.5	333	314	8.28	4.72	5.85
2017_0331	46.1	24.1	21.9	20.2	1.01	0.51	0.20
2017_0502	69.2	24.1	45.1	19.17	10.4	5.68	9.80
2017_0505	19.6	7.85	11.8	9.87	1.11	0.36	0.44
2017_0519	32.0	15.6	16.5	9.60	4.13	1.93	0.80
2018_0314	226	141	85.6	81.7	1.45	1.23	1.21
2018_0323	73.5	61.5	12.0	11.6	0.12	0.13	0.17
2018_0404	81.9	66.5	15.4	14.0	0.62	0.53	0.28
2018_0406	86.7	71.2	15.5	14.2	0.65	0.39	0.19
2018_0412	321	225	96.7	74.1	9.22	10.6	2.81
2018_0720	4.43	2.20	2.23	1.64	0.39	0.02	0.20
2018_0828	108	64.6	43.8	27.4	10.6	4.72	1.09
2018_0914	22.4	18.1	4.38	2.37	1.49	0.39	0.12
2018_0928	38.5	29.8	8.74	6.81	0.87	0.75	0.31

2018_1030	186	150	36.2	29.2	2.77	3.81	0.33
2018_1107	24.3	8.59	15.7	14.5	0.22	0.17	0.83
2018_1114	108	56.3	51.8	47.6	3.86	0.26	0.08
2018_1127	54.8	26.2	28.5	25.9	2.17	0.30	0.13
2018_1205	433	264	169	152	11.0	4.44	1.67
2018_1213	149	106	43.4	36.8	3.84	2.43	0.43
2018_1220	18.6	15.2	3.37	3.01	0.15	0.15	0.06
2019_0108	131	123	8.65	6.30	0.21	1.72	0.41

4NP (mg)

sample	part. + diss.	diss.	total	particular			
				< 63 µm	63 – 125 µm	125 – 250 µm	250 – 2000 µm
2017_0206	841	67.2	774	752	9.82	6.72	5.61
2017_0331	169	90.3	78.8	73.3	3.86	0.95	0.65
2017_0502	413	60.0	353	151	79.3	48.8	74.7
2017_0505	74.4	28.7	45.7	36.6	7.39	0.89	0.84
2017_0519	168	45.0	123	70.0	15.3	30.8	6.70
2018_0314	668	444	224	210	6.34	5.28	3.25
2018_0323	127	99.6	27.0	22.5	0.55	3.59	0.36
2018_0404	118	62.1	56.0	46.5	5.71	2.18	1.56
2018_0406	124	60.3	63.8	44.8	3.83	14.6	0.70
2018_0412	1250	733	517	414	55.3	41.1	6.39
2018_0720	30.1	12.3	17.8	12.6	3.79	0.20	1.25
2018_0828	406	205	201	112	41.6	41.8	4.93
2018_0914	90.2	60.9	29.3	20.2	7.57	1.30	0.18
2018_0928	143	92.2	51.3	41.8	5.42	3.61	0.50
2018_1030	880	619	262	161	31.2	69.0	0.94
2018_1107	113	38.9	74.6	67.3	4.54	2.35	0.38
2018_1114	747	311	435	395	33.8	4.64	1.29
2018_1127	158	80.2	77.6	69.0	5.93	2.16	0.43
2018_1205	1448	656	792	709	52.6	25.6	4.35
2018_1213	539	269	270	210	28.0	31.0	0.89
2018_1220	56.1	44.7	11.4	9.25	1.40	0.67	0.05
2019_0108	205	153	52.3	47.1	1.56	3.39	0.31

BT (mg)

sample	part. + diss.	diss.	total	particular			
				< 63 µm	63 – 125 µm	125 – 250 µm	250 – 2000 µm
2017_0206	3544	2524	1019	947	43.4	13.4	15.6
2017_0331	1475	1128	348	297	10.3	24.1	16.3
2017_0502	3140	2316	824	378	198	118	131
2017_0505	1858	1712	146	64.1	59.1	4.71	18.3
2017_0519	1815	1443	372	243	58.1	34.5	36.4
2018_0314	2563	1983	580	529	19.2	17.8	13.5
2018_0323	595	486	109	103	2.21	2.27	2.43
2018_0404	410	306	104	91.4	5.00	6.01	1.50
2018_0406	724	598	126	112	6.15	4.93	3.47
2018_0412	2663	1572	1091	826	115	124	25.4

2018_0720	75	30.9	44.2	2.23	1.72	0.02	40.2
2018_0828	5565	4332	1233	888	207	87.2	50.1
2018_0914	275	240	35.2	10.4	20.9	2.45	1.46
2018_0928	1699	967	732	691	15.3	22.3	3.06
2018_1030	13145	12216	928	821	63.3	20.0	23.9
2018_1107	2094	1677	418	387	12.6	6.79	11.2
2018_1114	6420	6285	135	84.6	25.9	12.7	11.7
2018_1127	1195	1103	92.3	67.1	1.99	13.7	9.5
2018_1205	13313	8974	4339	4127	116	69.7	26.0
2018_1213	1929	973	956	816	97.7	29.4	13.3
2018_1220	669	193	476	400	14.7	39.4	22.1
2019_0108	2355	714	1641	1493	54.5	42.2	51.5

MTBT (mg)

sample	part. + diss.	diss.	total	particular			
				< 63 µm	63 – 125 µm	125 – 250 µm	250 – 2000 µm
2017_0206	803	557	247	223	18.5	3.07	2.04
2017_0331	613	519	93.8	82.4	3.20	5.88	2.34
2017_0502	1901	1521	380	127	101	88.3	64.0
2017_0505	1033	855	178	137	36.6	3.22	1.13
2017_0519	2158	1768	389	246	89.1	10.4	43.7
2018_0314	1386	1121	264	241	8.94	7.24	7.20
2018_0323	815	524	291	288	1.97	0.88	0.52
2018_0404	362	311	51.0	44.5	1.33	2.19	2.98
2018_0406	491	427	64.7	59.5	2.47	0.24	2.47
2018_0412	2908	2441	468	406	19.3	22.8	19.9
2018_0720	104	81.6	22.5	11.0	1.73	0.19	9.6
2018_0828	5628	5225	403	255	87.0	29.8	30.8
2018_0914	519	484	35	7.51	22.5	2.23	2.78
2018_0928	667	565	102	79.1	6.81	12.5	3.73
2018_1030	3133	2853	281	259	13.7	3.36	4.04
2018_1107	802	643	158	152	2.54	1.11	2.29
2018_1114	2312	2188	123	93.3	20.1	6.75	3.22
2018_1127	863	791	72.1	65.1	1.57	2.77	2.62
2018_1205	4658	3089	1569	1498	39.4	19.4	12.4
2018_1213	2157	1908	249	199	20.5	19.5	9.5
2018_1220	166	90.0	76.1	64.3	4.06	6.70	0.95
2019_0108	576	390	185	159	4.02	15.2	7.40

TCEP (mg)

sample	part. + diss.	diss.	total	particular			
				< 63 µm	63 – 125 µm	125 – 250 µm	250 – 2000 µm
2017_0206	1186	1175	11.0	7.52	1.43	1.13	0.93
2017_0331	3653	3609	44.1	22.5	3.45	3.41	14.7
2017_0502	1397	1312	84.5	55.2	10.4	9.38	9.56
2017_0505	411	362	49.0	7.46	34.6	2.37	4.53
2017_0519	856	829	26.0	10.9	4.91	5.88	4.35
2018_0314	1769	1715	54.6	42.9	2.73	3.54	5.41

sample	part. + diss.	diss.	total	< 63 µm	63 – 125 µm	125 – 250 µm	250 – 2000 µm
2018_0323	513	494	19.0	11.7	3.27	2.01	1.96
2018_0404	417	401	16.5	11.7	2.62	1.55	0.56
2018_0406	483	475	7.51	5.87	0.50	0.24	0.90
2018_0412	3386	3280	106	45.9	24.6	27.2	8.57
2018_0720	122	114	7.61	4.14	0.60	1.72	1.16
2018_0828	2999	2868	132	70.4	29.4	15.3	16.6
2018_0914	534	515	18.7	11.6	2.24	2.79	2.04
2018_0928	320	302	17.6	6.24	0.92	9.72	0.69
2018_1030	5097	5051	46.7	34.3	5.64	3.73	2.98
2018_1107	513	501	12.1	9.27	0.90	0.95	0.97
2018_1114	1069	1049	19.9	15.5	1.58	1.90	0.88
2018_1127	494	469	25.6	23.3	0.58	0.57	1.22
2018_1205	3659	3484	175	138	19.3	15.9	1.43
2018_1213	946	935	10.3	7.27	0.90	0.85	1.30
2018_1220	239	233	6.46	3.05	0.52	2.33	0.56
2019_0108	557	526	30.79	5.49	0.69	23.6	1.03

TCPP (mg)

sample	part. + diss.	diss.	total	particular			
				< 63 µm	63 – 125 µm	125 – 250 µm	250 – 2000 µm
2017_0206	2558	1563	995	327	261	285	122
2017_0331	2219	1871	348	92.7	93.8	106	55.8
2017_0502	2844	1561	1283	237	305	329	412
2017_0505	711.97	568	144	28.9	58.0	28.2	29.3
2017_0519	2399	1048	1350	181	296	629	243
2018_0314	3691	2192	1499	398	396	563	143
2018_0323	1058.74	723	336	39.8	89.5	120	87.2
2018_0404	1088.23	795	294	50.2	92.5	120	31.3
2018_0406	1210.51	854	357	79.9	94.5	124	58.6
2018_0412	8246	4715	3531	585	977	1613	356
2018_0720	309.93	179	131	32.8	65.6	24.0	8.85
2018_0828	10484	5164	5320	851	2879	1158	431
2018_0914	1834.61	1661	173	90.9	37.9	33.3	11.0
2018_0928	2329	1957	371	94.4	154	110	13.3
2018_1030	15229	14343	886	311	392	129	54.1
2018_1107	2259	1806	452	195	100	97.2	59.9
2018_1114	4815	3451	1364	608	473	151	133
2018_1127	2062	1343	719	129	216	201	173
2018_1205	35311	17736	17575	2075	8407	4896	2196
2018_1213	5547	3767	1779	627	645	243	265
2018_1220	876.26	760	116	40.2	42.8	30.2	2.65
2019_0108	3981	3516	464	241	118	55.2	50.2

TPP (mg)

sample	part. + diss.	diss.	total	particular			
				< 63 µm	63 – 125 µm	125 – 250 µm	250 – 2000 µm
2017_0206	101	85.0	15.9	3.36	4.59	5.41	2.59
2017_0331	64.1	45.4	18.6	0.40	3.87	12.4	1.93

sample	part. + diss.	diss.	total	< 63 µm	63 – 125 µm	125 – 250 µm	250 – 2000 µm
2017_0502	133	29.2	103	16.6	35.1	28.7	23
2017_0505	21.6	11.4	10.2	1.14	5.09	1.33	2.61
2017_0519	65.1	10.7	54.4	5.38	14.4	15.3	19.3
2018_0314	57.6	40.1	17.5	3.01	4.23	8.28	1.97
2018_0323	42.4	39.7	2.63	0.18	0.56	0.45	1.44
2018_0404	28.2	24.7	3.53	0.50	1.65	1.11	0.28
2018_0406	15.9	14.2	1.71	0.51	0.57	0.49	0.14
2018_0412	147	112	34.8	2.57	10.0	14.6	7.62
2018_0720	11.4	3.7	7.74	2.13	5.23	0.14	0.24
2018_0828	212	127	85.2	6.72	35.6	31.6	11.39
2018_0914	26.2	24.6	1.61	0.07	0.52	0.39	0.63
2018_0928	67.5	63.5	3.99	0.68	1.85	0.79	0.67
2018_1030	85.5	64.7	20.8	1.47	10.2	7.58	1.53
2018_1107	30.7	18.1	12.7	0.54	4.28	7.14	0.71
2018_1114	117	95.8	21.3	1.89	10.3	8.52	0.65
2018_1127	59.5	21.6	37.9	0.68	14.1	18.7	4.38
2018_1205	848	608	240	6.03	91.9	127	15.6
2018_1213	95.2	48.0	47.2	2.16	17.5	18.1	9.37
2018_1220	20.5	16.5	4.05	0.09	2.23	1.10	0.63
2019_0108	44.2	36.3	7.88	0.57	2.42	4.08	0.82

TBY (mg)

sample	part. + diss.	diss.	total	particular			
				< 63 µm	63 – 125 µm	125 – 250 µm	250 – 2000 µm
2017_0206	70.1	63.3	6.78	2.28	1.39	1.67	1.44
2017_0331	120	118	1.47	0.28	0.56	0.38	0.25
2017_0502	316	274	41.6	12.8	6.79	12.98	9.04
2017_0505	91.6	88.7	2.96	1.41	0.38	1.00	0.17
2017_0519	191	186	4.78	0.98	1.57	1.15	1.08
2018_0314	99.6	97.8	1.81	0.06	0.46	0.81	0.49
2018_0323	26.3	25.9	0.43	0.05	0.14	0.16	0.08
2018_0404	43.6	40.4	3.20	0.20	0.73	0.66	1.60
2018_0406	50.0	48.8	1.25	0.17	0.37	0.31	0.39
2018_0412	156	151	4.56	0.86	1.50	1.44	0.76
2018_0720	63.6	53.6	10.0	7.18	1.19	0.56	1.07
2018_0828	917	885	32.2	7.33	7.10	8.27	9.45
2018_0914	120	118	1.73	0.10	0.50	0.90	0.23
2018_0928	196	194	2.05	0.16	0.76	0.26	0.87
2018_1030	392	389	2.37	0.57	0.51	0.36	0.93
2018_1107	68.1	66.6	1.49	0.65	0.07	0.20	0.56
2018_1114	187	181	5.75	0.72	1.60	1.35	2.09
2018_1127	35.2	31.4	3.88	0.82	2.00	0.31	0.75
2018_1205	115	109	5.85	1.45	0.32	0.61	3.47
2018_1213	41.9	39.6	2.24	0.20	0.38	0.31	1.35
2018_1220	15.9	15.6	0.22	0.08	0.03	0.06	0.05
2019_0108	33.8	32.9	0.92	0.31	0.11	0.23	0.28

CAF (mg)

sample	part. + diss.	diss.	total	particular			
				< 63 µm	63 – 125 µm	125 – 250 µm	250 – 2000 µm
2017_0206	860	847	12.8	3.69	5.96	2.02	1.14
2017_0331	2575	2568	7.13	0.24	4.10	1.38	1.40
2017_0502	1663	1583	80.7	37.5	3.25	24.7	15.2
2017_0505	1544	1530	14.0	7.40	4.25	0.87	1.48
2017_0519	672	668	4.70	0.08	1.03	0.76	2.83
2018_0314	2641	2633	8.22	0.17	0.75	1.07	6.22
2018_0323	933	933	0.74	0.08	0.25	0.21	0.20
2018_0404	413	412	0.94	0.11	0.40	0.30	0.12
2018_0406	990	989	0.66	0.06	0.10	0.41	0.08
2018_0412	1866	1863	2.78	0.46	0.61	0.24	1.47
2018_0720	26	26	0.32	0.19	0.09	0.02	0.03
2018_0828	1165	1160	4.73	0.54	0.81	1.91	1.48
2018_0914	290	289	1.08	0.20	0.63	0.07	0.18
2018_0928	457	456	0.82	0.17	0.16	0.25	0.24
2018_1030	6330	6325	4.92	0.35	1.07	1.62	1.89
2018_1107	737	736	1.24	0.47	0.22	0.46	0.08
2018_1114	2011	2010	0.90	0.10	0.43	0.17	0.20
2018_1127	1026	1021	4.88	0.02	0.17	1.65	3.04
2018_1205	1100	1098	1.57	0.91	0.30	0.21	0.16
2018_1213	1773	1770	3.76	0.18	0.82	0.65	2.12
2018_1220	1544	1538	6.39	0.47	4.09	0.63	1.19
2019_0108	1861	1858	2.68	0.31	1.14	0.61	0.62

DEET (mg)

sample	part. + diss.	diss.	total	particular			
				< 63 µm	63 – 125 µm	125 – 250 µm	250 – 2000 µm
2017_0206	36.2	36.2	0.03	0.00	0.01	0.01	0.01
2017_0331	26.4	26.3	0.05	0.00	0.01	0.01	0.03
2017_0502	33.3	33.0	0.25	0.07	0.04	0.10	0.04
2017_0505	9.48	8.64	0.84	0.08	0.56	0.10	0.11
2017_0519	21.7	21.6	0.05	0.00	0.03	0.01	0.02
2018_0314	34.9	29.4	5.51	2.72	1.07	1.17	0.56
2018_0323	10.0	9.87	0.13	0.02	0.01	0.04	0.06
2018_0404	7.35	7.23	0.11	0.00	0.04	0.07	0.00
2018_0406	8.54	8.51	0.03	0.00	0.00	0.02	0.01
2018_0412	58.9	57.9	1.01	0.12	0.24	0.50	0.15

MCP (mg)

sample	part. + diss.	diss.	total	particular			
				< 63 µm	63 – 125 µm	125 – 250 µm	250 – 2000 µm
2017_0206	189	188	0.39	0.14	0.11	0.10	0.04
2017_0331	2020	2018	2.16	0.39	0.24	0.31	1.22
2017_0502	8686	8584	102	49.3	34.80	11.44	6.38

sample							
2017_0505	664	662	2.15	1.34	0.36	0.23	0.21
2017_0519	3797	3791	6.29	1.79	1.48	1.42	1.60
2018_0314	148	147	0.88	0.08	0.14	0.29	0.36
2018_0323	92.5	92.3	0.20	0.02	0.06	0.06	0.05
2018_0404	131	131	0.26	0.01	0.11	0.08	0.05
2018_0406	345	345	0.49	0.06	0.03	0.29	0.11
2018_0412	1036	1033	2.54	0.99	0.30	0.55	0.69

CBZ (mg)

sample	part. + diss.	diss.	total	particular			
				< 63 µm	63 – 125 µm	125 – 250 µm	250 – 2000 µm
2018_0314	90.1	74.8	15.3	3.07	3.59	6.41	2.27
2018_0323	90.6	87.2	3.4	0.77	0.45	1.37	0.77
2018_0404	67.4	61.7	5.71	1.34	1.54	1.33	1.51
2018_0406	55.4	51.7	3.66	0.86	1.44	1.22	0.14
2018_0412	98.3	70.3	28.0	4.79	8.40	9.59	5.24

LID (mg)

sample	part. + diss.	diss.	total	particular			
				< 63 µm	63 – 125 µm	125 – 250 µm	250 – 2000 µm
2018_0314	73.3	62.2	11.1	3.41	2.42	2.85	2.46
2018_0323	20.8	19.6	1.16	0.24	0.29	0.44	0.19
2018_0404	18.8	16.6	2.12	0.56	0.66	0.59	0.31
2018_0406	24.9	23.4	1.52	0.42	0.41	0.36	0.33
2018_0412	86.8	74.9	11.9	1.94	3.11	3.59	3.26

Tab. C.16: Phase distribution of micropollutant load (%).

Substance	particulate fraction (%)					dissolved fraction (%)				
	min	max	mean	median	SD	min	max	mean	median	SD
16 EPA	70	95	87	89	6.1	4.7	30	13	11	6.1
NAP	2.3	78	34	32	19	22	98	66	68	19
ACY	5.7	70	41	43	20	30	94	59	57	20
ACN	23	91	55	52	21	9.3	77	45	48	21
FLE	14	88	46	44	20	12	86	54	56	20
PHE	58	93	77	74	11	7.0	42	23	26	11
ANT	48	96	75	76	12	4.1	52	25	24	12
FLU	68	98	90	90	7	2.1	32	10	10	7
PYR	85	98	93	95	4.5	1.5	15	6.5	5.2	4.5
BaA	90	99	96	96	2.4	1.5	10	4.0	4.3	2.4
CHR	86	99	95	96	3.7	0.9	14	4.7	3.6	3.7
BbF	90	99	97	97	2.2	90	99	97	97	2.2
BkF	89	99	96	96	2.1	1.3	11	4.2	4.1	2.1
BaP	92	99	96	97	1.9	1.1	7.8	3.5	3.3	1.9
IND	91	98	95	95	2.3	2.3	9.4	5.4	5.0	2.3
GHI	93	99	97	98	1.7	0.8	7.0	3.1	2.4	1.7
DBA	48	96	79	84	14	48	96	79	84	14
4tOP	6.6	93	39	38	21	7.4	93	61	62	21
4NP	20	92	49	49	19	8.0	80	51	51	19
BT	2.1	71	29	23	20	29	98	71	77	20
MTBT	5.3	46	19	17	11	54	95	81	83	11
TCEP	0.9	12	3.8	3.3	2.5	88	99	96	97	2.5
TCPP	5.8	56	30	31	15	44	94	70	69	15
TPP	5.9	84	33	26	23	16	94	67	74	23
DEET	0.1	16	3.1	1.0	5.2	84	100	97	99	5.2
MCP	0.1	1.2	0.3	0.2	0.3	99	100	100	100	0.3
TBY	0.6	16	4.5	2.8	4.2	84	99	95	97	4.2
CBZ	3.7	28	13	8.5	10	72	96	87	92	10
LID	5.6	15	10	11	4.4	85	94	90	89	4.4
CAF	0.1	4.9	0.6	0.3	1	95	100	99	100	1

Tab. C.17: Pearson correlation of particular pollutant concentration with POC concentrations on sample basis. *significant at the 0.05 level

	Pearson correlation coefficient: pollutant concentration (part.) with POC			
	< 63 µm	63 – 125 µm	125 – 250 µm	250 – 2000 µm
NAP	0.686*	0.632*	0.435*	0.079
ACY	0.226	0.102	0.624*	0.477*
ACN	0.514*	0.634*	0.592*	0.454*
FLE	0.426*	0.537*	0.838*	0.664*
PHE	0.886*	0.822*	0.884*	0.744*
ANT	0.769*	0.693*	0.492*	0.550*
FLU	0.924*	0.848*	0.888*	0.800*
PYR	0.879*	0.830*	0.886*	0.790*
BaA	0.754*	0.744*	0.847*	0.681*
CHR	0.823*	0.742*	0.856*	0.673*
BbF	0.872*	0.782*	0.850*	0.830*
BkF	0.671*	0.713*	0.874*	0.872*
BaP	0.721*	0.766*	0.868*	0.871*
IND	0.725*	0.842*	0.849*	0.809*
GHI	0.885*	0.837*	0.752*	0.721*
DBA	0.752*	0.664*	0.653*	0.456*
16EPA	0.909*	0.838*	0.880*	0.809*
4tOP	0.718*	0.731*	0.941*	0.688*
4NP	0.646*	0.587*	0.628*	0.694*
BT	0.324*	0.605*	0.773*	0.538*
MTBT	0.427*	0.589*	0.749*	0.488*
TCEP	0.155	0.717*	0.543*	0.799*
TCPP	0.394*	0.452*	0.488*	0.468*
TPP	0.744*	0.459*	0.418*	0.847*
DEET	-0.039	0.046	0.404	0.407
MCP	-0.022	0.067	0.004	0.110
TBY	0.442*	0.692*	0.893*	0.838*
CBZ	0.943*	0.989*	0.987*	0.325
LID	0.818*	0.948*	0.984*	0.711
CAF	0.166	0.042	0.597*	0.0167

Tab. C.18: Pearson correlation dissolved pollutant concentrations with DOC on sample basis.
*significant at the 0.05 level

	Pearson correlation coefficient: pollutant concentration (diss.) with DOC			
	< 63 µm	63 – 125 µm	125 – 250 µm	250 – 2000 µm
NAP	0.318*	-0.082	-0.028	0.177
ACY	0.008	0.113	0.066	0.198
ACN	0.308*	0.010	0.375*	0.561*
FLE	-0.041	0.117	0.170	0.354*
PHE	0.276*	0.471*	0.001	0.498*
ANT	0.230	0.323	0.052	0.437*
FLU	0.199	0.181	-0.082	0.005
PYR	0.330*	0.364*	-0.108	0.082
BaA	0.164	-0.314	-0.074	0.028
CHR	0.017	-0.227	-0.059	-0.037
BbF	N/A	N/A	N/A	N/A
BkF	N/A	N/A	N/A	N/A
BaA	N/A	N/A	N/A	N/A
IND	N/A	N/A	N/A	N/A
GHI	N/A	N/A	N/A	N/A
DBA	N/A	N/A	N/A	N/A
16EPA	0.267	0.167	0.028	0.454*
4tOP	-0.149	-0.078	-0.050	0.003
4NP	-0.057	-0.022	-0.083	0.070
BT	0.284*	0.454*	0.474*	0.619*
MTBT	0.384*	0.464*	0.392*	0.887*
TCEP	0.294	0.256	-0.008	0.072
TCPP	0.189	0.193	0.280	0.023
TPP	0.063	-0.181	-0.019	-0.108
DEET	0.313*	0.881*	0.700*	0.543*
MCP	0.203	0.875*	0.873*	-0.151
TBY	0.377	0.623	0.597	0.552
CBZ	-0.248	-0.174	-0.171	0.041
LID	0.204	-0.148	-0.115	0.471
CAF	0.076	0.033	0.076	-0.060
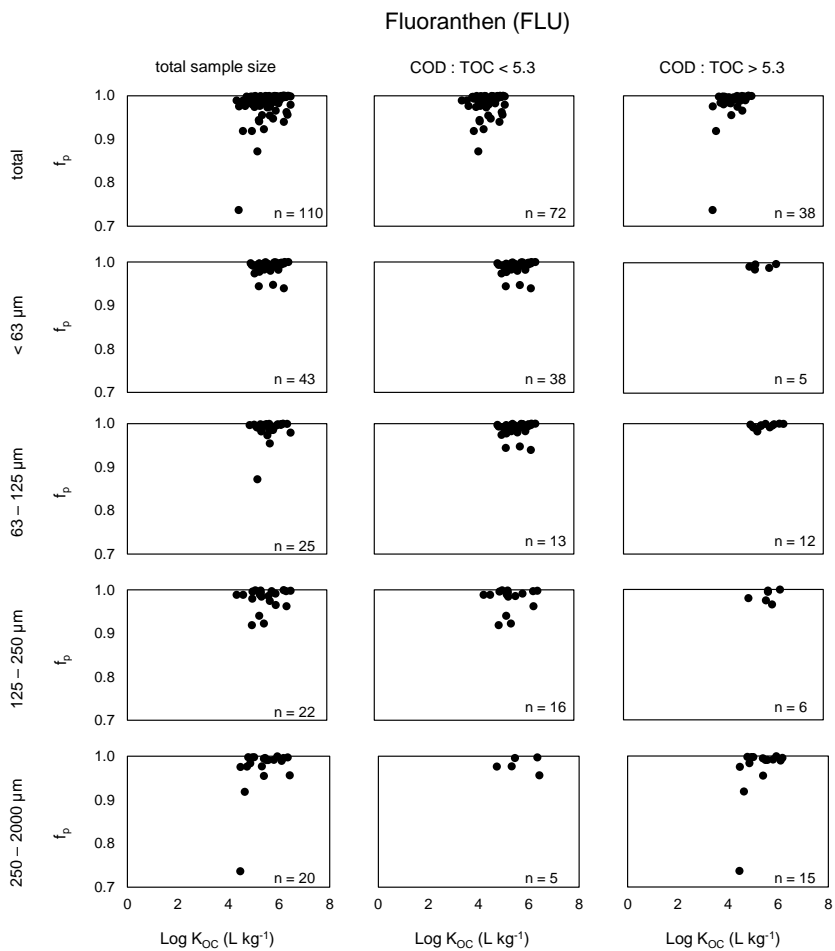
Fig. C.4:   Scatterplot-Analysis: phase distribution (fp) and log KOC of Flouranthen
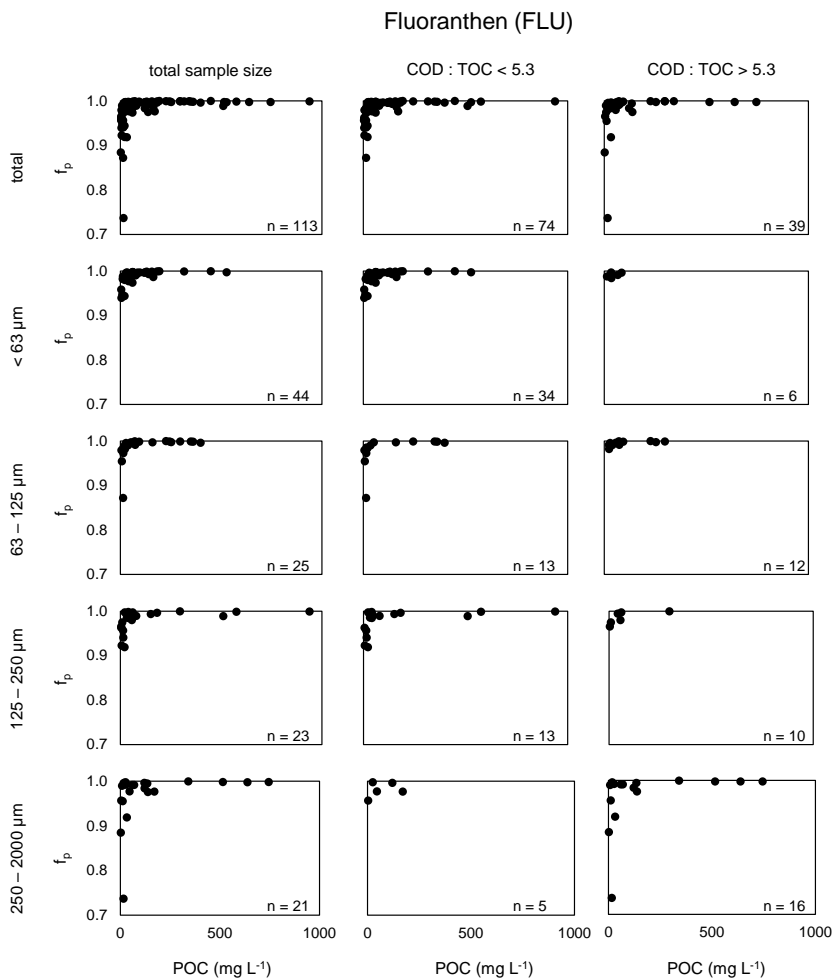
Fluoranthen (FLU)

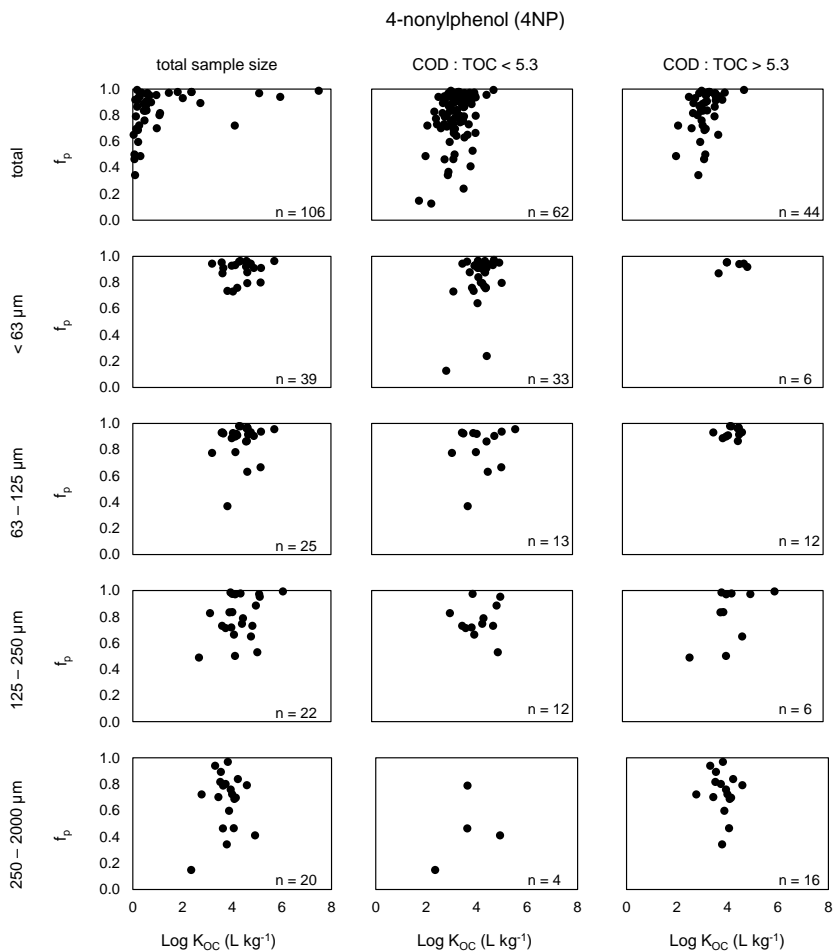Fig. C.5:   Scatterplot-Analysis: phase distribution (fp) of Flouranthen and particulate organic carbon

Fig. C.6: Scatterplot-Analysis: phase distribution (f_p) and log K_{OC} of 4-Nonylphenol
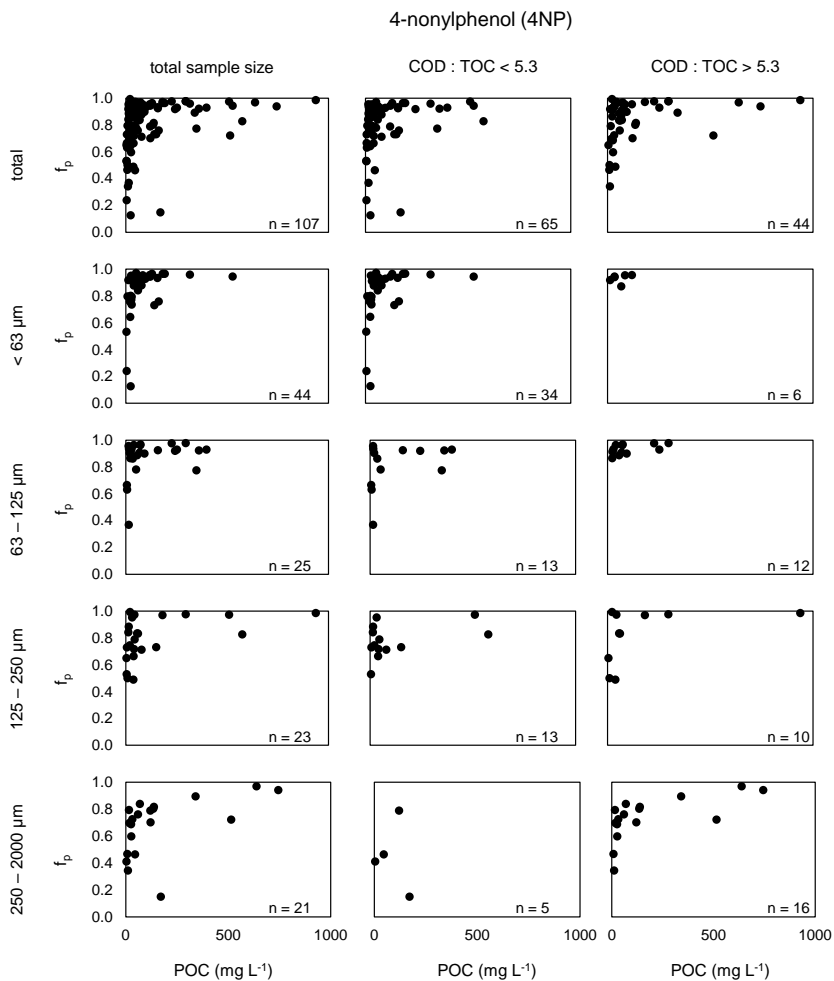
4-nonylphenol (4NP)

Fig. C.7: Scatterplot-Analysis: phase distribution (fp) of 4-Nonylphenol and particulate or-
ganic carbon

Tab. C.19: Descriptive statistics for the micropollutant removal efficiency. Sampling event 2018_0720 excluded

Sub-stance		part.+diss.	diss.	particulate-bound				
				total	< 63 µm	63-125 µm	125-250 µm	250-2000µm
NAP	min	0.03	0.03	0.06	0.03	0.03	0.05	0.31
	max	0.76	0.77	0.74	0.73	0.98	0.98	0.99
	mean	0.29	0.26	0.37	0.28	0.64	0.74	0.76
	median	0.25	0.23	0.40	0.22	0.80	0.80	0.87
	SD	0.19	0.18	0.20	0.19	0.35	0.26	0.24
ACY	min	0.06	0.03	0.04	0.01	0.12	0.25	0.07
	max	0.97	0.95	0.98	0.98	0.99	0.99	0.99
	mean	0.32	0.24	0.46	0.35	0.59	0.69	0.71
	median	0.29	0.16	0.48	0.29	0.49	0.77	0.75
	SD	0.22	0.22	0.25	0.25	0.31	0.27	0.27
ACN	min	0.06	0.02	0.10	0.01	0.13	0.00	0.21
	max	0.91	0.75	0.93	0.93	0.97	0.98	0.99
	mean	0.30	0.24	0.37	0.30	0.69	0.70	0.75
	median	0.21	0.17	0.28	0.22	0.78	0.76	0.78
	SD	0.22	0.20	0.24	0.25	0.28	0.28	0.22
FLE	min	0.06	0.01	0.07	0.02	0.11	0.14	0.10
	max	0.85	0.73	0.97	1.00	0.99	0.99	1.00
	mean	0.36	0.27	0.47	0.38	0.67	0.73	0.77
	median	0.28	0.13	0.34	0.28	0.84	0.84	0.82
	SD	0.26	0.25	0.28	0.28	0.32	0.28	0.25
PHE	min	0.10	0.02	0.12	0.10	0.19	0.13	0.25
	max	0.77	0.61	0.81	0.76	0.98	0.98	1.00
	mean	0.37	0.20	0.43	0.35	0.72	0.77	0.73
	median	0.29	0.11	0.43	0.25	0.82	0.87	0.79
	SD	0.21	0.18	0.23	0.22	0.27	0.24	0.24
ANT	min	0.13	0.06	0.17	0.11	0.16	0.08	0.18
	max	0.74	0.70	0.86	0.83	0.97	0.99	1.00
	mean	0.41	0.28	0.46	0.36	0.71	0.74	0.80
	median	0.41	0.26	0.43	0.27	0.78	0.82	0.89
	SD	0.20	0.19	0.24	0.23	0.28	0.24	0.23
FLU	min	0.12	0.01	0.12	0.10	0.18	0.15	0.27
	max	0.83	0.60	0.85	0.83	0.98	0.98	0.99
	mean	0.40	0.21	0.42	0.35	0.72	0.78	0.84
	median	0.32	0.16	0.35	0.25	0.86	0.87	0.91
	SD	0.21	0.17	0.22	0.23	0.28	0.25	0.19
PYR	min	0.12	0.01	0.12	0.10	0.18	0.15	0.27
	max	0.83	0.60	0.85	0.83	0.98	0.98	0.99
	mean	0.40	0.21	0.42	0.35	0.72	0.78	0.84
	median	0.32	0.16	0.35	0.25	0.86	0.87	0.91
	SD	0.21	0.17	0.22	0.23	0.28	0.25	0.19
BaA	min	0.13	0.03	0.13	0.10	0.16	0.22	0.26
	max	0.69	0.51	0.71	0.67	0.97	0.99	1.00
	mean	0.40	0.23	0.41	0.33	0.73	0.79	0.83
	median	0.37	0.29	0.40	0.28	0.84	0.87	0.90
	SD	0.19	0.17	0.19	0.20	0.27	0.20	0.19
CHR	min	0.12	0.03	0.12	0.10	0.18	0.16	0.25
	max	0.74	0.51	0.76	0.70	0.97	0.97	1.00
	mean	0.40	0.23	0.41	0.33	0.70	0.78	0.83
	median	0.32	0.26	0.35	0.23	0.81	0.86	0.89
	SD	0.20	0.16	0.21	0.21	0.29	0.21	0.19

Sub-stance		part.+diss.	diss.	particulate-bound				
				total	< 63 µm	63-125 µm	125-250 µm	250-2000 µm
BbF	min	0.12	0.04	0.12	0.00	0.10	0.18	0.36
	max	0.62	0.51	0.62	0.55	0.96	1.00	1.00
	mean	0.33	0.22	0.34	0.19	0.68	0.81	0.85
	me-dian	0.36	0.29	0.36	0.14	0.77	0.87	0.91
	SD	0.17	0.16	0.17	0.17	0.28	0.20	0.17
BkF	min	0.12	0.04	0.12	0.04	0.09	0.20	0.46
	max	0.58	0.51	0.61	0.58	0.97	1.00	0.99
	mean	0.33	0.22	0.33	0.19	0.68	0.83	0.86
	me-dian	0.35	0.29	0.36	0.13	0.79	0.90	0.88
	SD	0.15	0.16	0.15	0.14	0.27	0.20	0.16
BaP	min	0.10	0.04	0.10	0.05	0.21	0.12	0.19
	max	0.84	0.51	0.85	0.84	0.99	0.97	1.00
	mean	0.40	0.22	0.41	0.32	0.71	0.80	0.81
	me-dian	0.38	0.29	0.39	0.26	0.80	0.92	0.88
	SD	0.20	0.16	0.21	0.21	0.26	0.24	0.20
IND	min	0.15	0.04	0.15	0.10	0.18	0.21	0.39
	max	0.64	0.51	0.66	0.63	0.99	0.99	0.99
	mean	0.37	0.22	0.38	0.31	0.70	0.79	0.81
	me-dian	0.34	0.29	0.37	0.24	0.78	0.86	0.88
	SD	0.17	0.16	0.18	0.18	0.27	0.21	0.17
GHI	min	0.11	0.04	0.11	0.09	0.17	0.16	0.35
	max	0.66	0.51	0.68	0.66	0.99	0.98	0.99
	mean	0.37	0.22	0.38	0.31	0.70	0.79	0.81
	me-dian	0.34	0.29	0.35	0.30	0.80	0.89	0.87
	SD	0.17	0.16	0.17	0.17	0.28	0.23	0.18
DBA	min	0.10	0.04	0.10	0.07	0.17	0.09	0.00
	max	0.61	0.51	0.70	0.57	0.97	0.97	0.99
	mean	0.33	0.22	0.37	0.29	0.74	0.77	0.71
	me-dian	0.27	0.29	0.35	0.27	0.85	0.84	0.82
	SD	0.15	0.16	0.18	0.15	0.27	0.24	0.28
4tOP	min	0.07	0.03	0.09	0.06	0.12	0.09	0.25
	max	0.69	0.78	0.90	0.90	1.00	0.98	0.99
	mean	0.29	0.24	0.43	0.37	0.67	0.78	0.82
	me-dian	0.22	0.14	0.29	0.22	0.79	0.88	0.90
	SD	0.20	0.22	0.28	0.28	0.31	0.24	0.22
4NP	min	0.08	0.03	0.14	0.12	0.18	0.08	0.33
	max	0.61	0.95	0.84	0.82	0.99	0.99	0.99
	mean	0.32	0.26	0.41	0.33	0.68	0.77	0.69
	me-dian	0.30	0.24	0.39	0.24	0.82	0.79	0.75
	SD	0.18	0.22	0.23	0.22	0.29	0.23	0.22

Sub-stance		part.+diss.	diss.	particulate-bound				
				total	< 63 µm	63-125 µm	125-250 µm	250-2000 µm
BT	min	0.03	0.01	0.09	0.06	0.20	0.25	0.35
	max	0.61	0.70	0.96	0.98	0.99	1.00	0.98
	mean	0.27	0.23	0.40	0.34	0.69	0.70	0.74
	me-dian	0.20	0.17	0.30	0.24	0.79	0.73	0.78
	SD	0.20	0.21	0.27	0.29	0.27	0.23	0.21
MTBT	min	0.03	0.02	0.08	0.06	0.19	0.02	0.49
	max	0.80	0.80	0.84	0.83	0.99	0.99	0.99
	mean	0.25	0.24	0.35	0.29	0.67	0.65	0.80
	me-dian	0.21	0.21	0.28	0.22	0.76	0.76	0.88
	SD	0.21	0.22	0.24	0.24	0.27	0.29	0.17
TCEP	min	0.02	0.02	0.06	0.01	0.01	0.08	0.01
	max	0.80	0.80	0.96	0.92	1.00	0.98	0.98
	mean	0.26	0.25	0.43	0.29	0.56	0.65	0.61
	me-dian	0.22	0.22	0.38	0.18	0.54	0.73	0.69
	SD	0.22	0.22	0.25	0.29	0.34	0.27	0.30
TCPP	min	0.05	0.01	0.19	0.18	0.15	0.20	0.36
	max	0.63	0.58	0.92	0.88	0.97	0.98	1.00
	mean	0.36	0.23	0.67	0.46	0.71	0.76	0.82
	me-dian	0.37	0.23	0.74	0.37	0.84	0.87	0.91
	SD	0.17	0.17	0.22	0.24	0.29	0.24	0.20
TPP	min	0.10	0.01	0.29	0.38	0.28	0.27	0.29
	max	0.83	0.66	0.99	0.99	0.99	1.00	1.00
	mean	0.41	0.23	0.83	0.83	0.80	0.80	0.81
	me-dian	0.34	0.21	0.86	0.93	0.87	0.86	0.88
	SD	0.23	0.18	0.16	0.21	0.20	0.20	0.19
TBY	min	0.04	0.03	0.43	0.17	0.35	0.46	0.45
	max	0.75	0.74	0.99	1.00	0.99	0.99	1.00
	mean	0.28	0.26	0.81	0.74	0.76	0.81	0.83
	me-dian	0.25	0.21	0.84	0.85	0.82	0.86	0.90
	SD	0.21	0.20	0.16	0.25	0.21	0.18	0.18
CAF	min	0.02	0.02	0.16	0.07	0.02	0.06	0.05
	max	0.55	0.54	1.00	1.00	1.00	1.00	1.00
	mean	0.23	0.22	0.72	0.68	0.55	0.72	0.69
	me-dian	0.13	0.13	0.80	0.79	0.55	0.83	0.80
	SD	0.19	0.19	0.24	0.32	0.31	0.31	0.35

Tab. C.20: Fischer's z-transformation: lower (LL) and upper limits UL of the calculated 95 % Confidence interval (CI). n = 22, for metals n = 17

Parameter	95 % CI	NAP	ACY	ACN	FLE	PHE	ANT	FLU	PYR	BaA
TSS	LL	-7.4	-7.8	-7.5	-7.5	-7.0	-7.1	-7.3	-7.1	-7.2
	UL	9.7	9.3	9.6	9.6	10.1	10.0	9.8	10.0	9.9
TSS < 63 µm	LL	-7.2	-7.8	-7.5	-7.5	-6.6	-6.9	-7.2	-7.0	-7.1
	UL	9.9	9.3	9.6	9.6	10.5	10.2	9.9	10.1	10.0
TSS 63 – 125 µm	LL	-7.6	-7.8	-7.5	-7.6	-7.4	-7.3	-7.4	-7.3	-7.3
	UL	9.5	9.3	9.6	9.5	9.7	9.8	9.7	9.7	9.7
TSS 125 – 250 µm	LL	-7.7	-7.9	-7.8	-7.9	-7.6	-7.6	-7.6	-7.6	-7.6
	UL	9.3	9.1	9.3	9.2	9.5	9.5	9.5	9.5	9.4
TSS 250 – 2000 µm	LL	-7.5	-7.8	-7.7	-7.8	-7.5	-7.4	-7.6	-7.4	-7.5
	UL	9.6	9.3	9.4	9.3	9.6	9.6	9.5	9.7	9.6

Parameter	95 % CI	CHR	BbF	BkF	BaP	IND	GHI	DBA	∑16 EPA
TSS	LL	-7.44	-7.32	-7.28	-7.10	-7.20	-7.03	-7.26	-7.10
	UL	9.65	9.77	9.80	9.98	9.89	10.06	9.83	9.99
TSS < 63 µm	LL	-7.28	-7.05	-7.04	-6.99	-7.06	-6.84	-7.15	-6.96
	UL	9.81	10.04	10.04	10.10	10.02	10.25	9.94	10.13
TSS 63 – 125 µm	LL	-7.68	-7.58	-7.54	-7.19	-7.42	-7.43	-7.50	-7.35
	UL	9.41	9.50	9.55	9.90	9.67	9.66	9.59	9.74
TSS 125 – 250 µm	LL	-7.85	-7.72	-7.73	-7.59	-7.71	-7.62	-7.64	-7.62
	UL	9.24	9.37	9.35	9.49	9.38	9.46	9.45	9.47
TSS 250 – 2000 µm	LL	-7.80	-7.67	-7.63	-7.46	-7.59	-7.51	-7.55	-7.48
	UL	9.29	9.42	9.46	9.63	9.50	9.58	9.54	9.61

Parameter	95 % CI	4tOP	4NP	BT	MTBT	TCEP	TCPP	TPP	TBY	CAF
TSS	LL	-7.87	-7.52	-7.54	-7.59	-7.62	-7.64	-7.37	-7.72	-8.15
	UL	9.22	9.56	9.55	9.50	9.46	9.45	9.71	9.36	8.94
TSS < 63 µm	LL	-7.68	-7.35	-7.47	-7.58	-7.48	-7.54	-7.33	-7.81	-8.12
	UL	9.41	9.73	9.62	9.50	9.61	9.55	9.76	9.28	8.97
TSS 63 – 125 µm	LL	-8.01	-7.66	-7.73	-7.58	-7.74	-7.69	-7.41	-7.60	-8.26
	UL	9.08	9.42	9.36	9.51	9.34	9.39	9.68	9.48	8.82
TSS 125 – 250 µm	LL	-8.15	-7.89	-7.97	-7.86	-7.93	-7.95	-7.72	-7.77	-8.36
	UL	8.94	9.20	9.12	9.23	9.16	9.13	9.36	9.32	8.72
TSS 250 – 2000 µm	LL	-8.14	-7.84	-7.80	-7.72	-7.85	-7.90	-7.64	-7.71	-8.29
	UL	8.94	9.25	9.28	9.36	9.23	9.18	9.45	9.37	8.80

Tab. C.20: continued

Parameter	95 % CI	Cr	Cu	Zn	Cd	Pb
TSS	LL	-5.78	-6.04	-6.21	-6.17	-5.98
	UL	8.89	8.63	8.46	8.49	8.69
TSS	LL	-5.59	-5.81	-6.05	-5.96	-6.14
< 63 µm	UL	9.08	8.86	8.62	8.71	8.52

Tab. C.21: Sample specific metal event mean concentrations (µg L^{-1}), pH and temperature (°C)

					Chromium			
sample	pH	T(C°)	< 63 µm	63 – 125 µm	125 – 250 µm	250 – 2000 µm	total	dissolved
2018_0314	7.6	9.9	22.5	0.77	0.60	0.81	25.3	0.60
2018_0323	7.4	8.1	5.08	0.23	0.19	0.12	8.82	3.19
2018_0404	7.1	12.7	6.52	0.30	0.37	0.30	8.21	0.72
2018_0406	6.9	9.4	6.84	0.39	0.39	0.19	8.94	1.13
2018_0412	7.1	13.4	27.2	7.56	5.12	1.10	41.9	0.87
2018_0720	6.7	21.4	16.9	6.20	5.57	9.05	38.9	1.26
2018_0828	6.7	18.5	22.4	4.25	1.59	1.12	29.5	0.13
2018_0914	6.8	19.1	5.34	0.56	0.28	0.26	6.71	0.27
2018_0928	6.8	16.2	8.83	1.09	0.61	0.38	11.2	0.28
2018_1030	7.1	9.9	4.35	0.51	0.13	0.16	5.42	0.28
2018_1107	7.0	9.5	5.99	0.34	0.31	0.64	7.55	0.27
2018_1114	7.0	10.2	3.65	0.54	0.28	0.33	4.98	0.19
2018_1127	6.9	7.8	2.35	0.97	0.20	0.17	3.92	0.23
2018_1205	7.2	10.2	12.5	0.77	0.60	0.20	14.2	0.09
2018_1213	6.9	5.8	7.55	0.69	0.28	0.38	9.15	0.25
2018_1220	6.9	8.5	1.19	< 0.1	< 0.1	< 0.1	1.60	0.27
2019_0108	7.2	7.8	1.71	0.13	< 0.1	< 0.1	2.28	0.35
					Copper (Cu)			
sample	pH	T(C°)	< 63 µm	63 – 125 µm	125 – 250 µm	250 – 2000 µm	total	dissolved
2018_0314	7.6	9.9	28.6	2.07	1.56	3.29	45.8	10.2
2018_0323	7.4	8.1	18.5	0.50	0.31	0.36	24.7	5.03
2018_0404	7.1	12.7	20.6	1.08	1.03	0.70	37.2	13.8
2018_0406	6.9	9.4	23.2	1.48	1.19	0.79	38.7	12.0
2018_0412	7.1	13.4	65.4	16.1	13.0	3.22	108	10.3
2018_0720	6.7	21.4	38.1	19.2	11.0	18.2	102	15.1
2018_0828	6.7	18.5	10.7	2.09	0.81	2.19	22.3	6.49
2018_0914	6.8	19.1	11.3	0.93	0.16	0.77	28.9	15.8
2018_0928	6.8	16.2	7.39	4.46	0.85	2.01	26.6	11.9
2018_1030	7.1	9.9	1.75	1.99	1.15	0.81	19.3	13.6
2018_1107	7.0	9.5	23.3	0.67	0.29	0.81	44.1	19.1
2018_1114	7.0	10.2	3.92	1.17	0.12	1.55	15.3	8.49

			< 63 µm	63 – 125 µm	125 – 250 µm	250 – 2000 µm		
2018_1127	6.9	7.8	9.74	4.44	0.65	0.77	26.3	10.7
2018_1205	7.2	10.2	18.6	1.23	0.74	0.46	24.0	3.00
2018_1213	6.9	5.8	13.2	1.33	0.81	0.87	23.0	6.81
2018_1220	6.9	8.5	5.36	0.16	0.25	0.15	17.5	11.6
2019_0108	7.2	7.8	3.91	0.20	< 0.1	< 0.1	14.3	10.0

Zinc (Zn)

sample	pH	T(C°)	< 63 µm	63 – 125 µm	125 – 250 µm	250 – 2000 µm	total	dissolved
2018_0314	7.6	9.9	134	11.9	9.91	19.7	347	171.6
2018_0323	7.4	8.1	78.7	2.88	1.98	2.26	157	71.3
2018_0404	7.1	12.7	112	6.87	7.09	4.95	247	116
2018_0406	6.9	9.4	105	8.14	7.37	4.14	239	115
2018_0412	7.1	13.4	323	71.3	63.7	15.0	735	262
2018_0720	6.7	21.4	265	131	26.9	105	835	306
2018_0828	6.7	18.5	56.6	8.69	4.07	10.4	244	165
2018_0914	6.8	19.1	59.1	1.45	8.00	2.23	276	206
2018_0928	6.8	16.2	28.2	14.3	2.95	24.6	267	197
2018_1030	7.1	9.9	22.4	7.76	4.35	3.95	276	237
2018_1107	7.0	9.5	143	3.27	1.98	2.75	533	382
2018_1114	7.0	10.2	14.7	3.19	2.75	6.66	245	218
2018_1127	6.9	7.8	26.7	15.8	2.24	6.02	449	399
2018_1205	7.2	10.2	94.4	8.07	4.35	3.25	242	132
2018_1213	6.9	5.8	61.1	8.46	5.04	8.74	295	212
2018_1220	6.9	8.5	17.5	1.40	1.24	0.96	314	293
2019_0108	7.2	7.8	38.2	1.73	1.33	1.97	256	213

Cadmium (Cd)

sample	pH	T(C°)	< 63 µm	63 – 125 µm	125 – 250 µm	250 – 2000 µm	total	dissolved
2018_0314	7.6	9.9	0.10	< 0.1	< 0.1	< 0.1	0.20	< 0.1
2018_0323	7.4	8.1	< 0.1	< 0.1	< 0.1	< 0.1	< 0.1	< 0.1
2018_0404	7.1	12.7	< 0.1	< 0.1	< 0.1	< 0.1	0.13	< 0.1
2018_0406	6.9	9.4	< 0.1	< 0.1	< 0.1	< 0.1	0.11	< 0.1
2018_0412	7.1	13.4	0.21	< 0.1	< 0.1	< 0.1	0.50	0.21
2018_0720	6.7	21.4	0.18	< 0.1	< 0.1	< 0.1	0.58	0.20
2018_0828	6.7	18.5	< 0.1	< 0.1	< 0.1	< 0.1	0.12	< 0.1
2018_0914	6.8	19.1	< 0.1	< 0.1	< 0.1	< 0.1	0.15	< 0.1
2018_0928	6.8	16.2	< 0.1	< 0.1	< 0.1	< 0.1	0.12	< 0.1
2018_1030	7.1	9.9	< 0.1	< 0.1	< 0.1	< 0.1	0.09	< 0.1
2018_1107	7.0	9.5	0.11	< 0.1	< 0.1	< 0.1	0.28	0.16
2018_1114	7.0	10.2	< 0.1	< 0.1	< 0.1	< 0.1	0.13	0.10
2018_1127	6.9	7.8	< 0.1	< 0.1	< 0.1	< 0.1	0.15	0.10
2018_1205	7.2	10.2	< 0.1	< 0.1	< 0.1	< 0.1	0.11	< 0.1
2018_1213	6.9	5.8	< 0.1	< 0.1	< 0.1	< 0.1	< 0.1	< 0.1
2018_1220	6.9	8.5	< 0.1	< 0.1	< 0.1	< 0.1	< 0.1	< 0.1
2019_0108	7.2	7.8	< 0.1	< 0.1	< 0.1	< 0.1	0.11	< 0.1

			Lead (PB)					
sample	pH	T(C°)	< 63 μm	63 – 125 μm	125 – 250 μm	250 – 2000 μm	total	dissolved
2018_0314	7.6	9.9	6.37	0.73	0.65	0.97	8.87	0.15
2018_0323	7.4	8.1	2.65	0.13	< 0.1	< 0.1	2.97	< 0.1
2018_0404	7.1	12.7	4.07	0.27	0.27	0.15	4.82	< 0.1
2018_0406	6.9	9.4	4.80	0.40	0.33	0.15	5.73	< 0.1
2018_0412	7.1	13.4	18.7	4.45	3.90	0.70	29.0	1.28
2018_0720	6.7	21.4	10.8	6.64	2.68	11.3	31.5	< 0.1
2018_0828	6.7	18.5	2.48	0.28	0.18	0.41	3.40	< 0.1
2018_0914	6.8	19.1	3.11	0.22	0.55	0.11	4.03	< 0.1
2018_0928	6.8	16.2	1.55	1.04	0.17	0.38	3.20	< 0.1
2018_1030	7.1	9.9	0.20	0.46	0.24	0.19	1.14	< 0.1
2018_1107	7.0	9.5	11.3	0.25	< 0.1	0.18	11.8	< 0.1
2018_1114	7.0	10.2	0.83	0.23	< 0.1	0.33	1.46	< 0.1
2018_1127	6.9	7.8	2.29	0.71	0.15	0.17	3.37	< 0.1
2018_1205	7.2	10.2	4.48	0.37	0.19	0.11	5.20	< 0.1
2018_1213	6.9	5.8	3.94	0.41	0.22	0.28	4.92	< 0.1
2018_1220	6.9	8.5	0.65	< 0.1	< 0.1	< 0.1	0.88	0.12
2019_0108	7.2	7.8	0.75	0.23	< 0.1	< 0.1	1.29	0.25

Curiculum Vitae

2007 – 2014	Studium der Umweltschutztechnik (Dipl.-Ing.) an der Fakultät für Bau- und Umweltingenieurswissenschaften der Universität Stuttgart
2010 – 2012	Studentische Hilfskraft am Institut für Siedlungswasserbau, Wassergüte- und Abfallwirtschaft (ISWA) im Arbeitsbereich Wassergütewirtschaft und Wasserversorgung
2012	10-monatiges Praktikum und ASApreneurs Stipendienprogramm bei der Stiftung Sabab Lou (Grabenstetten) und der Rural Developement Organization (Gambia, West-Afrika) - Planung und Implementierung von nachhaltigen Trinkwassersystemen und Bewässerungslösungen im ländlichen Raum Gambias
2014 – 2020	Wissenschaftlicher Mitarbeiter an der Universität Stuttgart am Institut für Siedlungswasserbau, Wassergüte- und Abfallwirtschaft (ISWA) im Arbeitsbereich Urbanes Wassermanagement und Siedlungsentwässerung
2020 – 2021	Ingenieur bei der unteren Wasserbehörde am Landratsamt Rems-Murr-Kreis
seit 2021	Referent für Wasserwirtschaft beim Land Baden-Württemberg

Schriftenreihe Wasser Infrastruktur Ressourcen

bereits veröffentlicht wurden

wasser infrastruktur ressourcen